# Lithium-ion batteries and the transition to electric vehicles: environmental challenges and opportunities from a life cycle perspective

Xu, C.

# Lithium-ion batteries and the transition to electric vehicles — environmental challenges and opportunities from a life cycle perspective

**Chengjian Xu**

Chengjian Xu (2022)
Lithium-ion batteries and the transition to electric vehicles — environmental challenges and opportunities from a life cycle perspective
PhD Thesis at Leiden University, The Netherlands

ISBN: 9789051919899
Cover: Xuanlin Fan & Chengjian Xu
Layout: Chengjian Xu
Printing: GVO printers & designers B.V., Ede, The Netherlands

# Lithium-ion batteries and the transition to electric vehicles — environmental challenges and opportunities from a life cycle perspective

Proefschrift

ter verkrijging van
de graad van doctor aan de Universiteit Leiden,
op gezag van rector magnificus prof.dr.ir. H. Bijl,
volgens besluit van het college voor promoties
te verdedigen op woensdag 21 december 2022
klokke 16.15 uur

door

Chengjian Xu
geboren te Yancheng, China
in 1993

**Promotor:**
Prof. dr. A. Tukker
**Co-promotores:**
Dr. B. Steubing
Dr. M. Hu

**Promotiecommissie:**
Prof. dr. E. van der Voet
Prof. dr. H. X. Lin
Dr. S. Cucurachi
Prof. dr. D.B. Müller (Norwegian University of Science and Technology)
Dr. A. Nordelöf (Chalmers University of Technology)

**Table of Contents**

1 General introduction ..... 1

2 Future material demand for automotive lithium-based batteries ..... 11

3 Future greenhouse gas emissions of automotive lithium-ion battery cell production ..... 85

4 Future greenhouse gas emissions of global automotive lithium-ion battery cells and recycling potential till 2050 ..... 109

5 Electric vehicle batteries alone could satisfy short-term grid storage demand by as early as 2030 ..... 125

6 General discussion ..... 171

References ..... 187

Summary ..... 205

Samenvatting ..... 209

Acknowledgements ..... 213

Curriculum Vitae ..... 215

# 1 General introduction

## 1.1 Background

Global greenhouse gas (GHG) emissions continued to grow with the annual addition of 59 Gt CO2-Eq in 2019, despite slowed growth in recent years. Combating climate change and meeting the Paris Agreement's long-term temperature goal is only possible with urgent and ambitious actions across all sectors. These actions include a transition to low-carbon electricity production, electrification of transport, a low or nearly zero energy build environment and low-carbon industry processes, amongst others, next to implementing carbon capture and utilization and circular material use.

As the second-largest GHG-emitting sector next to the energy sector, the transportation sector accounts for ~15% of global annual GHG emissions in 2019[1]. Electrification of transportation services has been demonstrated as a technically feasible, cost-efficient, and rapidly scalable option to mitigate GHG emissions in the transportation sector. Vehicle electrification can significantly reduce GHG emissions of passenger cars[2], alongside reducing dependency on oil resources[3]. It can further contribute to the 'smart city' concept if electrification is combined with automated driving[4] and fleet sharing[5].

Passenger cars are the fastest growing segment of the transport sector that makes a shift from internal combustion engine vehicles (ICEVs) to electric vehicles (EVs). The global EV fleet grew from a few thousand vehicles in 2005 to 10.1 million vehicles in 2021[6]. Strong growth can be foreseen in the next decades. The International Energy Agency (IEA) projects 175-244 million EVs on the road globally in 2030, including 130-190 million battery electric vehicles (BEVs) and 45-54 million plug-in hybrid electric vehicles (PHEVs)[6,7], depending on policy support, technology advancements, and other factors.

## 1.2 Sustainability challenges and opportunities related to the EV transition with a focus on batteries

The EV transition faces technical challenges (*e.g.,* range and durability of EV batteries); economic challenges (*e.g.,* purchase price compared to ICEVs); and consumer awareness challenges (*e.g.,* environmental benefits of EVs). These EV transition

challenges relate to and impact each other[8]. Understanding this complexity will help address these EV transition challenges and even create opportunities that maximize the benefits of the EV transition.

The batteries play a key role in understanding the EV transition challenges[8,9]. Here, we focus on the challenges for achieving environmentally sustainable batteries, as well as the opportunities that battery use can bring to sectors other than the EV sector. The following sections introduce the challenges and opportunities of EV batteries from a battery life cycle perspective: battery production, battery use, and battery end-of-life.

**Battery production.** The future global EV fleet will demand massive amounts of batteries, reaching 1.8-3 terawatt-hour (TWh) of batteries in 2030[6]. This requires the rapid scale-up of battery production capacity and related supply chains, starting from materials extraction and concentration, smelting, leaching, cathode (and other components) production, cell production, to battery pack assembly. Concerns have been raised with regard to various aspects: economically available reserves for battery materials[10]; affordable, secure and sufficient supply of raw materials[11] (especially for lithium, cobalt, nickel); how to minimize carbon emissions related to battery production[12]; and other social and environmental impacts[13].

**Battery use.** The increasing EV fleet, supported by large-scale battery production, is set to reduce the demand for oil-based fossil fuels that would otherwise be required by ICEVs. EVs also increase net GHG emissions benefit because EVs are 2-4 times more efficient than ICEVs and the electricity supply is decarbonized by the transition to renewables[6]. EVs are expected to lead to a reduction of 3-4.5 million barrels of oil per day that would otherwise have been consumed by light-duty vehicles in 2030[6], depending on EV fleet size. The net reduction of GHG emissions can reach 460-580 million tons (Mt) CO2-Eq in 2030[6], where 280-340 Mt CO2-Eq (generated from EV use due to electricity consumption) are offset by the avoidance of 740-920 Mt CO2-Eq (which would have been emitted from ICEVs).

In addition, EV batteries on the vehicle board can provide energy storage service and economic value for the power system through vehicle-to-grid technology. Vehicle-to-grid charging can be smart to enable dynamic EV charging and load-shifting services to the grid. EVs can also store electricity and deliver it to the grid at peak times when power generation is more expensive[14]. These opportunities rely on standards and

market arrangements that allow for dynamic energy pricing and the ability of owners to benefit from the value to the grid (value includes deferred or avoided capital expenditure on additional stationary storage, and power electronic infrastructure, transmission build-out[14]).

**Battery end-of-life.** Battery useful capacity degrades as being used for EV driving and vehicle-to-grid service (hereafter called battery degradation). Usually, when the remaining battery capacity drops to between 70-80% of the original capacity batteries become unsuitable for use in EVs[15] (hereafter called retired batteries). However, these retired batteries may still have years of useful life in less demanding stationary energy storage applications[16]. These batteries can contribute to grid stability and generate substantial grid-based economic value.

Batteries with extremely poor state-of-health (SoH) are not useful anymore for any applications (hereafter called EoL batteries). Recycling can be applied to EoL batteries to recover valuable battery materials and used them for new battery production (*i.e.*, closed-loop recycling). In theory, closed-loop recycling can reduce the materials-related environmental impacts of EV batteries. The reduction efficiency depends on the input battery chemistry and recycling technology applied. Various recycling technologies are developed and optimized to increase the recycling rates of materials as well as lower the cost of input chemicals and energy[17].

The above points lead to questions with regard to insights that have to be developed on battery demand and associated battery material flows, battery production and related environmental impacts, the grid storage potential of EV battery use, *etc.* In the next section, we discuss analytical methods that can give insights into these aspects, followed by sections that specify research gaps, research questions, and the structure of this thesis.

## 1.3 Analytical methods to assess challenges and opportunities

Various modeling tools and approaches exist that can help to analyze and understand the challenges and questions discussed in the former section. The research methods include mainly the dynamic material flow analysis and the prospective life cycle assessment. Executing the dynamic material flow analysis and the prospective life cycle assessment methods requires detailed insights into the battery chemistry, chemistry mix, amongst others, battery lifetime, and compositions of batteries, which can be

provided via battery technology modeling. Below we describe each method applied in this thesis.

**Dynamic material flow analysis.** Dynamic material flow analysis (MFA) is a method used to quantify past, current, and future stock and flows of materials used in our society[18,19]. The inflow or in-use stock data of a product, a product lifetime distribution, and product material compositions are essential information for the calculation of dynamic MFA, and they can be extrapolated based on relevant social-economic variables (GDP, population, *etc.*) or summarized based on the social questionnaire. Inflow- or stock-driven dynamic MFA has been used widely to assess the flows of various materials, such as metals[16], plastics[20], rare earth elements[21], *etc*. The applications of dynamic MFA have increased the knowledge basement of materials flows, including both the quantity and quality of materials[16]. The flows of critical battery materials, mainly metals, can be assessed by dynamic MFA[22], combined with scenario analysis of EV fleet and battery chemistry.

**Prospective life cycle assessment.** Life cycle assessment (LCA) is a tool to assess the current environmental impacts of a product along the life cycle, *i.e.*, from raw materials extraction, via production and use, to end-of-life treatment/recycling[23]. To determine the environmental impacts of emerging technologies, prospective LCA approaches have been proposed by researchers[24]. A key aspect for prospective LCA is how to model the future performance[23] of the foreground technology system (*e.g.*, how to extrapolate a life cycle inventory from pilot to commercial scale[25]) as well as the background system (*e.g.*, taking into account the energy transition[26]). A common way to implement prospective LCA is to combine dynamic emerging foreground technology scenarios[27] (such as battery chemistry change), long-term background scenarios from integrated assessment models[28] (IAMs, such as the energy mix scenarios from REMIND model), and other important changes that are not considered well in IAMs. Prospective LCA methodology can provide a future dynamic perspective in environmental impact assessment, although it faces comparability, data, and uncertainty challenges that should be solved in future research[24]. When performing a prospective LCA for batteries, the changes in battery technology next to other changes in the foreground and background technology systems should be fully considered.

**Battery technology modeling.** Based on EV type, size, range, and other factors, various lithium-ion battery chemistries have been developed, including lithium iron

phosphate battery (LFP), lithium nickel cobalt manganese battery (NCM), and lithium nickel cobalt aluminum battery (NCA). LFP, NCA, and NCM differ in cost, special energy (Wh/kg), and cycle life, as well as in material compositions and production processes. LFP features lower cost and longer cycle life than NCM and NCA, while NCM and NCA show higher special energy than LFP[29]. In the next decade, LFP, NCA, and NCM are expected to dominate the EV market[7]. In the long term, solid-state lithium-based batteries, such as lithium-air and lithium-sulfur batteries[7], or sodium-ion batteries could breakthrough and gain a foothold in the EV market.

Modeling the technical characteristics of different chemistries and the future battery chemistry mix is significant for assessing the challenges and opportunities of battery sustainability. The battery models can provide information on battery material compositions, which can be used as inputs to the dynamic material flow analysis and prospective life cycle assessment to assess the battery sustainability challenges. Also, the battery models can give battery capacity degradation, which is an important input to assessing the battery capacity available for grid storage that represents one key battery sustainability opportunity.

## 1.4 Research gaps

Although dynamic MFA and prospective LCA methods have been applied to analyse the future impact of EV batteries, these two methods have rarely been combined with battery technology modeling. As indicated above, only such a combination of models can give insight into future material requirements and emissions related to battery production for the global EV market. With this combination of models, we aim to overcome four key research gaps that are only partially researched in the existing literature. Please see the four research gaps in detail in the following sections.

**Ⅰ. Future battery material demand.** Future demand for raw materials for EV batteries is essential for assessing potential supply risks as well as social and environmental impacts, which in turn is essential strategic information for both industry and policy makers. Studies have quantified the future demand for EV battery materials for specific regions such as Europe[30], the United States[31,32], and China[22], or for specific individual battery materials[33-35]. Weil et al.[36] assess the global material demand for EV batteries and find that shortages for key materials, including lithium and cobalt, can be expected. However, their model does not investigate the influence

of battery chemistry developments (*e.g.,* improved NCM chemistries or novel Lithium-Sulphur (Li-S) and Lithium-Air batteries (Li-Air)) as well as alternative fleet and different recycling scenarios. There is hence a major need for considering different EV fleet and battery chemistry scenarios and quantifying the global demand for different battery materials.

**Ⅱ. Future cradle-to-gate GHG emissions of battery production per kWh battery capacity.** Although EVs have environmental advantages over ICEVs[37-39], the impacts of battery production are still rather uncertain[40-42]. Studies find diverging life cycle impacts of battery production[43-45]. This is due to the use of different data and assumptions of battery performance and compositions[46], geographical scope[47], battery production life cycle inventory (LCI) data[48,49], and environmental impact assessment methodologies[50]. All these factors can lead to questionable conclusions on the magnitude of environmental impacts of battery production. Moreover, changes in environmental impacts of battery production in the next decades are often not taken into account, due to the challenges in estimating futurized background LCI data and modeling future battery production processes. There is hence a need for summarizing the up-to-date battery production LCI data (for different battery chemistries) and building a prospective LCA model that incorporates both the battery production LCI data and futurized background LCI data systematically. The prospective LCA model can then be used to estimate the future life cycle environmental impacts of different battery chemistries.

**Ⅲ. Future life cycle GHG emissions of global battery production.** Environmental impacts of global battery production[51,52] are normally quantified using battery life cycle assessments and used volumes of batteries[40-42]. We discussed the future life cycle GHG emissions of battery production under II. But the total GHG emissions related to battery production depend on the EV fleet size and battery capacity per vehicle, which will differ between the main EV markets (*e.g.,* US, EU, Asia). Further, the distribution of battery production over regions may change due to regional battery production capacity, resource constraints, and other factors. Therefore, there is a need for developing future (regional) battery demand scenarios incorporating the development of EV fleet size and battery capacity per vehicle, and further quantifying the future GHG emissions of global EV battery production considering the future split of battery

production over production regions.

**IV. Future global battery capacity available for grid storage.** The utilization of EV batteries for grid storage could improve the flexibility of electricity supply, while reducing the capital costs and material-related emissions associated with additional storage and power-electronic infrastructure. However, the total grid storage capacity of EV batteries depends on business models, consumer behaviour (in driving and charging), battery degradation, and more factors[53,54]. Investigating the future grid storage capacity of EV batteries is essential to understand the role EV batteries could play in the renewable energy transition. Previous global-level studies, including those on vehicle-to-grid capacity[55-57] and retired battery capacity[57,58], while informative, rarely consider factors such as: non-linear, empirically-based battery degradation (they often neglect the impact of battery chemistry[59-61]); geographical and/or temporal temperature variance (which impacts battery degradation); and, driving intensity by vehicle type in different countries/regions (which constrains the battery capacity available during the day). These factors determine the technical grid storage capacity. Additionally, consumer participation in the vehicle-to-grid market and in the second-use market impacts the actual grid storage capacity[54], which is significant but rarely quantified. There is hence a need for quantifying the total grid storage capacity of EV batteries including both vehicle-to-grid capacity and second-use capacity, which considers factors of the battery capacity degradation and market participation rates.

## 1.5 Aims and Research questions

With the aim of closing the above-mentioned research gaps, this thesis integrates the method of dynamic MFA, prospective LCA, and battery technology modeling to an integrated model. The model is used to assess the environmental impacts and co-benefits of EV batteries, and to address the overall research question (RQ): **What are the future environmental challenges and opportunities for automotive lithium-ion batteries from a life cycle perspective?**

To deal with the overall RQ, in relation to the research challenges discussed in section 1.4 we formulate four key sub-RQs (see Fig. 1.1):

**RQ1: What is the future material demand for automotive lithium-ion batteries?**

**RQ2: What are future cradle-to-gate GHG emissions per kWh automotive**

**lithium-ion battery production?**

**RQ3: What are the future GHG emissions of global automotive lithium-ion battery production?**

**RQ4: What is the future grid storage capacity available from global automotive lithium-ion batteries?**

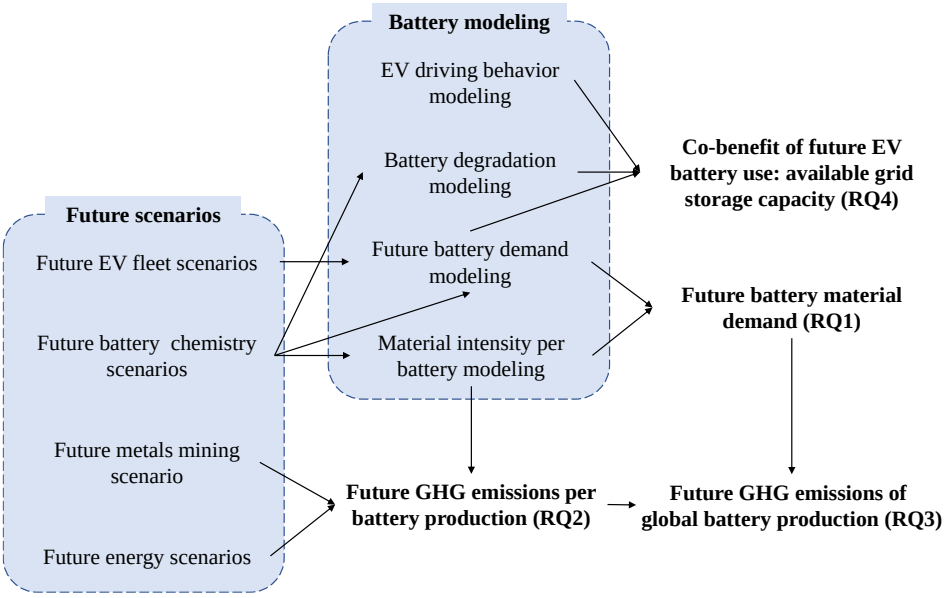


**Fig. 1.1: Overview of research methods and models for four research questions, including future scenarios and battery modeling.**

## 1.6 Thesis outline

In relation to the research questions above, this thesis consists of 6 chapters. Chapter 1 presents a general introduction to this thesis. Chapters 2 to 5 answer and discuss the RQs 1 to 4, respectively. Chapter 6 gives a general discussion of this research. In short, the next chapters discuss (see also Fig. 1.1):

Chapter 2 uses a dynamic MFA model that goes beyond previous analyses: including future EV fleet scenarios, future battery chemistry scenarios, and modelling material intensity per battery chemistry type. First, the future EV fleet scenarios cover information on EV technical parameters (range, fuel economy, and motor power) and

EV sales market share of small/mid-size/large BEVs/PHEVs. Second, the future battery chemistry scenarios include information on technical parameters of batteries (capacity in kWh and specific energy in Wh/kg) as well as future battery chemistry mixes. Last but not least, in the dynamic MFA model we incorporate battery material compositions that are modelled based on the technical parameters of both EV and battery. This chapter illuminates the future challenges related to strong demand growth of critical battery materials, such as sustainable supply of raw materials, social and environmental impact of materials production, *etc*. The methods and results of this chapter contribute to the analyses in following chapters 3-5.

Chapter 3 builds a prospective LCA model for battery production. The prospective LCA model incorporates future energy scenarios that indicate (regional) energy mixes and energy-related GHG emissions, in addition to the future metals mining scenarios, *i.e.*, technology changes for the supply of key battery metals. This chapter determines the (future) life cycle battery production GHG emission per kWh battery capacity for different battery chemistries, and gives a contribution analysis by battery components and materials.

Chapter 4 combines the dynamic MFA model in Chapter 2 and the prospective LCA model in Chapter 3 to assess the range of GHG emissions associated with global EV battery production under different scenarios. Sensitivity analysis with regard to key factors (such as closed-loop recycling) is further conducted.

Chapter 5 combines the dynamic MFA model in Chapter 2 (assess future battery stock and EoL batteries), the EV driving behavior model (model EV driving distance and charging behavior), and the battery degradation model (estimate battery capacity over time). This chapter evaluates the future available grid storage capacity - including both vehicle-to-grid capacity and second-use capacity - from EV battery use. Further, this chapter compares "the total available grid storage capacity from EV batteries" with "the demand for short-term storage capacity in an electricity system mainly using renewables".

Chapter 6 answers the RQs, discuss limitations of this work, give recommendations for future research, and provide policy implications of this research.

# 2 Future material demand for automotive lithium-based batteries[a]


## Abstract

The world is shifting to electric vehicles to mitigate climate change. Here, we quantify the future demand for key battery materials, considering potential EV fleet and battery chemistry developments as well as second-use and recycling of EV batteries. We find that in a lithium nickel cobalt manganese oxide dominated battery scenario, demand is estimated to increase by factors of 18-20 for Lithium, 17-19 for Cobalt, 28-31 for Nickel, and 15-20 for most other materials from 2020 to 2050, requiring a drastic expansion of Lithium, Cobalt, and Nickel supply chains and likely additional resource discovery. However, uncertainties are large. Key factors are the development of the electric vehicles fleet and battery capacity requirements per vehicle. If other battery chemistries were used at a large scale, *e.g.*, lithium iron phosphate or novel Lithium-Sulphur or Lithium-Air batteries, the demand for Cobalt and Nickel would be substantially smaller. Closed-loop recycling plays a minor, but increasingly important role in reducing primary material demand until 2050, however, advances in recycling are necessary to economically recover battery-grade materials from end-of-life batteries. Second-use of electric vehicle batteries further delays recycling potentials.


## 2.1 Introduction

Electric vehicles (EVs) generally have a reduced climate impact compared to internal combustion engine vehicles[52]. Together with technological progress and governmental subsidies, this advantage led to a massive increase in the demand for EVs[62]. The global fleet of light-duty EVs grew from a few thousand just a decade ago to 7.5 million vehicles in 2019[63]. Yet, the global average market penetration of EVs is still just around 1.5% in 2019 and future growth is expected to dwarf past growth in absolute numbers[63].

Lithium-ion batteries (LIBs) are currently the dominant technology for EVs[62]. Typical automotive LIBs contain lithium (Li), cobalt (Co), and nickel (Ni) in the cathode, graphite

[a] Published as: Xu, C., Dai, Q., Gaines, L., Hu, M., Tukker, A. & Steubing, B. Future material demand for automotive lithium-based batteries. *Communications materials* **1**, 1-10 (2020).

in the anode, as well as aluminum and copper in other cell and pack components. Commonly used LIB cathode chemistries are lithium nickel cobalt manganese oxide (NCM), lithium nickel cobalt aluminum oxide (NCA), or lithium iron phosphate (LFP), although battery technology is currently evolving fast and new and improved chemistries can be expected in the future[62,64].

Due to the fast growth of the EV market, concerns over the sustainable supply of battery materials have been voiced. These include supply risks due to high geopolitical concentrations of cobalt[65,66] and social and environmental impacts associated with mining[67,68], as well as the availability of cobalt and lithium reserves[36] and the required rapid upscaling of supply chains to meet expected demand[65].

Understanding the magnitude of future demand for EV battery raw materials is essential to guide strategic decisions in policy and industry and to assess potential supply risks as well as social and environmental impacts. Several studies have quantified the future demand for EV battery materials for specific world regions such as Europe[30], the United States[31,32], and China[22], or for specific battery materials only[33-35]. Weil et al.[36] assess the material demand for EV batteries at the global level and find that shortages for key materials, such as Li and Co, can be expected. However, their model does not investigate the influence of battery chemistry developments (*e.g.*, improved NCM chemistries or novel Lithium-Sulphur (Li-S) and Lithium-Air batteries (Li-Air)) as well as alternative fleet and different recycling scenarios.

Here, we go beyond previous studies by developing comprehensive global scenarios for the development of the EV fleet, battery technology (including potentially game-changing chemistries such as Li-S and Li-Air) as well as recycling and second-use of EV batteries. We assess the global material demand for light duty EV batteries for Li, Ni, and Co, as well as (for model see Supplementary Fig. 2.1) for manganese (Mn), aluminum (Al), copper (Cu), graphite and silicon (Si). We also relate material demands to current production capacities and known reserves and discuss key factors for reducing material requirements. The results presented are intended to inform the ongoing discussion on the transition to electric vehicles by providing a better understanding of future battery material demand and the key factors driving it.

## 2.2 Methods

**Model overview.** We develop a dynamic material flow analysis (MFA) model, which is

a frequently used approach to analyze material stocks and flows[69]. Our stock-driven MFA model estimates the future material demand for EV batteries as well as EoL materials available for recycling. It consists of an EV layer, a battery layer, and a material layer, and considers key technical and socio-economic parameters in three layers (Supplementary Fig. 2.1). The EV layer models the future EV stock (fleet) development until 2050 as well as required battery capacity. The EV stock then determines the battery stock, which in turn determines the battery inflows and, considering their lifespan distributions (Supplementary Fig. 2.2), the outflow of EoL batteries. The battery layer considers future battery chemistry developments and market shares. The material layer models material compositions of battery chemistries using the BatPaC model[70]. The fate of EoL batteries is modelled considering three recycling scenarios and a second-use scenario and these determine the material availability for closed-loop recycling. The model layers and parameters are described in the following.

**EV fleet scenarios and required battery capacity.** Projections for the development of the EV fleet vary, but most studies project a substantial penetration of EVs in the light duty vehicle (LDV) market in the future (Supplementary Fig. 2.3). We use two EV fleet development scenarios of the IEA until 2030: the stated policies (STEP) scenario and the sustainable development (SD) scenario[63] (and estimate the annual EV stock based on the equivalent IEA 2019 scenarios[71], see Supplementary Fig. 2.4). We then extrapolate the EV fleet penetration until 2050 using a logistic model (see Supplementary Fig. 2.5) based on a target penetration of EVs in the LDV market in 2050 of 25% in the STEP scenario and 50% in the SD scenario (which is in line with other EV forecasts, as shown in Supplementary Fig. 2.3). To estimate future EV fleet until 2050, we further assume a linear growth for global LDV stock from 503 million vehicles in 2019 to 3.9 billion vehicles in 2050, which is in line with projection by Fuel Freedom Foundation[72]. Global predictions of the future development of BEV and PHEV shares were not available. To estimate future shares of BEVs and PHEVs in the EV stock, we assumed that the global share of BEVs increases in the same way as the US BEV share projected by the US Energy Information Administration[73], but starting from the 2030 levels of the STEP and SD scenarios (*i.e.*, from 66% in 2030 to 71% in 2050 in STEP scenario and 70% in 2030 to 75% in 2050 in SD scenario, see Supplementary Fig. 2.6).

We classify EVs models into 3 market segments (small, mid-size, and large cars for both BEVs and PHEVs) based on vehicle size classes used in the Fuel Economy Guide by EPA

(see Supplementary Table 2.1)[74], and collect global sales of each EV model from the Marklines database[75] . We use the distribution of cumulative sales until 2019 to represent EV sales market shares among small, mid-size, and large segments (Supplementary Fig. 2.7 and Supplementary Fig. 2.8). As a result, we obtained 19%, 48%, and 34% for small, mid-size, and large cars for BEVs, and 23%, 45% and 32% for PHEVs. We assume EV sales market share remains constant, however, a sensitivity analysis is conducted to obtain the upper and lower bounds for material requirements if all vehicles were large BEV or small PHEV (see sensitivity analysis).

We collect range, fuel economy, and motor power of each EV model from Advanced Fuels Data Center of US DOE[76], and calculate sales-weighted average range, fuel economy, and motor power for 3 market segments for both BEVs and PHEVs[77] (Supplementary Table 2.2 and Supplementary Table 2.3). By assuming 85% available battery capacity for driving EVs based on BatPaC model[70], we obtain 33 kWh, 66 kWh, and 100 kWh for small, mid-size, and large BEVs (see Supplementary Table 2.3 for PHEV).

Passenger car lifespans have been found to vary from 9 to 23 years among countries with an average lifespan of around 15 years[78]. EV lifespan depends on consumer behavior, technical lifespan (see next section), and other factors. Here we use a Weibull distribution[79] to model the EV lifespan assuming the minimum, maximum, and most likely lifespans of EVs to be 1, 20, and 15 years respectively (see Supplementary Fig. 2.2). We do not consider battery remanufacture and reuse from one EV to another EV due to performance degradation, technical compatibility and consumer acceptance.

**Battery chemistry scenarios and market shares.** Although various EV battery chemistries have been developed for EVs to decrease cost and improve performance, current major battery roadmaps in US[80], EU[81], Germany[82], and China[83] focus on cathode material development considering high-energy NCM (transition to low cobalt and high nickel content) and NCA based chemistries to be the likely next generation of LIBs for EVs in next decade, as well as anode material development considering adding Si to graphite anode. This is also reflected in commercial activities by battery producers (*e.g.*, LG Chem or CATL)[84] and market share projections until 2030 by Avicenne Energy85, which we use in this study. We assume that NCM batteries continue to decrease cobalt content and increase nickel content after 2030 and compile the NCX scenario (where X represents either Al or Mn) until 2050 (including 8 chemistries, see Supplementary

Table 2.4. In the NCX scenario, we assume that NCM955 (90% nickel, 5% cobalt, 5% manganese) are introduced in 203086, and gradually replace other previous chemistries proportionally to reach a market share of one third by 2050 (*i.e.*, market shares of NCM111, NCM523, NCM622, NCM622-Graphite (Si), NCM811-Graphite (Si), NCA, and LFP batteries are assumed to decrease proportionally after 2030, see Fig. 2.2b).

Future battery chemistry developments after 2030 are uncertain, but conceivable battery chemistries, in addition to NCM and NCA batteries, include already existing LFP batteries[87,88], as well high-capacity Li-metal solid-state batteries, such as Li-S and Li-Air[81,89]. Therefore, we include two additional what-if scenarios next to the NCX scenario: an LFP scenario and a Li-S/Air scenario. In the LFP scenario, the market share of LFP chemistry is assumed to increase linearly from around 30% in 2019 to 60% by 2030 and remain at this level until 2050 (*i.e.*, other batteries lost market share proportionally compared to the NCX scenario, see Fig. 2.2b). In the Li-S/Li-Air scenario, we assume Li-S and Li-Air batteries to be commercially available in 2030 based on commercial plans of Li-S by OXIS Energy[90] and Li-Air by Samsung Electronics[91] and then they obtain linearly increasing market share to 30% each (totally 60%) by 2040, and maintain this share until 2050 (NCA and NCM batteries supply the rest of the market by historical proportions, see Fig. 2.2b).

The real-world lifespan of batteries is influenced by additional factors not modelled here, such as ambient temperature, depth, rates of charge and discharge, and driving cycles[92]. We use the technical lifespan of batteries. Before 2020, we assume that batteries are likely to last 8 years (based on the battery warranty of EV manufactures)[93], which is shorter than EV lifespan (Supplementary Table 2.5 and Supplementary Table 2.6). We assume a 50% battery replacement rate for EVs (*i.e.*, one EV requires 1.5 battery packs on average). Battery research agendas in the US[80], EU[81], and China[83] include targets to increase the lifespan of batteries, which is why we assume that after 2020 batteries will have the same lifespan distributions as EVs and no replacement of batteries is required. Note that we assume higher lifespans for LFP batteries (20 years on average) (Supplementary Fig. 2.2), which leads to a higher second-use potential than for the other battery types.

**Battery material compositions.** The battery material compositions are calculated by

using the BatPaC model version 3.1[70] as a function of the 2 EV types (BEVs or PHEVs), the 3 EV market segments (small, mid-size, and large cars), and the 8 battery chemistries (LFP, NCA, NCM11, NCM523, NCM622, NCM622-Graphite (Si), NCM811-Graphite (Si), NCM955-Graphite (Si)), which yields 48 unique battery chemistries. The input parameters include the EV range, fuel economy, and motor power, which determine the required capacity of each EV type and market segment (Supplementary Table 2.2 and Supplementary Table 2.3), and battery chemistry and other parameters (like the design of battery modules and cell components) for which we use the default values in the BatPaC model. To calculate the material compositions of battery chemistries that do not exist in BatPaC (*i.e.*, NCM523, NCM622-Graphite (Si), NCM811-Graphite (Si), NCM955-Graphite (Si)), we use the closest matching battery chemistry in BatPaC as a basis and then adapt technical parameters, such as Ni, Co, Mn contents in the positive active material and Si and graphite contents in the negative active material, by stoichiometry, as well as active material capacities and open circuit voltage (see Supplementary Table 2.7 and Supplementary Note 2.1). For Li-S and Li-Air chemistries, we performed a literature review on the specific energy and material compositions of Li-S and Li-Air cells (Supplementary Table 2.8 and Supplementary Table 2.9), and then scale these linearly to meet required battery capacities for each EV type and market segment. The pack components of Li-S and Li-Air are assumed to be based on the pack configurations of NCA chemistry (*i.e.*, the same weight ratio between cell components and pack components). Supplementary Table 2.10 shows the material compositions used in this paper.

**Recycling scenarios.** Recycling of EoL batteries provides a secondary supply of materials. Here we assume 100% collection rates and explore the effects of recycling efficiencies of three recycling scenarios (see Supplementary Table 2.11) on primary material demand, including recovered quantities and some discussion of recycled material qualities. The primary material demand when there is no collection and recycling of EoL batteries is captured by the "without recycling" scenario (Fig. 2.4). Currently commercialized recycling technologies include pyrometallurgical (pyro) and hydrometallurgical (hydro) recycling. Direct recycling is under development for cathode-to-cathode recycling. For NCX and LFP batteries, pyro, hydro, and direct recycling are assumed in the three recycling scenarios, respectively, while mechanical recycling is assumed for Li-S and Li-Air batteries in all three scenarios. Recycling

technologies differ in recycled materials, chemical forms, recovery efficiencies, and economic prospects[17,94,95] (Fig. 2.5).

The pyrometallurgical recycling scenario we consider is in fact a hybrid pyro and hydro process. After feeding disassembled battery modules and/or cells to the smelter, graphite is burnt off, aluminum and lithium end up in the slag, and nickel, cobalt, and copper end up in a matte. After leaching of the matte, copper ion is recovered as copper metal through electrowinning, while the nickel and cobalt ions are recovered as battery-grade nickel and cobalt compounds through solvent extraction or precipitation. The lithium in the slag can be refined to produce battery-grade lithium compounds, but it is only economical when lithium price is high and recycling at scale. Technically, aluminum in the slag can also be recovered, but it is not economical and not considered by pyro recycling companies (the slag may be used, *e.g.*, as aggregate in construction material).

The hydrometallurgical recycling scenario starts with shredding disassembled modules and/or cells. The shred then goes through a series of physical separation steps to sort the materials into cathode powder, anode powder, and mixed aluminum and copper scraps. Depending on the scrap metal prices, the mixed aluminum and copper scraps may be further sorted into aluminum scraps and copper scraps. The copper scraps can be incorporated back into the battery supply chain with minimal processing (*i.e.*, remelting). The closed-loop recycling of aluminum is more challenging as the recovered aluminum scraps are a mixture of different aluminum alloys (*e.g.*, from current collector and casing) and Al is, therefore, typically downcycled. Closed-loop recycling of aluminum would require separating the aluminum alloy before or during the recycling process, which may or may not be economical[96]. The cathode powder is subsequently leached with acid, where nickel, cobalt, and manganese leach out as ions, and recovered as battery-grade compounds after solvent extraction and precipitation. Lithium ends up in solid waste which can also be used as construction materials. Similar to pyro recycling, lithium in the solid waste can be recovered as battery-grade compounds, but the economic viability depends on the lithium price. The anode powder recovered through hydro, which can be a blend of graphite and silicon, is not battery-grade. Although they can be refined to battery-grade, at present the economic viability is unclear.

The direct recycling scenario is the same as hydro except for cathode powder recycling.

In the direct process, the cathode powder is recovered and then regenerated by reacting with a lithium source (re-lithiation and upgrading). Lithium, nickel, cobalt, and manganese are therefore recovered as one battery-grade compound. Since lithium refining is not needed here as with pyro and hydro, lithium recovery in direct process is economical at least from a lab-scale perspective.

The material recovery efficiencies for pyro, hydro, and direct are taken from the EverBatt[94] model developed at Argonne National Laboratory (Supplementary Table 2.11). As for mechanical recycling of Li-S and Li-Air batteries, we assume that only metallic lithium is recovered from the process. The material recovery efficiency of metallic lithium is assumed to be 90%, and the recovery is considered economical due to the relatively simple process and high value of recovered lithium metal.

**Second-use/use scenarios.** EoL EV batteries may experience a second-use for less demanding applications (non-automotive), such as stationary energy storage, as they often have remaining capacities of around 70-80% of their original capacity[97,98]. Technical barriers exist (*e.g.*, the performance of repurposed batteries) and economic uncertainty (the cost of repurposing including disassembly, testing, and repackaging) that depend on the battery chemistry, state-of-health, and the intended second-use application[98-100]. Here we distinguish the second-use rates of LFP and other chemistries due to the long cycle life[101] and the reduced chance of cascading failure of LFP[102]. LFP batteries are assumed to have a 100% second-use rate. For the rest of the battery chemistries, we assume a 50% second-use rate before 2020, rising to 75% during 2020-2050 because of improved technical lifespan of EV batteries (Supplementary Table 2.12). The second-use applications vary from home use to electricity system integration, resulting in the second-use lifespan varying from 6 to 30 years[103]. We assume a typical 10-year second-use lifespan[98] to explore the effects of second-use on the availability of materials for recycling. Note here the second-use assumes 100% reuse of battery modules, while pack components enter recycling directly.

**Sensitivity analysis.** The effect of important factors such as EV fleet size and battery chemistry are investigated in dedicated scenarios. In addition, we perform sensitivity analysis for a) battery lifespan, b) required battery capacity per vehicle, c) the market penetration of Co- and Ni-free battery chemistries, and d) the future specific energies of Li-S and Li-Air chemistries (for which conservative numbers were assumed).

(a) Battery lifespan has an important effect on the number of batteries required for EVs. We perform a sensitivity analysis of the effect of lower battery lifespans on battery material demand by assuming that also after 2020 one EV needs 1.5 batteries on average (results in Supplementary Fig. 2.9).

(b) Future market shares of BEVs and PHEVs and EV battery capacity are also key for determining the quantity of required materials. While battery capacity is driven by many factors like EV range, fuel economy, and powertrain configurations, we perform a sensitivity analysis on two extreme situations, 100% BEV with 110 kWh capacity (large SUVs such as Tesla Model S Long Range Plus[104], see Supplementary Table 2.13 for material compositions) and 100% PHEV with 10 kWh capacity, to explore the bounds of future material demand (see Supplementary Table 2.14 for material compositions, and annual results in Supplementary Fig. 2.10).

(c) Similarly, we also explore the effects of 100% market share of LFP in the LFP scenario and 100% market share of Li-S and Li-Air in the Li-S/Air scenario (see Supplementary Fig. 2.11 and associated material requirements in Supplementary Fig. 2.12 and Supplementary Fig. 2.13 respectively).

(d) The improvement of material performance of battery chemistry, especially specific energy (stored energy per weight), may reduce material demand dramatically. Here we chose Li-S and Li-Air chemistries in the Li-S/Air scenario to perform a sensitivity analysis of the potential specific energy improvement from 400 Wh/kg to 600 Wh/kg for Li-S and from 500 Wh/kg to 1000 Wh/kg for Li-Air (values based on review of industrial and lab-scale achievements, see Supplementary Table 2.10 for material compositions and associated material requirements in Supplementary Fig. 2.14).

## 2.3 Results

### 2.3.1 EV fleet growth

Fig. 2.1 shows the projected EV fleet development. We base our scenarios on two scenarios of the International Energy Agency (IEA) until 2030: the Stated Policies (STEP) scenario, which incorporates existing government policies and the Sustainable Development (SD) scenario, which is compatible with the climate goals of the Paris agreement and includes also the target of reaching a 30% global sales share for EVs

by 2030[63]. According to these scenarios, EVs will make up 8-14% of the total light duty vehicle fleet by 2030, of which 89-166 million are battery electric vehicles (BEVs) and 46-71 million are plug-in hybrid electric vehicles (PHEVs)[71]. We extend these scenarios until 2050 assuming logistic growth curves where the global fleet penetration of EVs in 2050 will be 25% in the STEP scenario and 50% in the SD scenario. This is in line with other projections, see Supplementary Fig. 2.3. In the STEP scenario, the EV stock will increase by a factor of 72 from 2020-2050 to nearly 1 billion vehicles and annual EV sales will rise to 109 million vehicles (Supplementary Fig. 2.15). In the SD scenario, the EV stock will increase by a factor of 102 from 2020-2050 to 2 billion vehicles and annual EV sales will rise to 211 million vehicles (Supplementary Fig. 2.15).

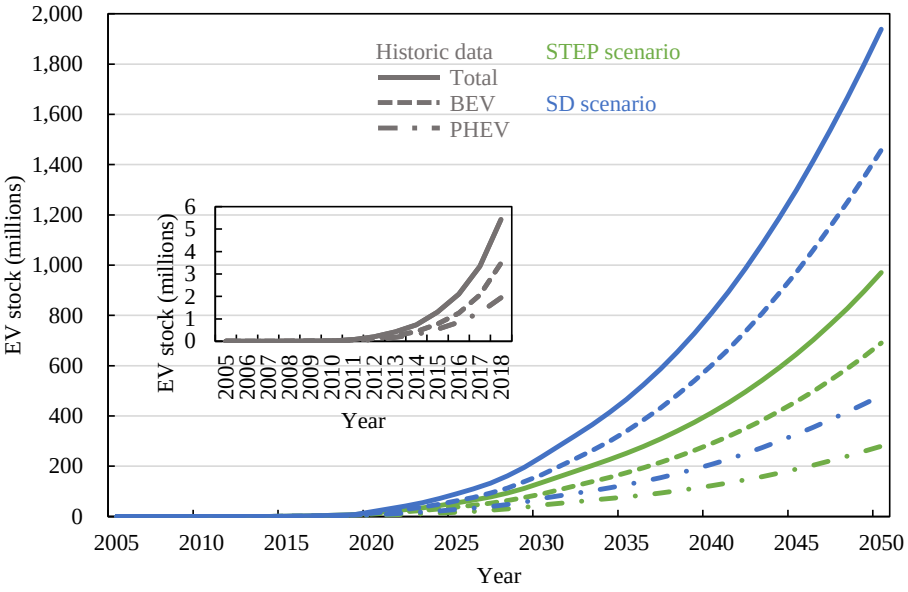


**Fig. 2.1: Global EV stock development projected until 2050.** BEV = battery electric vehicle. PHEV = plug-in hybrid electric vehicle. STEP scenario = the Stated Policies scenario. SD scenario = Sustainable Development scenario.

### 2.3.2 Battery capacity and market shares

Fig. 2.2 shows that in the STEP scenario approximately 6 TWh of battery capacity will be required annually by 2050 (and 12 TWh in the SD scenario, see Supplementary Fig. 2.16). The required future battery capacity depends on the development of the EV fleet

as well as the required battery capacity per vehicle (we assume 66 kWh and 12 kWh as average capacity for BEVs and PHEVs, respectively, see Supplementary Table 2.2 and Supplementary Table 2.3 for details) and the battery lifespans (see Supplementary Table 2.6 and Supplementary Fig. 2.2). The material requirements depend on the choice of battery chemistries used. Three battery chemistry scenarios are considered (see Fig. 2.2 and detailed description in methods).

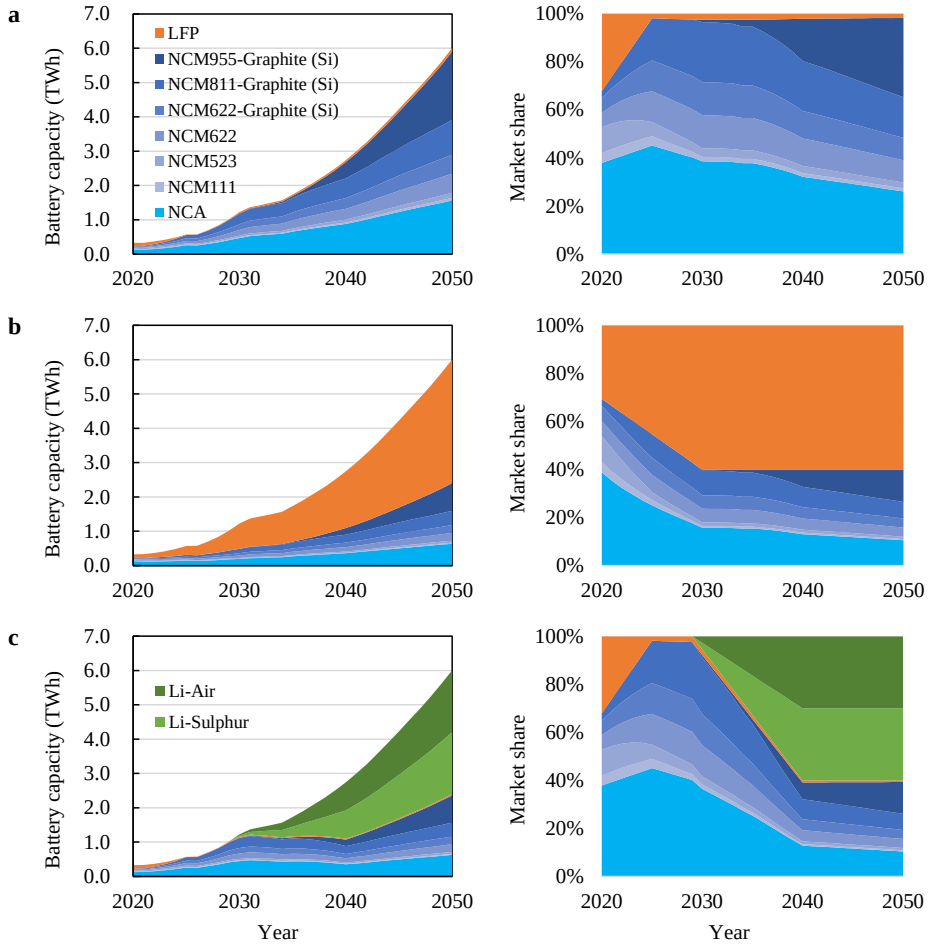


**Fig. 2.2: Battery market shares and yearly EV battery sales until 2050 for the fleet development of the STEP scenario. a** NCX scenario. **b** LFP scenario. **c** Li-S/Air scenario. See Supplementary Fig. 2.16 for the Sustainable Development scenario. See Supplementary Fig. 2.17 for battery sales in units.

The most likely NCX scenario follows the current trend of widespread use of lithium nickel cobalt aluminum (NCA) and lithium nickel cobalt manganese (NCM) batteries (henceforth called the NCX scenario with X representing either Al or Mn)[85]. Battery producers are seeking to replace costly cobalt with nickel, which has led to an evolution from NCM111 to NCM523, NCM622, and NCM811 batteries (numbers denote ratios of nickel, cobalt, and manganese)[85] and NCM955 (90% nickel, 5% cobalt, 5% manganese) are expected to be available by 2030[86]. Specific energies at the pack level assumed here range from 160 Wh/kg for NCM111 to 202 Wh/kg for NCM955-Graphite (Si) battery for typical mid-size BEVs (Supplementary Table 2.15), and lifespans are assumed to increase to an average of 15 years to match vehicle lifespans (Supplementary Fig. 2.2)[105].

The LFP scenario considers the possibility that LFP ($LiFePO_4$) batteries will be increasingly used for EVs in the future. The principle drawback of LFPs is their lower specific energy compared to NCA and NCM chemistries, which negatively impacts fuel economy and range of EVs. Advantages of LFPs are lower production costs due to the abundance of precursor materials, safety due to better thermal stability, and longer cycle life[101]. While LFP batteries have seen their main application in commercial vehicles, such as buses, there are prospects of a more widespread use of LFPs in light-duty EVs (*e.g.*, Tesla has recently announced to equip the Chinese version of its Model 3 with LFP batteries[87]). In this scenario, we assume that LFP batteries (with a specific energy of 129 Wh/kg at pack level for typical mid-size BEVs and on average lifespan of 20 years[106]) will have a market share of 60% from 2030-2050, while the rest of the market follows the trends in the NCX scenario.

In the Li-S/Air scenario, we consider the possibility of breakthroughs in Li-metal solid-state battery chemistries, specifically, Li-S and Li-Air batteries, which are seen as potential successors of LIBs[89,107]. Although Li-S and Li-Air batteries are still in early development and considerable challenges remain to be solved before commercialization, *e.g.*, low cycle life and safety issues[62,64], Li-S batteries could reach 2 times and Li-Air batteries up to 3 times the specific energy of current LIBs, which would likely lead to cost reductions and improved EV ranges[89]. Although it is highly uncertain if and when such batteries could reach market readiness, we assume that Li-S and Li-Air batteries (with specific energies of 308 and 383 Wh/kg, respectively, at pack level for typical mid-size BEVs and lifespans equal to NCM batteries) enter the market in

2030[81] and reach a market share of 60% by 2040, while the rest of the market follows the trends in the NCX scenario.

### 2.3.3 Battery material demand

Fig. 2.3a shows the global demand for Li, Co, and Ni for EV batteries (Mn, Al, Cu, graphite, and Si are shown in Supplementary Fig. 2.18a). It can be observed that higher EV deployments in the SD scenario lead to 1.7-2 times higher annual material demand than in the STEP scenario. The demand for Li is only slightly influenced by the battery chemistry scenario (although the Li-S/Air scenario requires slightly more Li due to the Li-metal anodes in Li-S and Li-Air batteries). The demand for Ni and Co is strongly influenced by the battery chemistry scenario and substantially smaller in the LFP and Li-S/Air scenarios due to the lower market shares of NCX batteries. From 2020 to 2050 in the more conservative STEP scenario, Li demand would rise by a factor of 17-21 (from 0.036 Mt to 0.62-0.77 Mt), Co by a factor of 7-17 (from 0.035 Mt to 0.25-0.62 Mt), and Ni demand by a factor of 11-28 (from 0.13 Mt to 1.5-3.7 Mt) (Supplementary Fig. 2.19, Supplementary Fig. 2.20, and Supplementary Fig. 2.21). Note that the demand increase for Co is smaller than for Ni due to the assumed partial replacement of Co by Ni in future NCM batteries. Mn and Si follow the same trend as Ni and Co in the three battery scenarios as they are also not used in LFP, Li-S, and Li-Air batteries. The demand for Al, Cu, and graphite in the LFP scenario is slightly higher than in the NCX scenario due to specific energy differences, and lower in the Li-S/ Air scenario, since Li-S and Li-Air batteries use less Al and Cu on a per kWh basis and typically do not contain graphite.

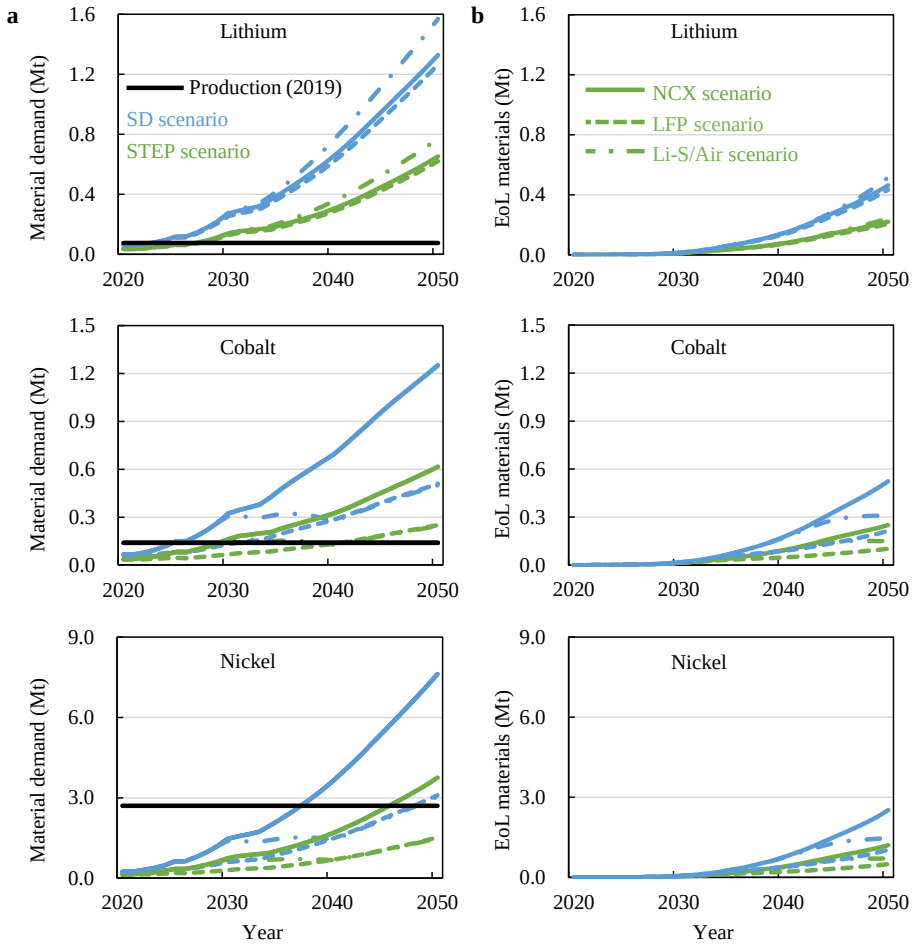


**Fig. 2.3: Battery material flows from 2020 to 2050 for lithium, nickel, and cobalt in the NCX, LFP and Li-S/Air battery scenarios. a** Primary material demand. **b** materials in end-of-life batteries. STEP scenario = the Stated Policies scenario. SD scenario = Sustainable Development scenario. See Supplementary Fig. 2.18 for other materials. Mt = million tons.

Fig. 2.4 shows the cumulative demand from 2020-2050. It ranges from 7.3-18.3 Mt for Li, 3.5-16.8 Mt for Co, and 18.1-88.9 Mt for Ni across fleet and battery chemistry scenarios (numbers for all materials are reported in Supplementary Table 2.16). The cumulative demand is twice as high in the SD scenario, and 2-2.5 times higher for Ni and Co in the NCX compared to the LFP and Li-S/Air scenarios. Consequently, there is a factor of 4-5 between the cumulative Ni and Co demands in the SD-NCX and the

STEP-LFP or STEP-Li-S/Air scenarios.

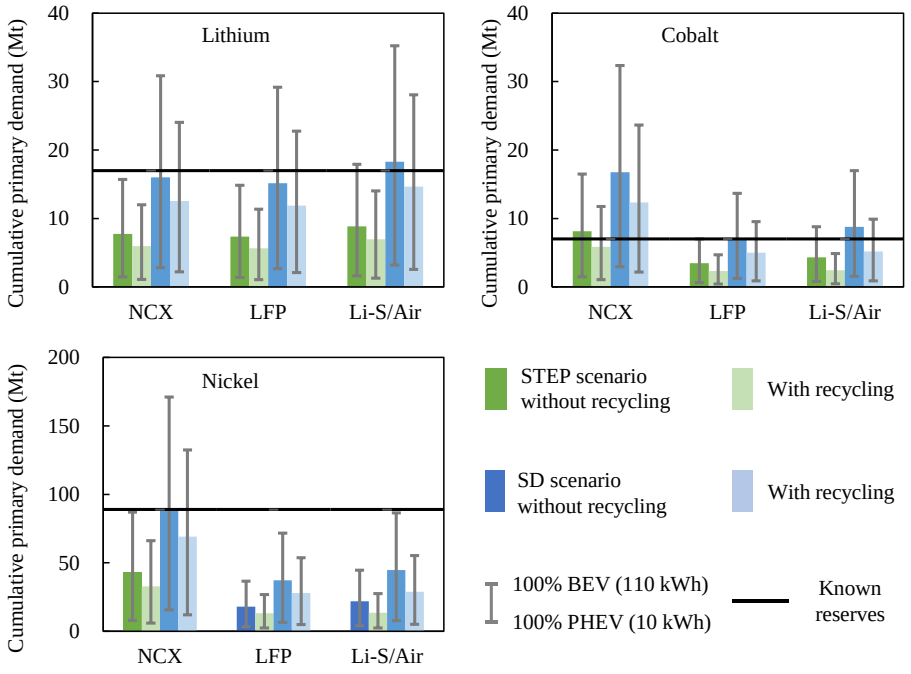


**Fig. 2.4: Cumulative primary material demand in 2020-2050 without recycling and with hydrometallurgical recycling.** STEP scenario = the Stated Policies scenario. SD scenario = Sustainable Development scenario. Grey error bars represent a sensitivity analysis for battery capacity considering two extreme cases (if all EVs were PHEVs with small 10 kWh batteries or if all EVs were large SUVs with 110 kWh batteries, *e.g.*, Tesla's Model S Long Range Plus[104], see annual results in Supplementary Fig. 2.10). The black line represents known reserves[108]. See Supplementary Fig. 2.22 for other materials.

### 2.3.4 Recycling potentials

Fig. 2.3b shows the materials contained in end-of-life (EoL) batteries over time (0.21-0.52 Mt of Li, 0.10-0.52Mt of Co, and 0.49-2.52Mt of Ni in 9-27 Mt EoL batteries, see Supplementary Fig. 2.23 for EoL battery weight, and Supplementary Fig. 2.24 and Supplementary Fig. 2.25 for other materials in EoL batteries). The recovery of these materials could help to reduce primary material production[33,109]. Current commercial recycling technologies for EV batteries include pyrometallurgical and hydrometallurgical processing[110]. Pyrometallurgical recycling involves smelting entire batteries or, after pretreatment, battery components. Hydrometallurgical processing

involves acid leaching and subsequent recovery of battery materials, *e.g.*, through solvent extraction and precipitation. In closed-loop recycling, pyrometallurgical processing is followed by hydrometallurgical processing to convert the alloy into metal salts, as illustrated in Fig. 2.5. Direct recycling aims at recovering cathode materials while maintaining their chemical structures, which could be economically and environmentally advantageous[49], however, it is currently still in early development stages[17]. In order to quantify recycling potentials, we consider three potential recycling scenarios: pyrometallurgical, hydrometallurgical, and direct recycling for NCX and LFP batteries as well as mechanical recycling for Li-S and Li-Air batteries. They differ in recovered materials and associated chemical forms (see methods and summary in Fig. 2.5).

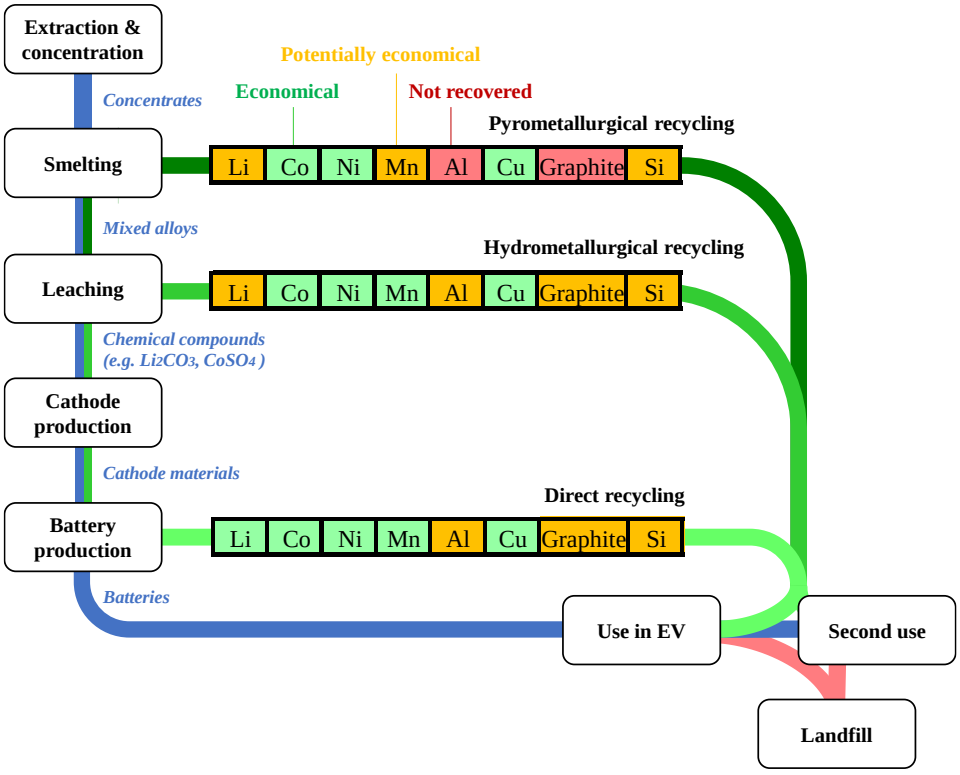


**Fig. 2.5: Conceptual schematic showing how the three considered recycling scenarios close battery material loops and which materials are recovered.** In reality not all materials go through all processing steps. For example, pyrometallurgical recycling (smelting) still requires hydrometallurgical

processing (leaching) before cathode materials can be produced, while direct recycling is designed to recover cathode materials directly. In pyro- and hydrometallurgical recycling the recovery of Li may not be economical and in pyrometallurgical recycling graphite is incinerated and Al not recovered from the slag (see also methods).

We also consider the potential second-use of EoL EV batteries. The exact second-use application, the battery state-of-health, battery chemistry, and other factors determine, if and for how long second-use is possible. For the sake of simplicity and to illustrate the effect of second-use, we assume that 50% of NCX, Li-S and Li-Air batteries before 2020 (increasing to 75% after 2020), and 100% of LFP batteries, due to their higher cycle life, experience a 10-year second-use in stationary energy storage, which is likely to be economically and environmentally beneficial[111], before finally entering recycling (Supplementary Table 2.12)

Fig. 2.4 shows the cumulative battery material demand from 2020-2050 for both fleet scenarios without recycling (representing the maximum primary material demand), and with hydrometallurgical recycling of NCX and LFP batteries and mechanical recycling of Li-S and Li-Air batteries without second-use (representing the minimum primary material demand) (Supplementary Fig. 2.26 shows the development over time for all materials). Considering additional material losses, *e.g.*, during collection and recycling, or material recovery delays due to second-use, would yield figures in between these bounds. This shows that battery recycling has, at best, the potential to reduce 20-23% of the cumulative material demand for Li until 2050 (8% for Li metal), 26-44% for Co, and 22-38% for Ni (see Supplementary Table 2.17 for other materials). The most important reason for this is the fast growth of the EV market and the time lag between the need for materials and the availability of EoL material. It should be noted that in a steady-state system, *i.e.*, once the battery stock of a saturated EV market has been built up, secondary material shares could, theoretically, be as high as recycling efficiencies, *i.e.*, above 90%. Supplementary Table 2.18 shows the increasing potential of recycling to mitigate primary material demand over time.

Fig. 2.6 shows the temporal evolution of the closed-loop recycling potential (CLRP), *i.e.*, the percentage of battery material demand that can be met with secondary material from battery recycling, for the next three decades. While the CLRP is small for the current decade (below 10%) it may reach as much as 20-71% during 2040-2050. The CLRP for Co and Ni are higher in the LFP and Li-S/Air scenarios, since LFP, Li-S, and Li-

Air battery chemistries do not require these materials and the total quantity of required materials for NCX batteries is growing much slower or even stagnating for some time (see Fig. 2.3). Note that CLRP of Li and Ni does not exceed 31% in the NCX and LFP scenario due to the continued growth of NCX chemistries, while it surpasses 50% in the Li-S/Air scenario (71% for Co) in 2040-2050 due to the higher stock of NCX batteries built up until 2030 when Li-S/Air chemistries are introduced (see Fig. 2.2). In the Li-S/Air scenario, lithium compounds (*e.g.*, $Li_2CO_3$ or LiOH) used for cathode production of LIBs need to be distinguished from lithium metal used for Li-S and Li-Air battery anodes (see demand for each in Supplementary Fig. 2.14), since existing recycling technologies recover lithium as compounds, and further processing of these compounds would be necessary to produce lithium metal. Although this is technically feasible, it is unlikely to be cost-competitive with primary lithium metal production from brine, which does not require the intermediate compounds production step and may work with lower-purity feedstock[112]. In the Li-S/Air scenario, the CLRP of lithium compounds surpasses 50% from 2040-2050. On the other hand, the CLRP for Li metal barely reaches 10% during 2040-2050 due to the fast growth of the Li-S and Li-Air batteries and the small historical stock (see also Supplementary Table 2.18).

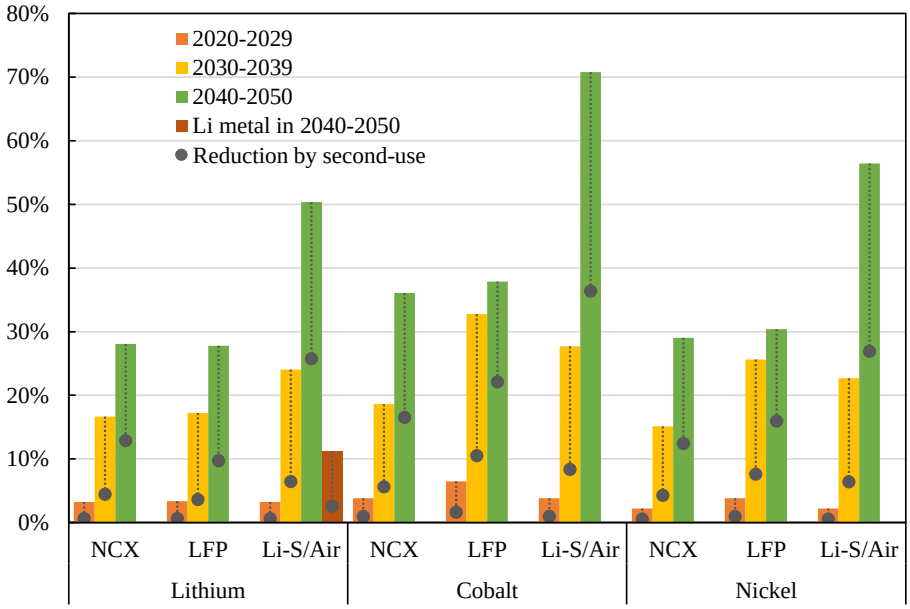


**Fig. 2.6: Closed-loop recycling potential of battery materials in periods of 2020-2029, 2030-2039, 2040-2050 in the STEP scenario.** Hydrometallurgical recycling is used for NCX and LFP batteries and mechanical recovery of Li-metal for Li-S and Li-Air batteries. Grey dot displays the reduction of closed-loop recycling potential as second-use delays the availability of end-of-life materials. See Supplementary Table 2.18 for other materials.

If a significant share of batteries experiences a second-use, the recovery of that material will be delayed in time and thus the CLRP will be substantially lower for the decades to come (shown by the dashed lines in Fig. 2.6). The CLRP of other materials follow similar patterns (see Supplementary Table 2.18).

## 2.4 Discussion

Given the magnitude of the battery material demand growth across all scenarios, global production capacity for Li, Co, and Ni (black lines in Fig. 2.3) will have to increase drastically (see Supplementary Table 2.19 and Supplementary Table 2.20). For Li and Co, demand could outgrow current production capacities even before 2025. For Ni, the situation appears to be less dramatic, although by 2040 EV batteries alone could consume as much as the global primary Ni production in 2019. Other battery materials could be supplied without exceeding existing production capacities (Supplementary

Table 2.20), although supplies may still have to increase to meet demands from other sectors[36,65]. The known reserves for Li, Ni, and Co (black lines in Fig. 2.4) could be depleted before 2050 in the SD scenario and for Co also in the STEP scenario. For all other materials known reserves exceed demand from EV batteries until 2050 (Supplementary Table 2.16). In 2019 around 64% of natural graphite and 64% of Si are produced in China[108], which could create vulnerabilities to supply reliability[113]. However, synthetic graphite has begun to dominate the LIB graphite anode market (56% market share in 2018) due to its superior performance and decreasing cost over natural graphite[85]. Thus, among EV battery materials Co and Li, and to a lesser extent Ni and graphite, can be considered to be most critical concerning the up-scaling of production capacities (see Supplementary Table 2.19), reserves and other supply risks, which confirms previous findings[30,36,65,113,114] even without taking into consideration the potential additional demand from heavy-duty vehicles[34] and other sectors[35]. In contrast to Li and Ni, Co reserves are also geographically more concentrated and partly in conflict areas[115], thus increasing potential supply risks[65]. Battery manufacturers are already seeking to decrease their reliance on cobalt, *e.g.*, by lowering the Co content of NCM batteries, however, as shown in Fig. 2.3, absolute decoupling is unlikely to occur in the coming decades. Shortages could also occur at a regional level, such as the access to Li and Ni for Europe[30]. Obviously, it is possible that the outlined supply risks change, *e.g.*, with the discovery of new reserves[116].

According to our model, lithium demand for EV batteries in 2050 (0.6-1.5 Mt) could be significantly lower than projected by Weil et al.[36] (1.1-1.7 Mt) and likely higher than projected by Hao et al.[34] (0.65 Mt), Deetman et al.[35] (0.05-0.8 Mt), and Ziemann et al.[33] (0.37-1.43 Mt). For cobalt, our estimations (0.25-1.25 Mt) are in line with the predictions by Weil et al.[36] (0.3-1.1 Mt) despite important differences in underlying scenarios and likely considerably higher than Deetman et al.[35] (0.06-0.62 Mt). For nickel our estimations (1.5-7.6 Mt) partly overlap but are generally higher than those by Weil et al.[36] (0.6-2.6). There are thus notable uncertainties concerning the primary material demand for EV materials related to several key factors that could be strategically addressed to mitigate supply risks. Probably the most important factor is the future required battery capacity. A sensitivity analysis is shown in Fig. 2.4 for two extreme battery capacity cases, *i.e.*, if all EVs were PHEVs with small 10 kWh batteries or if all EVs were large SUVs with 110 kWh batteries, such as Tesla Model S Long Range Plus[104].

While it is unlikely that the global average EV battery capacity will be close to either end of this range, this analysis illustrates the high importance of this factor. The demand for battery capacity depends on technical factors, such as vehicle design, vehicle weight, and fuel efficiency[117], and perhaps even more importantly, on socio-economic factors, such as the future EV fleet size (see also Fig. 2.4), consumer choices concerning the size and ranges of EVs, the cost of EV batteries and raw materials, the development of alternative transportation means and technologies (*e.g.*, fuel cell EVs[118]), and policy.

Opportunities lie in the development of battery technology. As shown here, Li-S and Li-Air batteries would reduce the dependency on Co, and Ni, while offering higher energy densities. Our analysis assumes conservative, *i.e.*, technically proven values, but if higher specific energies were to be achieved, *e.g.*, 600 instead of 400 Wh/kg for Li-S and 1000 instead of 500 Wh/kg for Li-Air (Supplementary Table 2.10 and Supplementary Table 2.21), the cumulative lithium demand in the Li-S/Air scenario could be reduced by 20% and the Li-metal demand by 40% (Supplementary Fig. 2.14). High market shares of Li-S/Air or LFP batteries or breakthroughs in post-Li batteries based on abundant elements such as sodium, magnesium, or calcium[64] could lead to an absolute decoupling from lithium, cobalt, and nickel (see Supplementary Fig. 2.11, Supplementary Fig. 2.12, and Supplementary Fig. 2.13).

It is also uncertain whether the lifespans assumed here will be reached in practice, especially for Li-S and Li-Air batteries[62]. Lower battery lifespans could require additional battery replacements and thus lead to considerably higher material demand (Supplementary Fig. 2.9 and Supplementary Table 2.22). On the other hand, batteries in a state-of-health that would typically be considered to mark their EoL (*i.e.*, 70-80%) may still be used by consumers who prefer to accept a shorter range over the expense of a battery replacement[34] (EVs with 80% residual battery capacity could still meet daily travel requirements in 85% of cases in the US[119] and widespread charging infrastructure could further support this[120]).

Truly circular EV batteries will not be available anytime soon. Over the next decades, we first need to produce the EV battery stock for a large fleet, mostly from primary materials. Closed-loop recycling will gain importance, depending on EV fleet and battery chemistry developments, second-use, and other factors, such as standardization[121], legislation, business models[122], eco-design or design for recycling[123],

collection systems, and recycling technology[17,109]. The difference between the recycling technologies is not so much in the recycling efficiency for individual materials, but whether materials are recovered and in what chemical form and purity[17,36]. All recovered battery materials can, in principle, be refined to battery-grade. For example, in the pyrometallurgical process, lithium ends up in the slag, while in the hydrometallurgical process, lithium ends up in the solid waste from the leaching step. Both slag and solid waste could be refined to produce battery-grade lithium carbonate, however, lithium has hardly been recovered so far as the lithium price did not enable a cost-effective recovery[36,124]. The most economically and environmentally promising technology for closed-loop recycling, although currently largely unproven outside of the lab, is direct recycling, which could recover cathode material "as is" without intermediate smelting or leaching step (Fig. 2.5). Challenges for direct recycling include the development of sorting processes that can separate cathode powder from different battery chemistries, re-lithiation and upgrading processes for cathode chemistries that have become obsolete and further standardization of batteries to support effective recycling[95].

The success of the transition to electric vehicles will depend partly on whether the material supply can keep up with the growth of the sector in a sustainable way and without damaging the reputation of EVs. Science-based sustainability assessments should guide the selection of alternative battery chemistries and raw materials to avoid unfavorable burden-shifts. The global demand scenarios presented here also provide a basis to assess the global economic, environmental, and social impacts related to EVs and batteries from a lifecycle perspective.

## 2.5 Data availability

The authors declare that the data used as model inputs supporting the findings of this study are available within the paper and its Supplementary Information files. Data and model are also provided as Excel files to facilitate further research (10.6084/m9.figshare.13042001).

## 2.6 Supplementary information

### 2.6.1 Supplementary Figures

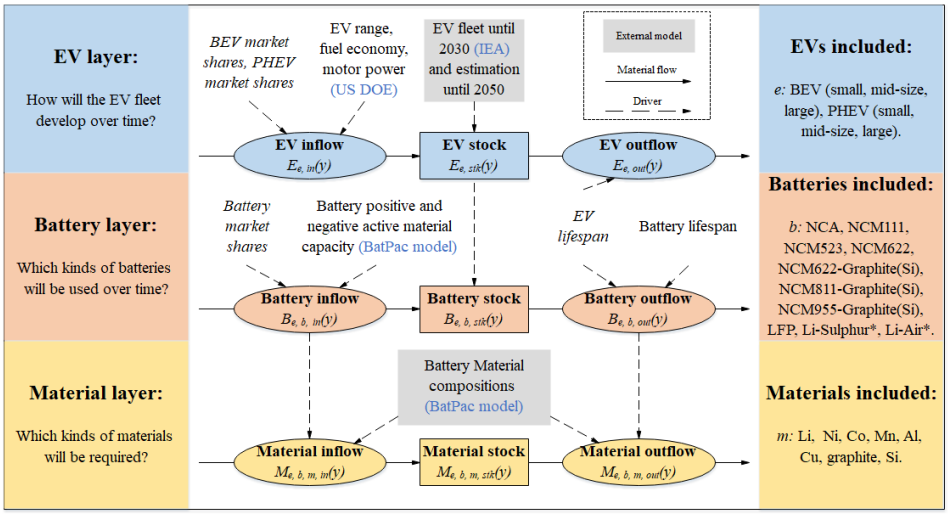


**Supplementary Fig. 2.1: Stock dynamics model on the EV, battery, and material layers: research questions (left), model structure (middle), and included categories (right).** Driving factors are classified into predominantly technical and socio-economic (in italic) drivers. We use two EC fleet development scenarios until 2030 from International Energy Agency (IEA)[57]. The EV range, fuel economy, and motor power of various EV models are collected from the US DOE (US Department of Energy)[125]. The material compositions for various battery chemistries are calculated by using the BatPaC (Battery Performance and Cost) model from Argonne National Laboratory[70], expected for Li-Sulphur and Li-Air chemistries (marked with * as they are associated with uncertainty for EV applications[81]). Abbreviations: E, B, and M = EV, battery, and material; e, b, and m = categories of EV, battery, and material; In, stk, and out = inflow, stock, and outflow; y = year. See the section on battery replacement and reuse for calculation equations.

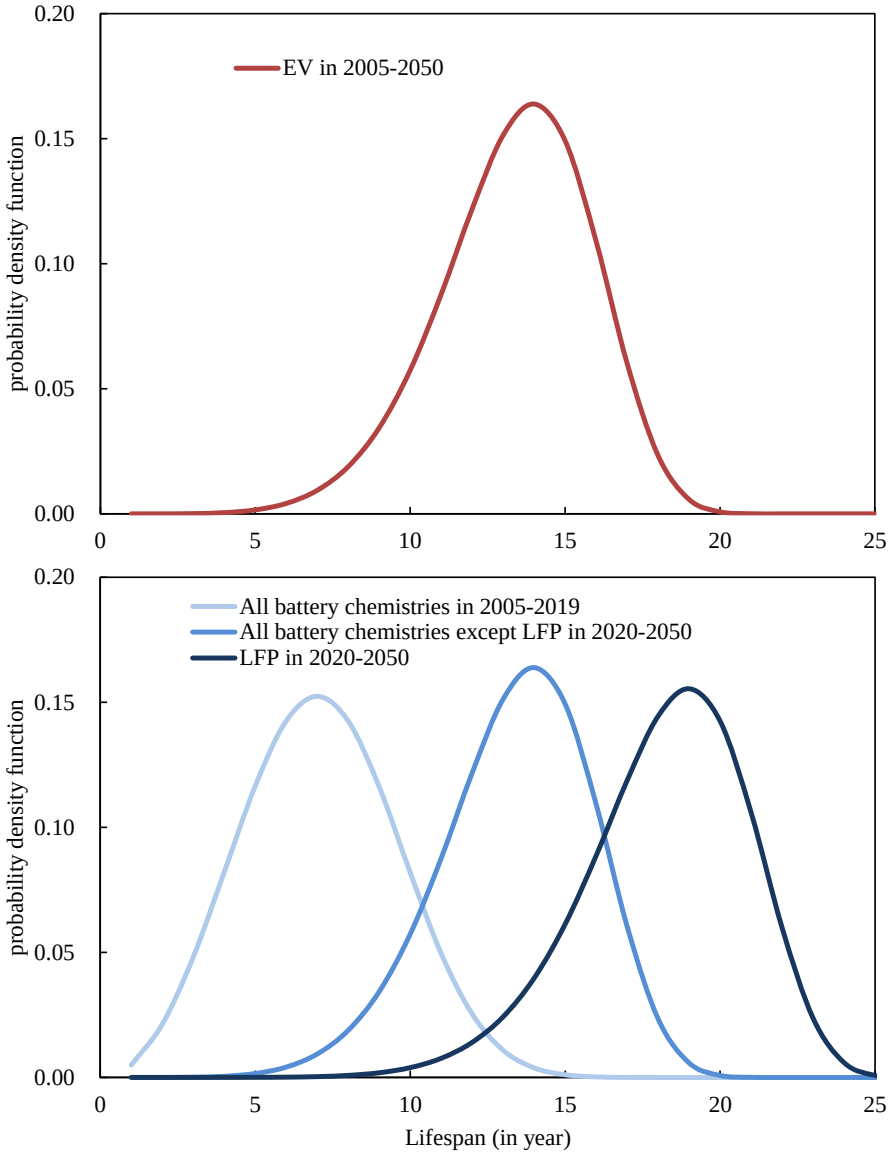


**Supplementary Fig. 2.2: Weibull lifespan distributions of EVs and batteries.**

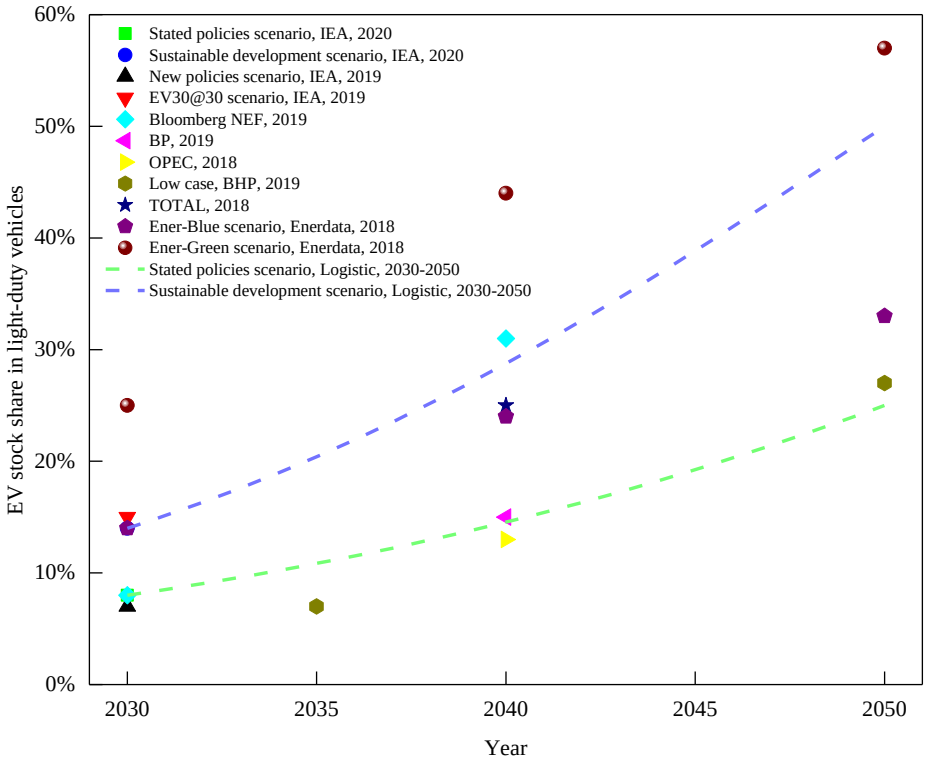


**Supplementary Fig. 2.3: Projections of EV stock share in light-duty vehicles from 2030 to 2050[57,126-132].** TOTAL projects 20%-30% of EV fleet share in 2040[130], which is shown as an average number of 25% in the figure. Green and blue dashed lines represent own estimations for the EV fleet share in the stated policies scenario and the sustainable development scenario of IEA[57] until 2050 by logistic model[133] respectively, which is comparable to other studies.

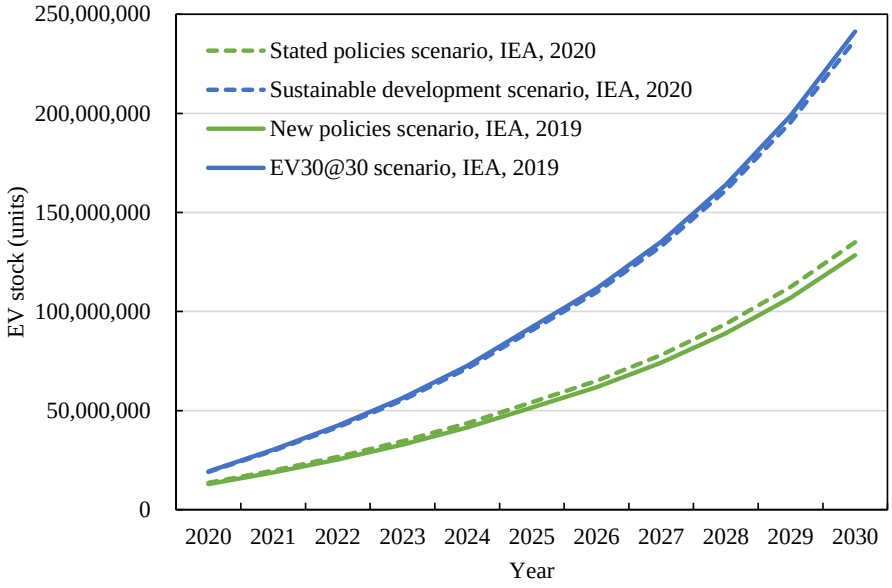


**Supplementary Fig. 2.4: EV stock estimations of stated policies scenario and sustainable development scenario from 2020-2030 of IEA global EV outlook 2020[57], in proportion with new policies scenario and EV30@30 scenario of IEA global EV outlook 2019[132], respectively.**

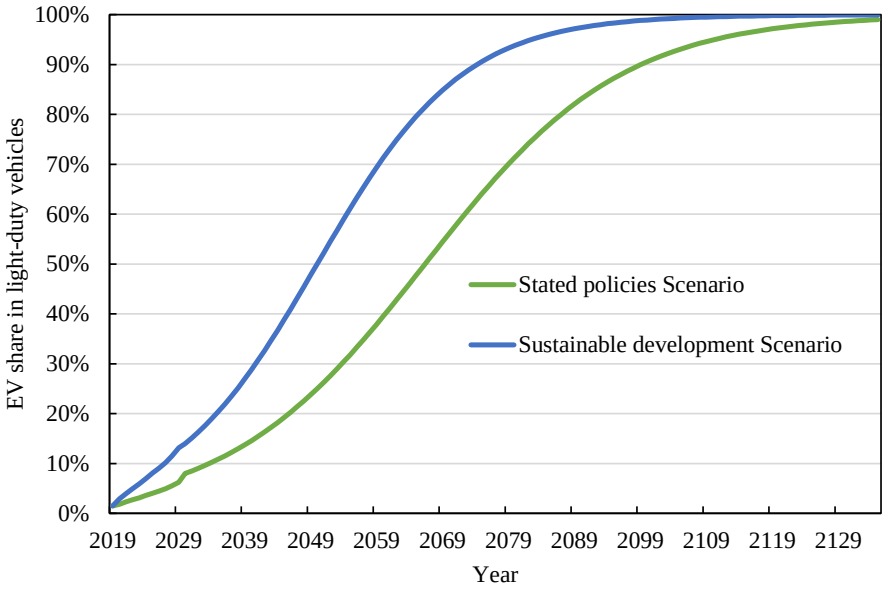


**Supplementary Fig. 2.5: Estimation of EV fleet penetration in stated policies scenario and sustainable development scenario of IEA (reach 100% until the year 2135).** The EV fleet penetration until 2030 is based on the stated policies scenario and the sustainable development scenario of IEA[57], and we model the EV fleet penetration after 2030 by logistic model[133]. Here the figure shows the process of full transition to EVs in light-duty passenger vehicle market, and the time point when EV fleet share reaches 100% in the stated policies scenario and the sustainable development scenario, if our estimations of 25%-50% of EV fleet share in 2050 are realized.

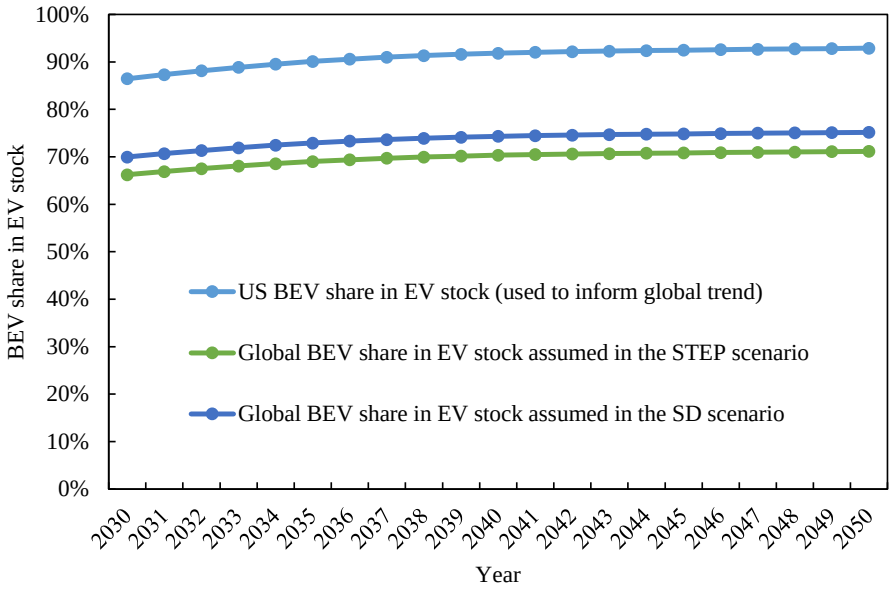


**Supplementary Fig. 2.6: Global BEV share in total EV stock in 2030-2050, in proportion with US BEV stock share projection by US Energy Information Administration[134].**

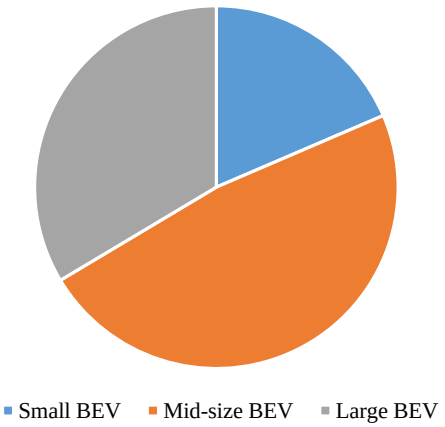


**Supplementary Fig. 2.7: BEV sales market shares among small/mid-size/large segments.** The market shares are based on cumulative sales until 2019 of each BEV model included in each BEV market segment. BEV sales market shares are assumed stable in 2020-2050, while sensitivity analysis is conducted.

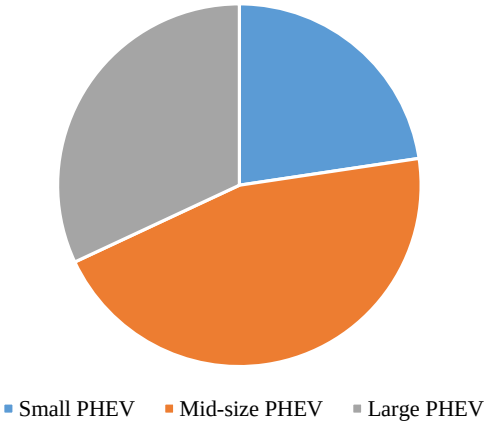


**Supplementary Fig. 2.8: PHEV sales market shares among small/mid-size/large segments.** The market shares are based on cumulative sales until 2019 of each PHEV model included in each PHEV market segment. PHEV sales market shares are assumed stable in 2020-2050, while sensitivity analysis is conducted.

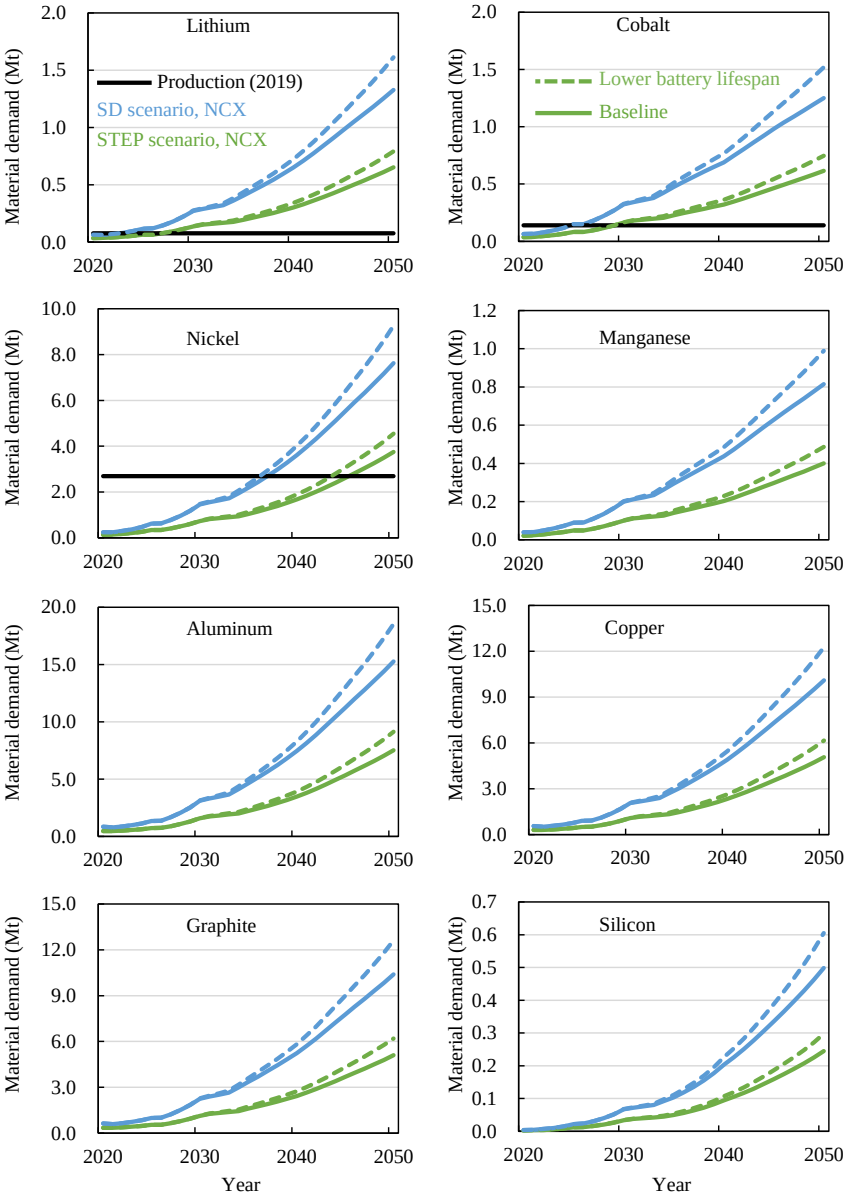


**Supplementary Fig. 2.9: Result of sensitivity analysis of lower battery lifespan (*i.e.*, one EV will use 1.5 battery packs on average after 2020, while in the baseline scenario one EV will use 1 battery pack after 2020) on annual demand for Li, Co, Ni, Mn, Al, Cu, graphite, and Si in 2020-2050 without recycling.**

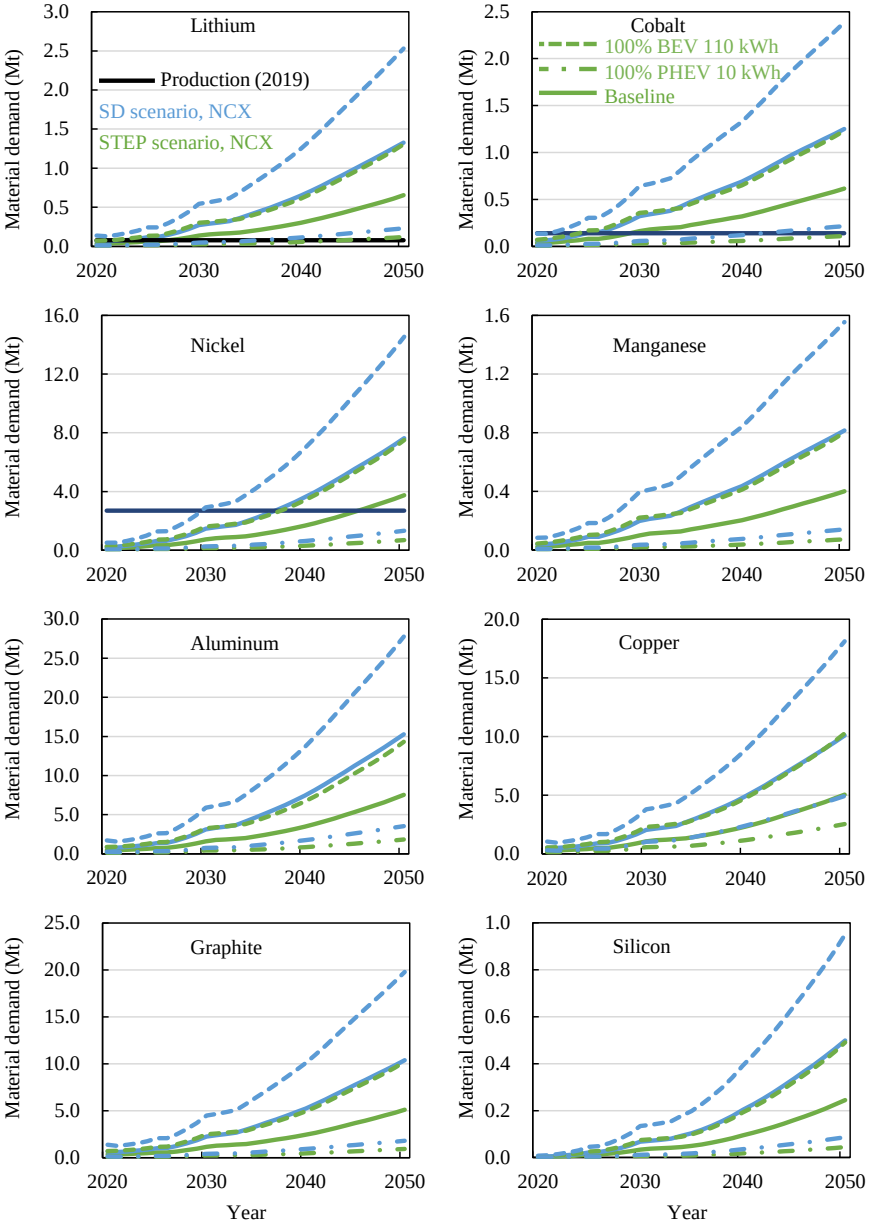


**Supplementary Fig. 2.10: Result of sensitivity analysis of required battery capacity (*i.e.*, 100% BEV with 110 kWh and 100% PHEV with 10 kWh) on annual demand for Li, Co, Ni, Mn, Al, Cu, graphite, and Si in 2020-2050 without recycling.**

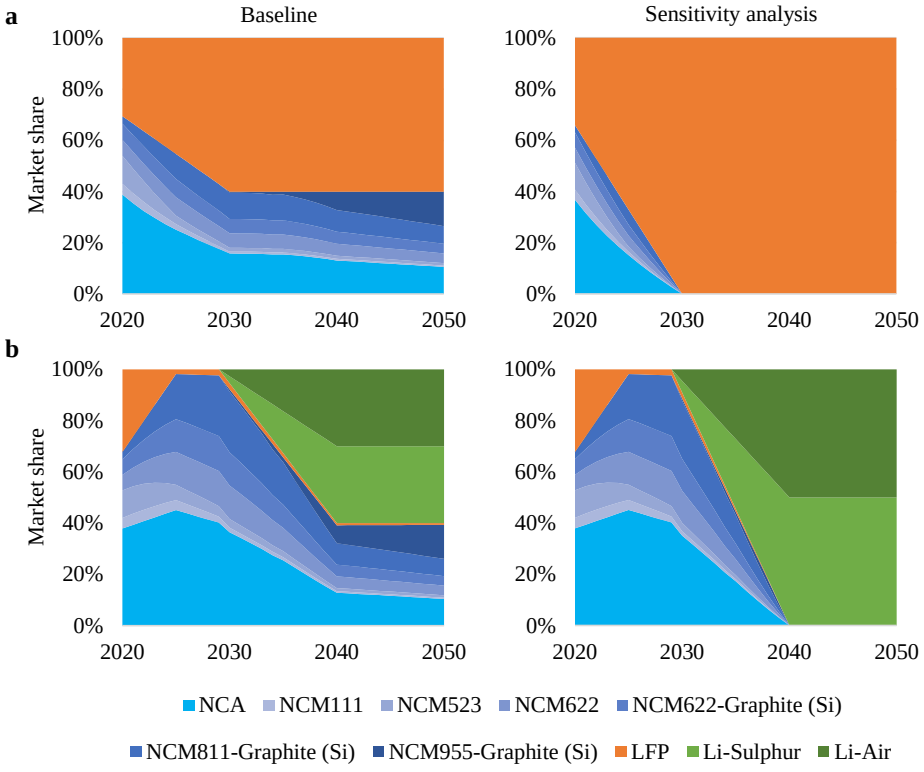


**Supplementary Fig. 2.11: Input of sensitivity analysis of LFP market share in the LFP scenario (a) and Li-S and Li-Air market shares in the Li-S/Air scenario (b).**

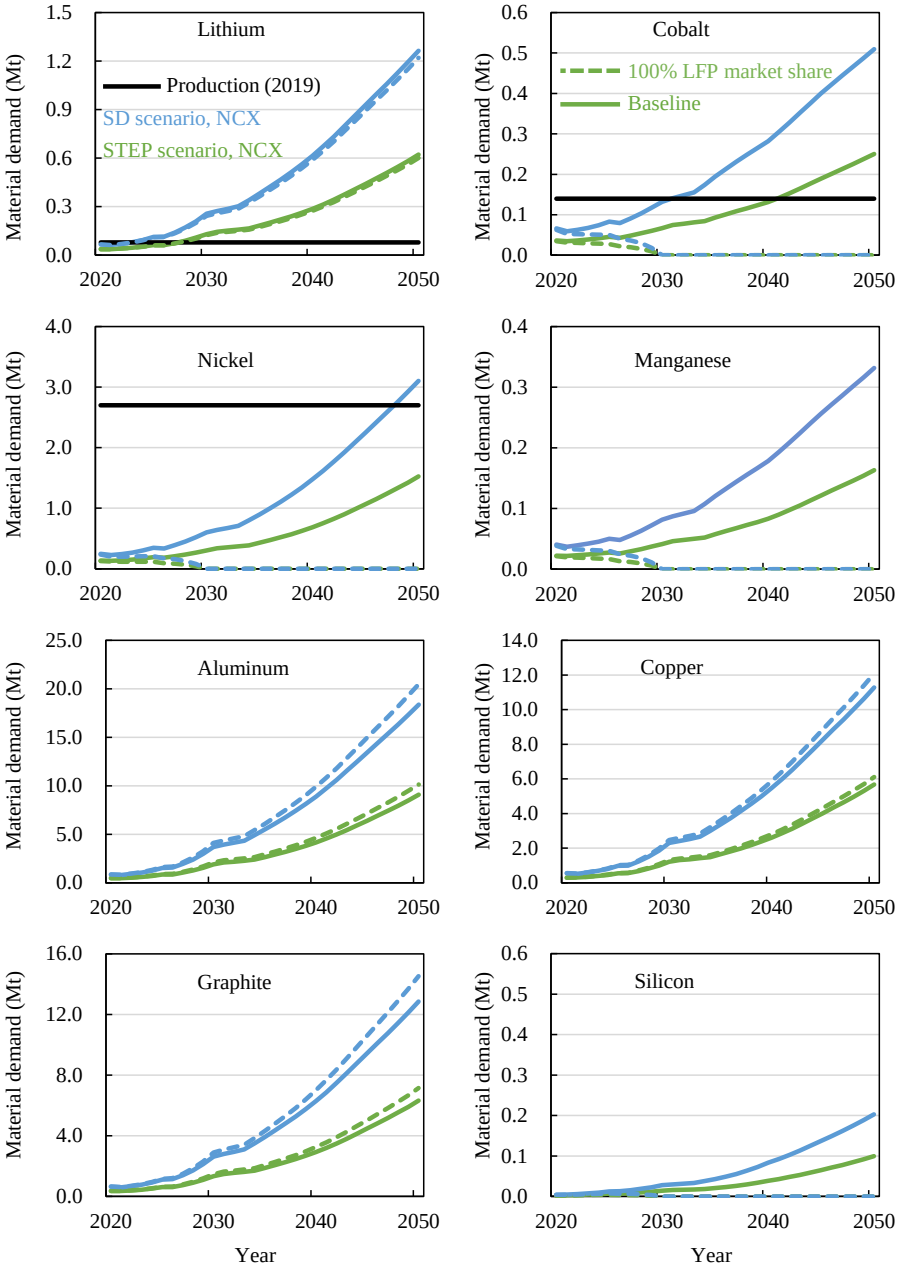


**Supplementary Fig. 2.12: Result of sensitivity analysis of 100% LFP market share (by 2030) on annual demand for Li, Co, Ni, Mn, Al, Cu, graphite, and Si in 2020-2050 without recycling.**

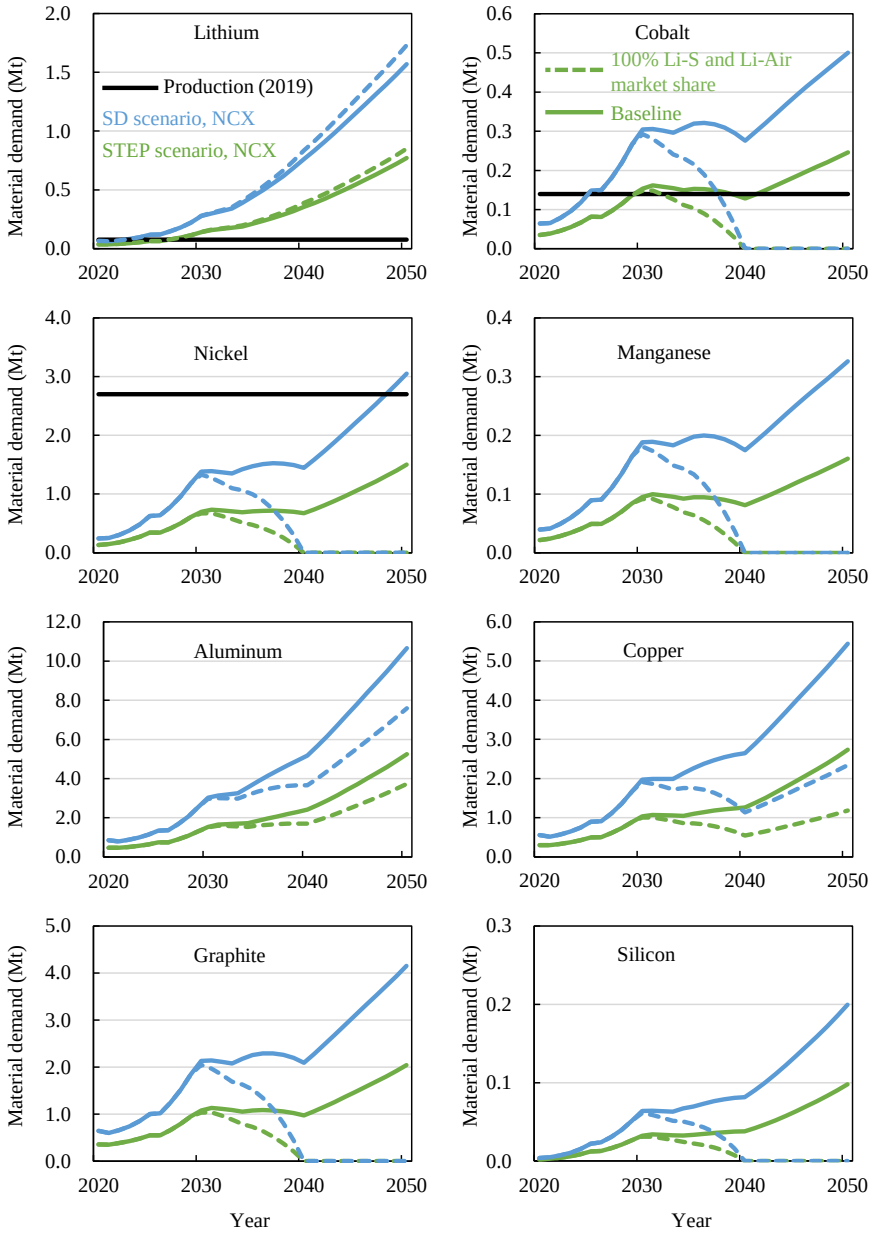


**Supplementary Fig. 2.13: Result of sensitivity analysis of 100% Li-S and Li-Air market share (by 2040) on annual demand for Li, Co, Ni, Mn, Al, Cu, graphite, and Si in 2020-2050 without recycling.**

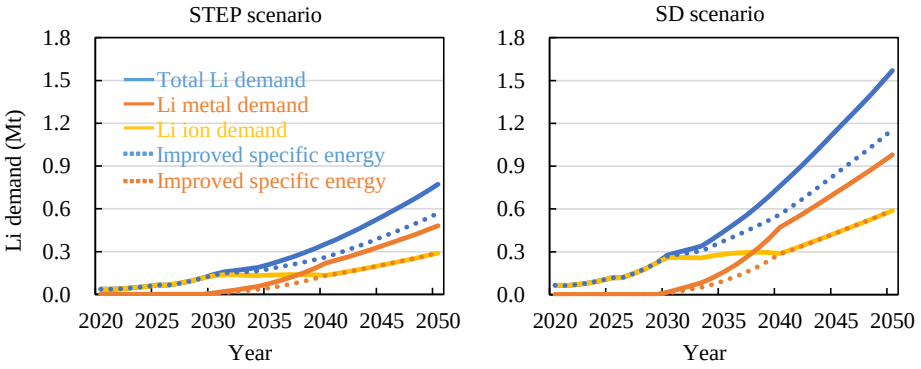


**Supplementary Fig. 2.14: Lithium demand split by Li ion (in the form of chemicals like $Li_2CO_3$, LiOH, *etc*.) and Li metal (in Li anode of Li-S and Li-Air chemistries) in the Li-S/Air scenario, including a sensitivity analysis for improved specific energy of Li-S and Li-Air chemistries.** Based on a review of the specific energy of Li-S and Li-Air cells from lab and commercial scales (see Supplementary Table 2.22 and Supplementary Table 2.1), the specific energy of Li-S cells is improved from 400 Wh/kg to 600 Wh/kg, and the specific energy of Li-Air cells from 500 Wh/kg to 1000 Wh/kg. Specific energy improvements of Li-S and Li-Air cells can make total Li demand in the Li-S/Air scenario lower than LFP and NCX scenarios.

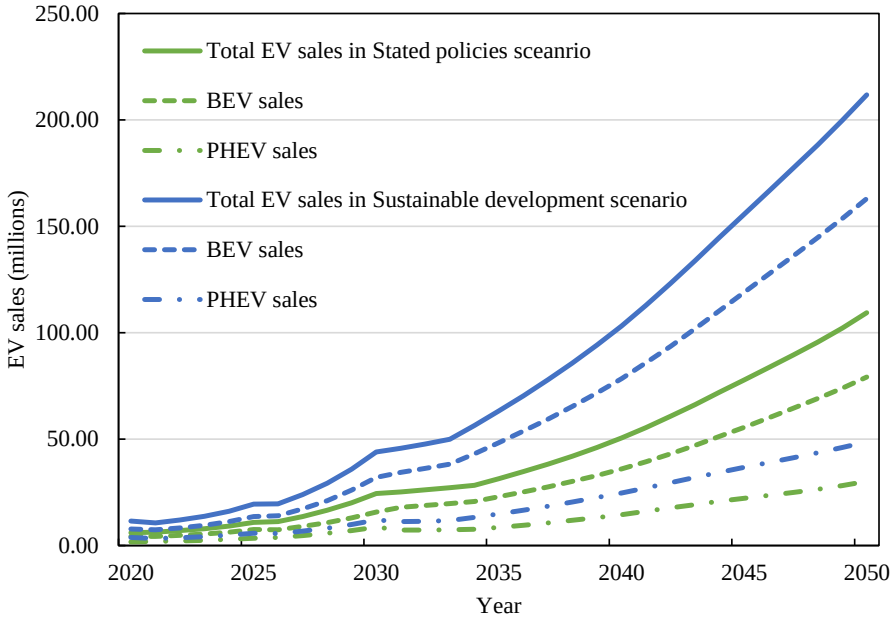


**Supplementary Fig. 2.15: Projections of global EV sales in the stated policies scenario and the sustainable development scenario in 2020-2050.** EV sales are in rapid growth phase until 2050, based on the projections of EV stock share in light-duty passenger vehicles.

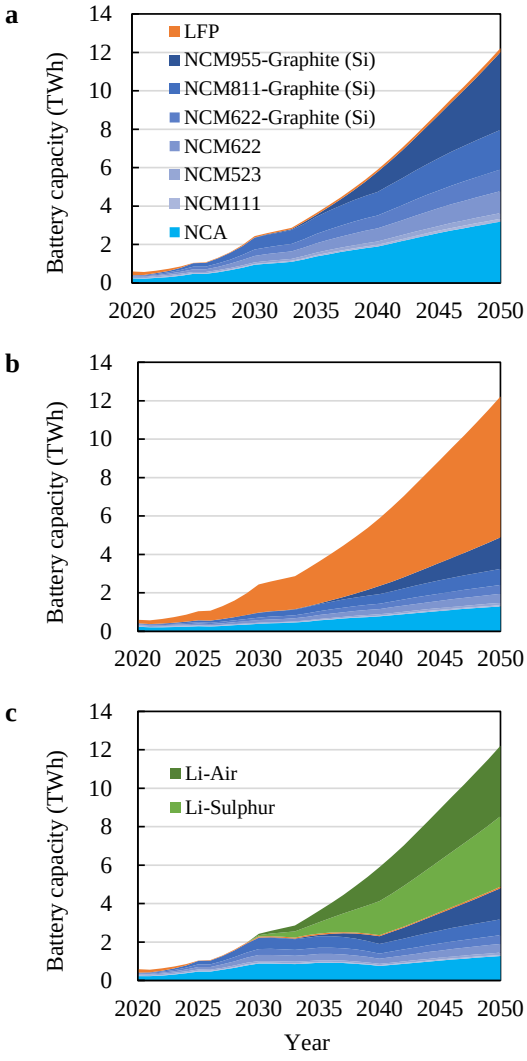


**Supplementary Fig. 2.16: EV battery sales by year in the NCX (a), LFP (b) and Li-S/Air (c) scenarios until 2050 for the fleet development of the SD scenario (unit: 1 TWh = $10^3$ GWh = $10^6$ MWh = $10^9$ kWh).**

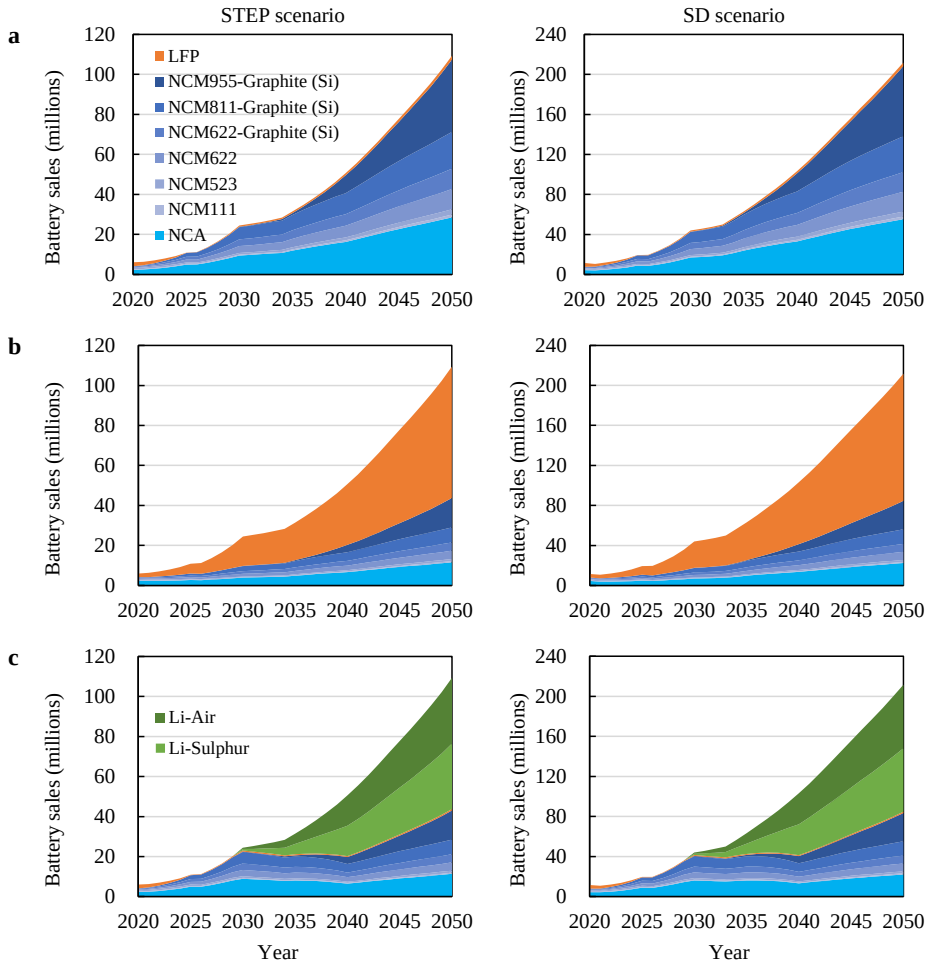


**Supplementary Fig. 2.17: EV battery sales by year in the NCX (a), LFP (b) and Li-S/Air (c) scenarios until 2050 for the fleet development of the STEP scenario and the SD scenario (unit: millions).**

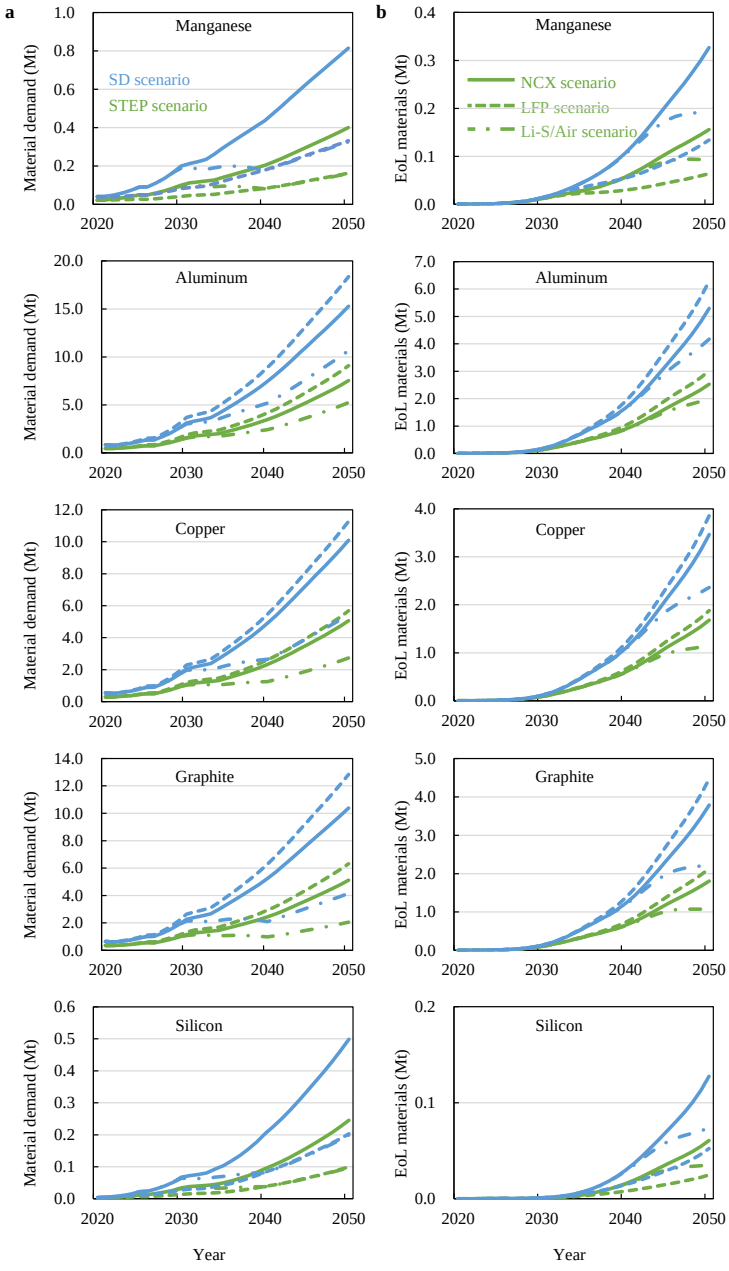


**Supplementary Fig. 2.18: Primary material demand (a) and materials in EoL batteries (b) from 2020 to 2050 for Mn, Al, Cu, graphite, and Si in the NCX, LFP and Li-S/Air battery scenarios.**

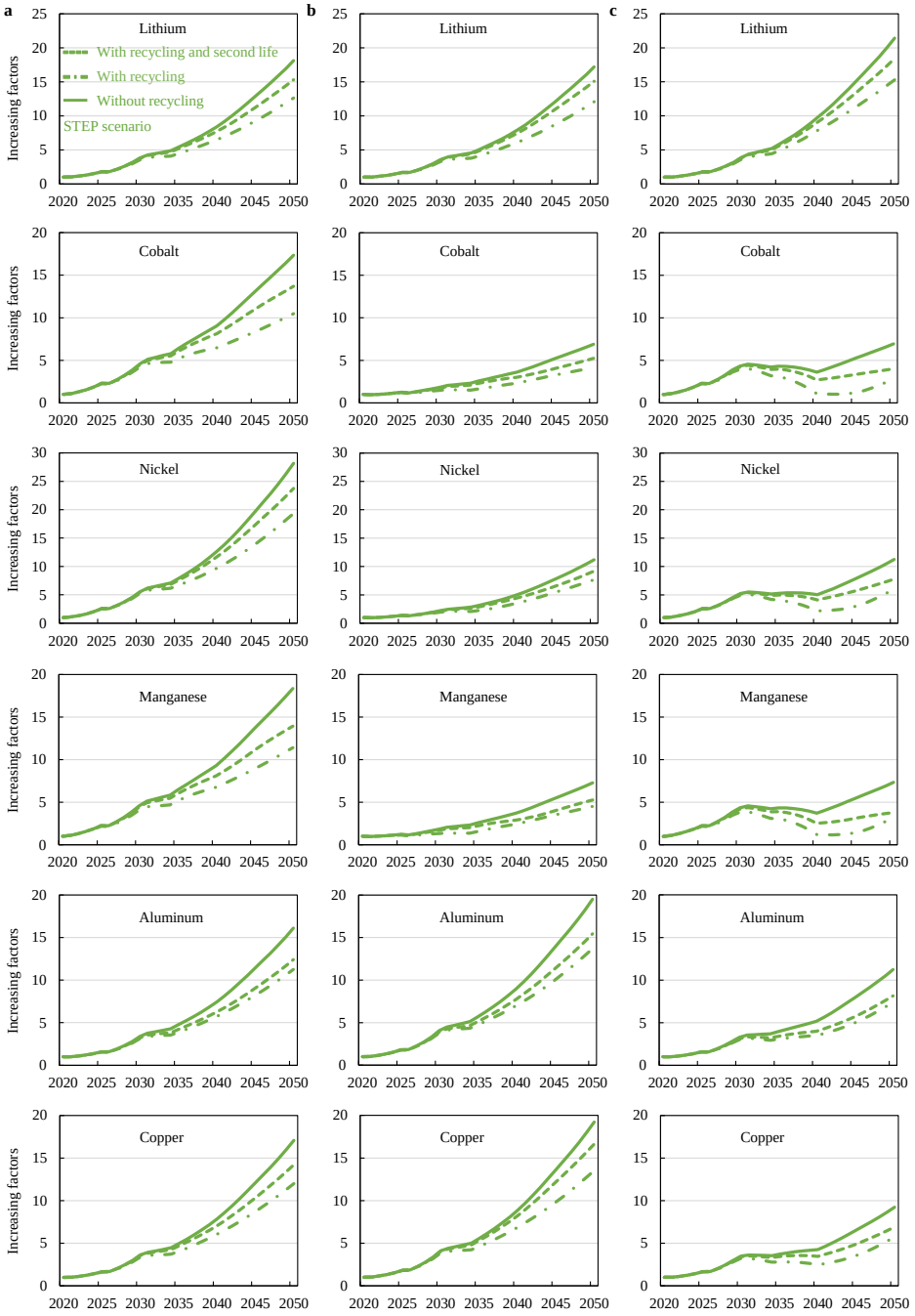
a
b
c
Lithium
Cobalt
Nickel
Manganese
Aluminum
Copper
With recycling and second life
With recycling
Without recycling
STEP scenario
Increasing factors
2020 2025 2030 2035 2040 2045 2050

Supplementary Figure 2.19 (Continued).

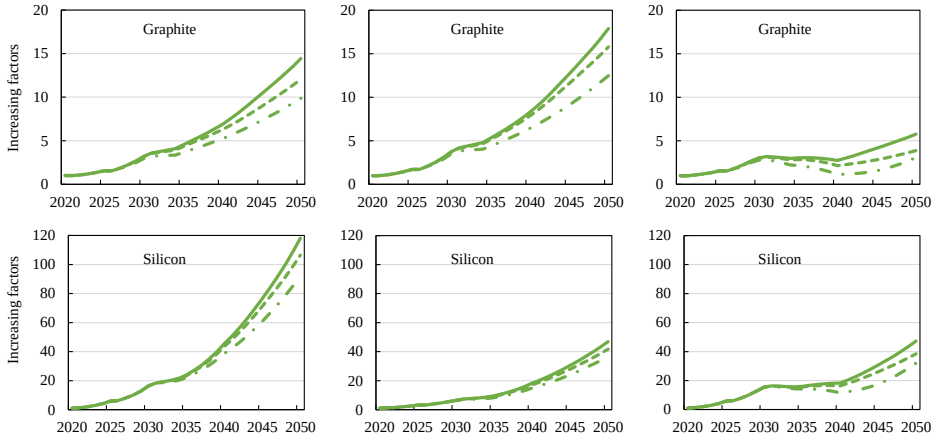


**Supplementary Fig. 2.19: Increasing factors for the primary demand for Li, Ni, Co, Mn, Al, Cu, graphite, and Si from 2020 to 2050 in the STEP scenario in the NCX (a), LFP (b) and Li-S/Air (c) scenarios.** Here recycling refers to hydrometallurgical recycling as an example.

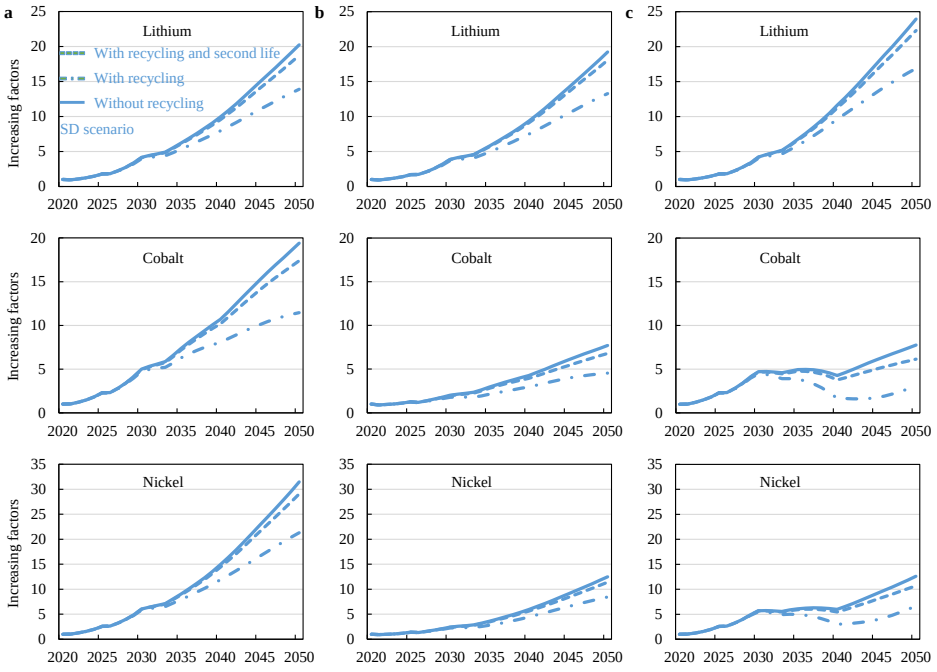

Supplementary Figure 2.20 (Continued).

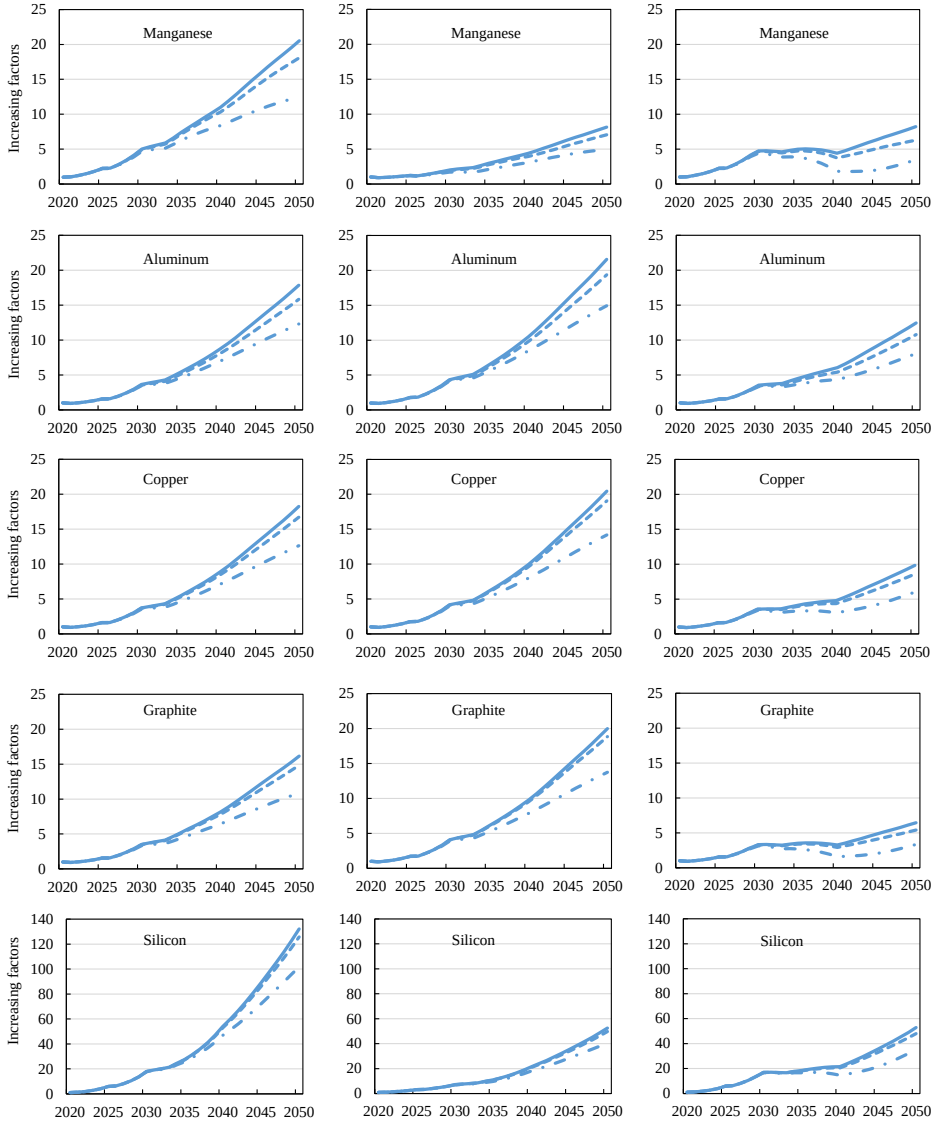


**Supplementary Fig. 2.20: Increasing factors for the primary demand of Li, Ni, Co, Mn, Al, Cu, graphite, and Si from 2020 to 2050 in the SD scenario in the NCX (a), LFP (b) and Li-S/Air (c) scenarios.** Here recycling refers to hydrometallurgical recycling as an example.

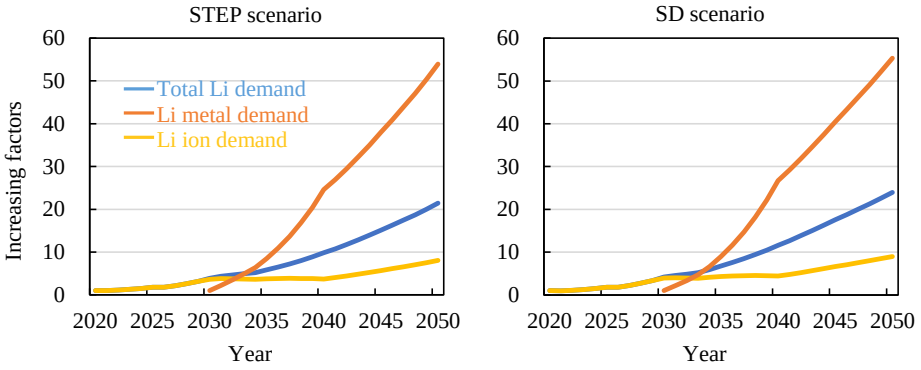


**Supplementary Fig. 2.21: Increasing factors for lithium demand split by Li ion (in the form of chemicals like Li2CO3, LiOH, *etc.*) and Li metal (in Li anode of Li-S and Li-Air chemistries) demand in the Li-S/Air scenario.**

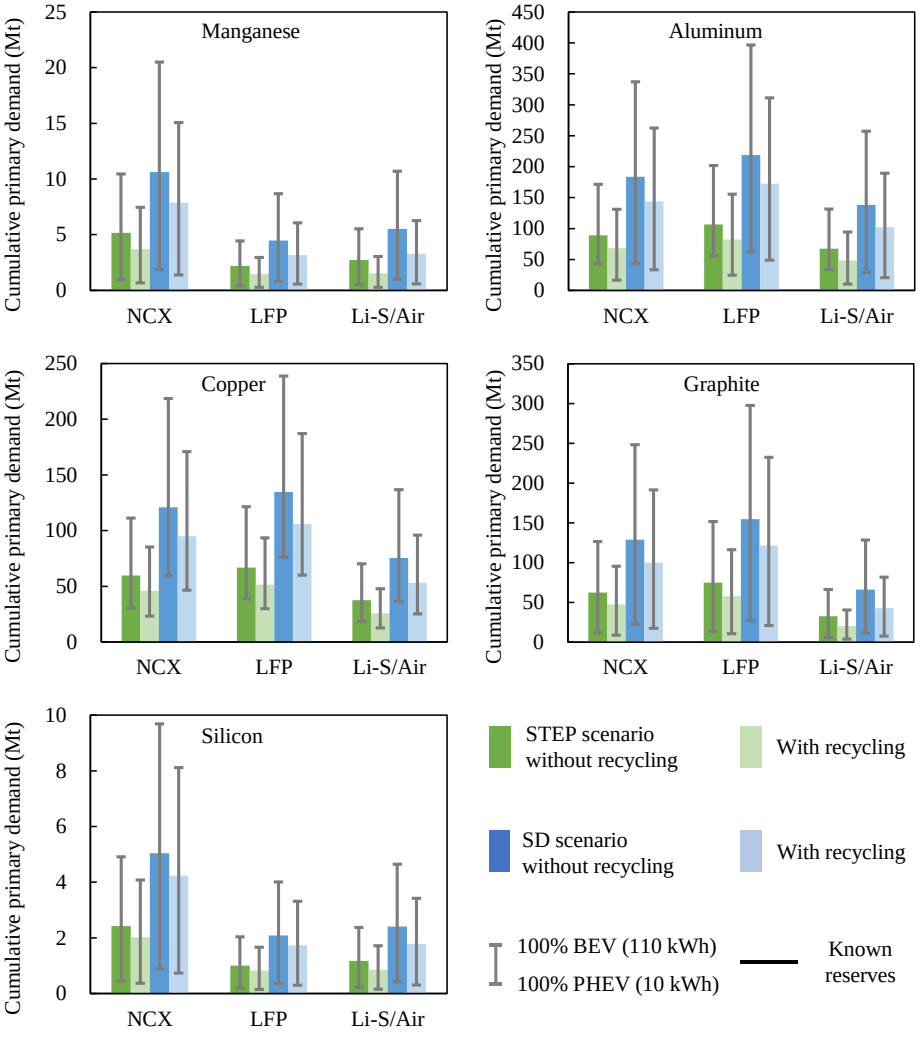


**Supplementary Fig. 2.22: Cumulative primary demand for Mn, Al, Cu, graphite, and Si in 2020-2050 without recycling or with hydrometallurgical recycling.** Grey error bars represent a sensitivity analysis for battery capacity considering two extreme cases (if all EVs were PHEVs with small 10 kWh batteries or if all EVs were large SUVs with 110 kWh batteries, *e.g.*, Tesla's Model S Long Range Plus[104]). The global known reserves in 2019 for Mn, Al, Cu, graphite, and Si are shown in Supplementary Table 2.2, which are much higher than cumulative primary material demand from EV batteries only.

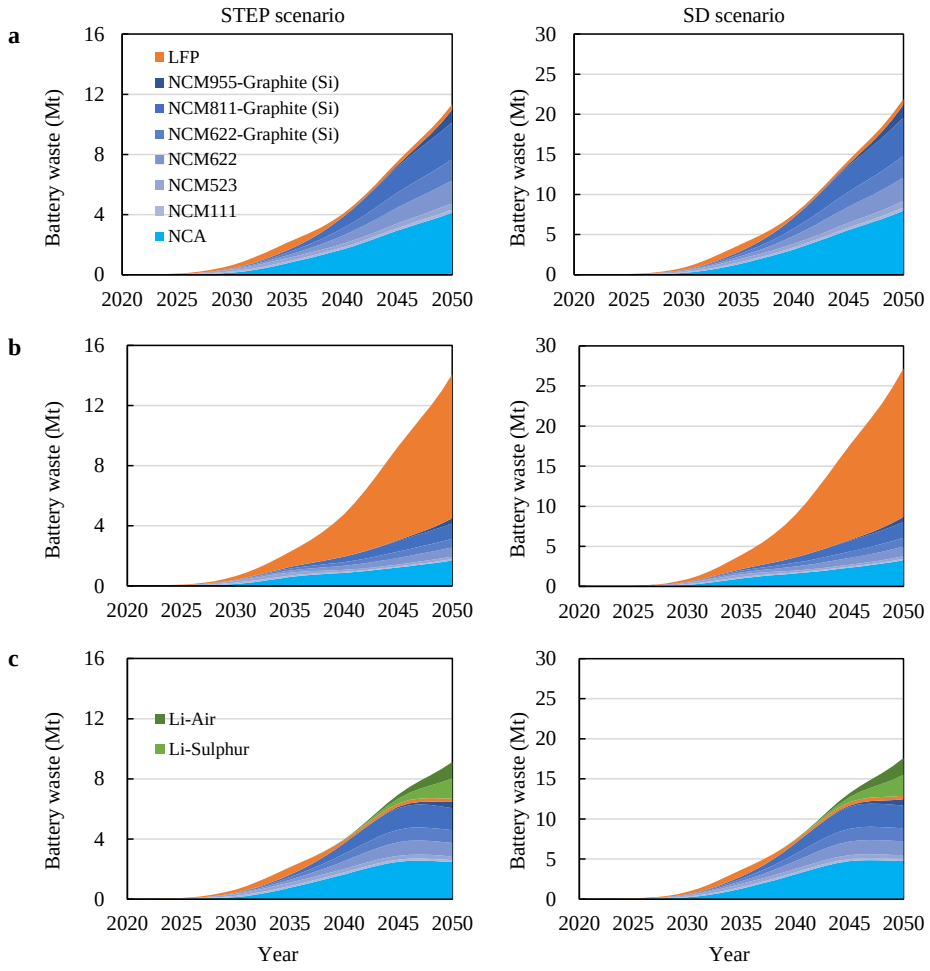


**Supplementary Fig. 2.23: Future battery waste stream by chemistry in the NCX (a), LFP (b) and Li-S/Air (c) scenarios until 2050 (unit: Mt = million tons).** Under the STEP scenario, the EV battery waste stream reaches around 11 Mt in 2050 if NCX scenario is realized, which is lower than the LFP scenario (14 Mt) and higher than the Li-S/Air scenario (9 Mt). The differences among three battery chemistry scenarios are associated with the relatively lower specific energy of LFP chemistry and higher specific energy of Li-S and Li-Air chemistries compared to NCA and NCM series chemistries. Driven by higher EV fleet deployments, the weight of EV battery waste stream reaches around 2 times in the SD scenario than the STEP scenario.

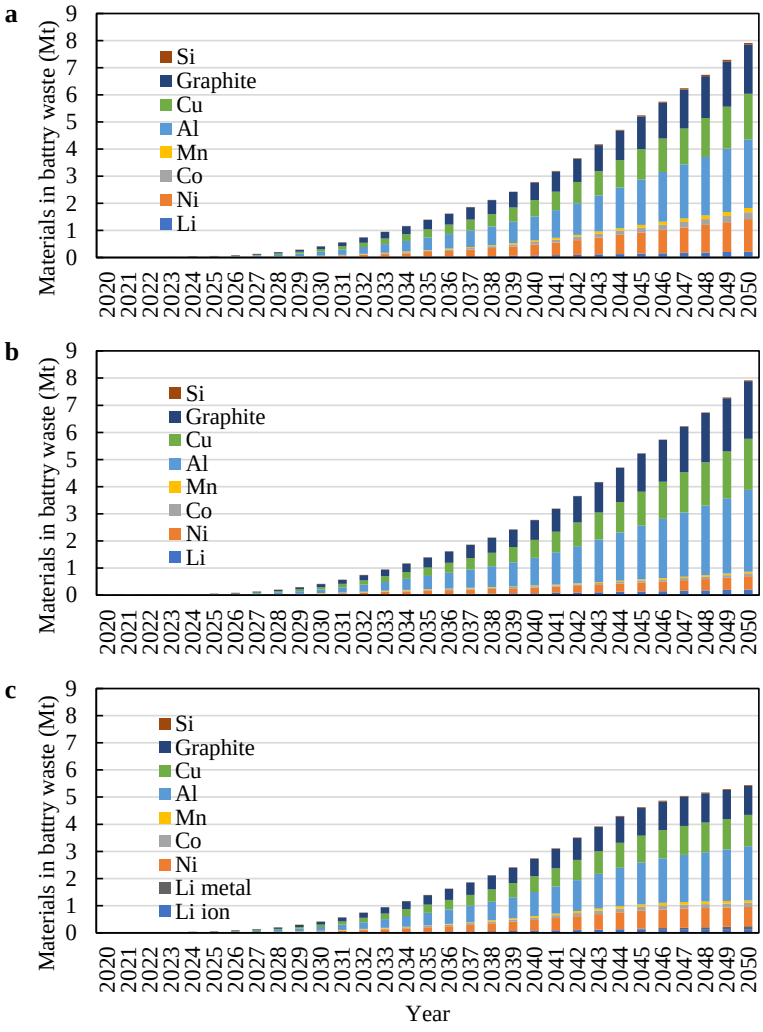


**Supplementary Fig. 2.24: Materials in future EV battery waste steam potentially available for recycling without second life use until 2050 in the STEP scenario in the NCX (a), LFP (b) and Li-S/Air (c) scenarios (unit: Mt = million tons).** The total weight of eight EoL materials in 2050 in the NCX scenario is almost equal to the LFP scenario, but with different material shares, especially for the EoL Ni weight in the NCX scenario is much higher than the LFP scenario. The total weight of eight EoL materials in the Li-S/Air scenario (Li includes Li ion in lithium chemical compounds and Li metal) is much lower than the other two battery scenarios, however, EoL Li weight is slightly higher.

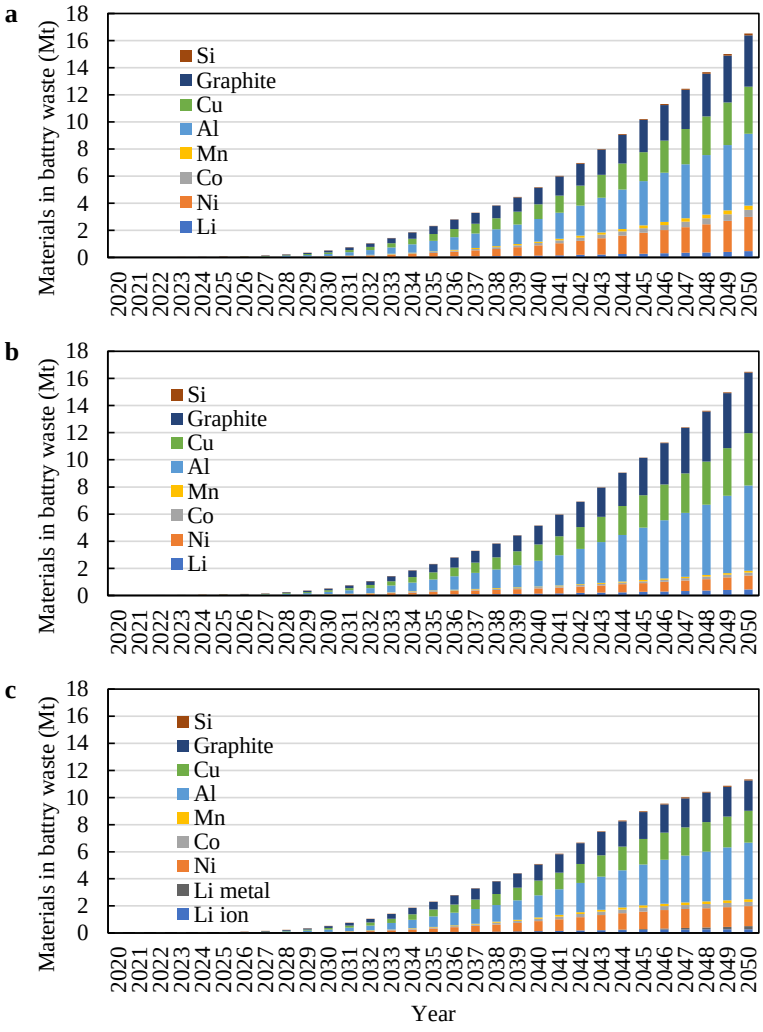


**Supplementary Fig. 2.25: Materials in future EV battery waste steam potentially available for recycling without second life use until 2050 in the SD scenario in the NCX (a), LFP (b) and Li-S/Air (c) scenarios (unit: Mt = million tons).** We can see the same pattern for EoL materials in the SD scenario as in the STEP scenario. However, the weight of EoL materials available for recycling in the SD scenario is around 2 times than STEP scenario.

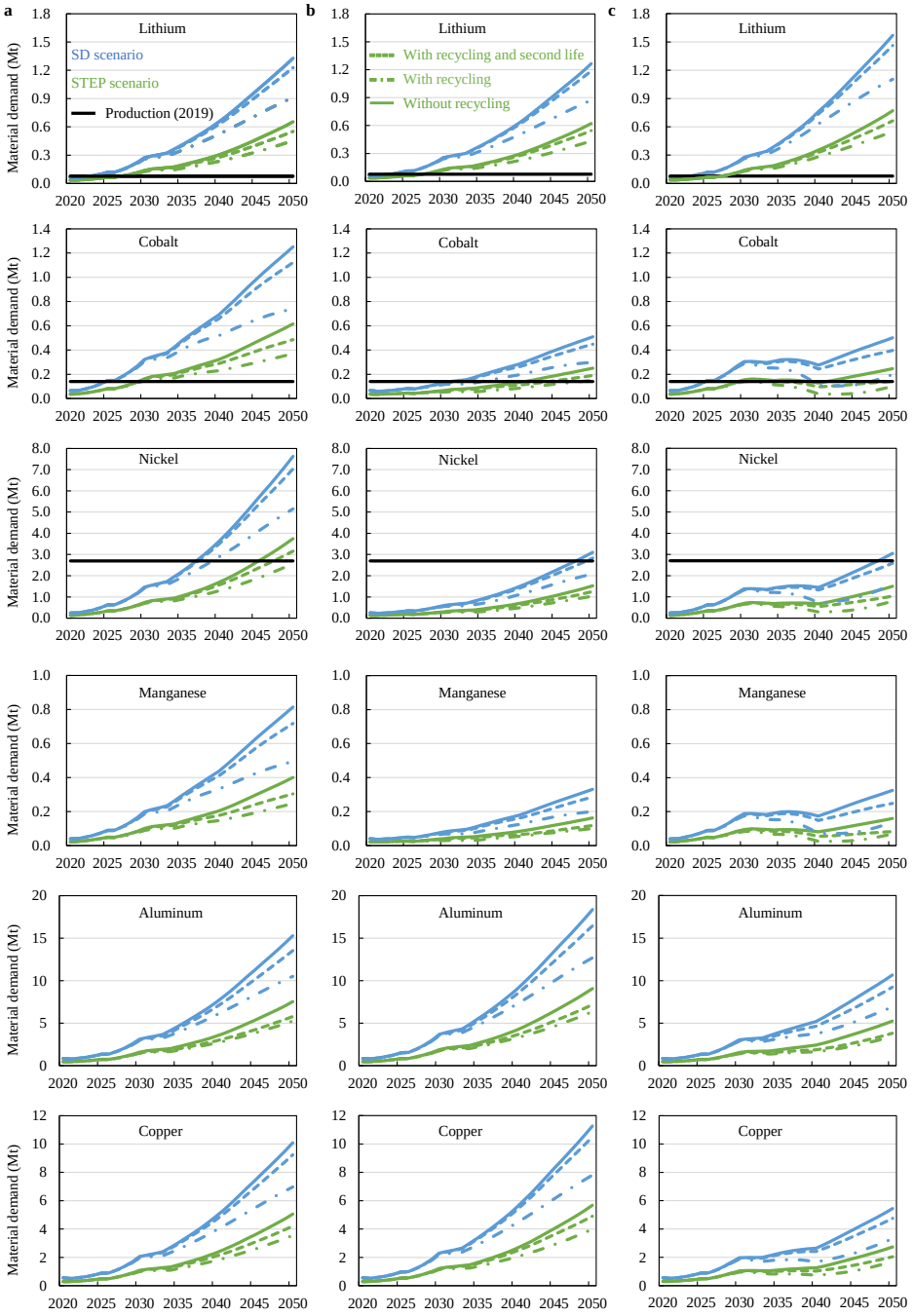
a
b
c
Lithium
Cobalt
Nickel
Manganese
Aluminum
Copper
Material demand (Mt)
SD scenario
STEP scenario
Production (2019)
With recycling and second life
With recycling
Without recycling
2020 2025 2030 2035 2040 2045 2050

Supplementary Figure 2.26 (Continued).

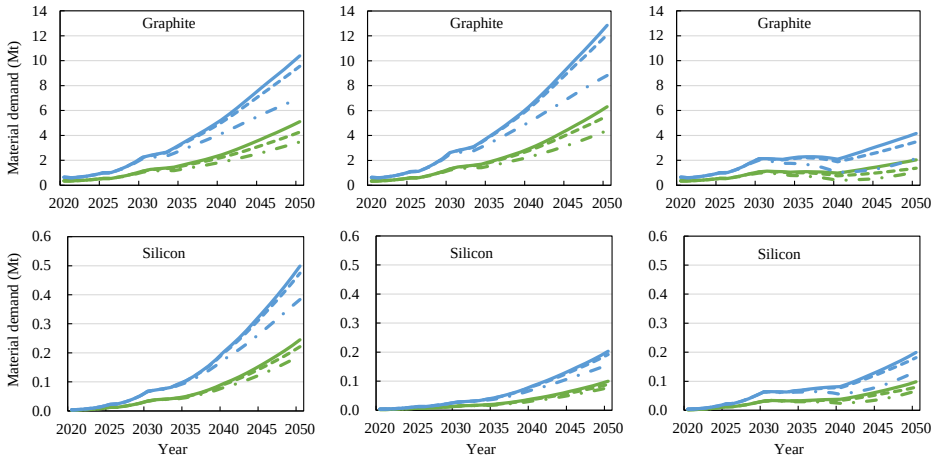


**Supplementary Fig. 2.26: Primary battery material demand in the NCX (a), LFP (b) and Li-S/Air (c) scenarios from 2020 to 2050 without recycling, with recycling, and with recycling and second life.** Here recycling refers to hydrometallurgical recycling as an example.

### 2.6.2 Supplementary Tables

**Supplementary Table 2.1: Compiled EPA car size class[74] used in this study.** Note here small cars include two-Seaters, minicompact sedans, subcompact sedans, and compact sedans by the EPA car size class. Large cars include large sedans, small station wagons, SUVs, and vans by the EPA car size class.

| Class | Passenger & Cargo Volume (Cu. Ft.) |
|---|---|
| Small | < 110 |
| Mid-size | 110 to 119 |
| Large | > 119 |

**Supplementary Table 2.2: Sales-weighted average BEV range, fuel economy, and motor power. We collect sales of each BEV model including in small/mid-size/large car segments until 2019[75], and calculate the distribution of cumulative sales until 2019 of three car segments (to represent BEV market shares among small/mid-size/large car segments).** The range, fuel economy, and motor power of each BEV segment are calculated by cumulative sales-weighted average method. The required battery capacity = EV range * fuel economy / 0.85, where 0.85 is the ratio of available battery capacity for driving EVs based on the assumption in the BatPaC model when calculating battery material compositions[70]. Average required battery capacity for BEVs reaches around 66 kWh.

| BEVs | Range (miles) | Fuel economy (Wh/mile) | Electric motor power (kW) | Required capacity (kWh) |
|---|---|---|---|---|
| Small BEVs | 96 | 291 | 101 | 33 |
| Mid-size BEVs | 194 | 291 | 169 | 66 |
| Large BEVs | 241 | 353 | 295 | 100 |

**Supplementary Table 2.3: Sales-weighted average PHEV range, fuel economy, and motor power.** Average required battery capacity for PHEVs reaches around 12 kWh.

| PHEVs | Range (miles) | Fuel economy (Wh/mile) | Electric motor power (kW) | Required capacity (kWh) |
|---|---|---|---|---|
| Small PHEVs | 44 | 336 | 123 | 17 |
| Mid-size PHEVs | 22 | 303 | 55 | 8 |
| Large PHEVs | 22 | 470 | 61 | 12 |

**Supplementary Table 2.4: Summary of capacity of the cathode and anode of battery chemistry as input to the BatPaC model.** The majority of cathode and anode capacity are kept as defaults in the BatPaC model[70], unless otherwise based on Supplementary Table 2.28, Supplementary Table 2.15, Supplementary Table 2.13, or references. We use composite graphite anode with 9 wt% Si to represent Graphite (Si) anode in this table, and its capacity is from[135].

| Battery chemistry | Cathode | Cathode capacity (mAh/g) | Anode | Anode capacity (mAh/g) |
|---|---|---|---|---|
| LFP | $LiFePO_4$ | 150 | Graphite | 360 |
| NCA | $LiNi_{0.8}0Co_{0.15}Al_{0.05}O_2$ | 200 | Graphite | 360 |
| NCM111 | $Li_{1.05}(Ni_{1/3}Mn_{1/3}Co_{1/3})_{0.95}O_2$ | 155 | Graphite | 360 |
| NCM523 | $Li_{1.05}(Ni_{0.5}Mn_{0.3}Co_{0.2})_{0.95}O_2$ | 158 | Graphite | 360 |
| NCM622 | $Li_{1.05}(Ni_{0.6}Mn_{0.2}Co_{0.2})_{0.95}O_2$ | 180 | Graphite | 360 |
| NCM622-Graphite (Si) | $Li_{1.05}(Ni_{0.6}Mn_{0.2}Co_{0.2})_{0.95}O_2$ | 180 | Graphite (Si) | 517[135] |
| NCM811-Graphite (Si) | $Li_{1.05}(Ni_{0.8}Mn_{0.1}Co_{0.1})_{0.95}O_2$ | 191 | Graphite (Si) | 517[135] |
| NCM955-Graphite (Si) | $Li_{1.05}(Ni_{0.9}Mn_{0.05}Co_{0.05})_{0.95}O_2$ | 211 | Graphite (Si) | 517[135] |

**Supplementary Table 2.5: The minimum, most likely, and maximum lifespans of EVs from 2005 to 2050 as input to the calculation of shape and scale parameters of Weibull lifespan distribution of EVs (unit: year, expect for shape and scale parameters).**

| Period | Minimum lifespan, a | Most likely lifespan, d | Maximum lifespan, c | Shape parameter, α | Scale parameter, β |
|---|---|---|---|---|---|
| 2005-2050 | 1 | 15 | 20 | 6.3 | 14.4 |

**Supplementary Table 2.6: The minimum, most likely, and maximum lifespans of EV batteries from 2005 to 2050 as input to the calculation of shape and scale parameters of Weibull lifespan distribution of batteries (unit: year, except for shape and scale parameters).** Other chemistries refer to all battery chemistries except LFP.

| Period | Chemistries | Minimum lifespan, a | Most likely lifespan, d | Maximum lifespan, c | Shape parameter, α | Scale parameter, β |
|---|---|---|---|---|---|---|
| 2005-2019 | All chemistries | 1 | 8 | 15 | 3.1 | 7.9 |
| 2020-2050 | Other chemistries | 1 | 15 | 20 | 6.3 | 14.4 |
| 2020-2050 | LFP | 1 | 20 | 25 | 8.1 | 19.3 |

**Supplementary Table 2.7: Reference chemistry and changing parameters as input to the BatPaC model for the calculation of the material compositions of the non-existing battery chemistries in the BatPaC model.** Here we assume a linear growth for open circuit voltage (OCV) at different levels of battery state of charge (SOC) from NCM523, to NCM622-Graphite (Si), to NCM811-Graphite (Si), to NCM955-Graphite (Si). The OCV of NCM523 = the average of OCV (NCM111) and OCV (NCM622) in the BatPaC model. The OCV of NCM622-Graphite (Si) = OCV (NCM622) – 0.076 (see Supplementary Note 2.1 for the assuming average voltage difference between graphite (Si) anode and graphite anode). Cathode capacity and Li, Ni, Co, and Mn content are from Supplementary Table 2.14.

| Battery chemistry | NCM523 | NCM622-Graphite (Si) | NCM811-Graphite (Si) | NCM955-Graphite (Si) |
|---|---|---|---|---|
| Reference chemistry | NCM111 | NCM622 | NCM622 | NCM622 |
| Cathode capacity (mAh/g) | 158 | 180 | 191 | 211 |
| Anode capacity (mAh/g) | 360 | 517 | 517 | 517 |
| OCV at 20% SOC (V) | 3.5405 | 3.489 | 3.5135 | 3.538 |
| OCV at 50% SOC (V) | 3.7105 | 3.674 | 3.7135 | 3.753 |
| OCV at 80% SOC (V) | 3.95 | 3.924 | 3.974 | 4.024 |
| OCV at 100% SOC (V) | 4.15 | 4.124 | 4.174 | 4.224 |
| Li (g/g active material) | 0.07751513 | 0.077221916 | 0.076949595 | 0.076813626 |
| Ni (g/g active material) | 0.296520724 | 0.354478904 | 0.470971788 | 0.528915777 |
| Co (g/g active material) | 0.119093288 | 0.118642798 | 0.059112203 | 0.031060614 |
| Mn (g/g active material) | 0.166530137 | 0.11060014 | 0.055105055 | 0.027508722 |

**Supplementary Table 2.8: Review of the specific energy of Li-S chemistry on cell level (unit: Wh/kg).**

| References | Battery shape | Specific energy | Technology readiness |
|---|---|---|---|
| Ref1[136] | | 400 | |
| Ref2[137] | | 370 | |
| Ref3[138] | | 300-620 | R&D |
| Ref4[90] | Pouch | 300-400 | |
| Ref4[90] | Pouch | 500-600 | R&D |
| Ref5[139] | | 400-620 | |
| Ref6[136] | Pouch | 350-400 | Commercial |
| Ref7[140] | Pouch | 300 | Lab |

**Supplementary Table 2.9: Review of the specific energy of Li-Air chemistry on cell level (unit: Wh/kg).**

| References | Battery shape | Specific energy | Technology readiness |
|---|---|---|---|
| Ref1[136] | | 1700 | |
| Ref2[137] | | 1700 | |
| Ref3[138] | | 500-900 | |
| Ref4[141] | Pouch | 362 | R&D |
| Ref5[91] | | 520 | |
| Ref6[142] | Coin | 1000 | |
| Ref7[143] | Folded structure | 1214 | |
| Ref8[139] | | 500-1000 | |

**Supplementary Table 2.10: Modelled material compositions of a Li-S (600 Wh/kg) and a Li-Air (1000 Wh/kg) pack used for sensitivity analysis.** (unit: kg per battery pack)

| EV types | Materials | Li-Sulphur | Li-Air |
|---|---|---|---|
| Small BEVs | Li ion | 0.19 | 0.12 |
| | Li metal | 3.62 | 1.69 |
| | Al | 16.42 | 9.92 |
| | Cu | 6.44 | 0.27 |
| | Al in modules | 6.86 | 4.18 |
| | Cu in modules | 6.14 | 0.10 |
| Mid-size BEVs | Li ion | 0.39 | 0.24 |
| | Li metal | 7.30 | 3.40 |
| | Al | 30.20 | 18.25 |
| | Cu | 13.33 | 0.77 |
| | Al in modules | 13.72 | 8.36 |
| | Cu in modules | 12.53 | 0.29 |
| Large BEVs | Li ion | 0.59 | 0.36 |
| | Li metal | 11.03 | 5.13 |
| | Al | 45.64 | 27.58 |
| | Cu | 21.75 | 2.12 |
| | Al in modules | 20.63 | 12.58 |
| | Cu in modules | 20.52 | 1.39 |
| Small PHEVs | Li ion | 0.10 | 0.06 |
| | Li metal | 1.91 | 0.89 |
| | Al | 7.26 | 4.39 |
| | Cu | 7.52 | 2.62 |
| | Al in modules | 3.53 | 2.15 |
| | Cu in modules | 4.37 | 2.62 |

Supplementary Table 2.10 (continued).

| EV types | Materials | Li-Sulphur | Li-Air |
|---|---|---|---|
| Mid-size PHEVs | Li ion | 0.05 | 0.03 |
| | Li metal | 0.88 | 0.41 |
| | Al | 3.97 | 2.40 |
| | Cu | 4.51 | 1.84 |
| | Al in modules | 1.70 | 1.04 |
| | Cu in modules | 3.06 | 1.84 |
| Large PHEVs | Li ion | 0.07 | 0.04 |
| | Li metal | 1.32 | 0.61 |
| | Al | 5.48 | 3.31 |
| | Cu | 7.26 | 3.05 |
| | Al in modules | 2.49 | 1.52 |
| | Cu in modules | 5.08 | 3.05 |

**Supplementary Table 2.11: Comparisons of three EV battery recycling technologies by recycled material type, recycling efficiency, and the quality of recovered materials, where mechanical recycling is especially for the recovery of Li metal (a different form compared to Li ion in chemicals), Al, and Cu form Li-S and Li-Air chemistry.** Numbers in the table show the material recycling efficiencies. The different colors show the feasibility of recovered materials being reused in new battery production (*i.e.*, closed-loop recycling). Yellow color indicates the economic feasibility of closed-loop recycling is in question, but maybe become potentially economical with future technology development and price fluctuance of recovered materials. Pyro and hydro recycling are already commercially available, while direct recycling and mechanical recycling marked with star (*) are in still lab-scale development.

| Technology | Li | Ni | Co | Mn | Al | Cu | Graphite | Si |
|---|---|---|---|---|---|---|---|---|
| Pyro | 90% | 98% | 98% | 90% | 0% | 90% | 0% | 0% |
| Hydro | 90% | 98% | 98% | 98% | 90% | 90% | 90% | 90% |
| Direct* | 90% | 90% | 90% | 90% | 90% | 90% | 90% | 90% |
| Mechanical* | 90% | | | | 90% | 90% | | |

| | |
|---|---|
| | Not present |
| | Lost |
| | Potentially economical |
| | Eonomical |

**Supplementary Table 2.12: Assumptions of second-use rate of batteries distinguished by LFP and other chemistries, based on the assumptions of EV and battery lifespan distribution** (Supplementary Table 2.19 and Supplementary Table 2.20).

| Periods | Battery chemistry | Second-use rate |
|---|---|---|
| 2005-2019 | LFP | 100% |
| | Others | 50% |
| 2020-2050 | LFP | 100% |
| | Others | 75% |

**Supplementary Table 2.13: Material compositions of a BEV battery with 110 kWh capacity used for sensitivity analysis.** (unit: kg per battery pack)

| EV types | Materials | LFP | NCA | NCM111 | NCM523 | NCM622 | NCM622-Graphite (Si) | NCM811-Graphite (Si) | NCM955-Graphite (Si) | Li-Sulphur | Li-Air |
|---|---|---|---|---|---|---|---|---|---|---|---|
| BEV with 110 kWh capacity | Li ion | 10.98 | 11.35 | 15.63 | 15.16 | 13.16 | 13.36 | 12.42 | 11.13 | 0.96 | 0.78 |
| | Li metal | 0.00 | 0.00 | 0.00 | 0.00 | 0.00 | 0.00 | 0.00 | 0.00 | 18.15 | 11.26 |
| | Ni | 0.00 | 73.36 | 38.42 | 55.88 | 58.02 | 59.22 | 73.36 | 73.79 | 0.00 | 0.00 |
| | Co | 0.00 | 13.81 | 38.58 | 22.45 | 19.42 | 19.82 | 9.21 | 4.33 | 0.00 | 0.00 |
| | Mn | 0.00 | 0.00 | 35.97 | 31.39 | 18.10 | 18.48 | 8.58 | 3.84 | 0.00 | 0.00 |
| | Al | 172.79 | 135.08 | 141.95 | 140.31 | 136.19 | 130.17 | 127.98 | 124.94 | 75.12 | 60.53 |
| | Cu | 99.58 | 86.46 | 87.62 | 86.66 | 85.42 | 86.01 | 85.07 | 84.02 | 35.80 | 4.66 |
| | Graphite | 130.80 | 117.71 | 120.79 | 119.27 | 116.56 | 78.64 | 77.26 | 75.60 | 0.00 | 0.00 |
| | Si | 0.00 | 0.00 | 0.00 | 0.00 | 0.00 | 7.78 | 7.64 | 7.48 | 0.00 | 0.00 |
| | Al in modules | 85.70 | 66.31 | 69.31 | 68.54 | 66.54 | 64.01 | 62.84 | 61.37 | 33.96 | 27.60 |
| | Cu in modules | 95.86 | 83.15 | 84.30 | 83.38 | 82.18 | 82.70 | 81.80 | 80.78 | 33.78 | 3.04 |

**Supplementary Table 2.14: Material compositions of a PHEV battery with 10 kWh capacity used for sensitivity analysis.** (unit: kg per battery pack)

| EV types | Materials | LFP | NCA | NCM111 | NCM523 | NCM622 | NCM622-Graphite (Si) | NCM811-Graphite (Si) | NCM955-Graphite (Si) | Li-Sulphur | Li-Air |
|---|---|---|---|---|---|---|---|---|---|---|---|
| PHEV with 10 kWh capacity | Li ion | 1.01 | 1.04 | 1.42 | 1.38 | 1.20 | 1.22 | 1.13 | 1.02 | 0.09 | 0.07 |
| | Li metal | 0.00 | 0.00 | 0.00 | 0.00 | 0.00 | 0.00 | 0.00 | 0.00 | 1.65 | 1.02 |
| | Ni | 0.00 | 6.66 | 3.49 | 5.07 | 5.27 | 5.37 | 6.66 | 6.70 | 0.00 | 0.00 |
| | Co | 0.00 | 1.25 | 3.50 | 2.04 | 1.76 | 1.80 | 0.84 | 0.39 | 0.00 | 0.00 |
| | Mn | 0.00 | 0.00 | 3.26 | 2.85 | 1.64 | 1.68 | 0.78 | 0.35 | 0.00 | 0.00 |
| | Al | 29.81 | 16.90 | 17.27 | 17.13 | 16.86 | 16.45 | 16.29 | 16.14 | 6.28 | 5.07 |
| | Cu | 34.74 | 23.03 | 22.70 | 22.67 | 22.74 | 23.23 | 23.22 | 23.30 | 6.50 | 3.02 |
| | Graphite | 11.83 | 10.71 | 10.99 | 10.86 | 10.61 | 7.16 | 7.03 | 6.88 | 0.00 | 0.00 |
| | Si | 0.00 | 0.00 | 0.00 | 0.00 | 0.00 | 0.71 | 0.70 | 0.68 | 0.00 | 0.00 |
| | Al in modules | 15.69 | 8.75 | 8.83 | 8.72 | 8.63 | 8.57 | 8.49 | 8.46 | 3.05 | 2.48 |
| | Cu in modules | 22.07 | 11.57 | 11.19 | 11.08 | 11.20 | 11.65 | 11.65 | 11.80 | 3.78 | 3.02 |

**Supplementary Table 2.15: Specific energy of EV battery pack (unit: Wh/kg).**

| EV types | LFP | NCA | NCM111 | NCM523 | NCM622 | NCM622-Graphite (Si) | NCM811-Graphite (Si) | NCM955-Graphite (Si) | Li-Sulphur | Li-Air |
|---|---|---|---|---|---|---|---|---|---|---|
| Small BEVs | 122 | 169 | 151 | 153 | 164 | 176 | 183 | 192 | 295 | 365 |
| Mid-size BEVs | 129 | 178 | 160 | 163 | 174 | 186 | 193 | 202 | 308 | 383 |
| Large BEVs | 128 | 176 | 159 | 162 | 172 | 185 | 191 | 201 | 308 | 384 |
| Small PHEVs | 101 | 151 | 132 | 134 | 147 | 155 | 161 | 169 | 265 | 327 |
| Mid-size PHEVs | 74 | 109 | 103 | 104 | 109 | 116 | 118 | 121 | 224 | 272 |
| Large PHEVs | 75 | 115 | 106 | 108 | 114 | 119 | 121 | 124 | 234 | 287 |

**Supplementary Table 2.16: Cumulative demand for Li, Co, Ni, Mn, Al, Cu, graphite, and Si in 2020-2050 without recycling, compared to global known reserves in 2019 (unit: Mt).** Note Li demand includes Li ion demand (in the form of chemicals like $Li_2CO_3$) and Li metal demand in the Li-S/Air battery scenario, for example, 9.1 (4.8) for Li demand under the STEP and Li-S/Air scenario is shown in the form of total Li demand (Li metal demand). * Yearend production capacity for Al reserve. ‡ Si reserves are not available, but ample for use. Known reserves in 2019 are referred from USGS[144].

| Materials | STEP scenario, NCX | STEP scenario, LFP | STEP scenario, Li-S/Air | SD scenario, NCX | SD scenario, LFP | SD scenario, Li-S/Air | Known reserves in 2019 |
|---|---|---|---|---|---|---|---|
| Li | 7.8 | 7.3 | 8.8 (4.6) | 16.0 | 15.1 | 18.3 (9.6) | 17 |
| Co | 8.1 | 3.5 | 4.3 | 16.8 | 7.1 | 8.8 | 7 |
| Ni | 43.0 | 18.1 | 21.9 | 88.9 | 37.2 | 44.7 | 89 |
| Mn | 5.2 | 2.2 | 2.7 | 10.6 | 4.5 | 5.5 | 810 |
| Al | 89.3 | 106.5 | 67.4 | 183.8 | 218.7 | 138.1 | 77.9* |
| Cu | 59.8 | 66.8 | 37.6 | 121.0 | 134.6 | 75.4 | 870 |
| Graphite | 62.4 | 74.8 | 32.6 | 128.8 | 154.4 | 66.2 | 300 |
| Si | 2.4 | 1.0 | 1.2 | 5.0 | 2.1 | 2.4 | Ample‡ |

**Supplementary Table 2.17: Effects of recycling on cumulative demand for Li, Ni, Co, Mn, Al, Cu, graphite, and Si in 2020-2050.** Numbers in the table represent reduction percentages by recycling compared to primary cumulative demand. Note Li demand includes Li ion demand (in the form of lithium chemicals) and Li metal demand in the Li-S/Air battery scenario. For example, 20.2% (8.0%) under the STEP scenario is shown in the form of the reduction percentage of total Li demand (reduction percentage of Li metal demand). The reduction percentage of total Li demand is more than 2 times the reduction percentage of Li metal demand. From this table, we can see the reduction of cumulative material demand through 2050 could reach around 20%-30% by recycling in the NCX and LFP scenarios, while it is raised to around 30%-40% in the Li-S/Air scenario due to the quick shift of battery chemistry in this scenario. There is no big difference in reduction percentages among materials and between the STEP scenario and SD scenario.

| Materials | STEP scenario, NCX | STEP scenario, LFP | STEP scenario, Li-S/Air | SD scenario, NCX | SD scenario, LFP | SD scenario, Li-S/Air |
|---|---|---|---|---|---|---|
| Li | 23.2% | 23.1% | 21.3% (8.4%) | 21.6% | 21.5% | 19.9% (8.3%) |
| Co | 28.2% | 32.5% | 44.0% | 26.3% | 29.5% | 41.0% |
| Ni | 23.6% | 26.6% | 37.7% | 22.2% | 24.6% | 35.4% |
| Mn | 28.1% | 33.0% | 44.1% | 25.9% | 29.4% | 40.6% |
| Al | 23.2% | 22.6% | 28.0% | 21.7% | 21.2% | 26.0% |
| Cu | 23.1% | 22.8% | 31.7% | 21.6% | 21.3% | 29.6% |
| Graphite | 24.2% | 23.0% | 38.2% | 22.5% | 21.5% | 35.6% |
| Si | 16.7% | 18.0% | 27.3% | 15.9% | 17.0% | 25.9% |

**Supplementary Table 2.18: Closed-loop recycling potential (CLRP) in 2020-2029, 2030-2039, 2040-2050 in the STEP scenario by battery chemistry scenarios, recycling technologies, and second life use.**

| *Battery scenarios* | | *NCX* | | | *LFP* | | | *Li-S/Air* | | |
|---|---|---|---|---|---|---|---|---|---|---|
| *Time periods* | | *2020-2029* | *2030-2039* | *2040-2050* | *2020-2029* | *2030-2039* | *2040-2050* | *2020-2029* | *2030-2039* | *2040-2050* |
| *Li ion* | *No second life, pyro* | 0.03 | 0.17 | 0.28 | 0.03 | 0.17 | 0.28 | 0.03 | 0.24 | 0.50 |
| | *No second life, hydro* | 0.03 | 0.17 | 0.28 | 0.03 | 0.17 | 0.28 | 0.03 | 0.24 | 0.50 |
| | *No second life, direct* | 0.03 | 0.17 | 0.28 | 0.03 | 0.17 | 0.28 | 0.03 | 0.24 | 0.50 |
| | *Second life, pyro* | 0.01 | 0.04 | 0.13 | 0.01 | 0.04 | 0.10 | 0.01 | 0.06 | 0.26 |
| | *Second life, hydro* | 0.01 | 0.04 | 0.13 | 0.01 | 0.04 | 0.10 | 0.01 | 0.06 | 0.26 |
| | *Second life, direct* | 0.01 | 0.04 | 0.13 | 0.01 | 0.04 | 0.10 | 0.01 | 0.06 | 0.26 |
| *Li metal* | *No second life, mechanical* | | | | | | | 0.00 | 0.00 | 0.11 |
| | *Second life, mechanical* | | | | | | | 0.00 | 0.00 | 0.03 |
| *Co* | *No second life, pyro* | 0.04 | 0.19 | 0.36 | 0.06 | 0.33 | 0.38 | 0.04 | 0.28 | 0.71 |
| | *No second life, hydro* | 0.04 | 0.19 | 0.36 | 0.06 | 0.33 | 0.38 | 0.04 | 0.28 | 0.71 |
| | *No second life, direct* | 0.03 | 0.17 | 0.33 | 0.06 | 0.30 | 0.35 | 0.03 | 0.25 | 0.65 |
| | *Second life, pyro* | 0.01 | 0.06 | 0.17 | 0.02 | 0.10 | 0.22 | 0.01 | 0.08 | 0.36 |
| | *Second life, hydro* | 0.01 | 0.06 | 0.17 | 0.02 | 0.10 | 0.22 | 0.01 | 0.08 | 0.36 |
| | *Second life, direct* | 0.01 | 0.05 | 0.15 | 0.02 | 0.10 | 0.20 | 0.01 | 0.08 | 0.33 |
| *Ni* | *No second life, pyro* | 0.02 | 0.15 | 0.29 | 0.04 | 0.26 | 0.30 | 0.02 | 0.23 | 0.56 |
| | *No second life, hydro* | 0.02 | 0.15 | 0.29 | 0.04 | 0.26 | 0.30 | 0.02 | 0.23 | 0.56 |
| | *No second life, direct* | 0.02 | 0.14 | 0.27 | 0.04 | 0.24 | 0.28 | 0.02 | 0.21 | 0.52 |
| | *Second life, pyro* | 0.01 | 0.04 | 0.12 | 0.01 | 0.08 | 0.16 | 0.01 | 0.06 | 0.27 |
| | *Second life, hydro* | 0.01 | 0.04 | 0.12 | 0.01 | 0.08 | 0.16 | 0.01 | 0.06 | 0.27 |
| | *Second life, direct* | 0.01 | 0.04 | 0.11 | 0.01 | 0.07 | 0.15 | 0.01 | 0.06 | 0.25 |
| *Mn* | *No second life, pyro* | 0.05 | 0.18 | 0.32 | 0.09 | 0.33 | 0.33 | 0.05 | 0.27 | 0.62 |
| | *No second life, hydro* | 0.06 | 0.20 | 0.35 | 0.10 | 0.36 | 0.36 | 0.06 | 0.30 | 0.68 |
| | *No second life, direct* | 0.05 | 0.18 | 0.32 | 0.09 | 0.33 | 0.33 | 0.05 | 0.27 | 0.62 |
| | *Second life, pyro* | 0.01 | 0.07 | 0.18 | 0.02 | 0.13 | 0.24 | 0.01 | 0.10 | 0.39 |
| | *Second life, hydro* | 0.02 | 0.07 | 0.19 | 0.03 | 0.14 | 0.26 | 0.02 | 0.11 | 0.43 |
| | *Second life, direct* | 0.01 | 0.07 | 0.18 | 0.02 | 0.13 | 0.24 | 0.01 | 0.10 | 0.39 |
| *Al* | *No second life, pyro* | 0.00 | 0.00 | 0.00 | 0.00 | 0.00 | 0.00 | 0.00 | 0.00 | 0.00 |
| | *No second life, hydro* | 0.03 | 0.17 | 0.28 | 0.03 | 0.16 | 0.28 | 0.03 | 0.21 | 0.36 |
| | *No second life, direct* | 0.03 | 0.17 | 0.28 | 0.03 | 0.16 | 0.28 | 0.03 | 0.21 | 0.36 |
| | *Second life, pyro* | 0.00 | 0.00 | 0.00 | 0.00 | 0.00 | 0.00 | 0.00 | 0.00 | 0.00 |
| | *Second life, hydro* | 0.02 | 0.11 | 0.21 | 0.02 | 0.09 | 0.18 | 0.02 | 0.13 | 0.27 |
| | *Second life, direct* | 0.02 | 0.11 | 0.21 | 0.02 | 0.09 | 0.18 | 0.02 | 0.13 | 0.27 |
| Cu | No second life, pyro | 0.03 | 0.17 | 0.28 | 0.03 | 0.16 | 0.28 | 0.03 | 0.23 | 0.43 |
| | No second life, hydro | 0.03 | 0.17 | 0.28 | 0.03 | 0.16 | 0.28 | 0.03 | 0.23 | 0.43 |
| | No second life, direct | 0.03 | 0.17 | 0.28 | 0.03 | 0.16 | 0.28 | 0.03 | 0.23 | 0.43 |
| | Second life, pyro | 0.01 | 0.06 | 0.15 | 0.01 | 0.04 | 0.11 | 0.01 | 0.08 | 0.24 |
| | Second life, hydro | 0.01 | 0.06 | 0.15 | 0.01 | 0.04 | 0.11 | 0.01 | 0.08 | 0.24 |
| | Second life, direct | 0.01 | 0.06 | 0.15 | 0.01 | 0.04 | 0.11 | 0.01 | 0.08 | 0.24 |
| Graphite | No second life, pyro | 0.00 | 0.00 | 0.00 | 0.00 | 0.00 | 0.00 | 0.00 | 0.00 | 0.00 |
| | No second life, hydro | 0.03 | 0.18 | 0.29 | 0.03 | 0.16 | 0.28 | 0.03 | 0.27 | 0.57 |
| | No second life, direct | 0.03 | 0.18 | 0.29 | 0.03 | 0.16 | 0.28 | 0.03 | 0.27 | 0.57 |
| | Second life, pyro | 0.00 | 0.00 | 0.00 | 0.00 | 0.00 | 0.00 | 0.00 | 0.00 | 0.00 |
| | Second life, hydro | 0.01 | 0.05 | 0.14 | 0.01 | 0.03 | 0.09 | 0.01 | 0.07 | 0.31 |
| | Second life, direct | 0.01 | 0.05 | 0.14 | 0.01 | 0.03 | 0.09 | 0.01 | 0.07 | 0.31 |
| Si | No second life, pyro | 0.00 | 0.00 | 0.00 | 0.00 | 0.00 | 0.00 | 0.00 | 0.00 | 0.00 |
| | No second life, hydro | 0.01 | 0.08 | 0.20 | 0.01 | 0.13 | 0.21 | 0.01 | 0.13 | 0.38 |
| | No second life, direct | 0.01 | 0.08 | 0.20 | 0.01 | 0.13 | 0.21 | 0.01 | 0.13 | 0.38 |
| | Second life, pyro | 0.00 | 0.00 | 0.00 | 0.00 | 0.00 | 0.00 | 0.00 | 0.00 | 0.00 |
| | Second life, hydro | 0.00 | 0.02 | 0.07 | 0.00 | 0.03 | 0.09 | 0.00 | 0.03 | 0.16 |
| | Second life, direct | 0.00 | 0.02 | 0.07 | 0.00 | 0.03 | 0.09 | 0.00 | 0.03 | 0.16 |

**Supplementary Table 2.19: Annual material demand in 2050 by three battery chemistry scenarios without recycling, with recycling, and with recycling and second life, and 2019 global mining production (unit: Mt) in the STEP scenario.** The annual demand in 2050 for Li, Ni, Co, and graphite (natural graphite) from EV batteries alone exceed global mining production in 2019.

| *Materials* | *Demand sceanrios* | *Battery scenarios / Mt* | | | *2019 annual production / Mt* | *Demand as percent of 2019 production* | | |
|---|---|---|---|---|---|---|---|---|
| | | *NCX* | *LFP* | *Li-S/Air* | | *NCX* | *LFP* | *Li-S/Air* |
| *Li* | *Without recycling* | 0.65 | 0.62 | 0.77 | 0.077 | 848% | 807% | 1002% |
| | *With recycling* | 0.45 | 0.43 | 0.55 | | 590% | 565% | 715% |
| | *With recycling and second life* | 0.55 | 0.54 | 0.66 | | 717% | 707% | 863% |
| *Co* | *Without recycling* | 0.62 | 0.25 | 0.25 | 0.14 | 440% | 179% | 176% |
| | *With recycling* | 0.37 | 0.15 | 0.10 | | 265% | 107% | 72% |
| | *With recycling and second life* | 0.49 | 0.19 | 0.14 | | 347% | 136% | 102% |
| *Ni* | *Without recycling* | 3.75 | 1.53 | 1.50 | 2.7 | 139% | 57% | 56% |
| | *With recycling* | 2.57 | 1.04 | 0.81 | | 95% | 39% | 30% |
| | *With recycling and second life* | 3.16 | 1.25 | 1.04 | | 117% | 46% | 38% |
| *Mn* | *Without recycling* | 0.40 | 0.16 | 0.16 | 19 | 2% | 1% | 1% |
| | *With recycling* | 0.25 | 0.10 | 0.07 | | 1% | 1% | 0% |
| | *With recycling and second life* | 0.30 | 0.12 | 0.08 | | 2% | 1% | 0% |
| *Al* | *Without recycling* | 7.53 | 9.08 | 5.25 | 64 | 12% | 14% | 8% |
| | *With recycling* | 5.25 | 6.37 | 3.45 | | 8% | 10% | 5% |
| | *With recycling and second life* | 5.79 | 7.18 | 3.81 | | 9% | 11% | 6% |
| *Cu* | *Without recycling* | 5.06 | 5.68 | 2.73 | 20 | 25% | 28% | 14% |
| | *With recycling* | 3.55 | 3.99 | 1.70 | | 18% | 20% | 8% |
| | *With recycling and second life* | 4.21 | 4.91 | 2.04 | | 21% | 25% | 10% |
| *Graphite* | *Without recycling* | 5.11 | 6.31 | 2.04 | 1.1 | 464% | 574% | 186% |
| | *With recycling* | 3.48 | 4.40 | 1.08 | | 317% | 400% | 98% |
| | *With recycling and second life* | 4.27 | 5.57 | 1.37 | | 388% | 506% | 125% |
| *Si* | *Without recycling* | 0.25 | 0.10 | 0.10 | 7 | 4% | 1% | 1% |
| | *With recycling* | 0.19 | 0.08 | 0.07 | | 3% | 1% | 1% |
| | *With recycling and second life* | 0.22 | 0.09 | 0.08 | | 3% | 1% | 1% |

**Supplementary Table 2.20: Annual material demand in 2050 by three battery chemistry scenarios without recycling, with recycling, and with recycling and second life, and 2019 global mining production (unit: Mt) in the SD scenario.**

| *Materials* | *Demand sceanrios* | *Battery scenarios / Mt* | | | *2019 annual production / Mt* | *Demand as percent of 2019 production* | | |
|---|---|---|---|---|---|---|---|---|
| | | *NCX* | *LFP* | *Li-S/Air* | | *NCX* | *LFP* | *Li-S/Air* |
| *Li* | *Without recycling* | 1.33 | 1.26 | 1.57 | 0.077 | 1724% | 1641% | 2038% |
| | *With recycling* | 0.91 | 0.87 | 1.11 | | 1183% | 1133% | 1435% |
| | *With recycling and second life* | 1.23 | 1.19 | 1.46 | | 1593% | 1542% | 1899% |
| *Co* | *Without recycling* | 1.25 | 0.51 | 0.50 | 0.14 | 894% | 364% | 358% |
| | *With recycling* | 0.74 | 0.30 | 0.20 | | 527% | 214% | 141% |
| | *With recycling and second life* | 1.12 | 0.45 | 0.40 | | 801% | 320% | 283% |
| *Ni* | *Without recycling* | 7.63 | 3.10 | 3.05 | 2.7 | 282% | 115% | 113% |
| | *With recycling* | 5.15 | 2.09 | 1.60 | | 191% | 77% | 59% |
| | *With recycling and second life* | 7.04 | 2.83 | 2.59 | | 261% | 105% | 96% |
| *Mn* | *Without recycling* | 0.81 | 0.33 | 0.33 | 19 | 4% | 2% | 2% |
| | *With recycling* | 0.49 | 0.20 | 0.14 | | 3% | 1% | 1% |
| | *With recycling and second life* | 0.72 | 0.29 | 0.25 | | 4% | 2% | 1% |
| *Al* | *Without recycling* | 15.27 | 18.37 | 10.66 | 64 | 24% | 29% | 17% |
| | *With recycling* | 10.51 | 12.71 | 6.91 | | 16% | 20% | 11% |
| | *With recycling and second life* | 13.54 | 16.47 | 9.22 | | 21% | 26% | 14% |
| *Cu* | *Without recycling* | 10.09 | 11.28 | 5.44 | 20 | 50% | 56% | 27% |
| | *With recycling* | 6.97 | 7.80 | 3.32 | | 35% | 39% | 17% |
| | *With recycling and second life* | 9.24 | 10.50 | 4.75 | | 46% | 53% | 24% |
| *Graphite* | *Without recycling* | 10.39 | 12.84 | 4.16 | 1.1 | 944% | 1167% | 378% |
| | *With recycling* | 6.98 | 8.82 | 2.15 | | 634% | 802% | 196% |
| | *With recycling and second life* | 9.55 | 12.09 | 3.48 | | 868% | 1099% | 317% |
| *Si* | *Without recycling* | 0.50 | 0.20 | 0.20 | 7 | 7% | 3% | 3% |
| | *With recycling* | 0.38 | 0.16 | 0.13 | | 5% | 2% | 2% |
| | *With recycling and second life* | 0.47 | 0.19 | 0.18 | | 7% | 3% | 3% |

**Supplementary Table 2.21: Selected specific energy of Li-S and Li-Air cells used for calculating material compositions and sensitivity analysis values for specific energy(unit: Wh/kg), which is based on Supplementary Table 2.22 and Supplementary Table 2.1.**

| Chemistry | Baseline | Sensitivity analysis |
|---|---|---|
| Li-S | 400 | 600 |
| Li-Air | 500 | 1000 |

**Supplementary Table 2.22: Sensitivity analysis of lower battery lifespan (*i.e.*, one EV will use 1.5 battery packs on average after 2020, while in the baseline scenario one EV will use 1 battery pack after 2020) for cumulative demand for Li, Co, Ni, Mn, Al, Cu, graphite, and Si in 2020-2050 without recycling, compared to global known reserves in 2019 (unit: Mt).** * Yearend production capacity for Al reserve. ‡ Si reserves are not available, but ample for use. Known reserves in 2019 are referred from USGS[144].

| Materials | STEP scenario, NCX scenario | STEP scenario, NCX scenario, with lower battery lifespan | SD scenario, NCX scenario | SD scenario, NCX scenario, with lower battery lifespan | Known reserves in 2019 |
|---|---|---|---|---|---|
| Li | 7.8 | 8.8 | 16.0 | 18.1 | 17 |
| Co | 8.1 | 9.2 | 16.8 | 18.9 | 7 |
| Ni | 43.0 | 49.0 | 88.9 | 100.6 | 89 |
| Mn | 5.2 | 5.8 | 10.6 | 12.0 | 810 |
| Al | 89.3 | 101.6 | 183.8 | 207.6 | 77.9* |
| Cu | 59.8 | 68.1 | 121.0 | 136.9 | 870 |
| Graphite | 62.4 | 70.9 | 128.8 | 145.3 | 300 |
| Si | 2.4 | 2.8 | 5.0 | 5.7 | Ample‡ |

**Supplementary Table 2.23: Review of cathode capacity of NCM523 (unit: mAh/g).** We use the average number in this table as input into the BatPaC model to calculate battery material compositions of NCM523 chemistry.

| References | Cathode capacity of NCM523 |
|---|---|
| Ref1[145] | 157 |
| Ref2[146] | 164 |
| Ref3[147] | 150 |
| Ref3[147] | 142 |
| Ref3[147] | 175 |
| Average | 158 |

**Supplementary Table 2.24: Review of cathode capacity of NCM811 (unit: mAh/g).** We use the average number in this table as input into the BatPaC model to calculate battery material compositions of NCM811-Graphite (Si).

| References | Cathode capacity of NCM811 |
|---|---|
| Ref1[148] | 207 |
| Ref2[145] | 200 |
| Ref3[147] | 194 |
| Ref3[147] | 185 |
| Ref3[147] | 178 |
| Ref3[147] | 186 |
| Ref3[147] | 188 |
| Ref3[147] | 193 |
| Ref4[149] | 192 |
| Average | 191 |

**Supplementary Table 2.25: Review of cathode capacity of NCM955 (unit: mAh/g).** We use the average number in this table as input into the BatPaC model to calculate battery material compositions of NCM955-Graphite (Si).

| References | Cathode capacity of NCM955 |
|---|---|
| Ref1[147] | 205 |
| Ref2[149] | 217 |
| Average | 211 |

**Supplementary Table 2.26: EV battery material compositions on pack level calculated by the BatPaC model (unit: kg per battery pack).** Note the material compositions of Li-S and Li-Air are calculated based on literature and report data. Table continued till Page 80.

| EV types | Materials | LFP | NCA | NCM111 | NCM523 | NCM622 | NCM622-Graphite (Si) | NCM811-Graphite (Si) | NCM955-Graphite (Si) | Li-Sulphur | Li-Air |
|---|---|---|---|---|---|---|---|---|---|---|---|
| Small BEVs | Li ion | 3.29 | 3.40 | 4.68 | 4.54 | 3.94 | 4.00 | 3.72 | 3.33 | 0.29 | 0.23 |
| | Li metal | 0.00 | 0.00 | 0.00 | 0.00 | 0.00 | 0.00 | 0.00 | 0.00 | 5.44 | 3.37 |
| | Ni | 0.00 | 21.97 | 11.50 | 16.73 | 17.38 | 17.74 | 21.97 | 22.10 | 0.00 | 0.00 |
| | Co | 0.00 | 4.14 | 11.55 | 6.72 | 5.82 | 5.94 | 2.76 | 1.30 | 0.00 | 0.00 |
| | Mn | 0.00 | 0.00 | 10.77 | 9.40 | 5.42 | 5.53 | 2.57 | 1.15 | 0.00 | 0.00 |
| | Al | 58.66 | 45.71 | 49.02 | 48.42 | 46.33 | 44.33 | 43.23 | 42.23 | 24.63 | 19.83 |
| | Cu | 29.14 | 24.51 | 26.74 | 26.29 | 24.71 | 24.97 | 24.16 | 23.88 | 9.66 | 0.55 |
| | Graphite | 39.18 | 35.30 | 36.19 | 35.74 | 34.95 | 23.58 | 23.17 | 22.67 | 0.00 | 0.00 |
| | Si | 0.00 | 0.00 | 0.00 | 0.00 | 0.00 | 2.33 | 2.29 | 2.24 | 0.00 | 0.00 |
| Mid-size BEVs | Li | 6.62 | 6.84 | 9.43 | 9.14 | 7.94 | 8.06 | 7.49 | 6.72 | 0.58 | 0.47 |
| | Li metal | 0.00 | 0.00 | 0.00 | 0.00 | 0.00 | 0.00 | 0.00 | 0.00 | 10.95 | 6.79 |
| | Ni | 0.00 | 44.26 | 23.18 | 33.71 | 35.00 | 35.73 | 44.26 | 44.51 | 0.00 | 0.00 |
| | Co | 0.00 | 8.33 | 23.27 | 13.54 | 11.71 | 11.96 | 5.55 | 2.61 | 0.00 | 0.00 |

| | | | | | | | | | | | |
|---|---|---|---|---|---|---|---|---|---|---|---|
| | Mn | 0.00 | 0.00 | 21.70 | 18.93 | 10.92 | 11.15 | 5.18 | 2.32 | 0.00 | 0.00 |
| | Al | 106.87 | 83.41 | 87.69 | 86.68 | 84.12 | 80.35 | 78.98 | 77.11 | 45.30 | 36.50 |
| | Cu | 56.33 | 49.16 | 49.70 | 49.17 | 48.54 | 49.08 | 48.58 | 48.03 | 20.00 | 1.53 |
| | Graphite | 78.84 | 70.93 | 72.79 | 71.87 | 70.24 | 47.39 | 46.55 | 45.55 | 0.00 | 0.00 |
| | Si | 0.00 | 0.00 | 0.00 | 0.00 | 0.00 | 4.69 | 4.60 | 4.51 | 0.00 | 0.00 |
| Large BEVs | Li | 10.01 | 10.34 | 14.24 | 13.81 | 11.99 | 12.17 | 11.32 | 10.15 | 0.88 | 0.71 |
| | Li metal | 0.00 | 0.00 | 0.00 | 0.00 | 0.00 | 0.00 | 0.00 | 0.00 | 16.54 | 10.27 |
| | Ni | 0.00 | 66.86 | 35.02 | 50.93 | 52.88 | 53.97 | 66.86 | 67.25 | 0.00 | 0.00 |
| | Co | 0.00 | 12.59 | 35.16 | 20.46 | 17.70 | 18.06 | 8.39 | 3.95 | 0.00 | 0.00 |
| | Mn | 0.00 | 0.00 | 32.78 | 28.60 | 16.50 | 16.84 | 7.82 | 3.50 | 0.00 | 0.00 |
| | Al | 162.87 | 127.52 | 134.00 | 132.45 | 128.57 | 122.92 | 120.86 | 118.01 | 68.46 | 55.16 |
| | Cu | 92.60 | 80.24 | 81.37 | 80.50 | 79.37 | 79.90 | 79.05 | 78.09 | 32.63 | 4.25 |
| | Graphite | 119.32 | 107.42 | 110.22 | 108.83 | 106.37 | 71.77 | 70.51 | 69.00 | 0.00 | 0.00 |
| | Si | 0.00 | 0.00 | 0.00 | 0.00 | 0.00 | 7.10 | 6.97 | 6.82 | 0.00 | 0.00 |
| Small PHEVs | Li | 1.74 | 1.79 | 2.47 | 2.39 | 2.08 | 2.11 | 1.96 | 1.76 | 0.15 | 0.12 |
| | Li metal | 0.00 | 0.00 | 0.00 | 0.00 | 0.00 | 0.00 | 0.00 | 0.00 | 2.86 | 1.78 |
| | Ni | 0.00 | 11.56 | 6.05 | 8.80 | 9.14 | 9.33 | 11.56 | 11.63 | 0.00 | 0.00 |

| | | | | | | | | | | | |
|---|---|---|---|---|---|---|---|---|---|---|---|
| | Co | 0.00 | 2.18 | 6.08 | 3.53 | 3.06 | 3.12 | 1.45 | 0.68 | 0.00 | 0.00 |
| | Mn | 0.00 | 0.00 | 5.66 | 4.94 | 2.85 | 2.91 | 1.35 | 0.60 | 0.00 | 0.00 |
| | Al | 35.16 | 21.27 | 26.66 | 26.32 | 21.82 | 20.95 | 20.38 | 19.59 | 10.89 | 8.78 |
| | Cu | 34.72 | 24.49 | 25.98 | 25.65 | 24.76 | 25.30 | 24.74 | 24.02 | 11.27 | 5.24 |
| | Graphite | 20.47 | 18.48 | 18.95 | 18.72 | 18.30 | 12.34 | 12.13 | 11.87 | 0.00 | 0.00 |
| | Si | 0.00 | 0.00 | 0.00 | 0.00 | 0.00 | 1.22 | 1.20 | 1.17 | 0.00 | 0.00 |
| Mid-size PHEVs | Li | 0.81 | 0.83 | 1.13 | 1.10 | 0.96 | 0.97 | 0.90 | 0.81 | 0.07 | 0.06 |
| | Li metal | 0.00 | 0.00 | 0.00 | 0.00 | 0.00 | 0.00 | 0.00 | 0.00 | 1.31 | 0.82 |
| | Ni | 0.00 | 5.30 | 2.77 | 4.04 | 4.19 | 4.28 | 5.30 | 5.33 | 0.00 | 0.00 |
| | Co | 0.00 | 1.00 | 2.79 | 1.62 | 1.40 | 1.43 | 0.66 | 0.31 | 0.00 | 0.00 |
| | Mn | 0.00 | 0.00 | 2.60 | 2.27 | 1.31 | 1.33 | 0.62 | 0.28 | 0.00 | 0.00 |
| | Al | 23.16 | 15.10 | 15.59 | 15.40 | 15.01 | 12.41 | 12.30 | 12.23 | 5.95 | 4.79 |
| | Cu | 29.89 | 20.06 | 20.05 | 19.82 | 19.63 | 20.37 | 20.32 | 20.35 | 6.76 | 3.67 |
| | Graphite | 9.43 | 8.55 | 8.77 | 8.66 | 8.46 | 5.71 | 5.61 | 5.49 | 0.00 | 0.00 |
| | Si | 0.00 | 0.00 | 0.00 | 0.00 | 0.00 | 0.56 | 0.55 | 0.54 | 0.00 | 0.00 |
| Large PHEVs | Li | 1.21 | 1.24 | 1.71 | 1.66 | 1.44 | 1.46 | 1.36 | 1.22 | 0.11 | 0.09 |
| | Li metal | 0.00 | 0.00 | 0.00 | 0.00 | 0.00 | 0.00 | 0.00 | 0.00 | 1.98 | 1.23 |

| | | | | | | | | | | |
|---|---|---|---|---|---|---|---|---|---|---|
| Ni | 0.00 | 7.99 | 4.18 | 6.09 | 6.32 | 6.45 | 7.99 | 8.04 | 0.00 | 0.00 |
| Co | 0.00 | 1.50 | 4.20 | 2.44 | 2.11 | 2.16 | 1.00 | 0.47 | 0.00 | 0.00 |
| Mn | 0.00 | 0.00 | 3.92 | 3.42 | 1.97 | 2.01 | 0.93 | 0.42 | 0.00 | 0.00 |
| Al | 35.69 | 20.27 | 21.45 | 21.17 | 20.16 | 19.75 | 19.56 | 19.41 | 8.23 | 6.63 |
| Cu | 44.74 | 30.21 | 30.86 | 30.52 | 29.50 | 30.42 | 30.39 | 30.45 | 10.90 | 6.10 |
| Graphite | 14.18 | 12.84 | 13.17 | 13.01 | 12.72 | 8.58 | 8.42 | 8.24 | 0.00 | 0.00 |
| Si | 0.00 | 0.00 | 0.00 | 0.00 | 0.00 | 0.85 | 0.83 | 0.82 | 0.00 | 0.00 |

**Supplementary Table 2.27: Al and Cu compositions in EV batteries on module level as results of BatPaC model (unit: kg in battery modules).** We include this table only for Al and Cu here as the second-use of EV batteries are assumed to happen on battery module level which will delay materials available for recycling. Note Li, Co, Ni, Mn, graphite, and Si compositions on battery module level are the same as that on the battery pack level in Supplementary Table 2.11.

| EV types | Materials | LFP | NCA | NCM111 | NCM523 | NCM622 | NCM622-Graphite (Si) | NCM811-Graphite (Si) | NCM955-Graphite (Si) | Li-Sulphur | Li-Air |
|---|---|---|---|---|---|---|---|---|---|---|---|
| Small BEVs | Al | 27.06 | 20.41 | 22.42 | 22.06 | 20.77 | 19.99 | 19.36 | 18.90 | 10.29 | 8.36 |
| | Cu | 28.24 | 23.73 | 25.95 | 25.50 | 23.93 | 24.17 | 23.36 | 23.09 | 9.22 | 0.19 |
| Mid-size BEVs | Al | 52.23 | 40.25 | 42.11 | 41.63 | 40.40 | 38.81 | 38.09 | 37.19 | 20.58 | 16.72 |
| | Cu | 53.87 | 47.07 | 47.58 | 47.07 | 46.45 | 46.94 | 46.46 | 45.92 | 18.79 | 0.57 |
| Large BEVs | Al | 79.49 | 61.56 | 64.36 | 63.64 | 61.78 | 59.43 | 58.36 | 57.00 | 30.95 | 25.15 |
| | Cu | 88.86 | 77.00 | 78.10 | 77.24 | 76.13 | 76.60 | 75.77 | 74.83 | 30.78 | 2.77 |
| Small PHEVs | Al | 18.18 | 11.30 | 12.69 | 12.47 | 11.71 | 11.30 | 10.91 | 10.37 | 5.30 | 4.30 |
| | Cu | 22.28 | 13.71 | 15.45 | 15.18 | 14.22 | 14.39 | 13.89 | 13.18 | 6.55 | 5.24 |
| Mid-size PHEVs | Al | 13.61 | 7.70 | 7.90 | 7.77 | 7.57 | 7.55 | 7.50 | 7.51 | 2.55 | 2.07 |
| | Cu | 19.41 | 10.42 | 10.37 | 10.19 | 10.04 | 10.49 | 10.52 | 10.69 | 4.59 | 3.67 |
| Large PHEVs | Al | 19.30 | 10.76 | 11.48 | 11.29 | 10.61 | 10.55 | 10.46 | 10.45 | 3.73 | 3.03 |
| | Cu | 27.58 | 14.55 | 15.29 | 15.02 | 14.07 | 14.63 | 14.65 | 14.85 | 7.62 | 6.10 |

**Supplementary Table 2.28: EV battery pack weight as result of the BatPaC model (unit: kg).** PHEV battery weight is much smaller than that of BEVs because of the difference in required battery capacity between BEVs and PHEVs. For any car type and segment, we can see a decrease in battery pack weight to provide the same energy capacity due to the improvements of the specific energy of battery chemistries (see Supplementary Table 2.27).

| EV types | LFP | NCA | NCM111 | NCM523 | NCM622 | NCM622-Graphite (Si) | NCM811-Graphite (Si) | NCM955-Graphite (Si) | Li-Sulphur | Li-Air |
|---|---|---|---|---|---|---|---|---|---|---|
| Small BEVs | 269.94 | 194.99 | 218.63 | 214.67 | 200.36 | 187.16 | 180.17 | 172.00 | 111.75 | 90.20 |
| Mid-size BEVs | 514.05 | 373.09 | 413.66 | 406.40 | 382.34 | 355.97 | 344.24 | 328.02 | 215.36 | 173.08 |
| Large BEVs | 782.36 | 568.63 | 630.24 | 619.15 | 582.64 | 542.50 | 524.53 | 499.89 | 325.13 | 260.91 |
| Small PHEVs | 171.05 | 114.88 | 131.51 | 129.27 | 118.20 | 111.85 | 108.01 | 102.71 | 65.34 | 53.07 |
| Mid-size PHEVs | 107.49 | 72.79 | 77.61 | 76.44 | 73.27 | 68.69 | 67.34 | 65.64 | 35.56 | 29.25 |
| Large PHEVs | 159.24 | 104.21 | 112.76 | 111.01 | 104.89 | 101.28 | 99.25 | 96.66 | 51.20 | 41.76 |

### 2.6.3 Supplementary Methods

#### Battery and EV lifespans

The probability of Weibull lifespan distribution[79] is given by equation (1):

$$f(y) = \begin{cases} \alpha\beta^{-\alpha}(y-a)^{\alpha-1}exp\left\{-\left(\frac{y-a}{\beta}\right)^{\alpha}\right\} & if\ y > a; \\ 0 & otherwise. \end{cases} \quad (1)$$

where α is the shape parameter (α > 0); β is the scale parameter (β > 0); y is the year; a is the minimum lifespan.

By assuming the cumulative probability of Weibull lifespan distribution function between the minimum and the maximum lifespans as 99.7% (based on the normal distribution), the α and β in the Weibull lifespan distribution can be calculated by equations (2) and (3)[79]:

$$1 - exp\left\{-\left(\frac{c-a}{\beta}\right)^{\alpha}\right\} = 99.7\% \quad (2)$$

$$d = a + \beta\left(\frac{\alpha-1}{\alpha}\right)^{1/\alpha} \quad (3)$$

where c is the maximum lifespan; d is the most likely lifespan.

#### Battery replacement and reuse

**Supplementary Table 2.29: Assumptions of battery replacement rate, based on the assumptions of EV and battery lifespan distribution (Supplementary Table 2.19 and Supplementary Table 2.20).**

| Period | Battery replacement rate |
|---|---|
| 2005-2019 | 50% |
| 2020-2050 | 0% |

#### Battery stock dynamics model

Based on assumptions on lifespan distributions of EVs and replacement rate and reuse rate of EV batteries, we calculate the battery flows by equations (4) and (5):

$$B_{e,b,out}(y) = B_{e,b,in}(y) - \Delta B_{e,b,stk}(y) \quad (4)$$

$$B_{e,b,out}(y) = 1.5 * (B_{e,b,in}(2005) \times \int_{y-2005}^{y-2004} f_E(y)dy + B_{e,b,in}(2006) \times \int_{y-2006}^{y-2005} f_E(y)dy + \cdots + B_{e,b,in}(y-1) \times \int_{1}^{2} f_E(y)dy \quad (5)$$

where E, B, in, stk, and out are abbreviations of EV, battery, inflow, stock, and outflow respectively; e and b are the categories of EV and battery; $f_E(y)$ are lifespan distributions of EVs. 1.5 in equation (5) refers to battery replacement means one single EV uses 1.5 battery packs on average during EV lifespan.

### 2.6.4 Supplementary Notes

**Supplementary Note 2.1**

Average battery cell voltage = Average voltage of cathode – average voltage of anode. Relative to $Li^+/Li$, the average voltage of graphite (360 mAh/g) and Si are 0.15 V and 0.4 V. The average voltage of the graphite (Si) anode with 517 mAh/g active capacity can be estimated as (360/517)*0.15 + (157/517)*0.4 = 0.226 (V), based on assumption of a capacity averaged linear combination of graphite and Si[150]. Therefore, compared to NCM622-Graphite, the open circuit voltage of NCM622-Graphite (Si) will be reduced by 0.226-0.15 = 0.076 (V)[150].

**Supplementary Note 2.2**

The cell material compositions of Li-S batteries are obtained from[140], where required cell materials are scaled linearly by a factor between cell level energy capacity and required capacity of BEVs/PHEVs). The pack components of Li-S are calculated based on the pack configurations of default NCA chemistry in the BatPaC model[70], which means the weight ratio of cell components and pack components, as well as the weight ratios of various components/materials in the pack configurations for Li-S are assumed equal to the NCA chemistry in the BatPaC model[70]. Similarly, we also use the same calculation methods for the material compositions of Li-Air packs, based on the cell level material compositions of the Li-Air battery from[141].

# 3 Future greenhouse gas emissions of automotive lithium-ion battery cell production[b]


## Abstract

Understanding the future environmental impacts of lithium-ion battery is crucial to enable a sustainable transition to electric vehicles. Here, we build a prospective life cycle assessment (pLCA) model for lithium-ion battery cells production for 8 battery chemistries and 3 production regions (China, US, and EU). The pLCA model includes scenarios for future life cycle inventory data for energy and key materials used in battery cell production. We find that greenhouse gas (GHG) emissions per kWh of lithium-ion battery cell production could be reduced from 41-89 kg $CO_2$-Eq in 2020 to 10-45 kg $CO_2$-Eq in 2050, mainly due to the effect of a low-carbon electricity transition. Cathode is the biggest contributor (33%-70%) of cell GHG emissions in the period between 2020-2050. In 2050, LiOH will be the main contributor to GHG emissions of LFP cathode, and $Ni_2SO_4$ for NCM/NCA cathodes. These results promote discussion on how to reduce battery GHG emissions.


## 3.1 Introduction

In the transportation sector, a global shift from internal combustion engine vehicles (ICEVs) to electric vehicles (EVs) has been widely recognized as one of the most effective ways to mitigate climate change[57,151]. The International Energy Agency (IEA) expects the global light-duty EV fleet to grow from around 10 million in 2021 to 124-199 million EVs in 2030[6]. Due to recent policy incentives and ongoing innovations in battery technologies and business models, amongst others, it is expected the global light-duty EV fleet size will grow to 970-1940 million EVs by 2050[7].

The transition to the use of EVs will impact the supply chain of the automotive industry[152]. One of the key changes exists in the production and use of batteries[89]. Due to low cost and high performance, lithium-ion batteries dominate the current EV market and are expected to dominate in the next decade. The most important battery

[b] Published as: Xu, C., Steubing, B., Hu, M., Harpprecht, C., van der Meide, M. & Tukker, A. Future greenhouse gas emissions of automotive lithium-ion battery cell production. Resources, Conservation & Recycling 187, 106606 (2022).

types include lithium nickel cobalt manganese oxide batteries (NCM), lithium nickel cobalt aluminum oxide batteries (NCA), and lithium iron phosphate batteries (LFP).

Although a lot of studies have found that EVs have environmental advantages over ICEVs[37-39], the impacts of battery production are still rather uncertain[40-42]. Current studies find quite diverging battery impacts[43-45]. This is due to the use of different data and assumptions on battery performance and compositions[46], battery production processes, geographical scope[47], and life cycle inventory (LCI) information[48,49], and environmental impact assessment methodologies[50], amongst others. All these factors can lead to questionable conclusions on the magnitude of environmental impacts of battery production. Moreover, changes in environmental impacts of battery production in the next decades are rarely estimated, due to the challenges in estimating futurized background LCI data and modeling future battery production processes.

In this paper, we aim to overcome most of the aforementioned knowledge gaps by building a prospective life cycle assessment (pLCA) model to estimate future GHG emissions of the battery cell production per kWh battery capacity. The pLCA model simulates the lithium-ion battery cell production for 8 types of battery chemistries in 3 production regions (China, US, and EU) for the period 2020-2050. The foreground system is complemented by prospective life cycle inventory (pLCI) of background data that considers i) future energy scenarios as modelled in the Integrated Assessment Model REMIND[153] for the Shared Socio-Economic Pathway 2 (SSP2)-Base (no climate policy) and the SSP2-PkBudg 1100 scenarios (with climate policies)[154] as well as ii) future supply chain of key battery metals including nickel, cobalt, copper, and others (see details in methods). In this way, this paper aims to contribute to a better understanding of the current and future GHG emissions of battery cell production and the discussion of how to minimize such impacts in the context of a mobility transition towards EVs.

The paper is structured as follows. In section 2 we discuss the approach to the pLCA, discerning the goal and scope definition, life cycle inventory, and life cycle impact assessment. Section 3 gives the results and interpretation. Section 4 ends with discussions and conclusions.

## 3.2 Methods

### 3.2.1 Goal and scope

The goal of our pLCA model is to evaluate GHG emissions per kWh of battery cell production in 2020, 2030, 2040, and 2050. The modeled battery cell is a lithium-ion battery cell used in battery electric vehicles. The modeled cell capacity is 0.275 kWh, the most common size of an EV battery cell. The functional unit is chosen as 1 kWh in terms of the nominal battery cell capacity. The study is an attributional LCA, with a contribution analysis to reveal the environmental hotspots of battery cell production. The results are intended to give prospective environmental information to battery technology developers and EV policy makers.

The pLCA model covers 8 different battery chemistries and 3 production regions:

**I. Battery chemistries.** Battery chemistry development will lead to differences in material compositions and production processes and corresponding environmental impacts. Here we explore chemistry-specific GHG emissions by distinguishing 8 chemistries: LFP-Graphite, NCA-Graphite, NCM111-Graphite, NCM523-Graphite, NCM622-Graphite, NCM622-Graphite (Si), NCM811-Graphite (Si), and NCM955-Graphite (Si) batteries. We include these 8 chemistries because they are currently seen as the most likely dominant battery chemistries in the future according to our previous study[7].

**II. Production regions.** Battery production region determines where material and energy are supplied from, which significantly influences the associated environmental impacts. Here, we cover China, EU, and US as three main battery production regions in the world to explore region-specific GHG emissions.

Emissions of batteries in the use phase are negligible to zero. In the end-of-life phase, there may be benefits from 2nd uses or recycling of components or materials, but such scenarios and hence the environmental benefits of them are highly uncertain[155]. Therefore, we apply cradle-to-gate system boundaries for this study which allocates all production impacts to the first use of the battery in an EV. We include the production of all battery cell components, *i.e.*, cathode, anode, electrolyte, separator, and cell container, as well as the electric energy used to assemble all components into a complete cell (Fig. 3.1). We do not account for the environmental impacts of processing

battery cells to battery modules and –packs, or other components such as battery management systems, as they are minor (less than 10%[40]) compared to the battery cell production itself.

In the impact assessment, we focus on GHG emissions. We use the IPCC GWP 100 characterization method of 2013 that expresses GHG emissions in kg CO2-Eq.[156]. For the LCA implementation, we use the Activity Browser software[157] to calculate the life cycle impacts for all battery chemistries, production regions, temporal boundary, and background scenarios.

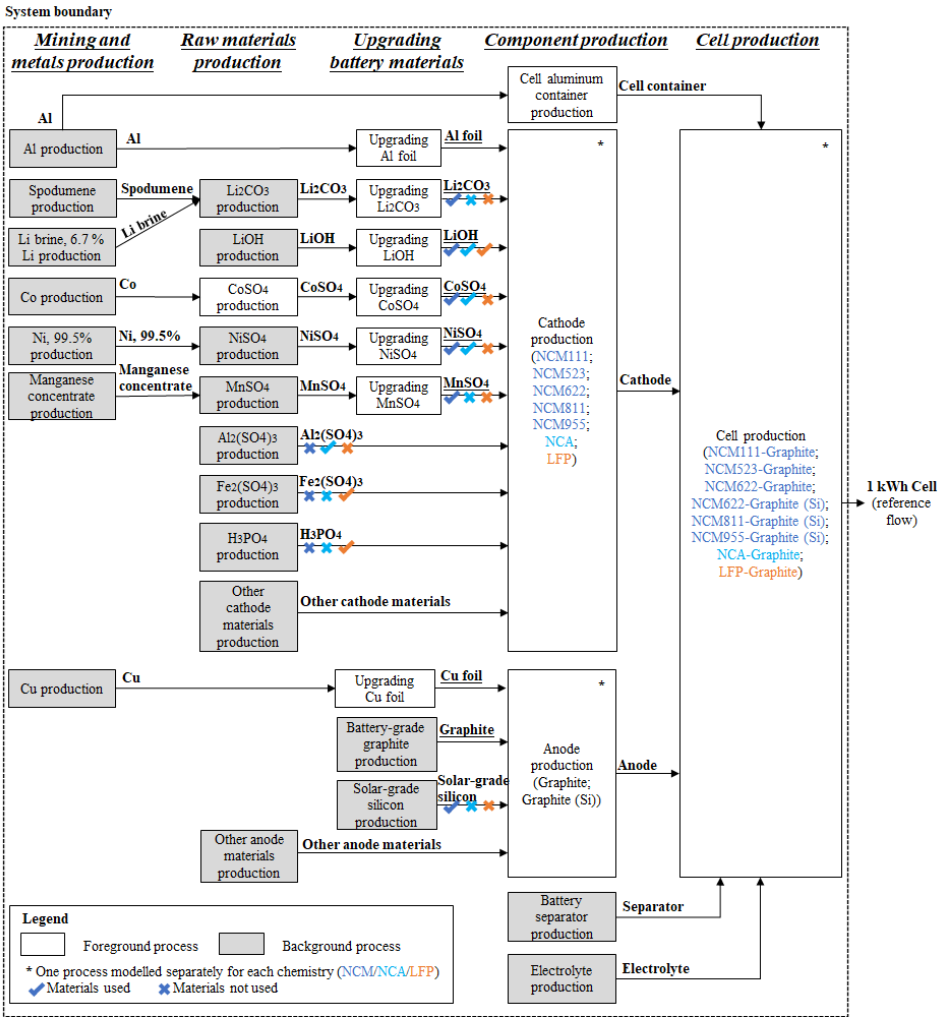


**Fig. 3.1: Flow chart of the production of battery cells.** Italicized underlined characters on top of the figure refer to life cycle stages. Materials with underlines indicate the quality of materials up to battery-grade, otherwise industry-grade.

### 3.2.2 Inventory analysis

#### Futurized background system

The futurized background system of our pLCA model is built based on the ecoinvent 3.6 database[158], considering future energy scenarios and supply chains of key battery

metals. Firstly, we use the premise[28] tool to build a futurized version of the ecoinvent 3.6 database[158] (cut-off system model). The tool systematically builds regional LCIs of future electricity production based on detailed regional energy scenarios from the Integrated Assessment Model REMIND[153]. Secondly, we incorporate technology scenarios for the future supply of key battery metals into the futurized version of the ecoinvent 3.6 database. Via this approach, we created the futurized background system of our pLCA model as follows.

**I. Processes obtained from ecoinvent 3.6.** We used ecoinvent 3.6[158] as a basis to build futurized LCIs of battery raw materials. From ecoinvent 3.6, we included $Li_2Co_3$, LiOH, $CoSO_4$, $NiSO_4$, $MnSO_4$, Al, and other materials for the production of the cathode. For the anode, we included graphite, silicon, Cu, and other materials. We further included all relevant raw materials and processes leading to the production of the separator, electrolyte, and cell container.

**II. REMIND energy scenarios.** We use the REMIND model[153] with Shared Socioeconomic Pathway 2 (SSP2)[159], a "middle-of-the-road" scenario with regard to future population and GDP growth. Under this SSP2 pathway, we use two future regional energy scenarios from REMIND model[153] to distinguish the effect of climate policy on the decarbonization of the electricity system. One is the "*SSP2-Base" scenario* where no specific climate policies are implemented and thus the global temperature could increase by more than 3.5 degrees Celsius by 2100. In the SSP2-Base scenario, the share of renewable energy (wind, solar, and hydro) will increase from only 24% in 2020 to 45% in 2050 for China, from 26% in 2020 to 63% in 2050 for EU, and from 14% 2020 to 54% in 2050 for US. The corresponding energy mix in 2050 will result in 0.4, 0.14, and 0.18 kg CO2-Eq per kWh electricity for China, EU, and US, respectively, reducing from 0.72, 0.36, and 0.48 kg CO2-Eq per kWh electricity in 2020. The second is the "*SSP2-PkBudg1100*" scenario, which has a goal to limit the cumulative global GHG emissions to 1,100 gigatons by 2100, thus limiting the global average temperature increase to well below 2 degrees Celsius by 2100. In the SSP2-PkBudg1100 scenario, the share of renewable energy (wind, solar, and hydro) will further increase to 68%, 92%, and 93% for China, EU, and US in 2050, which leads to 0.079, 0.029, and 0.033 kg CO2-Eq per kWh electricity, respectively. Please see details in Supplementary Fig. 3.1 and Supplementary Fig. 3.2 for regional energy mix and GHG emissions per kWh electricity production in 2020, 2030, 2040, and 2050.

**III. Future technology scenarios for the supply of key battery metals.** We incorporated the future technology supply scenarios of key battery metals as modelled by *Harpprecht et al.*[160] and *van der Meide et al.*[161] into the futurized version of the ecoinvent 3.6 database to create the background system. We consider future developments in the supply chains of the following key battery metals: copper[160], nickel[160], aluminum[162], lithium[163,164], and cobalt[161]. These future supply chains use LCIs for the current situation as provided by ecoinvent 3.6 as a basis. For copper, we use the scenario developed by *Harpprecht et al.*[160] to model future changes in ore grades, energy efficiency improvements, and market shares of primary and secondary production as well as of primary production routes. For nickel, we consider future ore grades and increased secondary production. For lithium, an increase of future secondary production share is assumed based on the work of[30,31]. For aluminum, an increase of future secondary production share is used based on the work of the International Aluminium Institute[162]. We use the future cobalt supply chain developed by *van der Meide et al.*[161]. This model takes into account cobalt ore grade development, changes in the market shares of primary cobalt production routes, and changes in the share of secondary cobalt production share.

**Battery cell production stages**

In relation to the futurized background system, this section describes the battery cell production stages and relevant modeling choices, data sources, and assumptions. Battery cell production is taking place in five life cycle stages, namely: mining, raw materials production, upgrading battery materials, component production, and cell production (Fig. 3.1).

**I. Mining and metals production.** This life cycle stage refers to the extraction and concentration, smelting, refining, and other necessary procedures to produce metals. This stage includes the production processes of Al, spodumene, Li brine, Co, Ni (99.5%), manganese concentrate, and Cu for NCM cathodes; Al, spodumene, Li brine, Co, Ni (99.5%), and Cu for NCA cathode; Al, spodumene, Li brine, and Cu for LFP cathode. The data source for this stage is the aforementioned futurized background system.

**II. Raw materials production.** Raw materials production refers to the production of raw materials from relevant metals, such as hydrometallurgical leaching of Ni to produce $NiSO_4$. At this stage, the processes for producing $Li_2CO_3$, LiOH, $CoSO_4$, $NiSO_4$,

$MnSO_4$, and other necessary battery raw materials are considered for NCM cathode; LiOH, $CoSO_4$, $NiSO_4$, $Al_2(SO4)_3$, and other necessary battery raw materials for NCA cathode; LiOH, $Fe_2(SO4)_3$, $H_3PO4$, and other necessary battery raw materials for LFP cathode. The data source for raw materials production is the aforementioned futurized background system, except for $CoSO_4$. We compile the LCIs for producing $CoSO_4$ from Co using information from the China battery industry reports in the period 2020-2022[165].

**III. Upgrading battery materials.** The raw materials produced from the last life cycle stage are at the level of industry-grade, which is not suitable for battery production yet. In this stage, raw materials are upgraded to a battery-grade level with additional materials and energy inputs. For the NCM cathode, this includes the production of battery-grade $Li_2CO_3$, battery-grade LiOH, battery-grade $CoSO_4$, battery-grade $NiSO_4$, battery-grade $MnSO_4$, and battery-grade Al; for the NCA cathode, battery-grade $Li_2CO_3$, battery-grade LiOH, battery-grade $CoSO_4$, battery-grade $NiSO_4$, and battery-grade Al foil are required; and for the LFP cathode battery-grade LiOH is needed. For the anode production, we include the process for producing battery-grade Cu foil, battery-grade graphite, as well as solar-grade silicon if silicon is required for the anode (*i.e.*, Graphite (Si) anode).

The LCI data for upgrading industry-grade chemicals to battery-grade LiOH, battery-grade $CoSO_4$, and battery-grade $NiSO_4$ are based on the EverBatt model[48] developed by Argonne National Laboratory to assess the cost and environmental impacts during the battery life cycle. The LCIs of battery-grade $Li_2CO_3$, battery-grade $MnSO_4$, battery-grade Al foil, and battery-grade Cu foil are compiled using information from the China battery industry reports[165]

**IV. Component production.** At the component production stage, the battery cell components, *i.e.*, cathode, anode, electrolyte, separator, and cell container, are produced from battery-grade materials. From the EverBatt model[48], we derive LCI data of cathode production from relevant battery-grade materials, including LFP, NCA, NCM111, NCM523, NCM622, and NCM811. These LCIs of cathode production are complemented by emissions inventory of nickel, cobalt, and manganese to air or water during cathode production (which is lost in the EverBatt model[48]), using the information given in the China battery industry reports[165]. In addition, we model the LCI of producing the NCM955 cathode based on that of NCM811 cathode, based on

their differences in material compositions.

**V. Cell production.** During this stage, all battery cell components are assembled into a complete cell. Our model for this stage considers material inputs and energy consumption. The material inputs are based on the composition of the battery cells as determined in previous work of the authors[7]. In cell production, electrical energy is used, and we need to account for the amount of electrical energy required to combine all battery components into a battery cell. There are only a few studies providing detailed energy consumption data for cell production, and they have large deviations[166]. The total energy consumption per Wh cell production is highly influenced by production volumes, and could range from over 1000 Wh in the lab and pilot-scale to below 100 Wh on an industrial scale[40]. Here, we use an average electricity consumption from 5 industrial-scale studies, *i.e.*, 74 Wh per Wh cell production[166].

## 3.3 Results and interpretation

### 3.3.1 GHG emissions

Fig. 3.2 shows the cradle-to-gate GHG emissions for producing 1 kWh of cell capacity in 2020 by type of battery chemistry and production region. From the figure, we find a significant variation in the cradle-to-gate GHG emissions per kWh of battery cell production in China, US, and EU in 2020. This is mainly due to a substantial difference in the share of renewable energy and resulting emission intensities for electricity used for battery cell production across the three regions. In 2020, the EU electricity mix has the lowest emission intensity (0.36 kg CO2-Eq per kWh electricity), followed by the US (0.48 kg CO2-Eq per kWh electricity) and China (0.72 kg CO2-Eq per kWh electricity). As a consequence, the GHG emissions per kWh of battery cells produced in EU are 16%-18% lower than in the US, and 38%-41% lower than in China in 2020.

In addition to production regions, GHG emissions depend on battery chemistry as different materials and production processes are used. For instance, LFP does not require nickel, cobalt, and aluminum metals whose production is very energy-intensive and generates significant amounts of polluting emissions, while these metals are used for NCM and NCA cell production. For this reason, LFP cell production generates 20%-28% lower GHG emissions than NCA and NCM cells in terms of per kWh cell production, depending on the production region.

As a result, LFP cells produced in the EU can generate the lowest GHG emissions, while NCA and NCM cells produced in China can generate the highest emissions in 2020. There is a factor of ~2.2 between the lowest and highest GHG emissions per kWh of battery cell production in 2020.

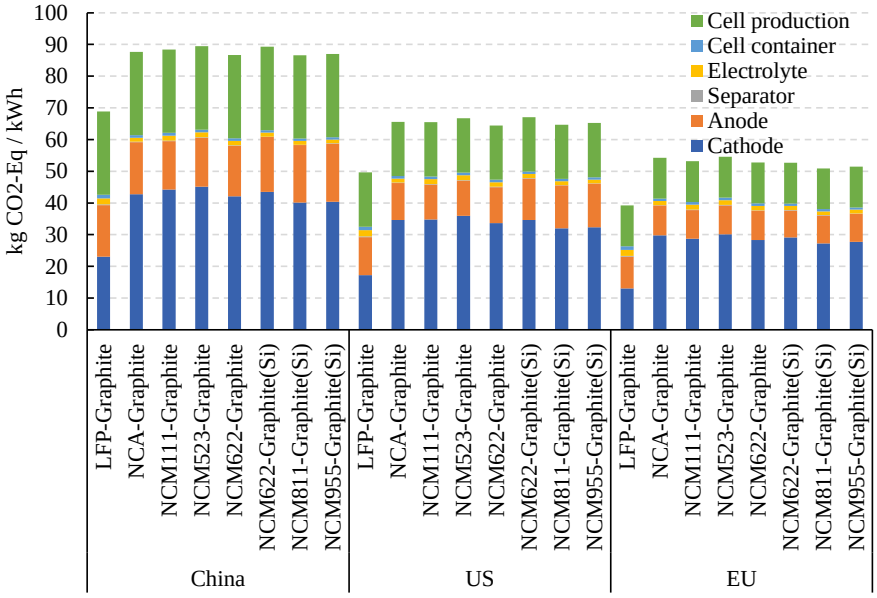


**Fig. 3.2: Cradle-to-gate GHG emissions per kWh of cell production by battery chemistry and production region in 2020.**

**Future GHG emissions.**

Given the similar GHG emissions of NCM and NCA chemistries, we show the future cradle-to-gate GHG emissions per kWh of battery cell production for two distinct chemistries in Fig. 3.3: LFP-Graphite cell and NCM622-Graphite cell (see results of other cell chemistries in Supplementary Fig. 3.3, Supplementary Fig. 3.4, and Supplementary Fig. 3.5). Mainly due to the development of renewable and low-carbon electricity used for cell production, the cradle-to-gate GHG emissions of cell production per 1 kWh capacity is significantly reduced significantly from 2020 to 2050. Depending on battery chemistry and production region, the GHG emissions could be reduced by 49%-52% under the SSP2-Base scenario in 2020-2050, and even 74%-81% under the SSP2-PkBudg 1100 scenario during the same period.

In addition, the absolute variation in GHG emissions between production region and battery chemistry is expected to decline between 2020 to 2050. In 2020, the cradle-to-gate GHG emissions range from 41 to 89 (difference of 48) kg CO2-Eq per kWh battery cell capacity. In 2050**,** the cradle-to-gate GHG emissions range from 21 to 45 (difference of 24) kg CO2-Eq per kWh battery cell capacity in the SSP2-Base scenario and from 10 to 17 (difference of 7) kg CO2-Eq in SSP2-PkBudg 1100 scenario. Depending on energy scenarios, the corresponding absolute variation for GHG emissions in 2050 is 2-6.5 times lower than that in 2020.

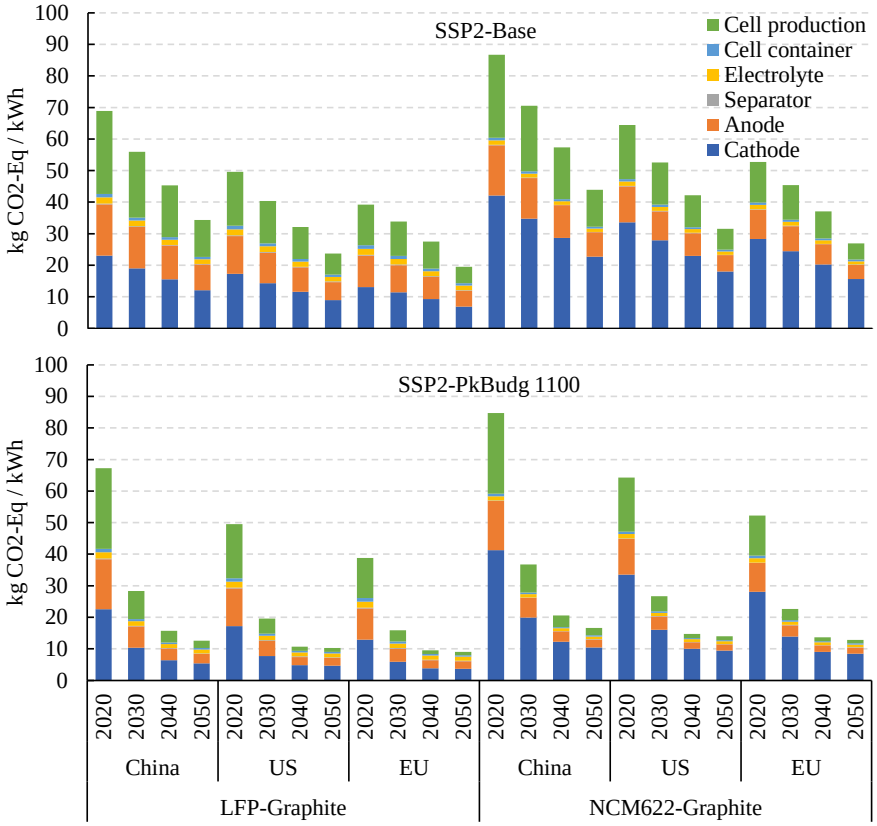


**Fig. 3.3: Future GHG emissions per kWh of cell production for LFP-Graphite and NCM622-Graphite in China, EU, and US.** Please see results for other cell chemistries in Supplementary Fig. 3.3, Supplementary Fig. 3.4, and Supplementary Fig. 3.5.

### 3.3.2 Contribution analysis of battery cell

Fig. 3.2 and Fig. 3.3 also present the contribution of different cell components to GHG emissions results. The cathode, anode, and cell production are the three most important contributors to GHG emissions. The relative contribution of the cathode for NCM/NCA cells is higher than that of LFP cells, while the relative contribution of the anode and cell production for LFP cells is higher than that of NCM/NCA cells. These are mainly due to different material compositions between NCM/NCA cells and LFP cells.

The NCM/NCA cathode is, with 46%-55% depending on battery chemistry and production region, the biggest contributor to GHG emissions in 2020, which is more than the total contributions from all other components. This is because NCM/NCA cathodes make up around 53%-59% of the weight of battery cells and also its production relates to the majority of metals contained in a battery cell which require GHG-intensive mining and refining processes (such as lithium, nickel, cobalt, and others). The NCM/NCA cathode is expected to remain the primary contributor to cradle-to-gate GHG emissions until 2050 (Fig. 3.3). Yet, its relative contribution is expected to increase to 49%-60% in the SSP2-Base scenario and 60%-70% in SSP2-PkBudg 1100 scenario during 2020-2050, depending on battery chemistry and production region.

Fig. 3.4 provides a relative contribution analysis by battery production life cycle stage. In 2020, the two most important life cycle stages from a GHG emissions perspective are “component production” followed by “cell production”. They together account for 74%-83% of GHG emissions for LFP cells and 54%-69% for NCM/NCA cells, depending on production region/cell chemistry. These numbers could decrease to 39%-76% for LFP cells and 23%-61% for NCM/NCA cells depending on energy scenarios, due to the stronger effects of low-carbon energy development on life cycle stages of “cell production” and component production” rather than other life cycle stages.

“Mining and metals production” could become a significant life cycle stage for NCM/NCA cells in the future, especially when considering a stronger low-carbon energy development scenario. The SSP2-PkBudg 1100 scenario could result in “mining and metals production” as the primary life cycle stage to GHG emissions, accounting for 33%-42% of NCA cells and 24%-47% of NCM cells in 2050. Note that for NCM cells,

the future transition from NCM111 chemistry to NCM955 chemistry will improve the contribution of "mining and metals production" to GHG emissions. This transition increases the content of Ni with relatively high GHG emissions (7 kg CO2-Eq in 2020 and 3-4.7 kg CO2-Eq in 2050 per kg $NiSO_4$ globally) and decreases the content of Co with relatively low GHG emissions (2.7 kg CO2-Eq in 2020 and 1.2-1.7 kg CO2-Eq in 2050 per kg $CoSO_4$ globally) for NCM cells, resulting in an overall increase in GHG emission during the life cycle stage of "mining and metals production".

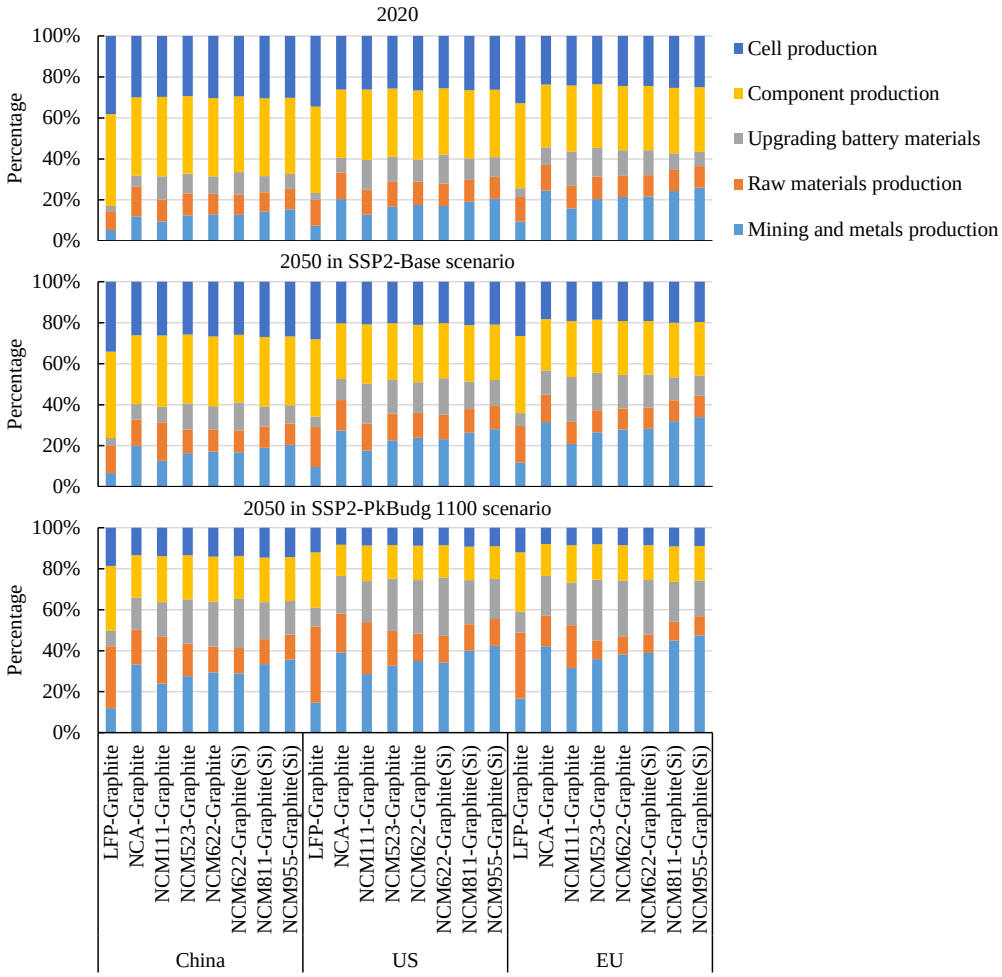


**Fig. 3.4: GHG emission contributions by life cycle stage for different battery cell chemistries and production regions in 2020 and 2050.**

### 3.3.3 Contribution analysis of cathode

Given the substantial contribution of the cathode in the battery GHG emissions, we perform an absolute contribution analysis for cathode disaggregated by life cycle stage, with each stage divided into energy and materials input. Fig. 3.5 presents the results for LFP and NCM622 cathodes produced in China in 2020 and 2050 (please see the results of US and EU in Supplementary Fig. 3.6 and Supplementary Fig. 3.7). The contribution analysis results differ a lot between LFP and NCM622 cathodes. For battery cells produced in China in 2020, the life cycle stage of "mining and metals production" and "cathode production" contributes to around 22% and 44% for NCM622 cathode respectively, while these numbers are 2% and 71% for LFP cathode.

In addition, the energy input dominates (around 78%) the cradle-to-gate GHG emissions of the LFP cathode, while the energy input and materials have almost equal contributions to GHG emissions for the NCM622 cathode in 2020. In the future, input materials, rather than input energy, will become more important contributors to GHG emissions due to the decarbonization of the electricity system. Input materials will even become the major source of cradle-to-gate GHG emissions for cathodes in 2050, with a relative contribution of up to 34%-81% for LFP cathodes and 52%-71% for NCM/NCA cathodes depending on energy scenarios/production regions/cell chemistries.

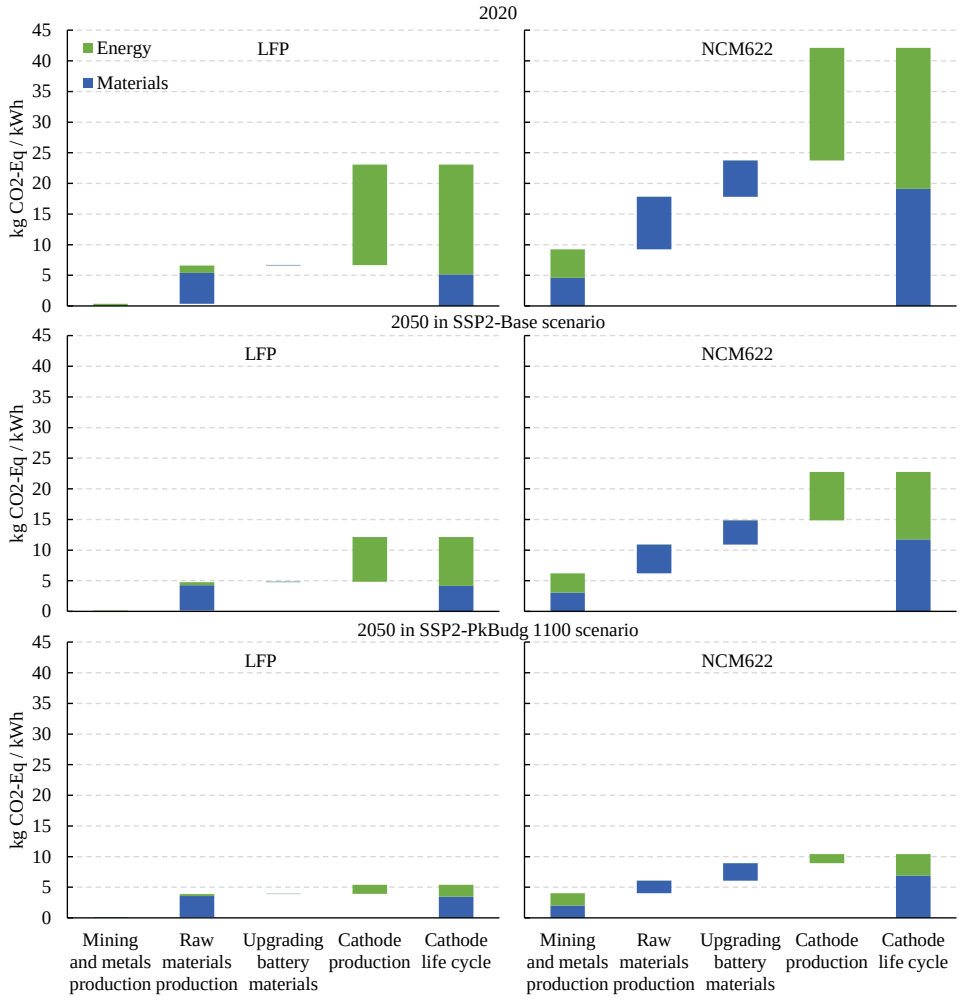


**Fig. 3.5: Absolute contribution analysis of cradle-to-gate GHG emission of the cathode production for 1 kWh battery cell capacity by life cycle stages, divided by input energy and input materials, for LFP and NCM622-Graphite in China in 2020 and 2050.** Please see results of US and EU in Supplementary Fig. 3.6 and Supplementary Fig. 3.7.

Fig. 3.6 further illustrates which specific materials and energy sources account for the GHG emissions for LFP and NCM622 cathodes. LiOH and electricity are key contributors to GHG emission of LFP cathodes. They together account for 82-86% in 2020 and 64%-82% in 2050 of GHG emissions for LFP cathodes, depending on the

production region. Taking the perspective of the production of the whole LFP cell, LiOH and electricity together contribute to 27%-29% in 2020 and 28%-35% in 2050 of GHG emissions for the production of LFP cells.

Looking at the cradle-to-gate GHG emissions of NCM622 cathode production, $NiSO_4$ and $Li_2CO_3$ materials, rather than $CoSO_4$ and other cathode materials, are important contributors. $NiSO_4$ and $Li_2CO_3$ can contribute to 18%-30% and 6%-11% of GHG emissions of NCM622 cathode in 2020 respectively. These numbers change to 25%-46% and 8%-21% in 2050, depending on the production region and energy scenarios. In other words, $NiSO_4$ and $Li_2CO_3$ can account for 16%-31% and 5%-14% of GHG emissions of NCM622 cells in 2050.

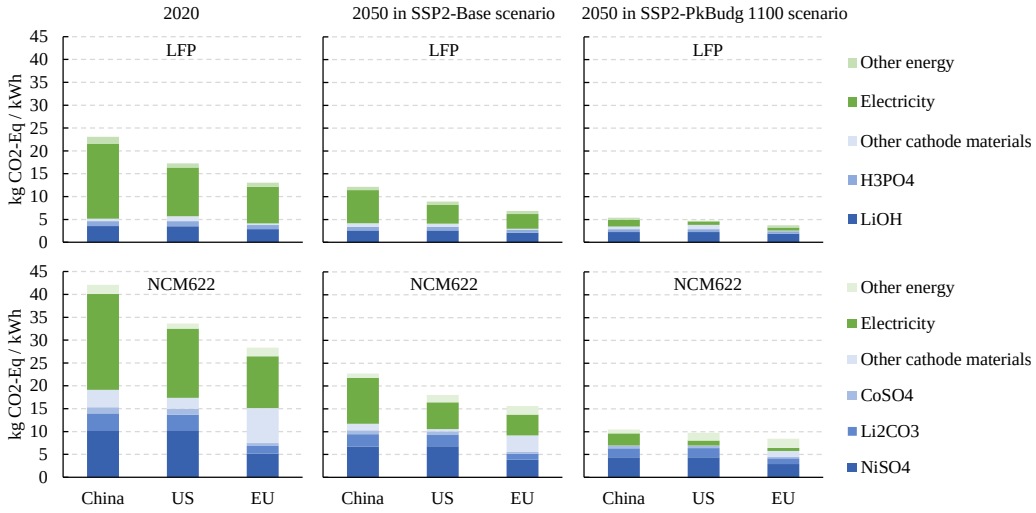


**Fig. 3.6: Absolute contribution analysis of GHG emissions of the cathode production split by materials and energy, in terms of 1 kWh battery cell capacity.**

## 3.4 Discussion

In this study, we build a prospective LCA model to quantify future cradle-to-gate GHG emissions per kWh battery cell production for 8 types of cell chemistries and 3 production regions until 2050. According to the pLCA model, our results for GHG emissions per kWh battery cell production (53-85 kg CO2-Eq per kWh in 2020 and 10-45 kg CO2-Eq per kWh in 2050) lie in the lower end of the range of earlier studies found in literature[44,49,167] (28-356 kg CO2-Eq per kWh). However, our results

compare well with the findings from the International Council of Clean Transportation [168] (34-77 kg CO2-Eq per kWh in 2021). There are various explanations for this. First, existing literature uses dated LCI data for battery cell production. Our modeling uses up-to-date LCI data based on the EverBatt model[48] and China battery industry reports in the period 2020-2022[165], which takes changes in battery chemistry next to cell production into account. Second, we take into account the effects of the low-carbon energy transition on battery production based on integrated assessment model REMIND. Results are intended to give reliable insights into future cradle-to-gate GHG emissions from battery cell production, which can form a basis for doing suggestions to further reduce impacts from this production.

Since LFP battery is expected to generate less GHG emissions than NCM/NCA batteries until 2050, one option is to support LFP battery deployment. The somewhat lower technical performance of LFP batteries compared to NCM/NCA batteries, in terms of specific energy (Wh/kg), may however be an obstacle for the large-scale deployment of LFP batteries. At the same time, advantages of LFP batteries are their relatively long useful lifetimes and low materials cost of LFP battery. Battery producers can take advantage of this, and at the same time invest in improving LFP battery performance. One example is that several battery producers started to improve the mass and space utilization of battery pack by removing modules and directly assembling cells into a pack (the LFP blade battery created by BYD can reach the specific energy of 140 Wh/kg at the pack level, which is higher than that of a standard NMC622 prismatic battery)[169].

Choosing battery production regions, which determine the electricity mix used to produce batteries, could be another important factor to consider for battery producers to reduce GHG emissions. China dominates the battery production market and is expected to continue so in the next decade. Reducing the emissions of China's electricity supply is key for achieving a lower GHG impact. EU and US provide greener electricity supply than China, and in theory, they are ideal regions for producing batteries with the lowest GHG emissions. However, it may not be possible to put a complete battery production supply chain in EU and US in the short term due to an uneven geographical distribution of extraction locations for primary materials required for batteries. Putting some part of the battery production life cycle stages in EU or US, rather than China, can be a pathway to start to reduce impacts of battery production.

This could be particularly considered for energy-intensive production stages such as cell production which uses electric energy to assemble all battery components into a complete cell.

We must emphasize the crucial role of a low-carbon electricity transition for reducing GHG emissions of battery production, reflected by the results of SSP2-PkBudg 1100 scenario. The energy supply for battery production should be as carbon-neutral as possible. For instance, Tesla's announced Giga watt-hour battery production factory is planned to be built together with a solar energy supply facility[170]. In this case, a 100% supply of solar power for battery production is ensured, which can lead to extremely low GHG emissions.

Given the major contribution of the use of $NiSO_4$ and $Li_2CO_3$ to the GHG emissions of the production of NCM/NCA batteries and of the use of LiOH to the production of LFP batteries, reduction of GHG emissions along the supply chain of Ni and Li metals is relevant too. Replacing fossil fuels with renewable electricity, improving energy efficiency, as well as controlling and capturing the GHG emissions during nickel mining and refining can be effective approaches to reduce impacts of $NiSO_4$ production. We can apply similar approaches to Li. Moreover, $Li_2CO_3$ produced from the leaching of spodumene with sulfuric acid can generate less GHG emission as when it is produced from concentrated brine[171]. The spodumene leaching pathway has currently still a minor market share of the $Li_2CO_3$ production market. Promoting this pathway is another option to reduce GHG emissions related to LFP battery production.

There are some future developments, which we did not consider in this study. Firstly, although we included a wide range of scenarios for battery chemistries, metal production, and energy generation, other scenarios may play out in the future (*e.g.*, lower or deeper decarbonisation of the energy system, or low-impact production processes for certain materials, such as the application of inert anodes in the Hall-Herault process for aluminum production[172]. Secondly, it is possible that the expected fast scaling up to high-volume production of the batteries considered in this study leads to considerable learning effects. This can result in significant efficiency improvements and lower costs and impacts, for instance by using automated manufacturing technologies using robots[173]. Thirdly, the development of new breakthrough battery technologies, such as solid-state Lithium-Sulphur and Lithium-

Air batteries [174], Na-ion[175], etc., may create radical changes in battery production processes and relevant materials supply chains. It is currently unclear if such technologies indeed will break through. There is further insufficient experience with such novel battery technologies to make a reliable quantitative estimate of life cycle inventory data, while also little is known about the impacts of such novel battery technologies once they have been scaled up from lab or pilot scale to full production plants.

## 3.5 Supplementary information

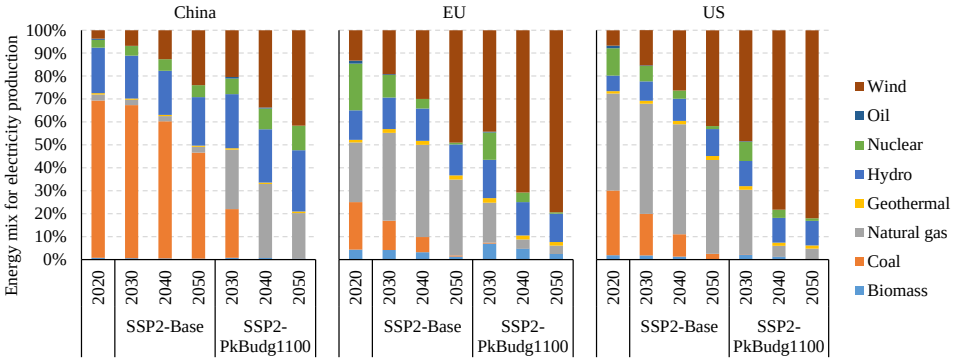


**Supplementary Fig. 3.1: Regional energy mix for electricity production in SSP2-Base and SSP2-PkBudg1100 scenarios.**

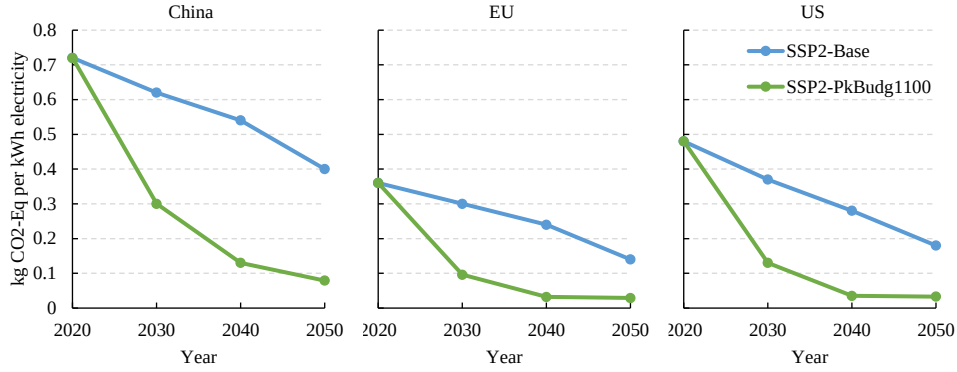


**Supplementary Fig. 3.2: Regional GHG emissions per kWh electricity production in SSP2-Base and SSP2-PkBudg1100 scenarios.**

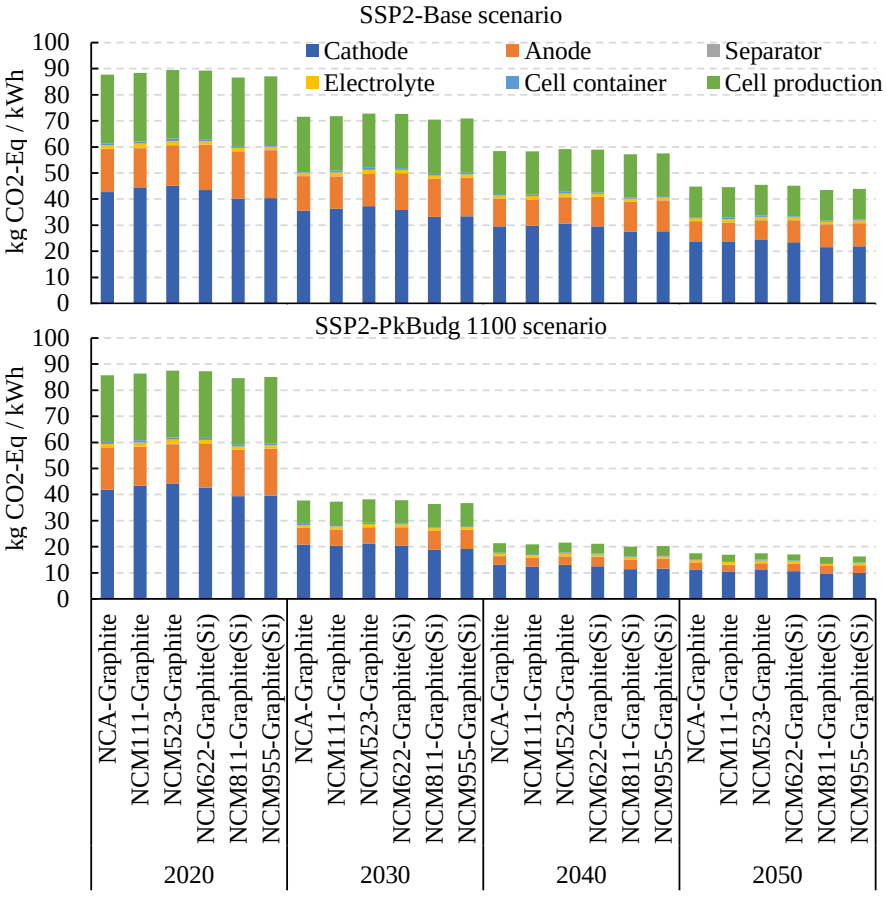


**Supplementary Fig. 3.3: Future GHG emissions per kWh of cell production by different cell chemistries in China.**

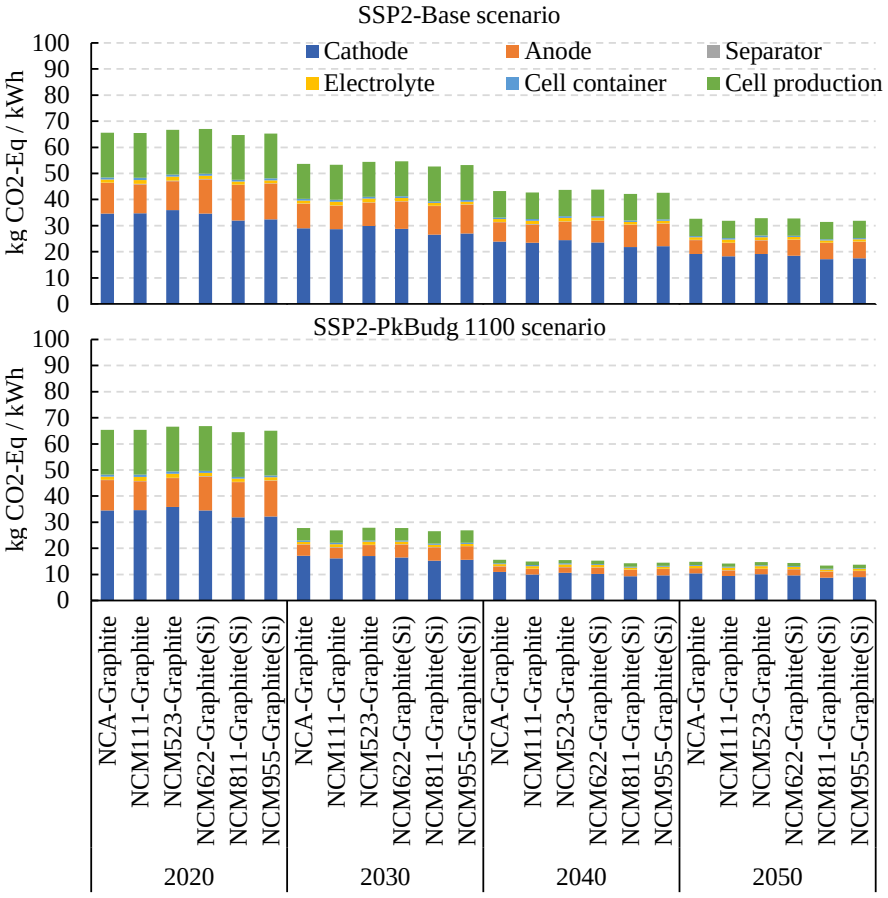


**Supplementary Fig. 3.4: Future GHG emissions per kWh of cell production by different cell chemistries in US.**

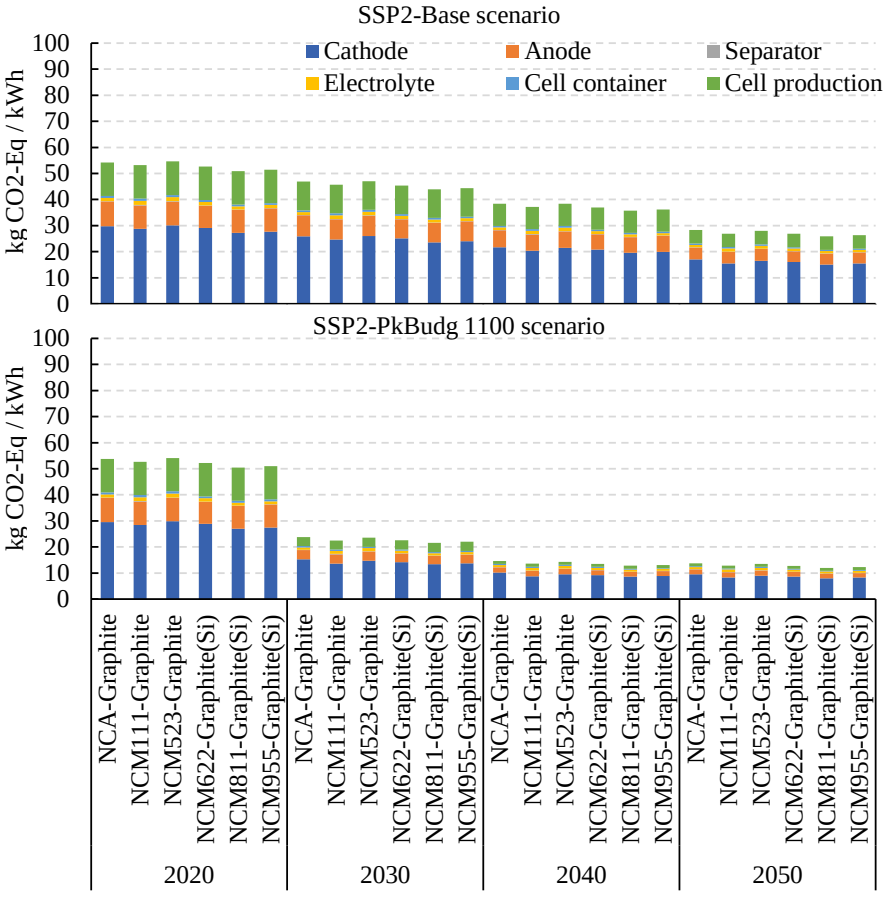


**Supplementary Fig. 3.5: Future GHG emissions per kWh of cell production by different cell chemistries in EU.**

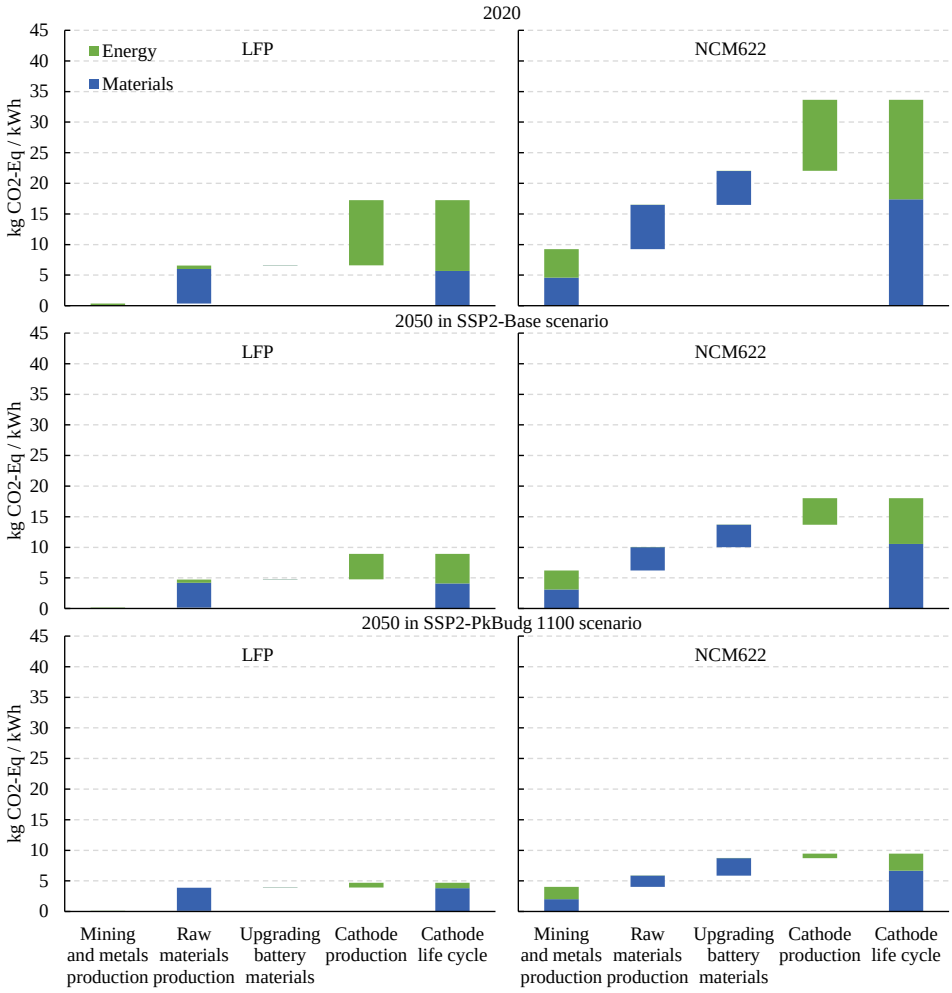


**Supplementary Fig. 3.6: Absolute contribution analysis of cradle-to-gate GHG emission of the cathode production for 1 kWh battery cell capacity by life cycle stages, divided by input energy and input materials, for LFP and NCM622-Graphite in US in 2020 and 2050.**

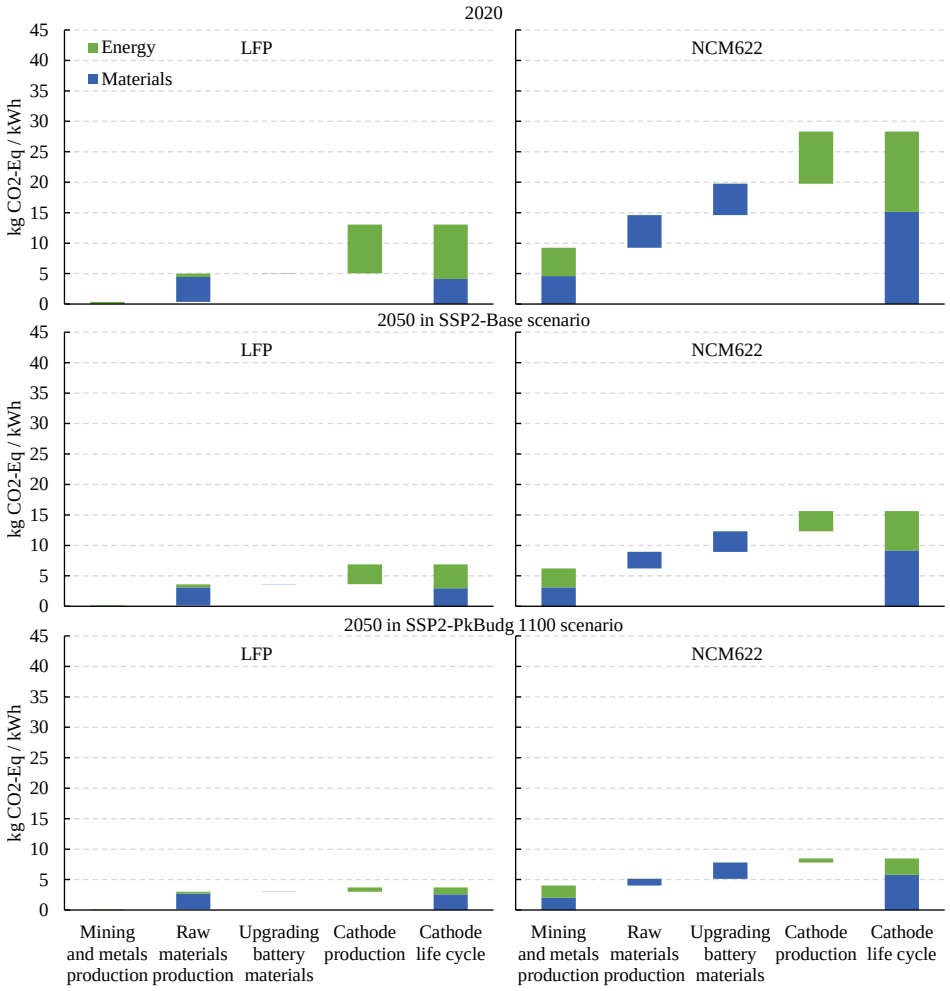


**Supplementary Fig. 3.7: Absolute contribution analysis of cradle-to-gate GHG emission of the cathode production for 1 kWh battery cell capacity by life cycle stages, divided by input energy and input materials, for LFP and NCM622-Graphite in EU in 2020 and 2050.**

# 4 Future greenhouse gas emissions of global automotive lithium-ion battery cells and recycling potential till 2050[c]


## Abstract

The global transition to electric vehicles (EVs) requires large-scale production of lithium-ion batteries which are the leading chemistry type for EV batteries (EVBs). To ensure a sustainable EV transition, greenhouse gas (GHG) emissions of EVB production have to be minimized. Given the fact that cells are the major source of life cycle GHG emissions of EVBs, we quantify the GHG emissions of global EVB cell production from 2020 to 2050. To this end, we build an integrated model that estimates the demand for EVB cells with a dynamic battery stock model, and the GHG emissions per EVB cell with a prospective life cycle assessment model. We find that GHG emissions of global EVB cell production will increase to 26-155 Mt CO2-Eq in 2030 and 58-468 Mt CO2-Eq in 2050, depending on EV demand growth, EV and related battery size, battery chemistry, and energy mix scenarios. Despite an average 8%-12% annual growth rate of global EVB cell demand between 2020 and 2050, global EVB cells GHG emissions only increase annually by 2%-10% in the same period due to the increasing use of renewable energy in EVB cell production and other factors. Decarbonization of energy used in EVB cell production and the use of small rather than big EVs are crucial factors to minimize growth in GHG emissions. EVB recycling offers potential GHG emissions reductions, however, only in the longer term after 2030.


## 4.1 Introduction

Transportation accounts for ~15% of global GHG emissions in 2019, making it the second-largest GHG emissions sector next to energy sector[1]. Cars for personal transport accounted in 2019 for about ~6 Gt emissions[1]. Technology developers proposed EVs, as an alternative to Internal Combustion Engine Vehicles (ICEVs), to reduce GHG emissions of transportation sector, along with reducing dependency on oil resources and (urban) air pollution[57,151]. As major deployments of EVs, the global

[c] Submitted to Renewable and Sustainable Enery Review as: Xu, C., Steubing, B., Hu, M. & Tukker, A. Future greenhouse gas emissions of global automotive lithium-ion battery cells and recycling potential till 2050.

light-duty EVs grew from a few thousand vehicles in 2005 to 10 million vehicles in 2021. EV fleet scenarios of the International Energy Agency[6], extended to 2050 in our previous paper[7], estimate 124-199 million EVs in 2030 and 970-1940 million EVs by 2050.

The transition to EVs reduces vehicle in-use emissions significantly due to improvements of vehicle energy efficiency[176] and use of renewable electricity[177]. However, it may increase vehicle production emissions because EVs require batteries that are carbon intensive to produce. For a 100 kWh battery, life cycle GHG emissions of the EVB cells production reach 4-9 t CO2-Eq in 2020[178] (equals to the in-use emissions of driving 16400-35600 km with a typical ICEV that emits on average 250 g CO2-eq GHG emissions per km[179]). In earlier work, we estimated the global EVB cells demand of 1.5-2.4 TWh in 2030 and 7-12 TWh in 2050[7]. This would lead to GHG emissions of 6-21 Mt CO2-Eq in 2030 and 30-104 Mt CO2-Eq in 2050 for global EVB cell production, if the life cycle emissions of EVB cell production would not change compared to 2020.

Most studies[51,52] on future GHG emissions from global EVB cell production use scenarios of future EVB demand growth and current life cycle emissions of EVB cell production[40-42]. There are few studies that take into account regional EVB demand and production and changes in battery production technology over the next decades, which strongly influence the life cycle emissions of battery production. This is due to two main challenges. First, future battery demand depends on the future EV fleet size and battery capacity per vehicle, which will both change and differ between the main EV markets (*e.g.*, US, EU, Asia). Second, regional battery production will change due to regional battery production capacity, resource constraints, and other factors. But at the same time, the climate policy and associated energy mix may differ between such regions, leading to potentially large differences in life cycle GHG emissions of battery production. Therefore, there is a need for developing future (regional) battery demand scenarios considering the development of EV fleet size and battery capacity per vehicle, and quantifying the future GHG emissions of global EV battery production considering the future distribution of battery production regions.

In this paper, we build an integrated model to estimate GHG emissions of global EVB cell production between 2020-2050. The integrated model combines a dynamic battery stock model[7] and a prospective life cycle assessment (LCA) model[178], which are

both developed in our earlier work to estimate future demand for EVB cells and life cycle GHG emission per kWh capacity of EVB cell production. Considering the future (regional) EV fleet size and battery capacity per vehicle, the dynamic battery stock model includes three battery demand scenarios (low, medium, and high) specified in future demand for EVB cells in China, EU, US, and rest of world (RoW) for the period from 2020-2050. The dynamic battery stock model also includes two global-level battery chemistry scenarios: an NCX scenario (NCA and NCM batteries dominate the EV market) and an LFP scenario (LFP battery dominates the EV market). Life cycle GHG emissions for EVB cell production for the period 2020-2050 are calculated by the prospective LCA model, giving specific results by region and battery chemistry[178]. The prospective LCA model further includes two energy mix scenarios, based on the Remind Integrated Assessment Model[180], reflecting different future regional energy mixes and related carbon emissions for electricity used in cell production.

Using the integrated model, we explore hence a range of GHG emissions of global EVB cell production between 2020-2050, using three different scenarios for battery demand, two different scenarios for battery chemistry, and two different scenarios for GHG emissions from electricity production. Next to this, we perform a sensitivity analysis related to a variation of EVB production regions, on the life cycle emissions of global EVB production. In this way, this paper contributes to a better understanding of the global future environmental impacts of EVB production and options to reduce these.

## 4.2 Methods

### 4.2.1 Model framework

The integrated model (Fig. 4.1) combines a dynamic battery stock model[7] and a (2) prospective LCA model[178]. The *dynamic battery stock model* estimates the global future demand for EVB cells, considering EV fleet size, battery lifespan, and battery material compositions, as well as the end-of-life (EoL) of EVB cells. The dynamic battery stock model was developed on a global scale in our previous study[7]. Here we apply the dynamic battery stock model to a regional scale, by distinguishing the regional EV fleet share, to project EVB cells demand and EoL materials from EVB cells in China, US, EU, and RoW during 2020-2050 based on an IEA projection[6]. This projection is only available until 2030 and the regional shares are kept as in 2030 for the years after.

Further details of the dynamic battery stock model are explained in Xu et al.[7].

The *prospective LCA model* estimates future production region and battery chemistry-specific life cycle GHG emissions per EVB cell production and cell material. The model from our previous study[178] combines i) the battery cell production data is simulated based on the EverBatt model[48] and China battery industry reports[165]; and ii) the prospective life cycle inventory (LCI) background database is derived from the ecoinvent database[158], but taking into account changes in production technologies of key battery metals (nickel, cobalt, copper, and others), next to changes in energy mixes by region (decarbonization of electricity generation due to climate policy) based on outputs of Remind Integrated Assessment Model[180]. The prospective LCA model presents results for 3 production regions (China, US, and EU) and 8 types of chemistries for the period 2020-2050. For details on this prospective LCA we refer to Xu et al.[178].

Based on the outputs of the dynamic battery stock model and prospective LCA model, we calculate GHG emissions of the global EVB cells production in 2030, 2040, and 2050 without considering the effects of recycling, under various scenarios of battery demand, battery chemistry, and energy mix (see section 2.2). Further, we perform sensitivity analysis of production region and recycling with regard to GHG emissions (see section 4.2.3).

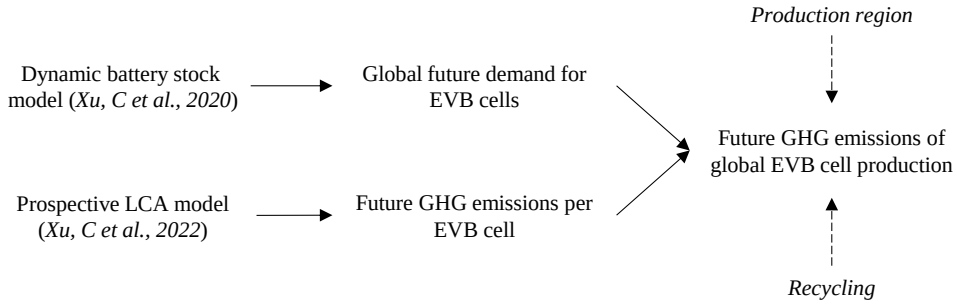


**Fig. 4.1: Integrated model to estimate future GHG emissions of global EVB cell production.** Dashed lines and italics indicate sensitivity analysis of GHG emissions.

### 4.2.2 Scenarios

The former section described how we build an integrated model to estimate the GHG emissions of global EVB cell production. We take into account 3 scenarios for EVB cell demand, 2 scenarios for battery chemistry, and 2 scenarios for energy mix between

2020-2050. This totally results in 12 scenarios.

**Battery demand scenarios.** We first use a medium battery demand scenario based on the EV fleet size of stated policy (STEP) scenario[7], which includes the fleet size of both battery electric vehicles (BEVs) and plug-in hybrid electric vehicles (PHEVs). The battery capacity per vehicle of small, mid-size, and large BEVs is assumed as 33, 66, and 100 kWh, respectively, while the average battery capacity of a PHEV is assumed as 14 kWh. The market share among small/mid-size/large is assumed as 19%, 48%, and 33% at any year between 2020-2050. We refer to Xu et al.[7] study for details of battery capacity per vehicle, share of BEVs/PHEVs, amongst others, share of small/mid-size/large BEVs.

The high battery demand scenario uses the same battery capacity per vehicle as the medium battery demand scenario, but a higher EV fleet size based on sustainable development (SD) scenario[7]. Since SD scenario suggests around double EV fleet size than STEP scenario, the high battery demand scenario indicates around two times demand for global EVBs capacity than the medium demand scenario.

The low battery demand scenario is developed based on the same EV fleet size as the medium battery demand scenario (*i.e.*, STEP scenario), but on a lower battery capacity per vehicle: we assume all BEVs are small BEVs with a 33 kWh battery capacity. This assumption is based on two arguments: first, small BEVs can provide most of the daily driving demand for consumers[181], even though they have a lower driving range than large BEVs equipped with a high-capacity battery. Second, the development of widespread EV charging infrastructure, including fast charging technology, could help to overcome the range anxiety of small BEV owners. The increasing use of small BEVs in the low battery demand scenario will reduce EVBs demand and GHG emissions significantly.

**Battery chemistry scenarios.** Given the uncertain battery chemistry development, we use two battery chemistry scenarios until 2050: the NCX scenario with the NCA and NCM series batteries dominating future EV market (including 1 NCA and 6 NCM batteries with X denoting manganese or aluminum, and NCX batteries will account for over 90% of EVBs market in 2030-2050), and the LFP scenario with LFP battery dominating the future EV market (LFP will reach a 60% market share in 2030-2050). We refer to the detailed descriptions of battery chemistry scenarios in our previous work[7].

We assume that battery chemistry scenarios would not differ between regions in view of limited data availability.

**Energy mix scenarios.** As indicated above, we take into account changes in energy mixes by region due to climate policy based on the Remind Integrated Assessment Model[180]. We apply two scenarios here, both based on Shared Socioeconomic Pathway 2 (SSP2) that indicates a 'middle-of-the-road' scenario with regard to future population and GDP growth. One is the '3.5 °C scenario' that projects the increase of global average temperature by more than 3.5 °C by 2100. Another is the 'well below 2 °C scenario' that aims to limit the cumulative global GHG emissions to 1,100 Gigatons (*i.e.*, SSP2-PkBudg1100 scenario as described in our previous paper[178]) and the increase of global average temperature by well below 2 °C by 2100. The two scenarios lead to quite different GHG intensities of electricity production per region, and as a consequence, life cycle GHG emissions of EVB production.

### 4.2.3 Sensitivity analyses with regard to GHG emissions

**Influence of EVB production region**

As shown above, we estimate the future GHG emissions of global EVB cells production during 2020-2050, based on global future demand for EVB cells and future life cycle GHG emissions per kWh capacity of EVB cell production (Fig. 4.1). However, the GHG intensities of EVB cell production differ between production regions, which are relatively high in China, medium in the US, and low in the EU. We assume China, EU, and US will produce 70%, 18%, and 12% of global EVBs during 2020-2050 while RoW is supplied by China, EU, and US proportionally. This assumption is based on predictions[182,183] of regional distribution of battery cell production capacity around the world in 2030.

It may however be that in future there will be a different production distribution mix. We, therefore, do a sensitivity analysis of battery production regions. Since EU generates the lowest energy-related GHG emissions and China generates the highest energy-related GHG emissions among three investigated battery production regions, here we perform sensitivity analysis between two extreme situations that all batteries supplied by EU producers (100% EU production) versus China producers (100% China production).

**Potential benefits of closed-loop, circular recycling**

In the above-mentioned scenarios (section 2.2), all life cycle GHG emissions are allocated to the use of batteries in EVs. No second uses or beneficial recycling of battery materials is assumed. We, therefore, perform a sensitivity analysis that includes a closed-loop, circular use of battery materials at their end of life. Battery recycling technologies, usually based on hydro[46]- or pyrometallurgy[48], develop fast and differ a lot according to battery chemistry, recycling volume, and other factors. This implies that using current LCI data for future battery recycling is unreliable. To avoid the use of highly uncertain estimates of environmental impacts during battery recycling, we define a 'maximum impact reduction potential by recycling': the GHG emissions of primary materials production that can be avoided if recycled materials would be used to substitute primary materials. This potential simply assumes that apart from a percentage loss in recycling all secondary materials available in EoL EVBs can be used as primary materials again, without considering *e.g.*, energy input, chemicals use, and emissions during recycling. Including reliable future-oriented LCI for recycling in future studies can promote insights into to what extent a circular use of battery materials may reduce life cycle GHG emissions of EVB production.

We calculate the maximum impact reduction potential by recycling based on global future EoL materials from EVB cells (recycled material) and future GHG emission of EVB cell materials that will be substituted by recycled materials. Calculating this recycling potential requires the match of type and quality between recycled materials and primary materials, as well as information on which and where primary materials, along the cell production chain, are substituted by recycled materials, as explained in the following.

**Recycled materials amount, type, and quality.** We consider two commercially available recycling technologies (pyro-[48] and hydro- recycling), and their recycled materials type, quality, recycling efficiency (Table 4.1). Although the outputs of both pyro- and hydro- recycling are industry-grade materials, the hydro- recycling can recycle more materials (such as graphite) with high recycling efficiency than pyro-recycling. The total amount of secondary/EoL materials available for re-use was calculated based on the amount of available EoL EVBs in a specific year from our dynamic battery stock model, and the recycling efficiencies in pyro- and hydrometallurgy assuming a 50%/50% market share of

pyrometallurgical/hydrometallurgical recycling. Since the uncertainty around market share between pyro- and hydro- recycling technologies, we conduct **s**ensitivity analysis of 100% pyro- and 100% hydro- recycling and investigate their effects on recycling potential.

**GHG emissions of primary cell materials that are substituted by recycled materials.** According to our prospective model[178], EVB cell production includes five life cycle stages: mining, raw materials production, upgrading battery materials, component production, and cell production. Here we assume recycled materials will substitute primary materials at the level of 'raw materials production' since pyro- and hydro- recycling can generate battery industry-grade materials.

Besides which and where primary materials are substituted, the GHG emissions of primary materials matter for the recycling potential. However, GHG emissions of primary materials are sensitive to their production regions where energy is supplied. We assume EoL EVBs are recycled and re-used in the same region where the EVBs are used. The EoL materials from EVB cells in China will be recycled in China and substitute primary cell materials produced in China, US for US, and EU for EU. While for RoW, we assume EoL EVB cells in RoW will be exported to China for recycling since the expansion of battery recycling capacity in China, and naturally the recycled materials will substitute primary cell materials produced in China. Consequently, around 50%/32%/18% of global EoL EVB cells are recycled and reused to substitute primary materials produced in China/EU/US respectively.

**Table 4.1: Recycling efficiency of battery materials by pyrometallurgical and hydrometallurgical technologies.**

| Materials | Pyrometallurgical[48] | Hydrometallurgical[46] |
|---|---|---|
| Copper | 90% | 100% |
| Aluminum foil | / | 100% |
| Graphite | / | 100% |
| Li+ in product | / | 80% |
| Co2+ in product | 98% | 98% |
| Ni2+ in product | 98% | 98% |
| Mn2+ in product | / | 80% |
| Al3+ in product | / | 80% |
| Electrolyte organics | / | 100% |
| Cell aluminum container | 90% | 90% |

## 4.3 Results and discussion

### 4.3.1 Battery cells demand

The global demand for EVB cells will increase from 0.4 TWh (terawatt hour) in 2020 to 1.5 TWh in 2030, and 7 TWh in 2050 in medium battery demand scenario (Fig. 4.2), with an increasing factor of 19 and an average annual growth rate of 10% during 2020-2050. China, EU, US, and RoW account for 47%, 22%, 12%, and 19% of global demand in 2050, respectively.

Compared to the medium demand scenario, low battery demand scenario sees 42% lower EVB cells demand in 2020-2050 due to lower battery capacity per vehicle, while high battery demand scenario finds a ~70% higher EVB cells demand in 2020-2050 because of double EV fleet size. As a result, global demand for EVB cells will reach as low as 0.9 TWh (low battery demand scenario) and as high as 2.4 TWh (high battery demand scenario) in 2030 and 4-12 TWh in 2050. Global demand is expected to increase by a factor of 11-31 and average annual growth rates of 8%-12% between 2020 and 2050.

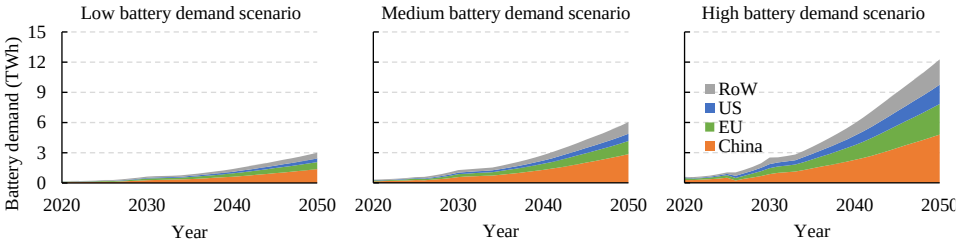


**Fig. 4.2: Scenarios of global future demand for EVB cells, including China, EU, US, and RoW.** 1 TWh = $10^9$ kWh.

### 4.3.2 GHG emissions

Fig. 4.3 presents the GHG emissions of global EVB cell production in 2030, 2040, and 2050, without considering effects of recycling. Note that the figure includes also the sensitivity analyses assuming full production in China or the EU, respectively. In the medium battery demand scenario, the global GHG emission of EVB cells production will range from 44-99 Mt CO2-Eq in 2030, 54-173 Mt CO2-Eq in 2040, and 99-287 Mt CO2-Eq in 2050 (range depends on battery chemistry and energy mix scenarios). High

battery demand scenario leads to 1.5-1.7 times higher annual GHG emissions than in the medium demand scenario, while low demand scenario results in 58%-59% of annual GHG emissions of the medium demand scenario. There is a factor of 2.6-2.9 for GHG emissions of global EVB cell production between the low demand scenario and the high demand scenario.

In addition to battery demand scenarios, scenarios of battery chemistry and energy mix also affect GHG emissions of global EVB cell production. Since LFP batteries generate lower GHG emissions than NCX batteries, the GHG emissions in LFP scenario are 12%-15% lower than NCX scenario (range depends on battery demand scenarios). Compared to battery chemistry, energy mix has a stronger impact on GHG emissions. The GHG emissions under well below 2 °C scenario are 48%-65% lower than under 3.5 °C scenario, because well below 2 °C scenario results in higher low-carbon energy use during battery production that can lead to over 50% reduction of GHG emission per EVB cell production. Consequently, in each battery demand scenario, GHG emissions of global EVB cell production range from low boundary in "LFP and well below 2 °C scenario" to high boundary in "NCX and 3.5 °C scenario".

Despite an 8%-12% annual growth rate of global demand for EVB cells during 2020-2050 across low-medium-high demand scenarios, associated GHG emissions only increase annually by 2%-10% in the same period. Therefore, EVB cells' GHG emissions relatively decouple, *i.e.*, emissions per kWh of battery decrease, while overall emissions continue to increase due to the fast growing demand. To illustrate this, we define a relative decoupling rate, based on[184], as the relative change of annual growth rates between GHG emissions and demand. The relative decoupling rate from 2020-2050 ranges from 19% to 70% for EVB cells, depending on battery demand, battery chemistry, and energy mix scenarios.

As indicated the region where EVBs will be produced is uncertain. Given the different GHG emission intensities of electricity production in China, US and EU this affects GHG emissions of global EVB cell production and the relative decoupling rate between GHG emissions and demand. Figure 3 shows also a sensitivity analysis assuming 100% production in China and the EU respectively. The effects are more limited in well below 2 °C scenario than in 3.5 °C scenario. The GHG emissions of global EVB cell production will increase to 61-519 Mt CO2-Eq in 2050 and the relative decoupling rate during 2020-2050 will decrease to 16%-68% if 100% China production; these numbers change

to 49-333 Mt CO2-Eq and 29%-77% if 100% EU production (error bars in Fig. 4.3).

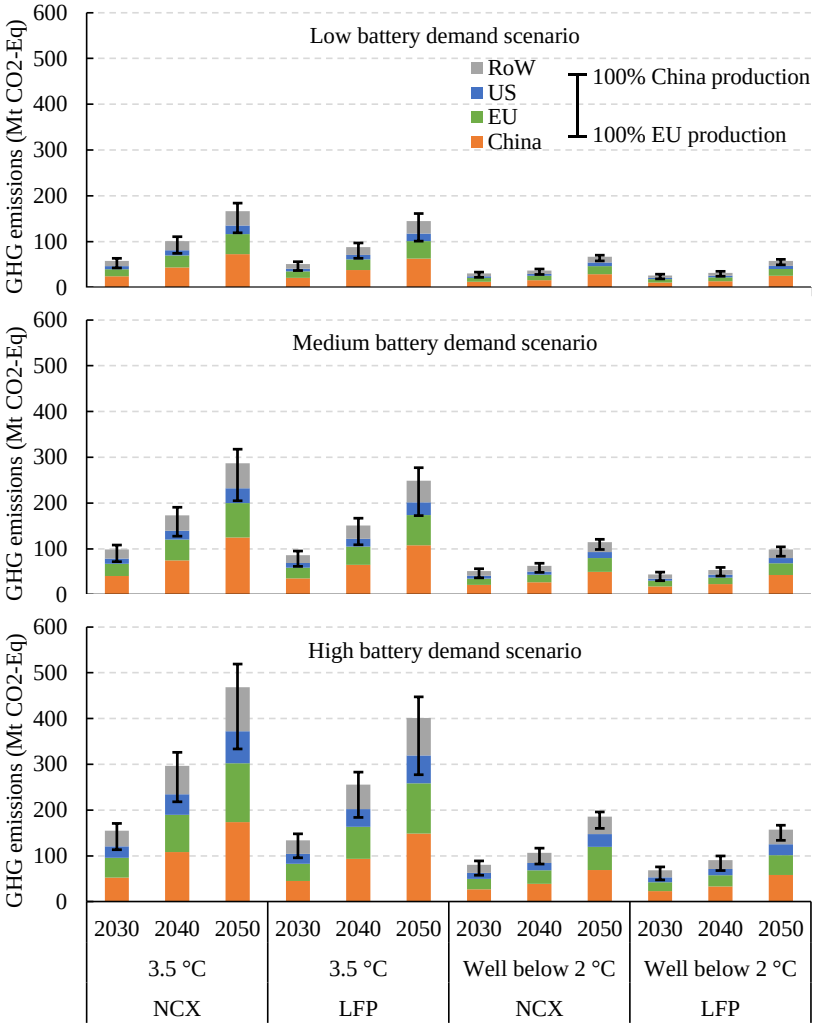


**Fig. 4.3: Future GHG emissions of global EVB cells production under different battery demand, battery chemistry, and energy mix scenarios.**

### 4.3.3 Potential benefits of closed loop recycling

EVB recycling can reduce the GHG emissions of EVB cells since recycled materials contain less embodied GHG emissions than primary materials[185]. We quantify

maximum impact reduction potential by recycling, *i.e.*, avoided GHG emissions of primary materials that can be substituted by recycled materials, while at the same time neglecting the environmental impacts during recycling. The higher GHG emissions of EVB cell production, the higher maximum impact reduction potential by recycling. In other words, the highest maximum impact reduction potential by recycling exists in 'high battery demand-NCX-3.5 °C' scenario, and the lowest potential in 'low battery demand-LFP-well below 2 °C' scenario. The global maximum impact reduction potential by recycling will range from 0.4 to 1.3 Mt CO2-Eq in 2030 and from 4 to 41 Mt CO2-Eq in 2050 (see Supplementary Fig. 4.1), which is 1-2 orders of magnitude lower compared to battery production GHG emissions (Fig. 4.3).

We further investigate the relative maximum impact reduction potential by recycling for the next three decades: maximum impact reduction potential by recycling divided by battery production GHG emissions, *i.e.*, the percentage of battery production GHG emission that can be mitigated by using recycled materials to substitute primary materials (see results in Fig. 4.4). Material recycling only has a minor but increasing contribution to reduce GHG emissions. The relative maximum impact reduction potential by recycling for GHG emissions is increasing from less than 1% in 2021-2030 to 2%-5% in 2031-2040, and to 3.5%-10% in 2040-2050 (left of Fig. 4.4). This is mainly because the volume of materials entering the EoL stage in a specific year is just a fraction of the required new use (5%-30%) due to the fast growth of the EV fleet. This situation can be only partly solved once the EV battery market has reached a steady state, *i.e.*, when recycled EoL materials can almost completely meet material demand. With a hypothetical future steady state after 2050 (right of Fig. 4.4), the relative maximum impact reduction potential by recycling can improve to 8%-22% in 2021-2030 to 10%-30% in 2031-2040, and to 13%-35% in 2040-2050. These potentials are still far below 100%. The reason is that recycled materials of pyro- and hydro-recycling can substitute/be used as industry-grade primary materials whose production generates fewer GHG emissions than the further processing to battery-grade materials or components.

The recycling potential depends on not only the amount of availability of EoL battery materials, but also on which primary battery materials will be substituted by recycled materials - affected by recycled material type and quality - and what GHG emission intensity of primary battery materials will be avoided. Pyro-recycling and hydro-

recycling can both recover industry-grade materials (lower quality than battery-grade materials), but hydro-recycling recovers more material types (such as graphite) than pyro- recycling. Compared to 100% pyro-recycling, 100% hydro-recycling only slightly improves the relative maximum impact reduction potential by recycling (error bars in Fig. 4.4). It is hence important to develop industrial-scale reconditioning technologies that allow the re-use of EoL battery components as components or battery-grade materials, such as direct recycling technology[186] that can recover and re-use battery cathode.

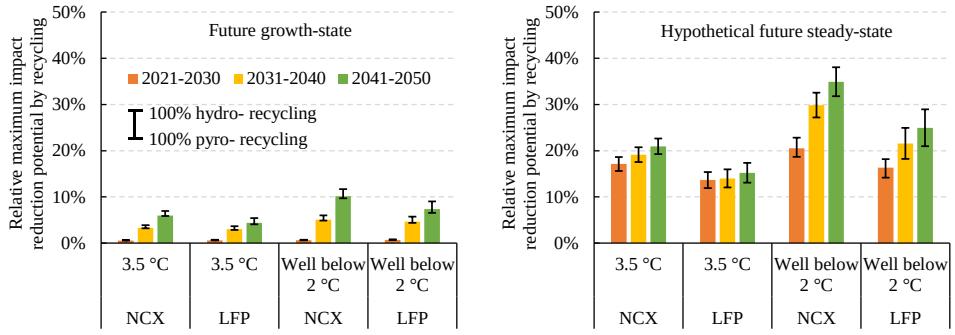


**Fig. 4.4: Relative maximum impact reduction potential by recycling for GHG emissions of global EVB cells production in periods of 2021-2030, 2031-2040, and 2041-2050, with future growth-state (left) and hypothetical future steady-state (right), under medium battery demand scenario.** Bar charts refer to a 50%/50% market share of pyro- /hydro- recycling. Error bars indicate 100% hydro-recycling and 100% pyro- recycling. Please see results under low and high battery demand scenarios in Supplementary Fig. 4.2 and Supplementary Fig. 4.3.

## 4.4 Conclusions

In this paper, we build an integrated model, consisting of a dynamic battery stock model and a prospective LCA model, to quantify future GHG emissions of global EVB cell production during 2020-2050. We further investigate the effect of different regional distributions of production and the GHG emissions reduction potential related to avoided primary material production due to closed-loop recycling. We find that:

(1) Due to demand growth for EVB cells, GHG emissions of global EVB cell production will increase to 26-155 Mt CO2-Eq in 2030 and 58-468 Mt CO2-Eq in 2050, depending on battery demand, battery chemistry, and energy mix scenarios.

(2) Despite 8%-12% average annual growth rate of global demand for EVB cells during 2020-2050, associated GHG emissions only increase annually by 2%-10% in the same period. There is thus a relative decoupling of GHG emissions related to demand by 19%-70% from 2020 to 2050. This is due to a reduction of the emission intensity of battery production by over 50% that mainly results from the decarbonization of the consumed electricity during battery production, especially under the well below 2 °C scenario.

(3) Maximum impact reduction potential by recycling for GHG emissions will reach 0.4-1.3 Mt CO2-Eq in 2030 and 4-41 Mt CO2-Eq in 2050, which is 1-2 orders of magnitude lower compared to battery production GHG emissions. Recycling offers initially only a small potential to reduce GHG emissions, but the potential increases after 2030 because of the increasing availability of EoL battery materials.

In short, to avoid important GHG emissions due to battery cell production for EVs it is crucial to realize the following. First, the energy system should be decarbonized strongly, since this is the single most important factor determining GHG emissions from EVB cell production. Second, we see that using small EVs that can operate using relatively low battery capacities reduces life cycle GHG production emissions even further. Third, we see that LFP batteries have slightly lower life cycle GHG emissions than NCX batteries. Finally, we see that recycling or re-use of secondary batteries on the short term will not reduce life cycle GHG emissions a lot since building up stocks of EVBs requires much more new materials as that there are EoL batteries available. These findings give clear recommendations to policy to reduce GHG emissions from EVB production. Particularly the stimulation of use of small EVs is crucial, next to ensuring batteries are designed and developed such that easy re-use after end of life is possible. An important other development that could be stimulated is the use of self-driving cars[4] and sharing vehicles[5]. These are likely to be used much more intensively by different users, which could reduce the required battery capacity and related life cycle GHG emissions for production additionally by several factors[187].

## 4.5 Supplementary information

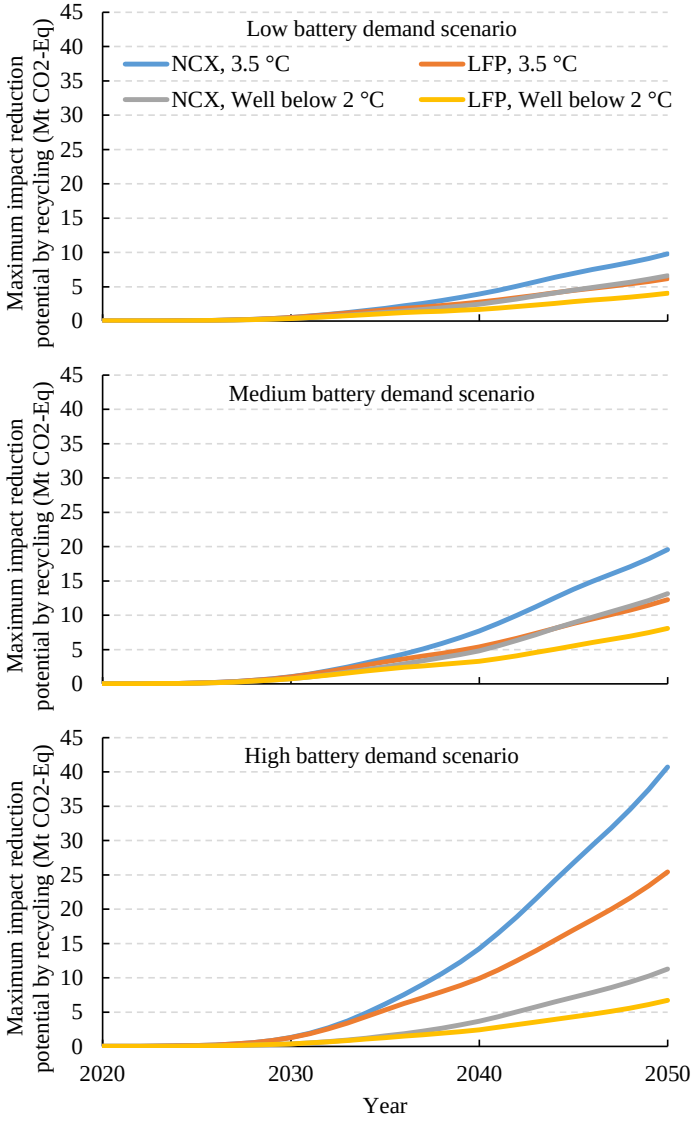


**Supplementary Fig. 4.1: Global maximum impact reduction potential by recycling for GHG emissions of global EVBs cells production under low, medium, and high battery demand scenarios.**

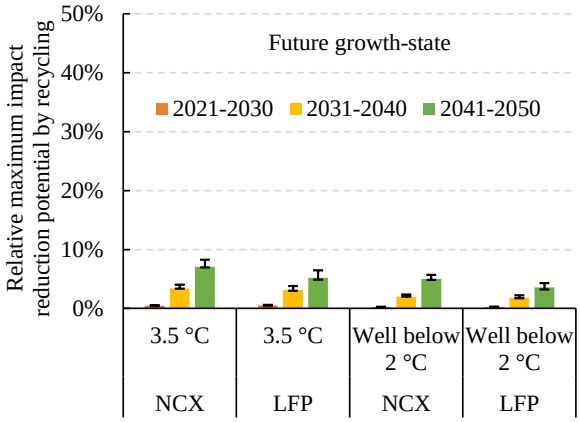


**Supplementary Fig. 4.2: Relative maximum impact reduction potential by recycling for GHG emissions of global EVBs cells production in periods of 2021-2030, 2031-2040, and 2041-2050, with future growth-state, under low battery demand scenario.** Bar charts refer to a 50%/50% market share of pyro- /hydro- recycling. Error bars indicate 100% hydro- recycling and 100% pyro-recycling.

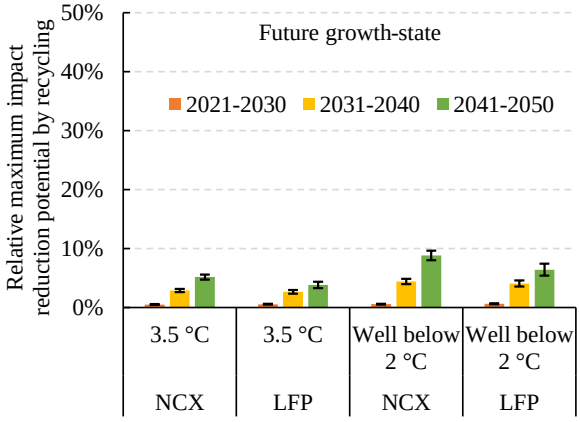


**Supplementary Fig. 4.3: Relative maximum impact reduction potential by recycling for GHG emissions of global EVBs cells production in periods of 2021-2030, 2031-2040, and 2041-2050, with future growth-state, under high battery demand scenario.** Bar charts refer to a 50%/50% market share of pyro- /hydro- recycling. Error bars indicate 100% hydro- recycling and 100% pyro-recycling.

# 5 Electric vehicle batteries alone could satisfy short-term grid storage demand by as early as 2030[d]


## Abstract

The energy transition will require a rapid deployment of renewable energy (RE) and electric vehicles (EVs) where mass transit or personal transit options are unavailable. EV battery storage could complement variable RE generation by providing short-term grid services. However, estimating the market size of this opportunity requires an understanding of many socio-technical parameters and constraints. We quantify global EV battery capacity available for grid storage using an integrated model which incorporates future EV battery deployment, battery degradation, and market participation rates. We include both the 'in-use' and 'end-of-life' potential of EV batteries. We find a technical capacity of 32-62 TWh by 2050 and that modest market participation rates (12%-43%) are needed to provide most if not all short-term grid storage demand globally. This demand could be met as early as 2030 across most regions. Our estimates are generally conservative and offer a lower bound of future opportunities.


## 5.1 Introduction

Electrification and the rapid deployment of renewable energy (RE) generation are both critical to a low-carbon energy transition[56,73]. They also address many other environmental issues, including air pollution. However, the variability of critical RE technologies, wind and solar, combined with increasing electrification may present a challenge to grid stability and security of supply[56,73]. To address this, there are several supply-side options for meeting demand including, in approximate ascending order of today's estimated cost: energy storage, firm electricity generators (such as nuclear or geothermal generators), long-distance electricity transmission to balance variations, over-building of RE (resulting in curtailment in periods of lower demand), and power-to-gas[188]. In addition to these supply-side options, demand-side management is also

[d] Under the second revision with Nature Communications, as: Xu, C., Behrens, P., Gasper, P., Smith, K., Hu, M., Tukker, A. & Steubing, B. Electric vehicle batteries alone could satisfy short-term grid storage demand by as early as 2030.

vital in shifting and flattening peak demand[189]. Given rapid cost declines, batteries are one of the major options for energy storage and can be used in various grid-related applications to improve grid performance. These declines in cost have also driven a cost-decline of EVs. Given that many batteries will be produced for light-duty transport these could offer a cost- and materially-efficient approach for the short-term storage requirements needed on electricity grids across the world[190].

EV batteries can be used while they are part of the vehicle in vehicle-to-grid approaches, or after the end of the life (EoL) of the vehicle (when they are removed and used separately to the chassis). Vehicle-to-grid charging can be smart to enable dynamic EV charging and load-shifting services to the grid. EVs can also be used to store electricity and deliver it to the grid at peak times when power generation is more expensive[14]. These opportunities rely on standards and market arrangements that allow for dynamic energy pricing and the ability of owners to benefit from the value to the grid (value that can include deferred or avoided capital expenditure on additional stationary storage, power electronic infrastructure, transmission build-out *etc*[14]).

There will also be substantial grid-based value for EV batteries at vehicle EoL (hereafter called retired batteries). Usually, when the remaining battery capacity drops to between 70-80% of the original capacity batteries become unsuitable for use in EVs[15]. However, these retired batteries may still have years of useful life in less demanding stationary energy storage applications[16]. These batteries can continue to buffer differences in supply and demand and contribute to grid stability.

The utilization of EV batteries could improve the flexibility of supply while reducing the capital costs and material-related emissions associated with additional storage and power-electronic infrastructure. However, the total grid storage capacity of EV batteries depends on different socio-economic and technical factors such as business models, consumer behaviour (in driving and charging), battery degradation, and more[53,54]. Investigating the future grid storage capacity of EV batteries is essential in understanding the role EV batteries could play in the energy transition. Previous global-level studies, including those on vehicle-to-grid capacity[55-57] and retired battery capacity[57,58], while informative, rarely consider several important factors such as: non-linear, empirically-based battery degradation (they often neglect the impact of battery chemistry[59-61]); geographical and/or temporal temperature variance (which impacts battery degradation); and, driving intensity by vehicle type in different

countries/regions (which constrains the total capacity available during the day). These factors determine the technical grid storage capacity. Additionally, consumer participation in the vehicle-to-grid market and in the second-use market impacts the actual grid storage capacity[54], which is important but rarely quantified.

Here we link three models and databases to provide an estimate of the grid storage capacity of EV batteries globally by 2050 for both vehicle-to-grid applications and EoL opportunities (see Methods and Supplementary Fig. 5.1). We cover the main EV battery markets (China, India, EU, and US) explicitly, and combine other markets in a Rest of the World region (RoW). The first model is a dynamic battery stock model, which estimates the future battery demand in each region as part of transport fleets per region (Supplementary Fig. 5.2). The model incorporates two EV fleet development scenarios from the IEA (International Energy Agency), the stated policy scenario (STEP) and the sustainable development scenario (SD). The scenarios include two battery chemistry variants to encompass different technological paths: one which is dominated by Lithium nickel cobalt oxides (NCX, representing NMC or NCA with X denoting manganese or aluminum) and another dominated by Lithium-ion phosphate or (LFP). The second model assesses EV use and provides potential EV driving and charging behavior for small, mid, and large size BEV (battery electric vehicles) and PHEV (plug-in hybrid electric vehicles) based on daily driving distance distributions for different regions (Supplementary Fig. 5.3, Supplementary Fig. 5.4, and Supplementary Fig. 5.5). The third model combines information from the other models on EV use behavior, battery chemistry, and temperature in each region with the latest battery degradation data for NCX[59,60,191] and LFP[61] chemistries to account for region- and chemistry-specific battery degradation (Supplementary Fig. 5.6).

We first analyze the technical capacity for short-term grid storage from vehicle-to-grid and second-use. We choose the industry standard, 4-hour storage capacity on a daily basis, as EV batteries are unsuitable for longer-term, seasonal storage due to their chemistries and use cases. We further analyze the impact of different participation rates of EV owners in vehicle-to-grid as well as the impact of different second-use participation rates of retired EV batteries in second-use business (see methods for further details). Finally, we compare these potentials against several scenarios for future storage requirements from the literature.

*Short-term grid storage demand scenarios.* Future electricity grids will require a

combination of short-term energy storage (discharge duration of several hours throughout a day, such as battery energy storage) and long-term storage (discharge duration of days, months, and seasons, such as pumped hydro storage technologies). We focus here on short-term energy storage since this accounts for the majority of the required power storage capacity[192]. Short-term energy storage demand is defined as a typical 4-hour storage system, referring to the ability for the storage system to operate at a capacity where the maximum power delivered from that storage over time can be maintained for 4 hours. For example, the 4-hour storage capacity of batteries that together deliver a maximum of 0.25 GW until depletion will be 1-Gigawatt hour[193] (GWh). The short-term storage capacity and power capacity are defined based on a typical 1-time equivalent full charging/discharge cycle per day (amounting to 4 hours of cumulative maximum discharge power per day).

We compare our results with storage requirements reported in the IRENA (International Renewable Energy Agency) Planned Energy Scenario (with a warming "likely 2.5°C" in the second half of this century) and the Transforming Energy Scenario (with a warming of "well below 2°C" in the second half of this century)[2]. We also compare our results with storage capacity requirements summarized by the influential Storage Lab for both conservative and optimistic scenarios[194]. Both Storage Lab scenarios result in a warming of "well below 2°C" by 2100, but differ in the role of grid storage in the energy system. For further details on these scenarios see Supplementary Table 5.1. These scenarios lead to short-term grid storage demands of 3.4, 9, 8.8, 19.2 TWh respectively, or 10 TWh on average by 2050. With the 4 hours delivery period, this implies that a power capacity demand is within a range of 850-4800 GW or 2500 GW on average by 2050.

## 5.2 Methods

### 5.2.1 Model overview

We develop an integrated model to quantify the future EV battery capacity available for grid storage, including both vehicle-to-grid and second-use (see Supplementary Fig. 5.1 for an overall schematic). The integrated model includes three sub-models:

1) A dynamic battery stock model[7] to estimate total future EV battery stock and the retired batteries at vehicle EoL. This model considers EV fleet (*i.e.*, battery stock) development and EV lifespan distribution (Supplementary Fig. 5.2), as

well as future chemistry development.

2) An EV use model which includes behavioral factors such as EV driving cycle and charging behavior (changing power, time, and frequency), based on daily driving distance data for small/mid-size/large BEVs and PHEVs (Supplementary Fig. 5.3, Supplementary Fig. 5.4, and Supplementary Fig. 5.5).

3) A battery degradation model based on the latest battery degradation test data, to estimate battery capacity fading over time under different EV use, battery chemistry, and temperature conditions (Supplementary Fig. 5.6).

### 5.2.2 Dynamic battery stock model

We build on results and methods from a previous study[7] where we built a global dynamic battery stock model to quantify the stock and flows of EV batteries. We model future EV fleet development (*i.e.*, battery stock) until 2050. We determine the retired battery availability based on battery stock development and EV lifespan distribution (which is assumed to determine the time when EV batteries are retired). Battery degradation does affect the technical performance (such as driving distance capability) of EVs, thus influencing consumers' choice of time when EVs come into EoL. Here, for model simplicity, we assume batteries will be retired only when EVs come into EoL. While for EV battery capacity, we use an average capacity of 33, 66, and 100 kWh for small/mid-size/large BEVs, and 21, 10, and 15 kWh for small/mid-size/large PHEVs.

**EV fleet scenarios.** We use two EV fleet scenarios until 2030 from the IEA: the stated policies (STEP) scenario and the sustainable development (SD) scenario. We further extend these two scenarios to 2050 based on a review of EV projections until 2050. We use the EV fleet share across 5 main EV markets (China, India, EU, US, and RoW) from the IEA until 2030, and keep the EV fleet share by countries/regions in 2030-2050 the same as the year 2030 due to lack of reliable data after 2030 (see Supplementary Data for EV fleet scenarios by countries/regions). Further, we include 56 cities in China, 9 cities in India, 32 cities in EU, 53 cities in US, and 9 cities in RoW. We compile future EV sales share among 159 cities globally in STEP scenario and SD scenario based on future EV fleet projections by counties/regions from the IEA[195] and other data sources[196,197] (see Supplementary Data).

**Battery chemistry scenarios.** We consider battery market shares by chemistry based on the market share projections until 2030 from Avicenne Energy[198] and potential trends until 2050[80,81,83]. Two battery chemistry scenarios are developed, including a

Lithium Nickel Cobalt Manganese Oxide and Lithium Nickel Cobalt Aluminum Oxide battery dominated scenario or NCX scenario (with X representing Manganese or Aluminum), and a Lithium Iron Phosphate battery dominated scenario or LFP scenario. The detailed battery market shares by chemistry in two scenarios are discussed in[7].

### 5.2.3 EV use model

**Daily driving distance (DDD).** We explore the EV driving behavior based on DDD distributions. We build historical EU DDD distributions for small/mid-size/large BEVs/PHEVs models based on data from Spritmonitor.de[199], which has been widely used in literatures[200,201]. We exclude the DDD less than 5 km from the dataset. By comparing various DDDs in multiples of EV range, we classify 5 DDD classes to formulate driving intensity and charging behavior. These 5 classes are divided between 0% of the EV range to 200% of the EV range (*i.e.*, a DDD twice the range of the EV) with intervals of 0-25%, 25-33%, 33-50%, 50-100%, 100-200%. We use the mean DDD of each class for calculations. Further, we compile future DDD in different countries/regions (Supplementary Fig. 5.7, Supplementary Fig. 5.8, Supplementary Fig. 5.9, and Supplementary Fig. 5.10) by assuming the future DDD is proportional to the future energy consumption per vehicle. We calculate future energy consumption per vehicle in different countries/regions based on the IEA's projection on future EV fleet size and associated energy consumption until 2030[195].

**EV driving cycle.** We assume two commuting trips between home and working place per day on weekdays and two entertaining trips on weekends for all countries/regions. Each trip distance is half of DDD. According to the required trip distance, we compile the driving cycle of each trip (speed versus time) based on the standard US combined driving cycle (*i.e.*, 55% city driving and 45% highway driving, see details in Supplementary Fig. 5.4 and Supplementary Fig. 5.5, and Supplementary Note 5.1).

**EV charging.** Charging behavior may be affected by charging infrastructure, amongst others, on-board EV charger, consumer preferences. We assume an immediate and slow home charging at constant charging power to full charge for all EV sizes and types because home charging is the major charging way (see Supplementary Data). We assume the home charging power as 1.92, 6.6, 22, and 1.92 kW for small, mid-size, large BEV, and PHEV, respectively[202]. We assume that due to high costs and limited utility no consumers will install higher power charging infrastructure at home. We

further anticipate the charging behaviors in terms of changing frequency by comparing the various DDDs in multiples of the EV range. As driving intensity increases, the higher charging frequency is assumed for 5 DDD classes (1x every four days, 1x every three days, 1x every two days, 1x each day, and 2x every day respectively). For example, if the DDD of mid-size BEV (with a 312 km EV range) increases from 75 km to 625 km, and the battery needs to be charged more frequently from 1 time per four days to 2 times per day.

**Battery State-of-Charge (SoC) profile.** We calculate the EV battery SoC second by second under three EV states: driving, parking and charging, and parking without charging. For battery SoC during driving, we use FASTSim model[202] developed by NREL to calculate EV battery SoC second-by-second based on inputs of the EV driving cycle, EV configurations, and battery performance parameters (specific energy and battery capacity). We select one representative EV model from the FASTSim model[202] for each EV size and type as EV configuration (Supplementary Table 5.2), and NCM622 as representative chemistry for all EV types; because it was found that EV configurations and battery performance parameters (such as specific energy) had small effects on the resulting battery SoC simulations. For battery SoC during charging, we assume the battery SoC increases linearly under a constant charging power with a 90% charging efficiency[203]. For battery SoC during parking without charging, the battery SoC decreases due to self-charging. A typical self-discharging rate of 5% per month is assumed for lithium-ion battery[204]. Note that for the sake of battery safety, a portion of battery capacity is unusable (15% for BEVs and 30% for PHEVs based on the BatPac model[205]), therefor we assume the usable battery SoC range as 5%-90% for BEV battery and 15%-85% for PHEV battery.

**Battery temperature**. The battery temperature depends on the heat generation from chemical reactions inside batteries, amongst others, ambient temperature and environment (such as solar power radiation), battery management system (air or liquid cooling system to control battery temperature). The temperature can also vary from cell to cell, module to module, and component to component in the battery pack. The modelling of battery temperature is complicated and out of scope of this study. Here we use city ambient temperature to represent battery temperature, which is then used to battery degradation. Here, we use the monthly average temperature of total 159 cities to capture the effects of geographic and temporal temperature variance on

battery degradation. The temperature data is collected from[206-209], which can be found in Supplementary Data.

### 5.2.4 Battery degradation model

**Degradation model development.** Battery degradation is crucially important for determining EV battery capacity both in use and for second life applications, but there are still many open research questions surrounding the importance of EV driving habits, charging behavior, and battery chemistries on capacity development[210]. Degradation model approaches include physics based degradation models[211] as well as machine learning models[75,212] though there is no agreed-upon best practice[213]. Here, to balance the complexity and accuracy of battery degradation model, we develop a semi-empirical battery degradation model based on method from[61]. The model considers both calendar life and cycle life aging (equation (1)), assuming a square-root dependence on time for calendar life (degradation rates depend on temperature and SoC, see equation (2)) and a linear dependence on energy throughput for cycle life (degradation rates depend on temperature, Depth-of-Discharge (DoD), and Current rate ($C_{rate}$) see equation (3)).

$$q = 1 - q_{Loss,Calendar} - q_{Loss,Cycling} \tag{1}$$

$$q_{Loss,Calendar} = k_{Cal} \cdot exp\left(\frac{-E_a}{RT}\left(\frac{1}{T} - \frac{1}{T_{ref}}\right)\right) \cdot exp\left(\frac{\alpha F}{R}\left(\frac{U_a}{T} - \frac{U_{a,ref}}{T_{ref}}\right)\right) \cdot \sqrt{t} \tag{2}$$

$$q_{Loss,Cycling} = k_{Cyc} \cdot (A \cdot DOD + B) \cdot (C \cdot C_{rate} + D) \cdot \left(E \cdot \left(T - T_{ref}\right)^2 + F\right) \cdot EFC \tag{3}$$

where q is the relative battery degradation, $q_{Loss,Calendar}$ is the relative calendar life degradation, $q_{Loss,Cycling}$ is the relative cycling life degradation, T is temperature, t is time (unit: days), EFC is equivalent full cycles. Note R is the universal gas constant (8.3144598 J/mol·K), $T_{ref}$ is the reference temperature (298.15 K), F is Faraday constant (96485 C/mol), $k_{Cal}$ (unit: $days^{0.5}$), $E_a$ (unit: J/mol·K), and α (no unit) are fitting parameters for calendar life degradation, and $k_{Cyc}$ (unit: $EFC^{-1}$). A, B, C, and D (no units) are fitting parameters for cycling life degradation. The value of the anode-to-reference potential, $U_a$ (unit: V), is calculated from the storage SoC using equations (4) and (5)[214].

$$\begin{aligned} U_a(x_a) = {} & 0.6379 + 0.5416 \cdot exp(-305.5309 \cdot x_a) + 0.044\, tanh\left(-\frac{x_a - 0.1958}{0.1088}\right) \\ & -0.1978\, tanh\left(\frac{x_a - 1.0571}{0.0854}\right) - 0.6875\, tanh\left(\frac{x_a + 0.0117}{0.0529}\right) - 0.0175\, tanh\left(\frac{x_a - 0.5692}{0.0875}\right) \end{aligned} \tag{4}$$

where $x_a$, which represents the lithiation fraction of the graphite, is a simple linear function of the SoC[215]:

$$x_a(SOC) = x_{a,0} + SOC \cdot (x_{a,100} - x_{a,0}), x_{a,0} = 0.0085, x_{a,100} = 0.78 \quad (5)$$

where $x_{a,0}$ is the lithiation fraction of the graphite at 0% SoC and $x_{a,100}$ is the lithiation fraction of the graphite at 100% SoC.

To obtain these fitting parameters, we collect publicly available battery degradation data, including calendar life aging and cycle life aging, for NCM[61] and LFP[59,60,191] chemistry. These data sets represent state-of-the-art lifetime performance for each chemistry; the LFP cells shown reach between 5000 and 8000 equivalent full cycles before reaching 80% remaining capacity, 4000~5000 equivalent full cycles for NCM cells. This experimental data was then fit with the semi-empirical model equations (1), (2), and (3) using a non-linear least squares solver in MATLAB. The NCM model has no $C_{rate}$ dependence, due to lack of data in the aging data set, so the parameters C and D are simply set at 0 and 1. We first fit the calendar fade data with the time-dependent portion of the model ($q_{Loss,Calendar}$, parameters $k_{Cal}$, $E_a$, and $\alpha$); the parameter $\alpha$ is bounded between -1 and 1, with other parameters unbounded. The parameters for the cycling fade (A, B, C, and D) are optimized on the cycling aging data. For both LFP and NCM, the raw cycling fade data was processed prior to optimizing a model based on expert judgement. For LFP, only cells with linear fade trajectories and data for at least 5000 EFCs were used for model optimization. For NCM, only data after 200 EFC at T > 5 °C and data at q < 0.85 at T < 5 °C was used for optimization of the NCM cycling model parameters. The optimized parameters for the LFP and NCM degradation models are shown in Supplementary Table 5.3. Fitting results are shown in Supplementary Fig. 5.11 and degradation rates are shown in Supplementary Fig. 5.12.

Note that we assume NCA battery has the same degradation patterns as NCM battery due to a lack of state-of-the-art open-source data for NCA batteries. Besides cell chemistry, capacity degradation characteristics vary with cell design, manufacturing process, and proprietary additives[210,216], which is out of scope of this study. We use cell degradation patterns to represent battery pack degradation without consideration of cell-to-cell and module-module differences.

**Battery degradation under different driving and temperature conditions.** For

simulation of the degradation under the EV driving loads (battery SoC evolution over time) and during dynamic temperature changes, the degradation model is reformulated to solve for the degradation occurring during consecutive timesteps[60]. We choose a timestep of 1 day for making SoH updates and update the SoC timeseries for each day by the current SoH. At each timestep, the temperature is the average temperature during the simulation month at cities from different countries/regions. Average SoC, DoD, $C_{rate}$, and the number of EFCs is extracted from the SoC timeseries. Average SoC refers to the time-averaged value of SoC. DoD is the difference between the maximum and minimum values of SoC. $C_{rate}$ is calculated using the absolute change of SoC per second, and then taking the average of all $C_{rates}$ greater than 0 during the entire timeseries. The number of EFCs is calculated by summing the changes to SoC over the timeseries. Dependence of the expected degradation rate on current SoH is incorporated by calculating a 'virtual time'[60]. The virtual time is found by inverting the calendar degradation equation to solve for time:

$$t_{virtual} = \left( q_{Current} \Big/ k_{Cal} \cdot exp\left(\frac{-E_a}{RT}\left(\frac{1}{T} - \frac{1}{T_{ref}}\right)\right) \cdot exp\left(\frac{\alpha F}{R}\left(\frac{U_a}{T} - \frac{U_{a,ref}}{T_{ref}}\right)\right) \right)^2 \tag{6}$$

The degradation change Δq during any given timestep Δt is then calculated by the following equation:

$$\Delta q = \left( k_{Cal} \cdot exp\left(\frac{-E_a}{RT}\left(\frac{1}{T} - \frac{1}{T_{ref}}\right)\right) \cdot exp\left(\frac{\alpha F}{R}\left(\frac{U_a}{T} - \frac{U_{a,ref}}{T_{ref}}\right)\right) \Big/ 2 \cdot \sqrt{t_{virtual} + \Delta t} \right) \cdot \Delta t + k_{Cyc} \cdot (A \cdot DOD + B) \cdot (C \cdot C_{rate} + D) \cdot \left(E \cdot \left(T - T_{ref}\right)^2 + F\right) \cdot \Delta EFC \tag{7}$$

For cycling fade, the virtual EFC does not need to be calculated, as the degradation rate is constant with respect to the change of EFC during any given timestep. This reformulation of the degradation model captures the path-dependent degradation observed in real-world battery use. See Supplementary Note 5.2 for modelled battery degradation for NCM and LFP.

### 5.2.5 Available capacity from EV batteries

**Battery capacity during use and when retired from EV.** Vehicle EoL does not necessarily correspond to battery EoL. With technological improvements in battery

reliability and durability, many batteries in EoL vehicles may still have years of useful life at the end of vehicle end of life. Vehicle battery EoL is usually as defined the time at which remaining battery capacity is between 70%-80% of the original capacity[15]. We assume an EV lifespan distribution, as in our previous work[7] to account for EoL of EV. In our modelling approach, the vehicle lifespan distribution determines when batteries are not used in EVs any more (*i.e.*, retired batteries). Retired batteries may have quite different capacity under different use conditions. When vehicles reach EoL due to consumer choices or other issues before the battery pack reaches 70% relative capacity, retired batteries will still have over 70% relative SoH and are assumed to be used in a second-life application. When battery pack reaches 70% relative SoH before a vehicle reaches its EoL, we assume that batteries may still be used in EVs for low distances-driving. Retired batteries from such vehicles will have lower than 70% relative SoH and are assumed to be recycled rather than for a second-use. We assume any battery with a relative SoH lower than 60% is recycled and removed from potential grid storage capacity[217]. However, even batteries with a relative SoH of 60%-70% have a limited economic value and can have relatively high safety risks. (methods)[218].

**Vehicle-to-grid capacity.** We define technical vehicle-to-grid capacity as the availability of EV battery stock capacity for vehicle-to-grid application, considering the capacity reserved for EV driving, the capacity of PHEVs that will not participate in vehicle-to-grid due to low capacity, and capacity fade due to battery degradation. We further define the actual vehicle-to-grid capacity as the availability of technical vehicle-to-grid capacity for the grid under different consumer participation rates in the vehicle-to-grid business. Results focus on investigating under which participation rate can actual vehicle-to-grid capacity meet grid storage demand.

**Second-use capacity.** The technical second-use capacity is defined as the retired battery capacity that can be repurposed (*i.e.*, retired batteries with over 70% relative SoH). We further investigate actual second-use capacity under different market participation rates (*i.e.*, not all retired batteries will participate in second-use). The results are intended to determine the required market participation rate for the actual second-use capacity to meet grid storage demand.

## 5.3 Results

**Total technical capacity.** We define technical capacity as the total cumulative available

EV battery capacity in use and in second use at a specific time, taking into account battery degradation and the capacity needed to meet driving demand. Globally, the SD scenario sees total technical capacity twice that of the STEP scenario due to the larger fleet size (see Supplementary Fig. 5.13 and Note 1). The LFP scenario sees a higher cumulative capacity than NCX due to the lower degradation of LFP across most countries/regions (see Supplementary Data for a comparison of LFP and NCM battery degradation). As shown in Fig. 5.1, the highest total technical capacity is provided in the SD-LFP scenario that is 48% higher by 2030 and 91% higher by 2050 than in the STEP-NCX scenario (respectively 3.8 TWh and 2.6 TWh in 2030 and 32 TWh and 62 TWh in 2050).

Under all scenarios, the cumulative vehicle-to-grid and second use capacity will grow dramatically, by a factor of 13-16 between 2030 and 2050. Putting this cumulative technical capacity into perspective against future demand for grid storage we find that our estimated growth is expected to increase as fast or even faster than short-term grid storage capacity demand in several projections[56,194] (Fig. 5.1). Technical vehicle-to-grid capacity or second-use capacity are each, on their own, sufficient to meet the short-term grid storage capacity demand of 3.4-19.2 TWh by 2050. This is also true on a regional basis where technical EV capacity meets regional grid storage capacity demand (see Supplementary Fig. 5.14).

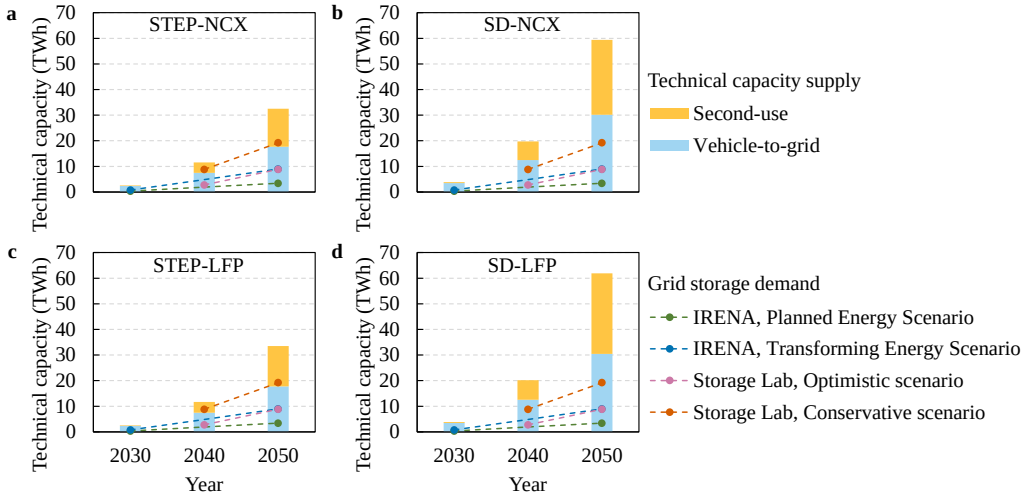


**Fig. 5.1: Total technical capacity for EV batteries and comparison to grid storage demand. a** STEP-

NCX scenario. **b** SD-NCX scenario. **c** STEP-LFP scenario. **d** SD-LFP scenario. The storage requirements of grids are 0.37-0.745 TWh in 2030 based on the IRENA[56], and that of 2050 from both IRENA and Storage Lab[194] (see details in Supplementary Table 5.1).

**Factors limiting total technical capacity.**

*Vehicle-to-grid.*

Examining the vehicle-to-grid opportunity alone, without considering second use, we find that 21%-26% of the global theoretical battery stock capacity (*i.e.*, on-board EV battery capacity of the entire EV fleet without considering battery degradation) could be available for vehicle-to-grid services by 2050 (Fig. 5.2a). The most important limiting factor is the battery capacity required to meet consumer driving demands[195,199] which can limit the technically available stock capacity by 57%-63%. PHEVs, which make up around 11% of the theoretical stock capacity in 2050, are not considered for vehicle-to-grid as they have a low storage potential due to low capacities. On average, just 5% of the theoretical stock capacity is lost due to battery degradation by 2050. These losses vary between 7% in India and 4% in RoW due to differences in regional factors such as use conditions and temperature (see regional results in Supplementary Fig. 5.15). Overall, taking these factors into account yields a technical vehicle-to-grid capacity of roughly 18-30 TWh by 2050 (see Fig. 5.2).

However, there are other factors that may limit actual available storage capacity. The vehicle-to-grid participation rate is the most important of these. That is, not all EV consumers will necessarily participate in the market. The impact of different participation rates, defined as the percentage of the technical vehicle to grid capacity actually connected to the grid, is shown in Fig. 5.2b. To satisfy the short-term storage demand of 10 TWh in 2050, participation rates of 38% and 20% are required for the STEP-NCX and SD-NCX scenarios, respectively. In practice, it is likely that EVs with high battery capacities and low degradation will be used for providing vehicle-to-grid services since these will provide the highest revenue for EV owners[219] (the full battery capacity distributions by 2050 across countries/regions is available in Supplementary Fig. 5.16, Supplementary Fig. 5.17, Supplementary Fig. 5.18, Supplementary Fig. 5.19, and Supplementary Fig. 5.20).

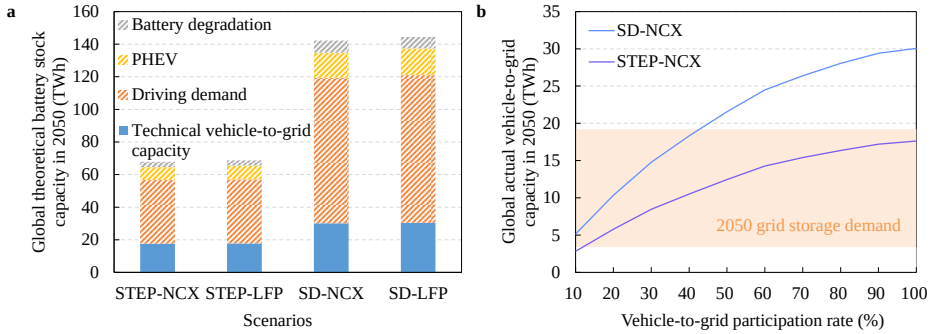


**Fig. 5.2: Global available vehicle-to-grid capacity in 2050. a** Technical vehicle-to-grid capacity. Hatched bars indicate the capacity limits due to key factors and blue bars the technical vehicle-to-grid capacity. **b** Actual vehicle-to-grid capacity as a function of participation rates. Results are shown for the STEP-NCX and the SD-NCX scenarios with a comparison to the range of storage demand computed by IRENA and Storage Lab models in 2050 (orange shading). Please see Supplementary Fig. 5.21 for global actual vehicle-to-grid capacity under the STEP-LFP and the SD-LFP scenarios, which shows similar results as STEP-NCX and SD-NCX scenarios. Supplementary Fig. 5.22, Supplementary Fig. 5.23, Supplementary Fig. 5.24, and Supplementary Fig. 5.25 for regional actual vehicle-to-grid capacity.

*Second-use.*

Over time EV batteries degrade so far that they cannot be used to power vehicles[7]. This is typically when the battery relative State of Health (SoH), defined as actual capacity as percentage of original capacity, has reached 70%-80%[15], although the relative SoH could fall even lower if a consumer is willing to accept relatively poor battery health and shorter ranges[119]. Given their high value, size and end of life regulations in many countries we assume all retired batteries will be collected[17]. Once collected, batteries are health tested to determine if the retired EV battery can be used in a less critical second-use application, or if the battery must be recycled[220].

Given the technical and economic feasibility of retired batteries for a second-use[218], we consider batteries with an SoH of 70% and higher only for second-use (this threshold is often assumed as a technically and economically feasible value for second-use businesses[218]). Using this criterion, we find that for all scenarios between 2030 and 2050 74% of the retired NCX batteries can be repurposed for second-use globally (*i.e.*, repurposing percentage), while 26% goes to recycling by 2050. Regional differences can be significant due to the impact of temperature on NCX battery degradation (see Supplementary Fig. 5.26 and Supplementary Data). In contrast, virtually all LFP retired

batteries can be repurposed.

Business models are still developing, and repurposing is highly dependent on the technical specifications and market requirements of second-use applications[221]. Since battery disassembly is costly[218], battery repurposing will likely happen on the pack level instead of modules and cell level. Repurposing will consist mainly of rebalancing and reconnecting the retired battery packs. There is no strong technical reason to model a capacity difference before and after the repurposing processes.

For these assumptions, 2.1-4.8 TWh of retired batteries are estimated to become available as annual technical second-use capacity globally in 2050, as shown in Fig. 5.3a. The cumulative technical second-use capacity is expected to reach 14.8-31.5 TWh by 2050 when using a 10-year second-use life scenario[222] (Fig. 5.3b). The actual second second-use lifespan is uncertain due to uncertainties surrounding the retired battery SoH, use conditions, *etc*. Another uncertainty is the further battery degradation during secondary use, which is difficult to model due to complicated degradation mechanisms of retired batteries[223]. Further research into degradation and second-use life span is required to improve estimates of technical second-use capacity.

Similar to estimates for actual vehicle-to-grid capacity, the second use participation rate determines which percentage of the technical second-use capacity is actually available and connected to the grid. To meet the requirement of a 10 TWh short-term storage capacity in the STEP-NCX scenario (14.8 TWh technical capacity) a participation rate 68% is required, while in the SD-LFP scenario (31.5 TWh technical capacity) a participation rate of 32% is needed.

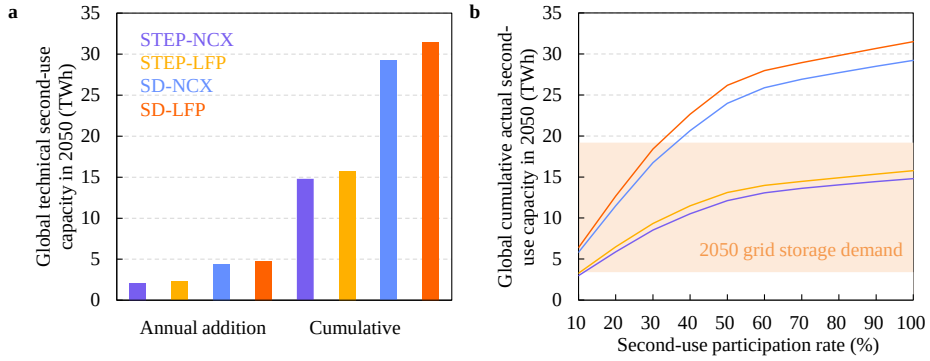


**Fig. 5.3: Global available second-use capacity in 2050. a** Annual addition and cumulative technical capacity in 2050. Capacity refers to the technically available capacity considering battery degradation, or maximum theoretical potential second-use capacity without considering the battery second-use participation rate. **b** Impacts of second-use participation rate on cumulative actual second-use capacity and a comparison to storage demand in 2050 (orange shading). See Supplementary Fig. 5.27, Supplementary Fig. 5.28, Supplementary Fig. 5.29, and Supplementary Fig. 5.30 for regional actual second-use capacity.

### Combining vehicle-to-grid and second-use participation rates.

As we describe above, the global technical capacity for short-term grid storage of EV batteries grows rapidly in all scenarios. However, the actual available capacity depends strongly on the vehicle-to-grid and second-use participation rates. We show the actual available capacity as a function of these participation rates in Fig. 5.4 for the STEP-NCX scenario (please see Supplementary Fig. 5.31, Supplementary Fig. 5.32, and Supplementary Fig. 5.33 for other scenarios). If 50% participation rates can be realized for both vehicle-to-grid and second-use, the combined actual available capacity is 25-48 TWh by 2050, far above requirements estimated from the literature. Changes in vehicle-to-grid participation rates of 23%-96%[224,225] could influence this actual available capacity in 2050 by as much as -24% to +21%. When second use participation rates vary 10%-100%, the actual available capacity varies between -41% and 12%. Taken together, vehicle-to-grid participation rate and second use participation rate could alter the actual available capacity in 2050 by -61% to +32%.

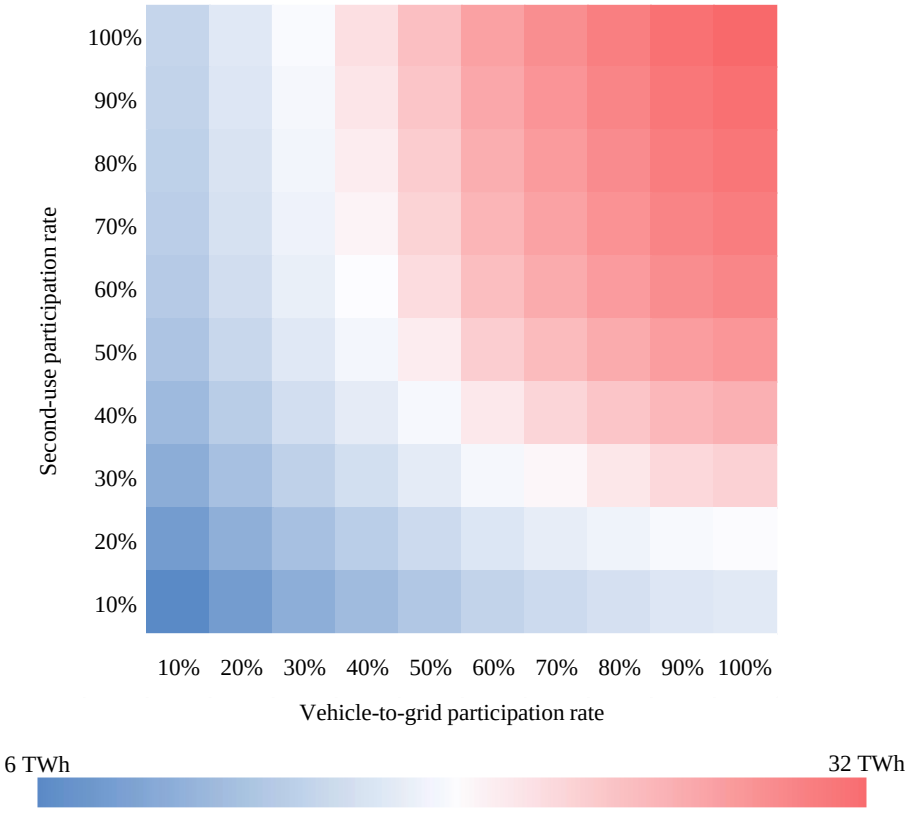


**Fig. 5.4: Total actual available capacity under various conditions in STEP-NCX scenario in 2050.** Blue, white, and red colors depict minimum, average, and maximum values. See Supplementary Fig. 5.31, Supplementary Fig. 5.32, and Supplementary Fig. 5.33 for other scenarios.

## 5.4 Discussion

Previous research has suggested that large EV fleets could exert additional stress on grid stability (*e.g.*, if the majority of EVs are charged at grid peak time)[226]. Our findings, from a different perspective, show EV batteries could promote electricity grid stability via storage solutions from vehicle-to-grid and second-use applications. We estimate a total technical capacity of 32-62 TWh by 2050. This is significantly higher as the 3.4-19.2 TWh (10 TWh on average) as required by 2050 in IRENA and Storage lab scenarios.

The actual available capacity depends on participation rates for vehicle-to-grid and second use. Participation rates may vary regionally depending on future market

incentives and infrastructure along with other factors[227]. However, we show how EV batteries in primary and secondary use could provide the 10 TWh short-term grid storage capacity required in the IRENA and Storage Lab scenarios by 2050. The STEP-NCX scenario presented in Fig. 5.4 has the lowest technical capacity (32 TWh compared to 62 TWh in the SD-LFP scenario) which already easily meets requirements at participation rates of 40%-50% for vehicle-to-grid and second-use. At a regional level, even lower participation rates may still contribute significantly to grid stability. Overall, EV batteries could meet short-term grid storage demand by as early as 2030 (if we assume lower requirements from the literature and higher levels of participation). By 2040-2050 storage demands are met across almost all scenarios and even low participation rates. Harnessing this potential will have critical implications for the energy transition and policymakers should be cognizant of the opportunities.

As we include a broader set of limitations for the total opportunity our results are difficult to compare with other literature. Our estimated global EV fleet capacity in 2050 (68-144 TWh) is considerably higher than the estimate from IRENA (7.5-14 TWh)[56]. This is due to the IRENA's very conservative scenarios on future EV fleet size and battery capacity per vehicle. The IRENA scenario also does not consider the availability of EV fleet capacity for grid services. An IEA estimate does not extend beyond 2030[57] but highlights the importance of including battery degradation in analyses, which we include here to project until 2050 (Fig. 5.3).

We note several limitations in our approach that could be improved as data availability improves. For example, while we include battery degradation by using state-of-art data, future battery degradation is highly uncertain and depends on further technological breakthroughs in battery chemistry such as Na-ion, Li-Air, and Li-Sulphur[228] along with developments in battery management systems. Further, while we derived driving behaviour from empirical data, future changes in driving habits are uncertain and dependent on various factors such as EV-related infrastructure. Vehicle chargers increase in power output over time and 50 kW charging is already common across many countries[229]. Frequent fast charging could lead to faster degradation, especially in hot/cold climates[230]. This challenge may be addressed by future technology improvements to battery materials[231], electrode architectures, and optimized synergy of the cell/module/pack system design[169]. A further limitation is that we compare technical and actual available vehicle-to-grid capacity with an average 4-hour storage

requirement as provided in the scenarios by IRENA and Storage Lab. This omits potential differences in storage requirements at shorter time scales (seconds/minutes). Improved modelling and data can overcome this gap. It is however likely that the technical vehicle-to-grid capacity will be sufficient given low vehicle utilization rates of just 5% for many regions[232]. Additionally, development of smart charging infrastructure and grid digitization is likely to provide additional flexibility for matching electricity demand and supply[233].

A final limitation is that we assume that the rated capacity per vehicle remains the same in the future and that a small number of large BEVs might provide large actual vehicle-to-grid capacity (Supplementary Fig. 5.22, Supplementary Fig. 5.23, Supplementary Fig. 5.24, and Supplementary Fig. 5.25). These capacities may change further in the future due to policy incentives, vehicle design, consumer preferences, charging infrastructure, among other factors. Further, the transportation system could see radical and fundamental changes. A significant and rapid shift away from private car use to mass transit, a move to shared electric vehicles, autonomous driving, and the success of battery swap systems[234] could all alter the available capacity via utilization rates and other factors by 2050.

**Glossary**

***Dynamic battery stock model:***

**EV**: electric vehicles.

**BEV**: battery electric vehicle.

**PHEV**: plug-in hybrid electric vehicle.

**LFP**: lithium-iron-phosphate / graphite battery.

**NCM**: lithium Nickel Cobalt Manganese Oxide / graphite battery.

**NCA**: lithium Nickel Cobalt Aluminum Oxide / graphite battery.

**NCX**: NCM and NCA, with X denoting manganese or aluminum.

***EV use model:***

**Ambient temperature:** the temperature of the air surrounding the EVs under consideration.

**Daily driven distance (DDD):** assumed as the mean value of DDD distribution.

**State of Charge (SoC)**: level of charge of a battery relative to its rated capacity, and the units of SoC are percentage points (0% = empty; 100% = full).

$\mathbf{C_{rate}}$: the charge or discharge current divided by the battery's capacity to store an electrical charge. The unit of the $\mathbf{C_{rate}}$ is $hour^{-1}$.

**Depth of discharge (DOD):** the fraction or percentage of the battery's capacity which is currently removed from the battery with regard to its (fully) charged state.

**Equivalent full cycles (EFCs):** the charge throughput of partial cycles relative to a full charge/discharge cycle.

***Battery degradation model:***

**Rated capacity:** the maximum energy of the battery at the start of life.

**Battery degradation:** the amount of charge a rechargeable battery can deliver at the rated voltage decreases with use, depending on lots of stress factors: Ambient temperature SoC, Crate, DoD, and EFCs.

**Battery capacity:** a property of that a battery's maximum capability to store the energy at a given moment in time and conditions, as the battery degradation.

**Relative SoH:** state of health, is assumed as Battery capacity / Rated capacity.

***Vehicle-to-grid model:***

**Theoretical battery stock capacity:** on-board EV battery capacity of total EV fleet, without considering capacity lost due to battery degradation. Theoretical battery stock capacity = Rated capacity per EV * number of total EVs.

**Technical vehicle-to-grid capacity:** availability of theoretical battery stock capacity for vehicle-to-grid applications, considering driving demand, battery degradation, and PHEV. Technical vehicle-to-grid capacity = Theoretical battery stock capacity – Battery capacity reserved for BEV driving – Battery capacity of PHEV - Battery capacity lost due to battery degradation.

**Vehicle-to-grid participation rate:** Number of EVs participating in vehicle-to-grid / Number of total EVs.

**Actual vehicle-to-grid capacity:** availability of technical vehicle-to-grid capacity for vehicle-to-grid applications. Actual vehicle-to-grid capacity = number of EVs participating in vehicle-to-grid * technical vehicle-to-grid capacity per EV.

***Second-use model:***

**Retired battery:** battery out of service from first life of EV.

**Capacity per retired battery**: battery capacity when coming to the end of the first life of EV.

**Collection rate per year:** number of collected batteries per year / number of retired batteries per year. Number of collected batteries per year = number of repurposed batteries + number of recycled batteries.

**Repurposing battery:** retired battery that is suitable for electricity storage. The model assumes collected battery with relative SoH above 70% will be repurposed.

**Recycled battery:** retired battery that is collected for material recycling.

**Repurposing rate per year:** rate of repurposing batteries in collected batteries. Repurposing rate per year = number of collected batteries with relative SoH above 70% per year / number of collected batteries per year.

**Recycling rate per year:** rate of recycled batteries in collected batteries. Recycling rate per year = 1- repurposing rate per year.

**Technical second-use capacity per year:** battery capacity of repurposed batteries per year. Technical second-use capacity per year = number of retired batteries per year * collection rate per year * repurposing rate per year * capacity per retired battery.

**Second-use participation rate per year:** number of batteries participating in second-use / number of repurposing batteries (or collected batteries with relative SoH above 70%) per year.

**Actual second-use capacity per year:** availability of technical second-use capacity per year for second-use applications. Actual second-use capacity per year = technical second-use capacity per year * second-use participation rate per year * capacity per retired battery.

## 5.5 Supplementary information

### 5.5.1 Model overview

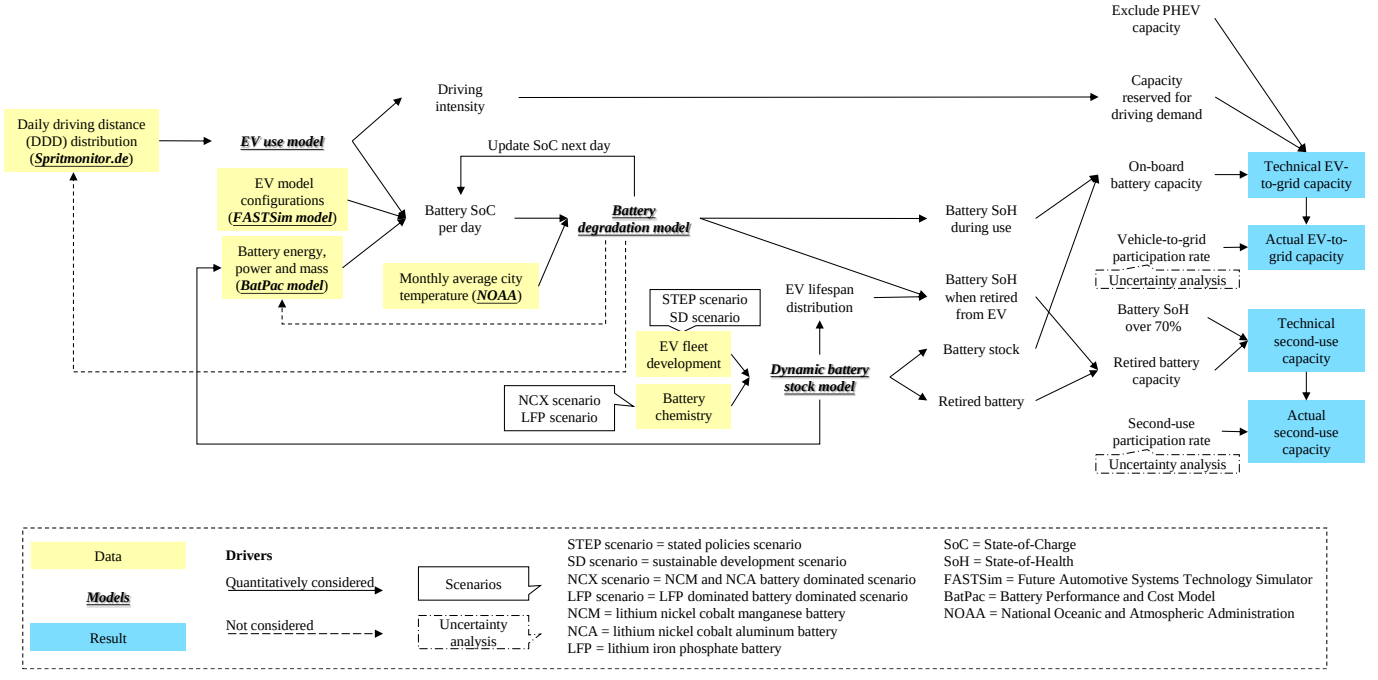


**Supplementary Fig. 5.1: Model framework consisting of a dynamic battery stock model, a EV use model, and a battery degradation model.**

## Dynamic battery stock model

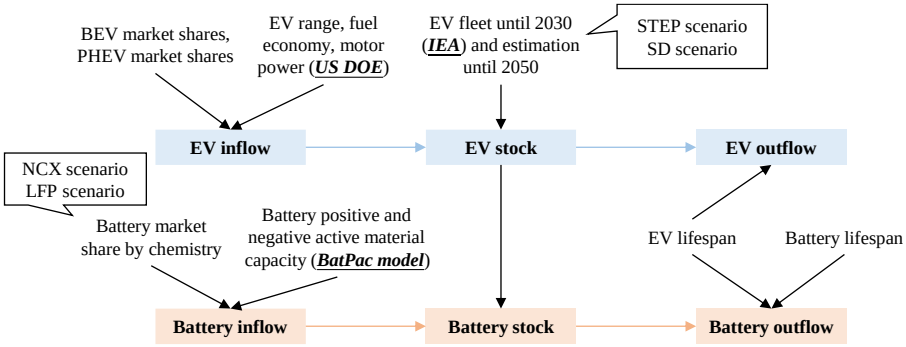


STEP scenario = stated policies scenario
SD scenario = sustainable development scenario
NCX scenario = NCM and NCA battery dominated scenario
LFP scenario = LFP dominated battery dominated scenario
NCM = lithium nickel cobalt manganese battery
NCA = lithium nickel cobalt aluminum battery
LFP = lithium iron phosphate battery

IEA = International Energy Agency
USDOE = U.S. Department of Energy
BatPac = Battery Performance and Cost Model

**Supplementary Fig. 5.2: Dynamic battery stock model[7].**

## EV use model

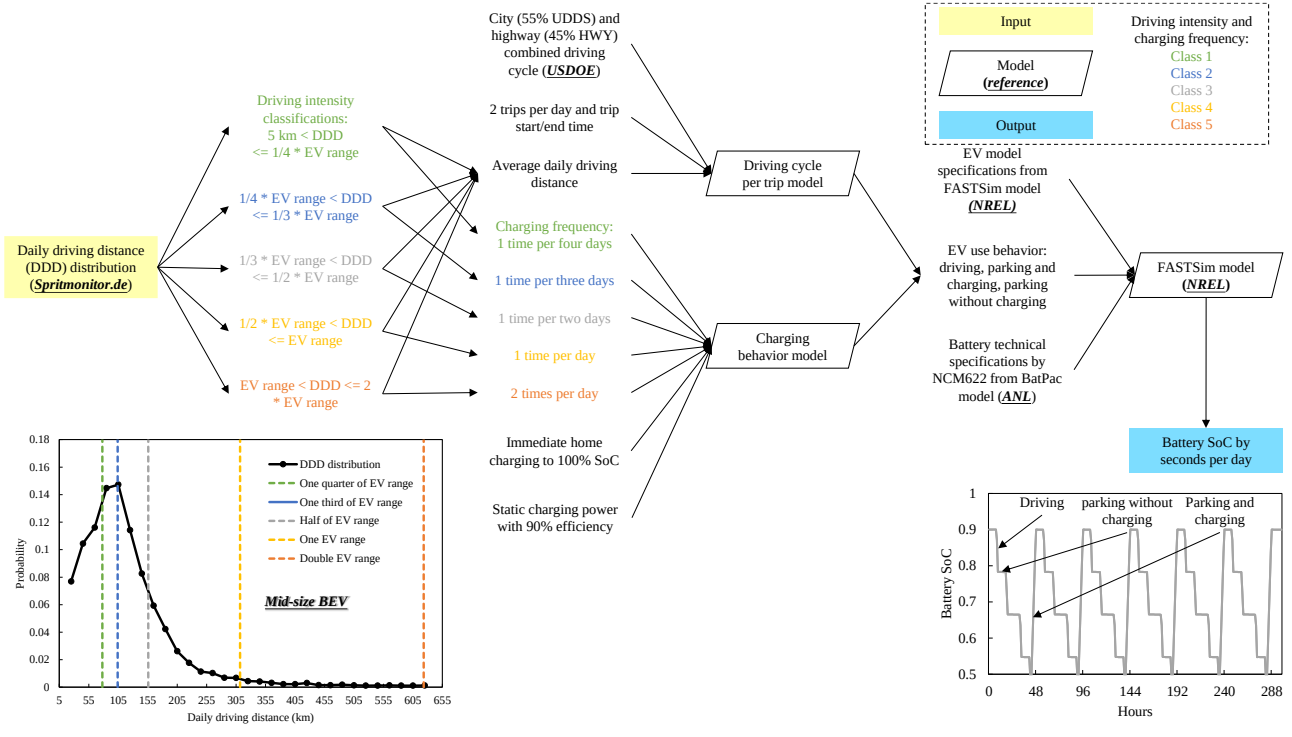


**Supplementary Fig. 5.3: EV use model.** NREL National Renewable Energy Laboratory. ANL Argonne National Laboratory.

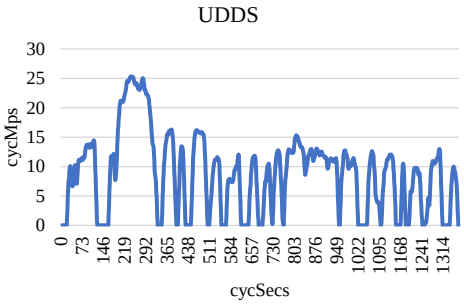


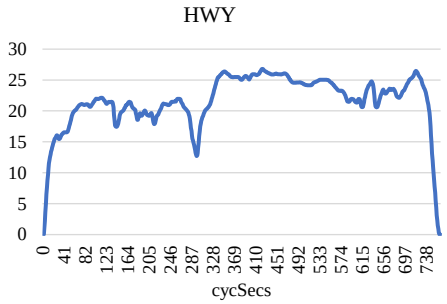


| UDDS | |
|---|---|
| Cumkm | 11.99043319 |
| Average speed (m/s) | 8.752141014 |
| Time (s) | 1369 |

| HWY | |
|---|---|
| Cumkm | 16.50681747 |
| Average speed (m/s) | 21.54937007 |
| Time (s) | 765 |

Average daily driving distance = x

Trip distance = 0.5*x

Required UDDS trip distance = 0.55*0.5*x

Required UDDS trip time = ROUND (0.55*0.5*x / UDDS average speed, 0)

**Required multiples of UDDS** = FLOOR (Required UDDS trip time / UDDS trip time, 1)

**Required downsize factor UDDS** = Round (UDDS trip time / MOD (Required UDDS trip time / UDDS trip time), 2)

Required HWY trip distance = 0.45*0.5*x

Required HWY trip time = ROUND (0.45*0.5*x / HWY average speed, 0)

**Required multiples of HWY** = FLOOR (Required HWY trip time / HWY trip time, 1)

**Required downsize factor HWY** = Round (HWY trip time / MOD (Required HWY trip time / HWY trip time), 2)

For UDDS and HWY, **first scale the resolution from 1s to 0.01 s**. new cycMps (for cycSecs in 0.00-0.49, 0.01s interval) = old cycMps (0); new cycMps (0.50-1.49) = old cycMps (1); new cycMps (1.50-2.49) = old cycMps (2) …

**Downsized cycMps (0)** = average ( new cycMps (0, downsize factor) );

**Downsized cycMps (1)** = average ( new cycMps (downsize factor+0.01, 2*downsize factor+0.01) ) …

**Supplementary Fig. 5.4: EV use model where driving cycle is compiled on trip distance and standard UDDS and HWY driving cycle.**

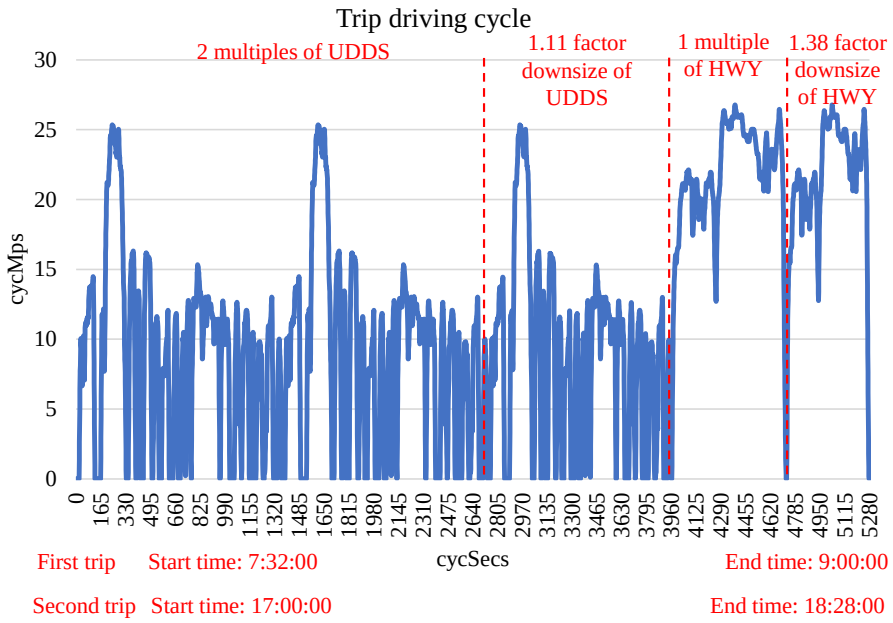


**Supplementary Fig. 5.5: EV use model where a drive cycle example is compiled for a mid-size BEV when the daily driving distance is 126.3 km.**

## Battery degradation model

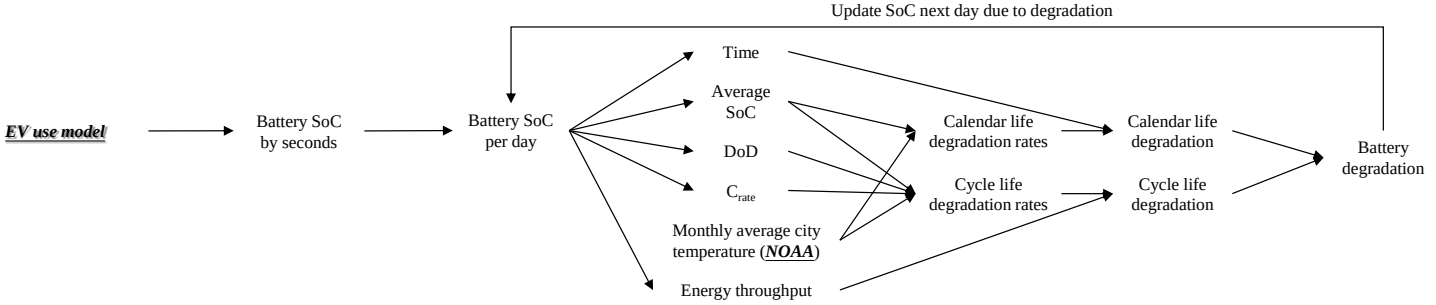


**Supplementary Fig. 5.6: Battery degradation model.**

### 5.5.2 Additional Figures and Tables

## Supplementary Figures

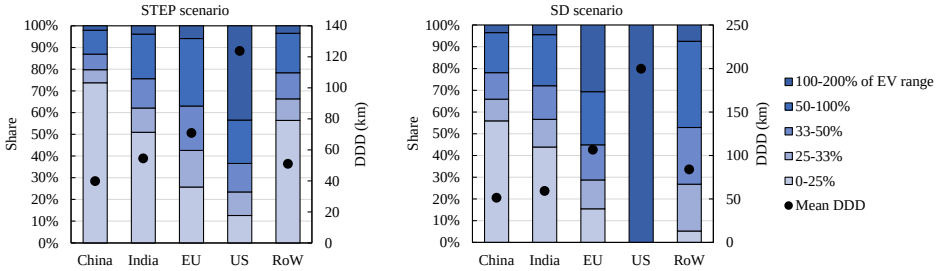


**Supplementary Fig. 5.7: Daily driving distance (DDD) distributions for small BEV across counties/regions.** The historic DDD distribution for EU is collected from Spritmonitor.de[199]. Combined with the IEA's projection of future EV fleet energy consumption for China, India, EU, US, and RoW[195], we compile the future DDD distributions for countries/regions.

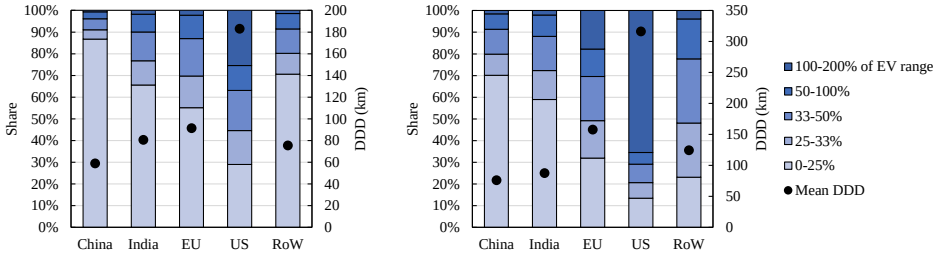


**Supplementary Fig. 5.8: Daily driving distance (DDD) distributions for mid-size BEV across counties/regions.** The historic DDD distribution for EU is collected from Spritmonitor.de[199]. Combined with the IEA's projection of future EV fleet energy consumption for China, India, EU, US, and RoW[195], we compile the future DDD distributions for countries/regions.

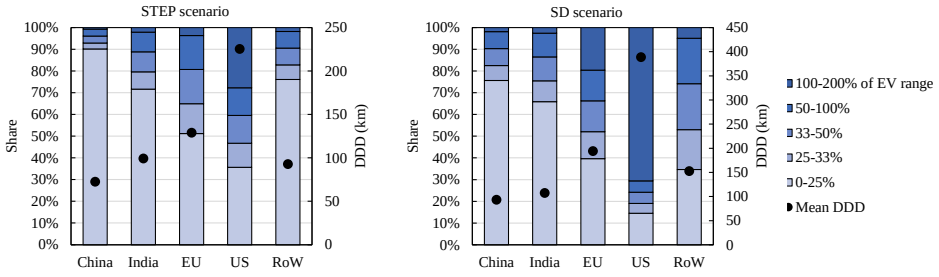


**Supplementary Fig. 5.9: Daily driving distance (DDD) distributions for large BEV across**

**counties/regions.** The historic DDD distribution for EU is collected from Spritmonitor.de[199]. Combined with the IEA's projection of future EV fleet energy consumption for China, India, EU, US, and RoW[195], we compile the future DDD distributions for countries/regions.

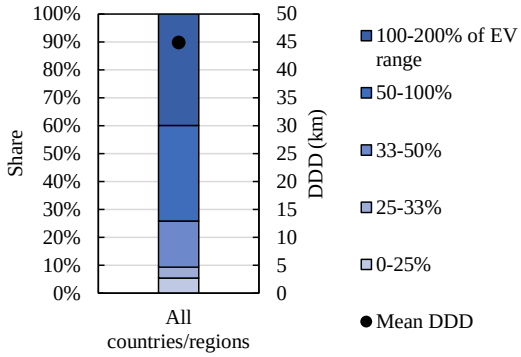


**Supplementary Fig. 5.10: Daily driving distance (DDD) distributions assumed for PHEVs for all counties/regions.**

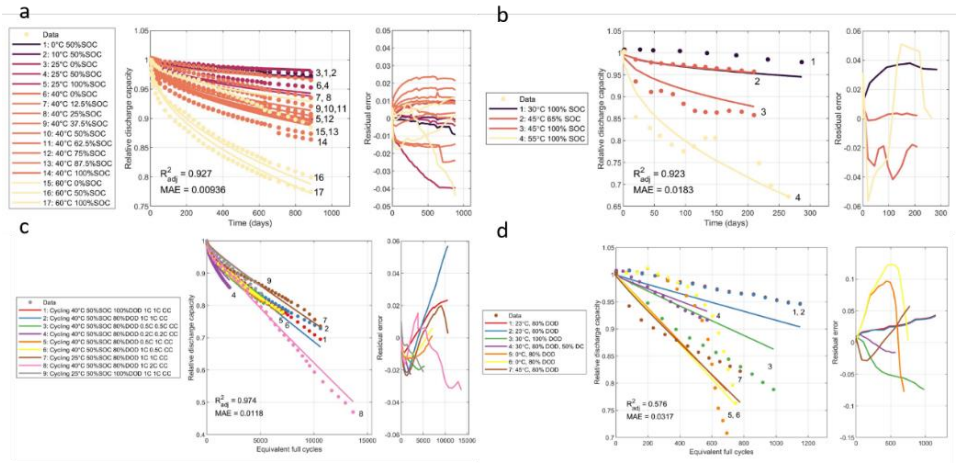


**Supplementary Fig. 5.11: Battery degradation model fitting results. a** calendar life aging of LFP. **b** calendar life aging of NCM. **c** cycling life aging of LFP. **d** cycling life aging of NCM. Residual errors are plotted to the right of each fit.

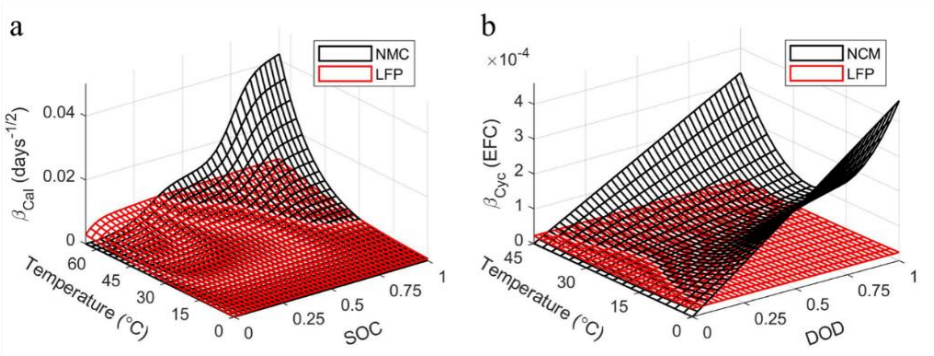


**Supplementary Fig. 5.12: LFP and NCM battery degradation rates. a** Calendar life degradation rate versus the square-root of time as a function of temperature and SoC (state-of-charge). **b** Cycle life degradation rate versus energy throughput, in units of EFCs (equivalent full cycles), as a function of temperature and DOD (depth-of-discharge).

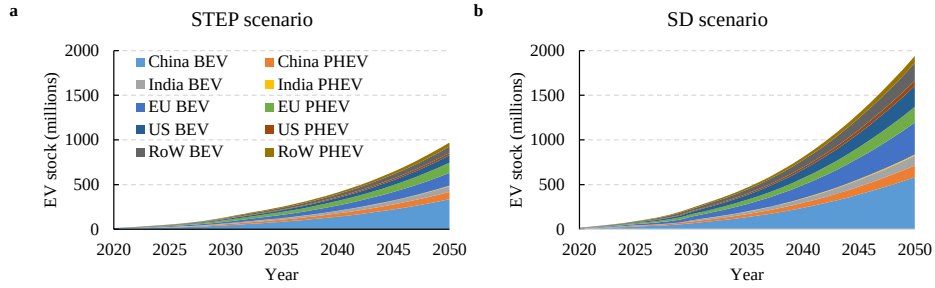


**Supplementary Fig. 5.13: Global EV stock development projected until 2050 for STEP and SD fleet scenarios. a** STEP scenario. **b** SD scenario. BEV battery electric vehicle, PHEV plug-in hybrid electric vehicle, STEP scenario the Stated Policies scenario, SD scenario Sustainable Development scenario.

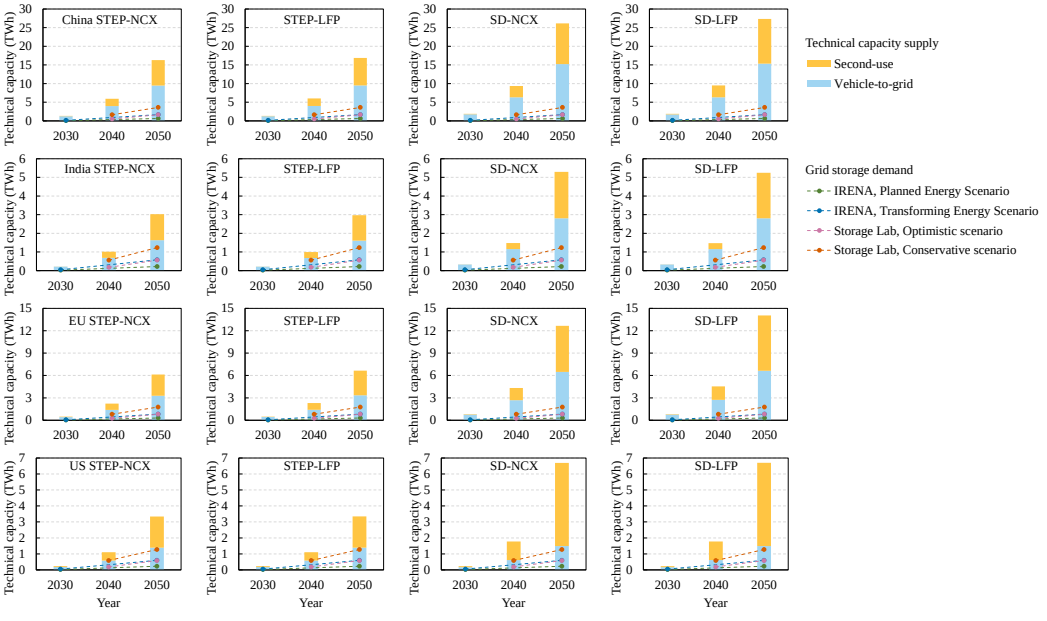


**Supplementary Fig. 5.14: Total technical capacity from EV batteries and comparison to grid storage demand in countries and regions.** The grid storage demand in countries/regions is estimated based on future peak power demand in countries/regions, where assuming a proportional relationship between grid storage demand and peak power demand for countries/regions is the same as global. Global peak power will increase to 6686 GW in 2030 and 10000 GW in 2050, derived from Storage Lab[194]. China's peak power will increase to 1258 GW in 2030 and 1881 GW in 2050. India's peak power will increase to 430 GW in 2030 and 643 GW in 2050. EU peak power will increase to 616 GW in 2030 and 922 GW in 2050. US peak power will increase to 445 GW in 2030 and 665 GW in 2050. Regional peak demand is from the IEA[57].

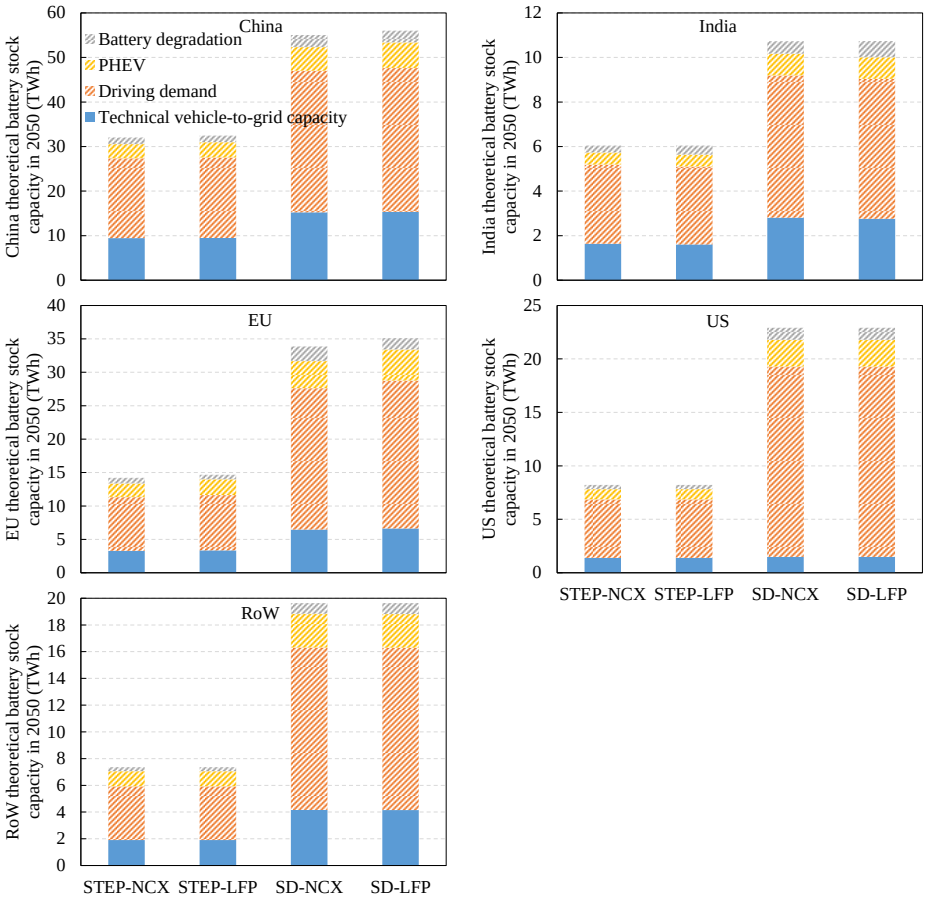


**Supplementary Fig. 5.15: Available vehicle-to-grid capacity in 2050 by countries/regions.** Hatched bars indicate the capacity limits due to key factors and blue bars the technical vehicle-to-grid capacity. It is found higher technical vehicle-to-grid capacity for LFP scenario compared to NCX scenario in China, EU, and US, while higher vehicle-to-grid capacity for the NCX scenario in India and RoW (Rest of World).

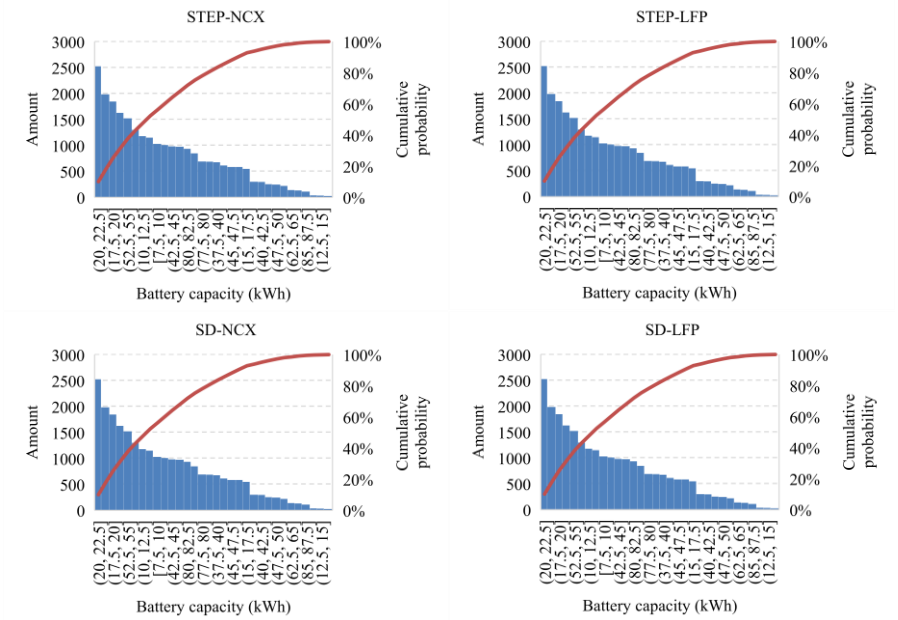


**Supplementary Fig. 5.16: Battery capacity distribution for China battery stock by 2050.**

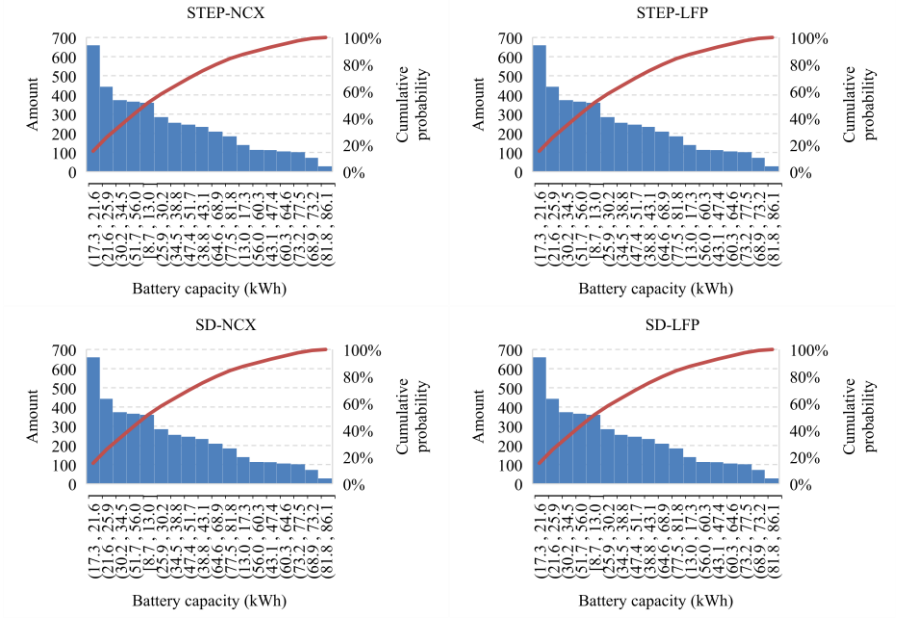


**Supplementary Fig. 5.17: Battery capacity distribution for India battery stock by 2050.**

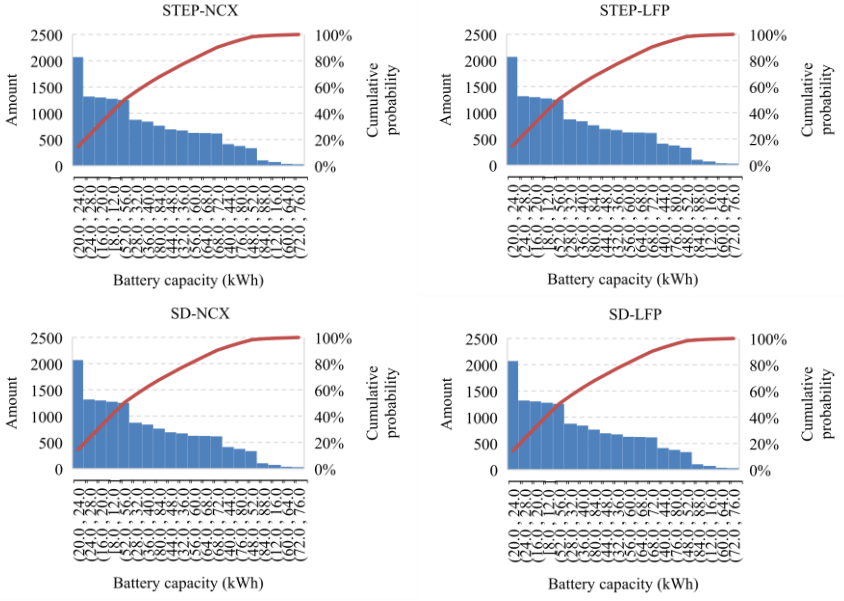


**Supplementary Fig. 5.18: Battery capacity distribution for EU battery stock by 2050.**

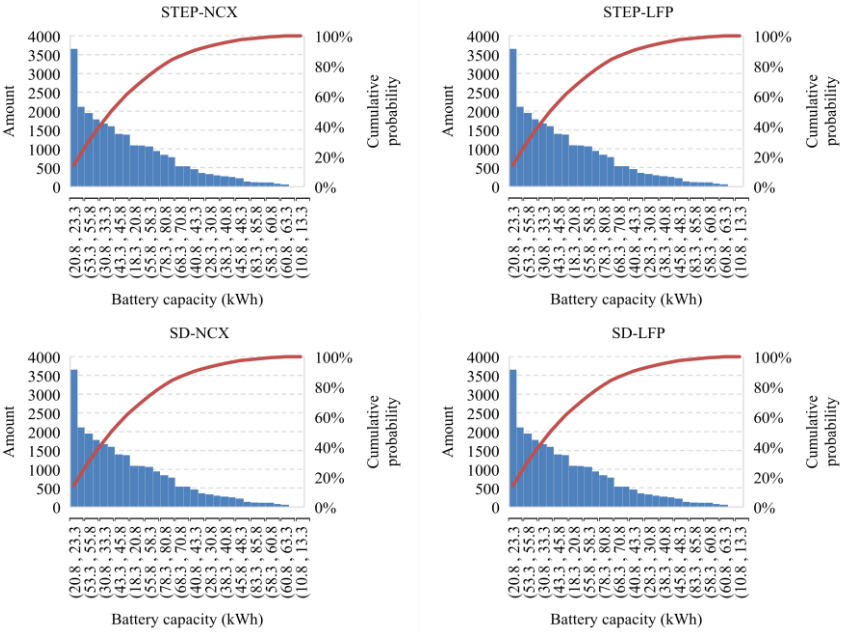


**Supplementary Fig. 5.19: Battery capacity distribution for US battery stock by 2050.**

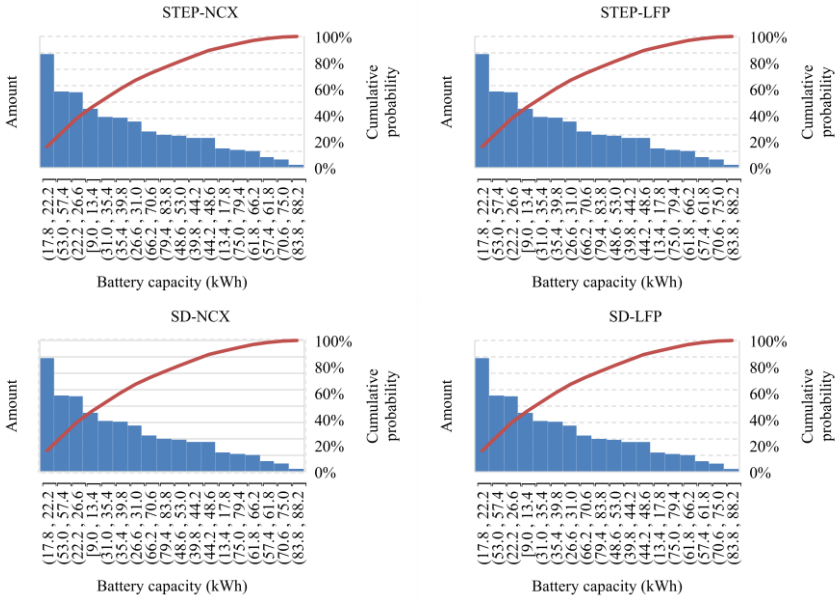


**Supplementary Fig. 5.20: Battery capacity distribution for RoW battery stock by 2050.**

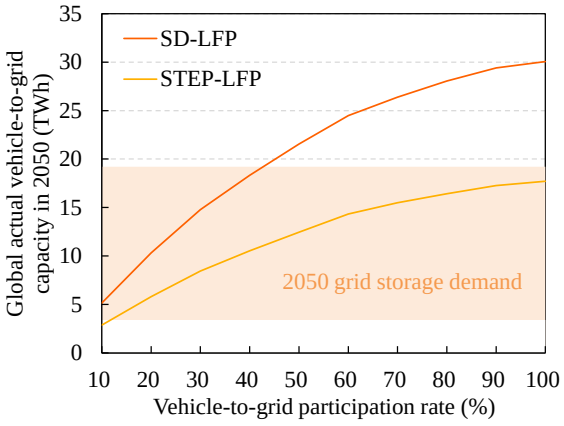


**Supplementary Fig. 5.21: Global actual vehicle-to-grid capacity as a function of participation rates in STEP-LFP and SD-LFP scenarios, and comparison to grid storage capacity demand in 2050.**

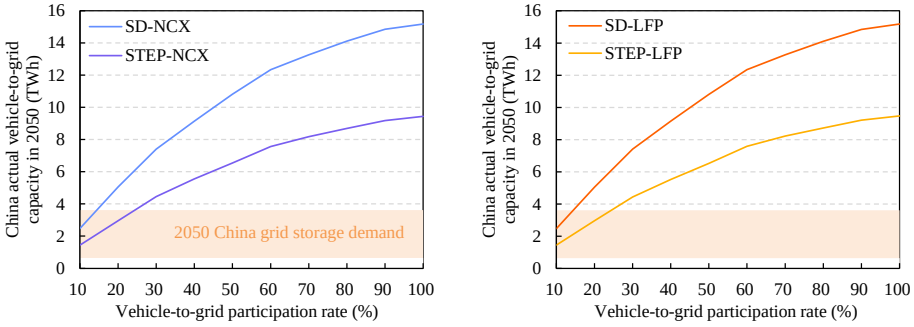


**Supplementary Fig. 5.22: China actual vehicle-to-grid capacity as a function of participation rate and comparison to grid storage capacity demand in 2050.**

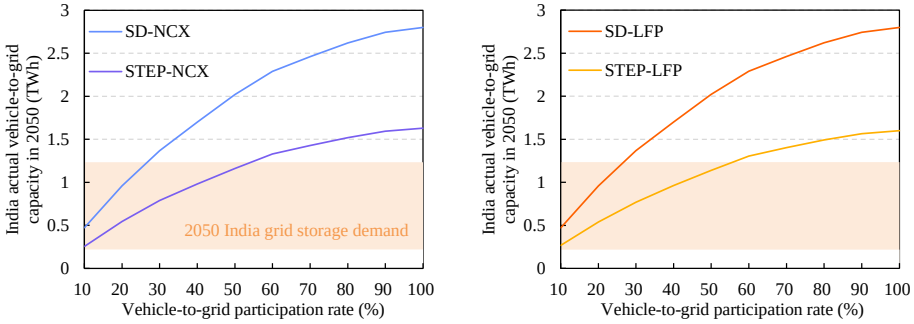


**Supplementary Fig. 5.23: India actual vehicle-to-grid capacity as a function of participation rate and comparison to grid storage capacity demand in 2050.**

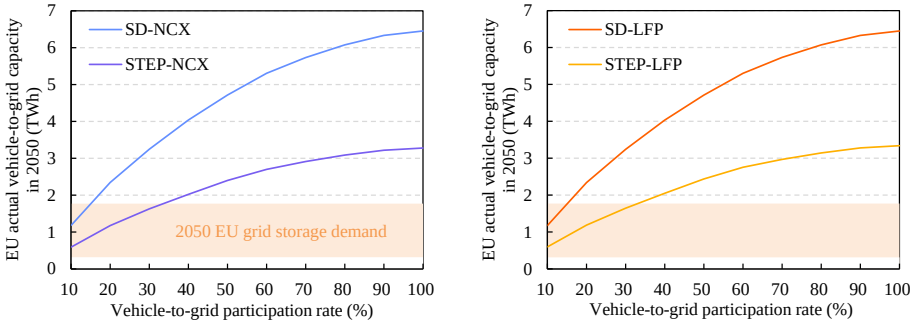


**Supplementary Fig. 5.24: EU actual vehicle-to-grid capacity as a function of participation rate and comparison to grid storage capacity demand in 2050.**

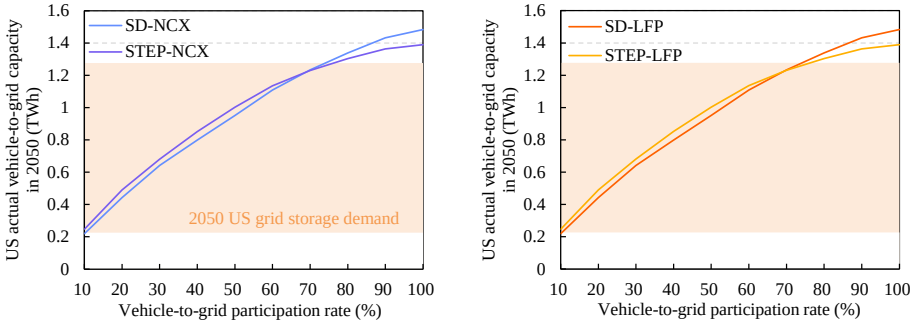


**Supplementary Fig. 5.25: US actual vehicle-to-grid capacity as a function of participation rate and comparison to grid storage capacity demand in 2050.**

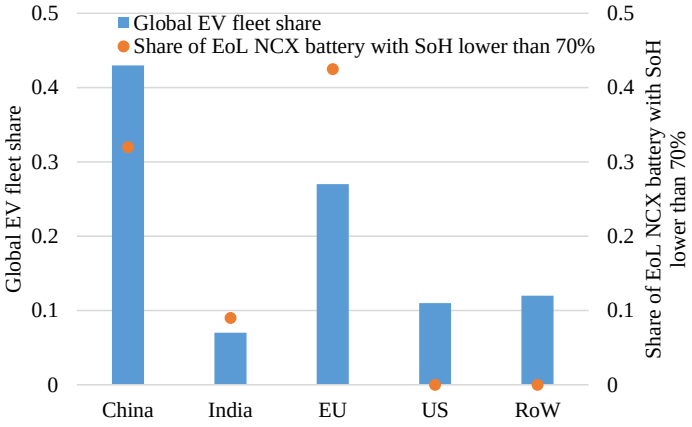


**Supplementary Fig. 5.26: Global share of retired NCX batteries with SoH lower than 70% in total retired NCX batteries (*i.e.*, repurposing rate per year).** Repurposing rate per year = number of collected batteries with relative SoH above 70% per year / number of collected batteries per year.

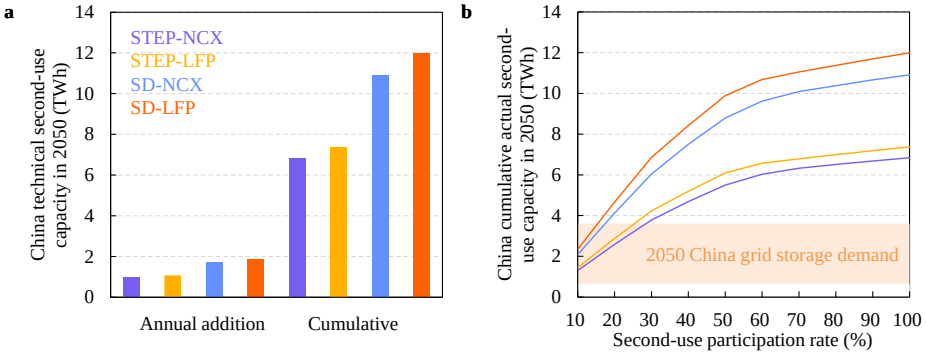


**Supplementary Fig. 5.27: China available second-use capacity in 2050. a** Annual addition and cumulative technical capacity in 2050. Capacity refers to the technically available capacity considering battery degradation, or maximum theoretical potential second-use capacity without considering the battery second-use participation rate. **b** Impacts of second-use participation rate on cumulative actual second-use capacity and a comparison to storage demand in 2050 (orange shading).

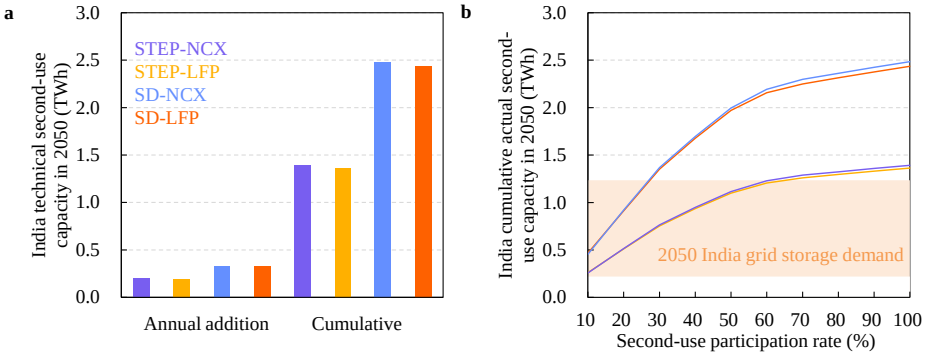


**Supplementary Fig. 5.28: India available second-use capacity in 2050. a** Annual addition and cumulative technical capacity in 2050. Capacity refers to the technically available capacity considering battery degradation, or maximum theoretical potential second-use capacity without considering the battery second-use participation rate. **b** Impacts of second-use participation rate on cumulative actual second-use capacity and a comparison to storage demand in 2050 (orange shading).

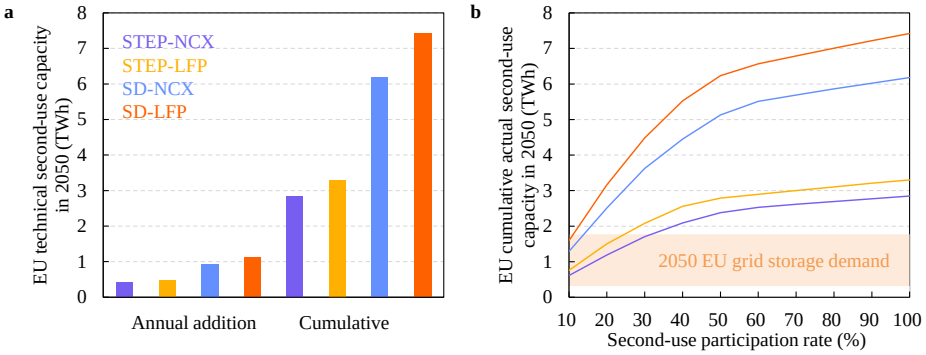


**Supplementary Fig. 5.29: EU available second-use capacity in 2050. a** Annual addition and cumulative technical capacity in 2050. Capacity refers to the technically available capacity considering battery degradation, or maximum theoretical potential second-use capacity without considering the battery second-use participation rate. **b** Impacts of second-use participation rate on cumulative actual second-use capacity and a comparison to storage demand in 2050 (orange shading).

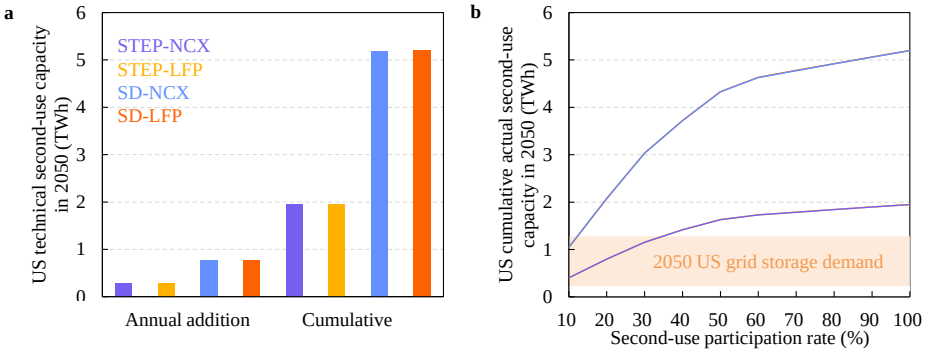


**Supplementary Fig. 5.30: US available second-use capacity in 2050. a** Annual addition and cumulative technical capacity in 2050. Capacity refers to the technically available capacity considering battery degradation, or maximum theoretical potential second-use capacity without considering the battery second-use participation rate. **b** Impacts of second-use participation rate on cumulative actual second-use capacity and a comparison to storage demand in 2050 (orange shading).

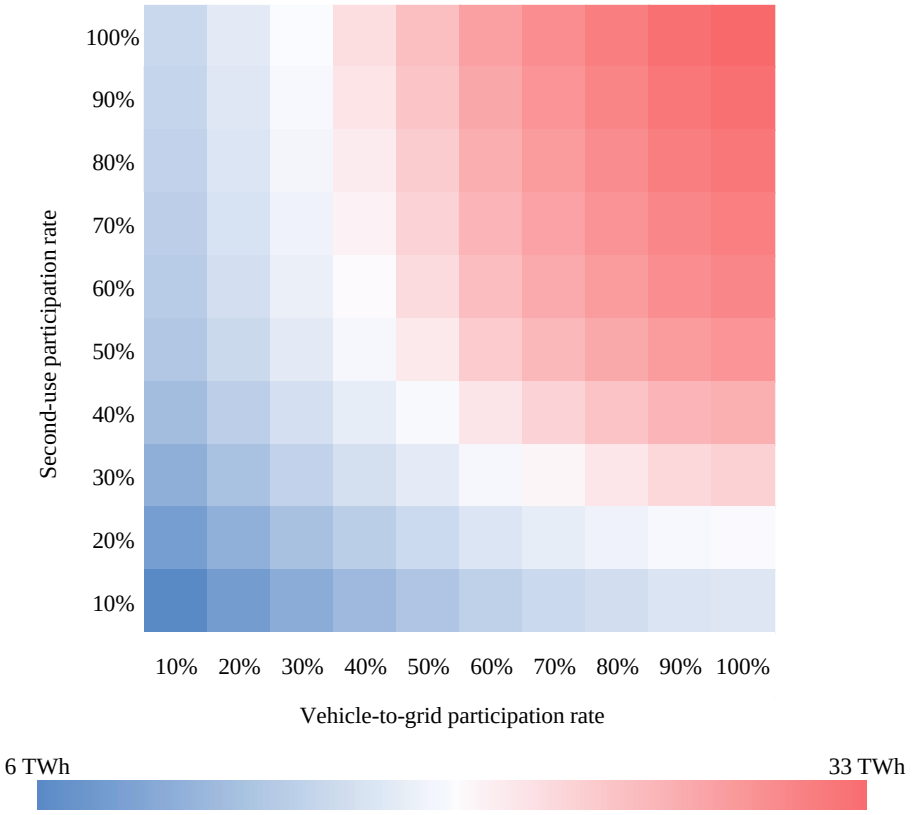


**Supplementary Fig. 5.31: Total actual available capacity under various conditions in STEP-LFP scenario in 2050.** Blue, white, and red colors depict minimum, average, and maximum values.

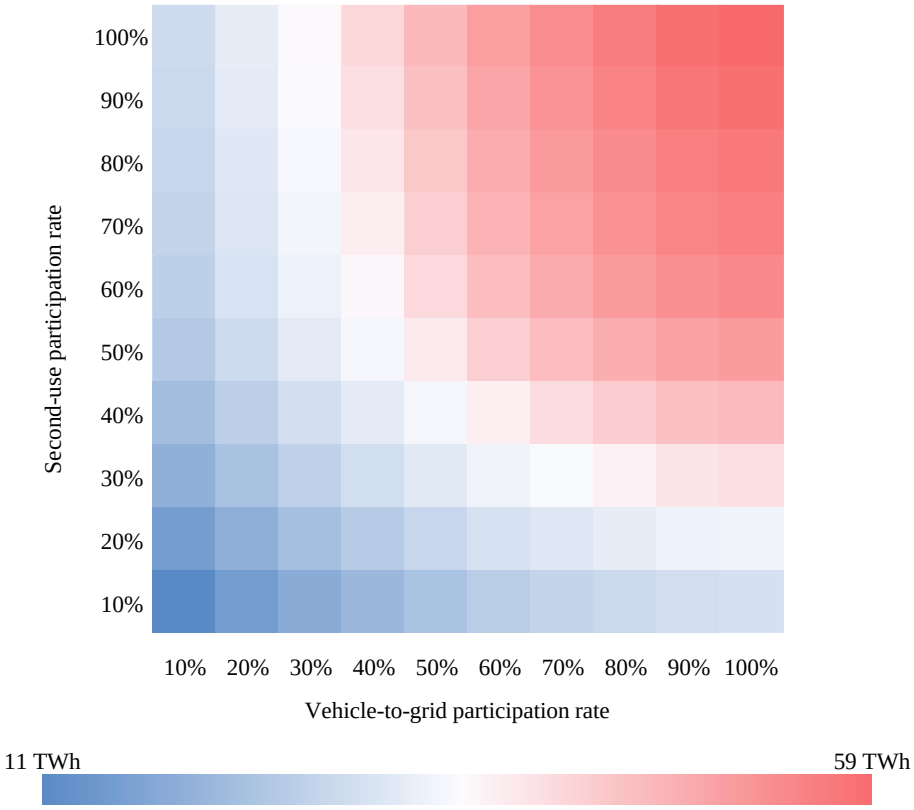


**Supplementary Fig. 5.32: Total actual available capacity under various conditions in SD-NCX scenario in 2050.** Blue, white, and red colors depict minimum, average, and maximum values.

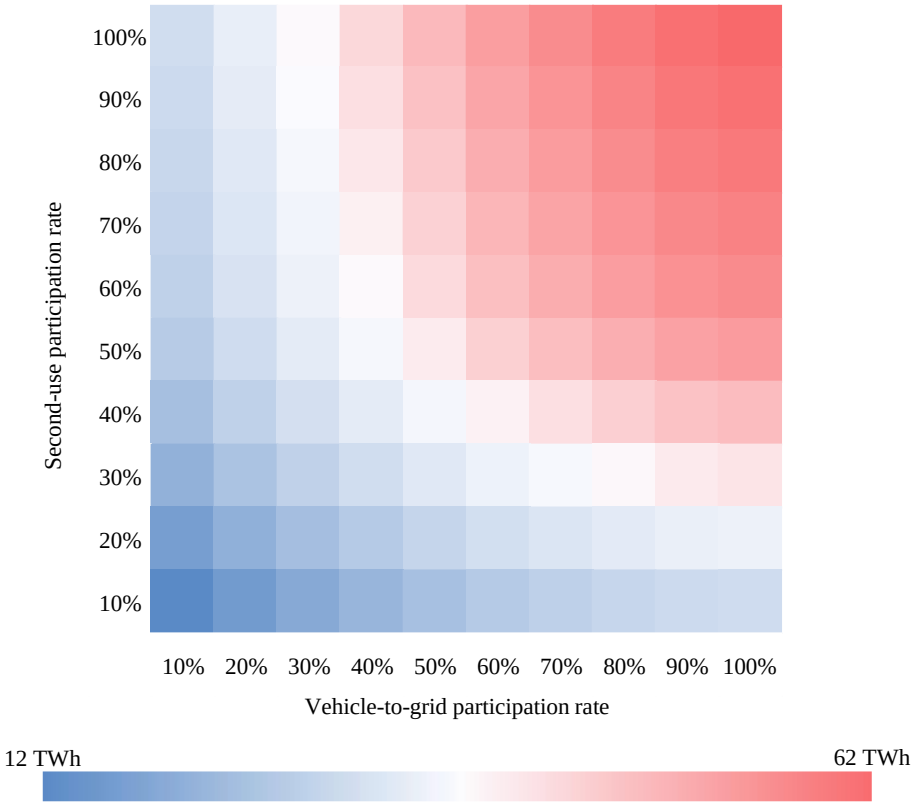


**Supplementary Fig. 5.33: Total actual available capacity under various conditions in SD-LFP scenario in 2050.** Blue, white, and red colors depict minimum, average, and maximum values.

## Supplementary Table

**Supplementary Table 5.1: Future grid storage capacity demand.** IEA = International Energy Agency. IRENA = International Renewable Energy Agency. BNEF = Bloomberg New Energy Finance. SD scenario = sustainable development scenario. Remap = Renewable Energy Roadmap. PES = Planned Energy Scenario. The "Planned Energy Scenario (PES)" is the primary reference case for this study, providing a perspective on energy system developments based on governments' current energy plans and other planned targets and policies (as of 2019), including Nationally Determined Contributions under the Paris Agreement unless the country has newer climate and energy targets or plans. TES = Transforming Energy Scenario. The "Transforming Energy Scenario (TES)" describes an ambitious, yet realistic, energy transformation pathway based largely on renewable energy sources and steadily improved energy efficiency (though not limited exclusively to these technologies). This would set the energy system on the path needed to keep the rise in global temperatures to well below 2 degree Celsius (°C) and towards 1.5°C during this century. Unit: TWh. TWh = $10^9$ kWh.

| Reference | Capacity demand | Scenarios | 2030 | 2040 | 2050 | Annual growth rate /increasing factor in 2030~2050 | Annual growth rate /increasing factor in 2040~2050 |
|---|---|---|---|---|---|---|---|
| IEA[235] | Stationary storage batteries | SD | / | 2.9884 | / | | |
| IRENA[236] | Behind the meter storage batteries | Remap | / | / | 9 | | |
| IRENA[237] | Electricity storage energy capacity | Reference scenario | 7.22 | / | / | | |
| IRENA[237] | Electricity storage energy capacity | Doubling scenario | 13.58 | / | / | | |
| IRENA[56] | Stationary storage | PES | 0.37 | / | 3.4 | 0.12/9.19 | |

Supplementary Table 5.1 (Continued).

| Reference | Capacity demand | Scenarios | 2030 | 2040 | 2050 | Annual growth rate /increasing factor in 2030~2050 | Annual growth rate /increasing factor in 2040~2050 |
|---|---|---|---|---|---|---|---|
| IRENA[56] | Stationary storage | TES | 0.745 | / | 9 | 0.13/12.08 | |
| BNEF[238] | Energy storage installations | / | / | 2.85 | / | | |
| Storage Lab[194] | Flexibility grid storage capacity | Optimistic approaches | / | 2.8 | 8.8 | | 0.12/3.14 |
| Storage Lab[194] | Flexibility grid storage capacity | Conservative approaches | / | 8.8 | 19.2 | | 0.08/2.18 |

**Supplementary Table 5.2: Selected EV models for modeling daily driving distance (DDD) distributions and driving cycles.**

| Vehicle type and class | EV models for modeling DDD distribution | Representative model for modeling drive cycles |
|---|---|---|
| Small BEV | Smart fortwo, Mitsubishi i-MiEV, BMW i3, Volkswagen e-Golf | Mitsubishi i-MiEV |
| Mid-size BEV | Nissan Leaf, Mercedes-Benz B250e, Honda Clarity EV, Hyundai Ioniq Electric, Tesla Model 3 | Nissan Leaf 30 kWh |
| Large BEV | Tesla Model S, Kia Soul Electric, Hyundai Kona Electric | TESLA Model S60 2WD |
| PHEV | Toyota Prius, Ford C-MAX Energi Plug-In Hybrid, Hyundai Ioniq Plug-in Hybrid | Prius Prime |

**Supplementary Table 5.3: Optimized parameters for LFP and NCM degradation model.**

| Parameter | LFP | NCM |
|---|---|---|
| $k_{Cal}$ | 1.9234E-3 ($days^{0.5}$) | 4.0149E-4 ($days^{0.5}$) |
| $E_a$ | 3.0233E4 (J/mol·K) | 5.9178E4 (J/mol·K) |
| $\alpha$ | -0.05590 | -1 |
| $k_{Cyc}$ | 2.93583E-6 | 4.3131332E-6 |
| A | 1.4761E-11 | 0.3549361 |
| B | 7.4008E-3 | 1.2308964E-4 |
| C | 0.082035 | 0 |
| D | 0.0313111 | 1 |
| E | 0.33344256 | 0.6149392 |
| F | 331.652158 | 63.619859 |

### 5.5.3 Supplementary Notes

#### Supplementary Note 5.1

As shown in Supplementary Fig. 4, we compile the trip driving cycle based on a standard US combined driving cycle (*i.e.*, 55% UDDS city driving and 45% HWY highway driving). We first model the required trip distance and time for UDDS city driving and HWY highway driving, respectively. By comparing the required driving distance with the distance of the standard driving cycle, the required multiples (*i.e.*, the repeated times of standard UDDS or HWY driving cycle) and downsizing factor (the downscaling of standard UDDS or HWY driving cycle to satisfy a small driving distance) are modeled, respectively, thus scaling up or down of standard driving cycle to the required driving distance. Supplementary Fig. 5 shows the driving cycle example of

mid-size BEV, where the mean driving distance between 33%-50% EV range is 126.3 km. A 63.1 km of trip distance requires 2 multiples of standard UDDS city driving and 1 multiple of standard HWY highway driving, as well as 1 downsized standard UDDS driving distance with a downsizing factor of 1.11 and 1 downsized standard HWY driving with a downsizing factor of 1.38.

**Supplementary Note 5.2**

According to degradation models fit with aging data from state-of-the-art NCM and LFP batteries, LFP batteries show lower levels and less variance of degradation than NCX as LFP is less sensitive to temperature variation, state-of-charge, and depth of discharge in both calendar-life and cycle-life degradation rates (Supplementary Figs. 32 and 33). For a mid-size battery electric vehicle (BEV), an increase of daily driving distance (DDD) from 0%-25% EV range to 100%-200% of EV range could reduce the relative battery State-of-health (SoH) at 8 years (*i.e.*, battery lifetime warranty by most EV manufacturers) by 5.5-22% for NCM and 1-1.5% for LFP, depending on temperature conditions (see Supplementary Data for degradation for different EV size and type). Higher utilization of plug-in hybrid vehicle (PHEV) batteries leads to higher degradation for PHEV batteries than for BEV batteries. Battery degradation variations among countries/regions are driven by driving intensity and climate conditions; the lifetime of NCM batteries in Europe is expected to be substantially shorter than other regions due to increased degradation caused by cycling at low average temperatures, while the lifetime of LFP batteries is shortest in India due to increased calendar degradation rate at high average temperatures (see Supplementary Figs. 28~31 for DDD distributions, Supplementary Data for city temperature and battery degradation).

# 6 General discussion

## 6.1 Answers to research questions

Table 6.1 summarizes the related research questions identified in the introduction as well as the methods applied and the answers provided in the previous chapters.

**Table 6.1: Summary of research questions, and the methods applied to come to answers on the research questions.**

| Questions | Methods | Results |
|---|---|---|
| What is the future material demand for automotive lithium-ion batteries? | ✓ Dynamic MFA<br>✓ EV fleet and battery chemistry scenarios | ✓ Strong demand growth for lithium, cobalt, nickel<br>✓ Closed-loop recycling only matters after 2030 |
| What are future cradle-to-gate GHG emissions per kWh automotive lithium-ion battery production? | ✓ Prospective LCA model including 8 battery chemistries and 3 production regions | ✓ GHG emissions per kWh storage capacity during 2020-2050<br>✓ LiOH matters for LFP emissions, NiSO4 for NCA/NCM emissions |
| What are the future GHG emissions of global automotive lithium-ion battery production? | ✓ Combine dynamic MFA and prospective LCA | ✓ Global EV battery demand will result 149-266 Mt CO2-Eq of GHG emissions in 2050<br>✓ GHG emissions reduce from 50%-75% by 2050 per kWh of battery, which results in a relative decoupling<br>✓ Battery demand matters more than recycling for GHG emissions reduction |
| What is the future grid storage capacity available from global automotive lithium-ion batteries? | ✓ Vehicle-to-grid and second-use<br>✓ EV driving behavior and battery degradation | ✓ Electric vehicle batteries alone could satisfy short-term grid storage demand by as early as 2030 |

### 6.1.1 RQ1: What is the future material demand for automotive lithium-ion batteries?

*Methods*

**Dynamic MFA.** To project battery material flows, we build a battery stock dynamics model[7] that consists of an EV layer, a battery layer, and a material layer. The EV layer models future EV fleet size (*i.e.*, EV stock) and battery capacity demand. EV stock determines battery stock. The battery stock determines the battery demand and end-of-life (EoL) batteries each year, considering EV and battery lifespan distributions. The battery layer reviews battery chemistry development and models future market shares by chemistry. The material layer uses the BatPac model[70] to model material compositions of different battery chemistries, with parameter inputs of intended EV type (BEV or PHEV), EV performance (range, fuel economy, motor power[76]), and battery performance (positive and negative electrodes and their active capacity[70]).

**EV fleet and battery chemistry scenarios.** We use two EV fleet scenarios of IEA: the stated policies (STEP) scenario and the sustainable development (SD) scenario[63]. The IEA scenarios only project EV fleet size until 2030, split by BEVs and PHEVs. We further project the EV fleet size in the period from 2030-2050 based on literature reviews of EV fleet penetration and global vehicle stock[72] during this period. We assume that the future share of BEV in the global EV fleet in 2030-2050 increases at the same rate as that in the US[73].

NCM, NCA, and LFP are three common lithium-ion battery chemistries used for EVs, and they are expected to dominate the EV market in the next decade. However, NCM/NCA/LFP chemistries differ in technical lifespan, specific energy (Wh stored energy capacity/kg battery weight), stability, and other performance factors[29]. NCM and NCA batteries (NCX, with X denoting manganese and aluminum) possess higher specific energy and power performance than LFP. LFP has advantages of materials cost, cycle life, and thermal stability over NCX. Researchers also develop lithium-based solid-state chemistries, such as Li-Air and Li-Sulphur batteries that have a potentially very high specific energy and that are very safe to use. But given the current development stage, only after 2030 Li-Air and Li-Sulphur batteries[7] can be expected to be practically applied in EVs at a large scale. Based on reviews of battery technology development roadmaps, we therefore develop an NCX scenario where NCM and NCA

batteries will dominate the EV market until 2050, an LFP scenario where LFP batteries will dominate the EV market by 60% after 2030, and a Li-S/Air scenario where Li-Air and Li-Sulphur batteries will dominate the EV market by 30% each (totally 60%) during 2040-2050.

*Results*

**Strong demand growth for lithium, cobalt, nickel.** The SD scenario results in a 1.7-2 times higher annual material demand than the STEP scenario since the EV fleet in that scenario is almost twice as big. The annual material demand for lithium does not differ a lot between the three chemistry scenarios, but for nickel and cobalt the chemistry scenario influences demand a lot. The annual demand for nickel and cobalt is lower in LFP scenario and Li-S/Air scenario since lower market shares of NCX batteries, which contain nickel and cobalt, in these two scenarios. Depending on EV fleet and battery chemistry scenarios, demand is estimated to increase by factors of 18-20 for lithium, 17-19 for cobalt, 28-31 for nickel, and 15-20 for most other materials during 2020-2050. The cumulative material demand during 2020-2050 is in the range of 7.3-18.3 Mt for lithium, 3.5-16.8 Mt for cobalt, and 18.1-88.9 Mt for nickel.

**Closed-loop recycling only matters after 2030.** EVs are a fast-growing market and EVBs hence inevitably need primary material input. Given the average battery lifetimes of ~15 years, in the coming decades the amount of EoL batteries materials are hence just a fraction of primary material demand for batteries. So closed-loop recycling can, at best (*i.e.*, without delay of recycling), reduce 20%-23% of the cumulative material demand for lithium during 2020-2050, 26%-44% for cobalt, and 22%-38% for nickel. A crucial condition for realizing this closed-loop recycling potential is that recycling technologies are developed that can economically recover battery-grade. Second-use of batteries will obviously delay recycling.

### 6.1.2 RQ2: What are future cradle-to-gate GHG emissions per kWh automotive lithium-ion battery production?

*Methods*

**Prospective LCA model including 8 battery chemistries and 3 production regions.** To project cradle-to-gate GHG emissions per kWh automotive lithium-ion battery production, we build a prospective LCA model that simulates battery production by

five life cycle stages: "mining", "raw materials production", "upgrading battery materials", "component production", and "cell production". We present 24 combinations of LCIs for battery production: 8 battery chemistries, which result in different material compositions and production processes, and 3 production regions (China, US, and EU), which affect where raw materials and energy are supplied. We compile a battery production Life Cycle Inventory (LCI) based on the EverBatt model[48], China battery industry reports[165], and literature assumptions[40] where applicable. The prospective LCA model also incorporates a prospective LCI background database that is derived from the ecoinvent 3.6 database[158], but takes into account changes in the production of key battery metals (nickel[160], cobalt[161], copper[160], and others), next to changes in energy/electricity mixes by region based on outputs of the Remind Integrated Assessment Model[180], for the period between 2020 and 2050.

*Results*

**GHG emissions per kWh storage capacity during 2020-2050.** GHG emissions per kWh automotive lithium-ion battery production vary significantly between the 3 production regions (China, US, and EU). The GHG emissions per kWh battery cell produced in EU are 16%-18% lower than in the US, and 38%-41% lower than in China in 2020. This is mainly due to the substantial difference in the share of renewable energy and resulting emission intensities for electricity used for battery cell production across the regions: 0.36 kg CO2-Eq per kWh electricity in EU (low), 0.48 kg CO2-Eq per kWh electricity in US (middle), and 0.74 kg CO2-Eq per kWh electricity in China (high) in 2020.

The battery chemistry also affects GHG emissions since different materials and production processes are used. A clear example is that LFP production does not require nickel and cobalt - their production is energy intensive and generates significant emissions - while NCX cell production requires these metals. Due to this and other differences in production processes between LFP and NCX, LFP cell production generates 20%-28% lower GHG emissions per kWh storage capacity than NCX cell production in 2020.

Depending on production regions and battery chemistry, GHG emissions per kWh of automotive lithium-ion battery production are in the range of 41-89 kg CO2-Eq in 2020. Compared to 2020, GHG emissions could more than halve to 10-45 kg CO2-Eq in 2050,

mainly due to the development and use of low-carbon electricity for cell production.

**LiOH matters for LFP emissions, $NiSO_4$ for NCA/NCM emissions.** The production of the cathode is the biggest contributor (33%-70%) to the cradle-to-gate cell GHG emissions between 2020-2050, followed by anode production and cell production, the latter using energy (such as electricity) to assemble battery components to a cell. Cathode production requires the supply of different battery materials.

Cathode production requires the supply of different battery materials, especially metal-based chemicals and compounds. These metal-based materials may contribute significantly to the battery cell's GHG emissions. The contribution analysis of different battery materials to GHG emissions will differ between cathodes of LFP and NCA/NCM since their differences in the production process and the required materials (LiOH, Fe2(SO4)3, H3PO4, *etc.,* are necessary materials for the production of LFP cathode, while NiSO4, CoSO4, LiOH/Li2CO3, *etc.,* for NCA and NCM cathodes).

The production and use of LiOH and electricity together account for 82%-86% in 2020 and 64%-82% in 2050 of GHG emissions for LFP cathodes, depending on the production regions. From the perspective of the whole battery cell, LiOH and electricity together contribute to 27%-29% in 2020 and 28%-35% in 2050 of the GHG emissions of LFP cells.

Fore NCX cells a different picture arises. There, the production of $NiSO_4$ and $Li_2CO_3$ is the most important contributor to GHG emissions. $CoSO_4$ and other cathode materials are less important. Using NCM622 as an example, $NiSO_4$ and $Li_2CO_3$ contribute to 18%-30% and 6%-11% of GHG emissions of NCM622 cathode in 2020 respectively. These numbers change to 25%-46% and 8%-21% in 2050, depending on the production region and energy scenarios. In other words, $NiSO_4$ and $Li_2CO_3$ account for 16%-31% and 5%-14% of the life cycle GHG emissions of NCM622 cell production in 2050.

### 6.1.3 RQ3: What are the future GHG emissions of global automotive lithium-ion battery production?

*Methods*

**Combine dynamic MFA and prospective LCA.** We build a model to estimate the GHG emissions of global automotive lithium-ion battery cell production during 2020-2050. The model framework combines the dynamic MFA model discussed under RQ1[7], which

projects global demand for EV battery cells, and the prospective LCA model discussed under RQ2[178], which projects cradle-to-gate GHG emissions per kWh battery production. As main scenarios discern a low, medium, and high demand for batteries. The low demand scenario follows the STEP scenario but combined with an average battery capacity of 33 kWh per BEV and 14 kWh per PHEV; the medium demand scenario follows the STEP scenario in section 2.1.1 combined with an average battery capacity of 66 kWh per BEV and 14 kWh per PHEV; The high demand scenario assumes the same battery capacity per vehicle as the medium demand scenario, but follows the SD scenario in section 2.1.1 that is about double EV fleet size than the STEP scenario. We incorporate further in these battery demand scenarios with 2 battery chemistry scenarios (in section 2.1.1) and two energy mix scenarios (in section 2.1.2). In addition to scenario analysis, we conduct sensitivity analysis of battery production region and closed-loop recycling with regard to total GHG emissions for global battery production.

*Results*

**Global EV battery demand will result in 149-266 Mt CO2-Eq of GHG emissions in 2050.** We find the life cycle GHG emissions of the global EVB cell production will increase to 26-155 Mt CO2-Eq in 2030 and 58-468 Mt CO2-Eq in 2050, depending on EV demand growth, battery chemistry, and energy mix scenarios. In the medium battery demand scenario, the global GHG emission of EVB cells production will range 44-99 Mt CO2-Eq in 2030, 54-173 Mt CO2-Eq in 2040, and 99-287 Mt CO2-Eq in 2050 (the range depends on battery chemistry and energy mix scenarios). The high battery demand scenario leads to 1.5-1.7 times higher annual GHG emissions than in the medium demand scenario, while the low demand scenario results in 58%-59% of the annual GHG emissions of the medium demand scenario. Between the high and low demand scenario there is a factor of 2.6-2.9 difference in GHG emissions of global EVB cell production in 2050.

In addition to the battery demand scenarios, the battery chemistry and energy mix scenarios also affect the GHG emissions of global EVB cell production. Since LFP battery production generates lower GHG emissions than production of NCX batteries, the GHG emissions in the LFP scenario are 12%-15% lower than in the NCX scenario (range depends on battery demand scenarios). Changes in the GHG intensity of energy have a higher influence on GHG emissions as changes in the battery chemistry. In a GHG emission scenario that aims to keep temperature rise well below 2 °C, GHG

emissions from battery production are 48%-65% lower than in a GHG emission scenario that will end up with 3.5 °C temperature rise.

**GHG emissions reduce from 50%-75% by 2050 per kWh of battery, which results in a relative decoupling.** Despite an 8%-12% annual growth rate of the global demand for battery cells during 2020-2050, life cycle emissions of battery production only increase annually by 2%-10% in the same period. There is hence relative decoupling, which can be defined as the relative change of annual growth rates of life cycle emissions of battery production, and battery demand. The relative decoupling rate can range from 19% to 70%, depending on battery demand, battery chemistry, and energy mix scenarios.

**Battery demand matters more than recycling for GHG emissions reduction.** Battery demand - determined by the EV fleet size and battery capacity per vehicle - provides a promising opportunity to reduce battery GHG emissions. This is reflected by the GHG emissions comparison among three battery demand scenarios. The comparison indicates that drastic reductions are possible if mainly small EVs are used with 33kWh storage capacity, as opposed to the 66 kWh we used on average. If additionally, self-driving cars breakthrough, which are more intensively used, a further reduction could be realized of required battery stock and related life cycle GHG emissions of their production.

Materials recycling only has a minor but increasing role to reduce life cycle GHG emissions of battery production. The relative maximum impact reduction potential by recycling for GHG emissions (see methods in Chapter 4) is increasing from 0.25%- 0.76% in the period from 2021-2030 to 2%-5.4% in 2031-2040, and to 3.8%-10.7% in 2040-2050. This is mainly because the volume of materials entering the EoL stage in a specific year is, given the vast expansion of the EV fleet, just a fraction of the required new use (5%-30%). This situation can be only partly solved once the EV battery market has reached a steady state, *i.e.*, when recycled EoL materials can almost completely meet material demand. Under a hypothetical future steady state, the relative maximum impact reduction potential can improve from 8%-22% in 2021-2030 to 10%-30% in 2031-2040, and to 13%-35% in 2040-2050. Note that this potential is not taking into account the GHG emissions from collection and recycling processes. It is hence essential that efficient, low-carbon techniques for battery recycling are developed.

### *6.1.4* RQ4: What is the future grid storage capacity available from the global use of automotive lithium-ion batteries?

*Methods*

**Vehicle-to-grid and second-use.** We develop an integrated model[155] to assess the future available (both technical and actual) grid storage capacity from EV batteries. In the following, we describe both vehicle-to-grid capacity (*i.e.*, batteries in use in EVs) and second-use capacity (*i.e.*, EV batteries that reached their end of life but can be used in less critical storage applications).

We define the technical vehicle-to-grid capacity as the availability of EV battery stock capacity for vehicle-to-grid application, considering the capacity reserved for EV driving, the capacity of PHEVs that will not participate in vehicle-to-grid, and capacity loss due to battery degradation. We further define the actual vehicle-to-grid capacity, under different consumer participation rates, as the actual availability of technical vehicle-to-grid capacity for the grid.

We assume that batteries will retire from EVs when vehicles reach their EoL. Typically, the retired batteries should have over 70% of their original capacity to meet the technical and economic feasibility of the second use. We define the technical second-use capacity as the capacity of the retired batteries that can be repurposed for a second use, considering the capacity loss during their use in EVs. We further investigate the actual second-use capacity under different market participation rates (*i.e.*, not all retired batteries maybe end up as second-use).

*Results*

**EV driving behavior and battery degradation.** A battery degradation model - based on the latest battery degradation test data differed by battery chemistries (LFP and NCM) - is developed to estimate battery capacity loss over time under different conditions of EV use, battery chemistry, and temperature. The model builds upon the battery degradation method of Smith. et al. from NREL[61] and considers both calendar life and cycle life aging. The calendar life aging consists of all aging processes that result in a degradation of a battery cell independent of charge and discharge cycles, which is modeled based on factors of battery temperature and state-of-charge; the cycle life aging refers to a degradation of a battery cell due to charging and discharging

cycles, which is modeled based on factors of battery temperature, depth-of-discharge, and current rate. The calendar life aging is an important factor than the cycle life aging for the lithium-ion batteries applied in EVs where the driving periods are substantially shorter than the idle parking periods.

We build an EV use model including behavioral factors such as the EV driving cycle and charging behavior (charging power, time, and frequency), based on daily driving distance datasets for small/mid-size/large BEVs and PHEVs provided by Spritmonitor.de[199]. In this model, EV battery SoC (state-of-charge) is simulated second-by-second under three EV states: driving; parking and charging; and parking without charging. For battery SoC during driving, we use the FASTSim model[202], developed by NREL, to simulate battery SoC second-by-second with inputs information on the EV driving cycle (vehicle speed over time), EV configurations (such as drag coefficients), and battery performance parameters (specific energy and battery capacity). For battery SoC during parking and charging, we assume a constant charging power with a 90% charging efficiency[203] such that the battery SoC increases linearly until a full charge state. If an EV is parked without charging, the SoC of the battery is slowly decreasing due to losses caused by battery self-discharging. We assume a typical discharge rate of 5% per month for lithium-ion batteries[204].

**Electric vehicle batteries alone could satisfy short-term grid storage demand by as early as 2030.** The expanding use of wind and PV for electricity generation will lead to a need for short- and long-term storage of electricity. Here, we focus on short-term electricity storage since this accounts for the majority of the required power storage capacity in kW[192]. We have used the Planned Energy Scenario and the Transforming Energy Scenario developed by the International Renewable Energy Agency[2] as well as the conservative and optimistic scenarios[194] developed by the Storage Lab. These scenarios all give the level of penetration of renewable wind and PV technologies. These levels of penetration estimate a short-term storage capacity requirement of respectively 3.4, 9, 8.8-19.2 TWh by 2050 globally. The future demand for short-term grid storage refers to the 4-hour storage capacity defined as a typical 1-time equivalent full charging/discharge cycle per day, amounting to 4 hours of cumulative maximum discharge power per day.

EV and second-use batteries are in principle an option to provide this storage capacity. We define total technical storage capacity as the cumulative available EV battery

capacity in use and in second use at a specific time, taking into account battery degradation and the capacity needed to meet the demand for driving. Under all EV fleet and battery chemistry scenarios, the total technical capacity will grow dramatically, by a factor of 13-16 between 2030 and 2050. Putting this total technical capacity into perspective against the future demand for short-term grid storage, we find that our estimated capacity growth is expected to increase as fast or even faster than short-term grid storage capacity demand in several projections[56,194]. Technical vehicle-to-grid capacity or second-use capacity are each, on their own, sufficient to meet the short-term grid storage capacity demand of 3.4-19.2 TWh by 2050. This is also true on a regional basis where technical EV capacity meets regional grid storage capacity demand. Modest market participation rates (12%-43%) are needed to provide most if not all short-term grid storage demand globally.

### 6.1.5 Answers to overall research question

**Overall RQ: What are the future environmental challenges and opportunities for automotive lithium-ion batteries from a life cycle perspective?**

*Methods*

We build an integrated model that links dynamic MFA, prospective LCA, and state-of-art battery technology modeling. The model was adjusted to answer various specific RQs. First, we use this model to estimate the future battery material demand (challenge 1). It links the dynamic MFA method and the battery chemistry model (including battery chemistry mix and material compositions). Second, we use this model to assess the GHG emissions per kWh of battery production (challenge 2). It links the prospective LCA method and the battery chemistry model. Third, we use this model to quantify the GHG emissions of global battery production (challenge 3). It links the dynamic MFA approach, the prospective LCA method, and battery chemistry modeling. Last, we use this model to explore available grid storage capacity from global EV battery use (opportunity 1). It links the dynamic MFA method and battery degradation modeling (*i.e.*, battery capacity over time).

*Results*

According to our model, EV battery production poses several challenges to the environment. There are however ways to limit these challenges. First, increasing EV

battery deployments will lead to strong demand growth for raw materials - especially lithium, cobalt, and nickel, which are defined as critical materials by the European Commission. We can reduce battery material demand by developing batteries that use low amounts of (critical) material (such as batteries based on chemistries using low amounts of cobalt), closed-loop material recycling, and stimulating the use of small cars using mall batteries. Self-driving cars that are driven much more intensively than private cars could lower materials demand even further. Further, transparent, secure, and sustainable supply chains of battery raw materials should be promoted. Second, battery production will generate a significant amount of GHG emissions. The future GHG emission per kWh battery storage capacity varies a lot by production region (China/EU/US) and battery chemistry, and most importantly the energy mix (the share of low-carbon renewable energy). Therefore, the use of low-carbon renewable energy, especially for energy-intensive processes, during battery production should be promoted. Third, the GHG emissions related to global battery production will increase due to battery demand growth. This increase in GHG emissions can be reduced if we use smaller cars with smaller batteries that have a lower GHG emission intensity. And as already discussed under material demand, the use of self-driving cars could reduce battery requirements and related GHG emissions from production even further.

Although the production of EV batteries will pose challenges to the environment, they obviously will lead to a massive reduction in driving emissions in the first place (an issue not further researched in this thesis). The use of EV batteries can further generate co-benefits in terms of providing energy storage capacity for the power system. This co-benefit, including both vehicle-to-grid capacity and second-use capacity, could satisfy short-term grid storage demand by as early as 2030. The co-benefit/opportunity of EV batteries to the power system should be promoted by supporting policy, innovative business, and consumer participation.

## 6.2 Limitations and recommendations for future research

**Projecting EV fleet size.** We compiled two EV fleet scenarios for the period between 2020 and 2050. Such scenarios were done in 2020, however, are by definition uncertain. They should be updated regularly, maybe even on a yearly basis, to incorporate the implications of the fast development of EV technology, supply equipment (such as charging infrastructure), and policy incentives. For instance, the IEA publishes a global

EV outlook report and updates EV fleet scenarios each year, with projections until 2030 only. The IEA's projection of EV fleet size in 2022[6] is slightly higher than that in previous years 2020[47] and 2021[239]. Also, instead of two EV fleet scenarios in 2020 and 2021, IEA in 2022 presents three EV fleet scenarios that are associated with different climate and EV policy goals: a stated policy scenario; an announced policy scenario; and a net-zero emissions by 2050 scenario[6]. Among the three scenarios, the net-zero emissions by 2050 scenario projects the highest EV fleet size that follows a net-zero emissions trajectory for energy system[6], which should be included in future research.

Moreover, we do not consider self-driving vehicles[4] and vehicle sharing[5] in our EV fleet scenarios. This is rarely considered in current studies, due to uncertainties with regard to commercialization timelines and consumer acceptance of these potential developments. Yet, such developments have potentially dramatic impacts on EV fleet sizes and battery demand. Future research is hence recommended to include the impacts of self-driving and sharing vehicles, since these technologies could lead to lower EV fleet size and battery demand while at the same time reducing challenges with regard to material requirements and life cycle GHG emissions of battery production.

**Battery chemistry.** Three battery chemistry scenarios are developed on a global level, and used also on a regional level. However, battery chemistry scenarios will differ in regions, depending on regional battery policies and development roadmaps. For instance, China prefers LFP batteries over NCA and NCM batteries, while the US and EU prefer NCA and NCM batteries over LFP batteries[240]. Future research can develop regional-specific battery chemistry scenarios, which will increase the accuracy of projecting regional battery materials demand and environmental impacts.

Further, battery technologies develop fast, and including the impacts of uncertain, but potentially breakthrough battery technologies in our results is challenging. Although we include a Li-S/Air scenario, we do not include any other chemistries beyond lithium-based chemistries, such as aluminum, and sodium-based batteries[64]. Such novel chemistries can also be potentially used for EVs. For example, CATL started the production of first-generation sodium-ion batteries for EVs[241], which do not require lithium, cobalt, and nickel during battery production. Broader scenario analyses of such possible future changes in battery chemistries are recommended.

**Battery production.** When simulating battery cell production in the prospective LCA model, future development of material efficiency is not incorporated in the model[242]. Higher material efficiency will result in lower material use and thus lower GHG emissions. This can be achieved in many ways, such as designing batteries requiring lower amounts of materials, reusing battery components and materials during production, *etc*[243]. Future research should include the future development of material efficiency and investigate its potential to reduce GHG emissions of battery cells.

Our analysis showed that the decarbonization of the energy system has a crucial impact on the life cycle GHG emission of battery production. Various energy scenarios exist from different Integrated assessment models, which can result in different life cycle environmental impacts for future energy production. Selecting and adjusting such energy scenarios to match battery production technology developments is hence crucial in further research. Future research should include close-to-reality and specific energy transition scenarios for different battery production stages/processes.

**Battery use.** We use state-of-art data to model battery degradation for LFP and NCM. However, if drastic innovations in battery technology take place (such as Na-ion, Li-Air, and Li-Sulphur[228], as discussed before), this may have a significant impact on battery lifespans and degradation rates. Further, while we derived driving behaviour from empirical data, future changes in driving habits are uncertain and dependent on various factors such as EV-related infrastructure. Vehicle chargers increase in power output over time and 50 kW charging is already common across some countries[229]. Frequent fast charging could lead to faster degradation, especially in hot/cold climates[230]. This challenge may be addressed by future technology improvements to battery materials[231], electrode architectures, and optimized synergy of the cell/module/pack system design[169].

Our research found that technically EV batteries alone could satisfy by 2030 short-term storage demand in electricity grids relying on input of PV and wind. Optimizing vehicle-to-grid capacity or second-use capacity of EV batteries may enhance the penetration level and use efficiency of renewable energy[244,245]. This may, in turn, result in lower GHG emissions for battery production. An interesting subject for future research could be building a model which can simulate interactions between EV battery use, renewable energy production and storage, and battery production.

**Battery end-of-life.** The battery lifespan strongly affects the demand for new batteries and the end of life scenarios (second-use or recycling). It is uncertain due to consumer behavior, battery state-of-health[246], *etc*. Actual battery lifespan data should be collected alongside the EV fleet exapansion, and included in future research to increase the reliability of results.

Since recycling can reduce material demand and GHG emissions for EV batteries, we do include the impacts of recycling in the analysis. However, the energy and materials input to recover materials from EoL batteries during recycling are neglected due to the lack of reliable data. Recycling may generate more GHG emissions than the emissions mitigated by recovered materials (such as pyrometallurgical recycling of LFP batteries[49]), depending on battery chemistry and recycling technologies. It is necessary to collect reliable LCI data on battery recycling and use the data along with a consistent methodology for quantifying environmental costs and benefits of battery recycling.

## 6.3 Policy implications of this research

**Battery materials.** Given the expected strong demand growth for battery materials, the global production capacity for critical materials - lithium, cobalt, and nickel - needs to expand drastically. For lithium, demand from global light-duty EVs alone can exceed the 2019 global lithium production, now mainly used in applications such as portable batteries, ceramics, and catalysts in the next decade. This potential lithium supply bottleneck is reflected by the recent lithium price spike of 438% in 2020[247], due to COVID lockdowns and supply chain issues[248]. It is hence crucial to start lithium mining and refinement projects well ahead of the demand increase given the fact that such projects have years of lead time; considering alternative methods of extracting and refining lithium (such as lithium from seawater) that can expand and speed up the supply[247]. Similar problems can be expected for cobalt. Cobalt demand for EV batteries alone in the next decade will be as high as the global cobalt production in 2020. Using batteries with low cobalt content (such as NCM batteries in which cobalt content is gradually reduced) or even batteries not containing cobalt (Li-Sulphur and Li-Air batteries) can relieve the potential cobalt supply shortage[7]. For nickel, demand from global EV battery production only, could surpass the 2019 global nickel production used in all applications between two and three decades. The situation for nickel is hence somewhat less critical as for lithium and cobalt in the long term. Increasing the

mining and refining capacity of Class 1 nickel, which is required for batteries, can avoid a nickel supply shortage for EV batteries[249]. Note the criticalities and supply chain vulnerabilities of different battery materials can change dramatically in a short term due to material trade restrictions, social and political disruptions (such as the recent war between Russia and Ukraine[250]), and the concentration of material production in a few countries and regions. Building new production sources and developing material reserves for battery materials, such as deep-sea mining[251] and the recent mining project in Greenland[252], can improve the security of the materials supply chain.

In sum, a vast ramp-up of extraction and production of battery materials is required to maintain an adequate supply. However, such a development poses environmental challenges, along with social and governance complexities[13]. Since GHG emissions of battery materials vary significantly under different conditions including production technologies, battery chemistries, and the pace of the low-carbon energy transition, we should stimulate conditions that lead to lower GHG emissions related to battery production. Our results in Chapters 3 and 4 provide a basic understanding of how GHG emissions related to battery production could be minimized.

**Low-carbon energy transition.** We must highlight the importance of low-carbon energy transition in reducing GHG emissions of battery cell production (over 50% reduction of battery GHG emissions). Increasing the share of low-carbon energy (such as wind and solar) in the energy system and, at the same time, the use of low-carbon energy during battery production should be a priority measure to reduce GHG emissions from battery production. One practical measure is to install a solar power generation facility along with a battery production factory[170] - such that low-carbon electricity is generated and directly used for battery production without long-distance electricity transmission.

Given the fact that the low-carbon energy transition is mainly driven by solar and wind power installments, we should speed up the installations of solar and wind that generate low-carbon electricity. However, electricity production by solar and wind fluctuates due to weather variability (if no/weak/strong wind and sunshine), and they require solutions to ensure a match of supply and demand on the electricity grid, such as stationary battery energy storage. For large-scale deployment of stationary battery energy storage, cutting down battery costs is necessary but challenging[253]. The opportunity that EV batteries alone could satisfy short-term grid storage demand by

as early as 2030 should not be missed and used as a cost-effective storage solution (*i.e.*, vehicle-to-grid and second use) for an energy system based on solar and wind. To realize vehicle-to-grid, policy incentives should support the development of an EV charging infrastructure that is capable of using as well vehicle-to-grid services, business models to encourage the participation of EV consumers, and the inclusion of EV battery energy storage in future electricity market design are all necessary supports. The energy storage opportunity can also be provided by the second use of retired EV batteries. Policies should focus on the establishment of a collection system for retired batteries, the technology for rapid battery health checks and remanufacturing, and business that can maximize the value of second-use batteries in the grid storage applications.

# References


1 Pörtner, H. O. et al. Climate change 2022: impacts, adaptation and vulnerability. (2022).

2 Michalek Jeremy, J. et al. Valuation of plug-in vehicle life-cycle air emissions and oil displacement benefits. *Proceedings of the National Academy of Sciences* **108**, 16554-16558 (2011).

3 Richter, A., Löwner, M.-O., Ebendt, R. & Scholz, M. Towards an integrated urban development considering novel intelligent transportation systems: Urban Development Considering Novel Transport. *Technological Forecasting and Social Change* **155**, 119970 (2020).

4 Coppola, P. & Silvestri, F. in *Autonomous Vehicles and Future Mobility* (eds. Coppola, P. & Esztergár-Kiss, D.) 1-15 (Elsevier, 2019).

5 Mounce, R. & Nelson, J. D. On the potential for one-way electric vehicle car-sharing in future mobility systems. *Transportation Research Part A: Policy and Practice* **120**, 17-30 (2019).

6 *Global EV Outlook 2022* (International Energy Agency Paris, France, 2022). https://www.iea.org/reports/global-ev-outlook-2022

7 Xu, C. et al. Future material demand for automotive lithium-based batteries. *Commun. Mater.* **1**, 99 (2020).

8 Berkeley, N., Bailey, D., Jones, A. & Jarvis, D. Assessing the transition towards Battery Electric Vehicles: A Multi-Level Perspective on drivers of, and barriers to, take up. *Transportation Research Part A: Policy and Practice* **106**, 320-332 (2017).

9 Skeete, J.-P., Wells, P., Dong, X., Heidrich, O. & Harper, G. Beyond the EVent horizon: Battery waste, recycling, and sustainability in the United Kingdom electric vehicle transition. *Energy Research & Social Science* **69**, 101581 (2020).

10 Turcheniuk, K., Bondarev, D., Amatucci, G. G. & Yushin, G. Battery materials for low-cost electric transportation. *Materials Today* **42**, 57-72 (2021).

11 Schade, W., Haug, I. & Berthold, D. The future of the automotive sector. (2022).

12 Mancini, L. & Nuss, P. Responsible Materials Management for a Resource-Efficient and Low-Carbon Society. *Resources* **9** (2020).

13 Lèbre, É. et al. The social and environmental complexities of extracting energy transition metals. *Nat. Commun.* **11**, 4823 (2020).

14 Guille, C. & Gross, G. A conceptual framework for the vehicle-to-grid (V2G) implementation. *Energy Policy* **37**, 4379-4390 (2009).

15 *Identifying and Overcoming Critical Barriers to Widespread Second Use of PEV Batteries*

(National Renewable Energy Lab, 2015). https://www.osti.gov/biblio/1171780

16 Haram, M. H. S. M. et al. Feasibility of utilising second life EV batteries: Applications, lifespan, economics, environmental impact, assessment, and challenges. *Alexandria Engineering Journal* **60**, 4517-4536 (2021).

17 Harper, G. et al. Recycling lithium-ion batteries from electric vehicles. *Nature* **575**, 75-86 (2019).

18 Müller, E., Hilty, L. M., Widmer, R., Schluep, M. & Faulstich, M. Modeling Metal Stocks and Flows: A Review of Dynamic Material Flow Analysis Methods. *Environmental Science & Technology* **48**, 2102-2113 (2014).

19 Brunner, P. H. & Rechberger, H. *Handbook of material flow analysis: For environmental, resource, and waste engineers*. (CRC press, 2016).

20 Kawecki, D., Scheeder, P. R. & Nowack, B. Probabilistic material flow analysis of seven commodity plastics in Europe. *Environmental science & technology* **52**, 9874-9888 (2018).

21 Du, X. & Graedel, T. E. Global in-use stocks of the rare earth elements: a first estimate. *Environmental science & technology* **45**, 4096-4101 (2011).

22 Song, J. et al. Material flow analysis on critical raw materials of lithium-ion batteries in China. *Journal of Cleaner Production* **215**, 570-581 (2019).

23 Finnveden, G. et al. Recent developments in Life Cycle Assessment. *Journal of Environmental Management* **91**, 1-21 (2009).

24 Thonemann, N., Schulte, A. & Maga, D. How to Conduct Prospective Life Cycle Assessment for Emerging Technologies? A Systematic Review and Methodological Guidance. *Sustainability* **12** (2020).

25 Tsoy, N., Steubing, B., van der Giesen, C. & Guinée, J. Upscaling methods used in ex ante life cycle assessment of emerging technologies: a review. *The International Journal of Life Cycle Assessment* **25**, 1680-1692 (2020).

26 Mendoza Beltran, A. et al. When the Background Matters: Using Scenarios from Integrated Assessment Models in Prospective Life Cycle Assessment. *Journal of Industrial Ecology* **24**, 64-79 (2020).

27 van der Giesen, C., Cucurachi, S., Guinée, J., Kramer, G. J. & Tukker, A. A critical view on the current application of LCA for new technologies and recommendations for improved practice. *Journal of Cleaner Production* **259**, 120904 (2020).

28 Sacchi, R. et al. PRospective EnvironMental Impact asSEment (premise): A streamlined approach to producing databases for prospective life cycle assessment using integrated assessment models. *Renewable and Sustainable Energy Reviews* **160**, 112311 (2022).

29 Ryu, H.-H., Sun, H. H., Myung, S.-T., Yoon, C. S. & Sun, Y.-K. Reducing cobalt from lithium-ion batteries for the electric vehicle era. *Energy & Environmental Science* **14**, 844-852 (2021).

30 Simon, B., Ziemann, S. & Weil, M. Potential metal requirement of active materials in lithium-ion battery cells of electric vehicles and its impact on reserves: Focus on Europe. *Resour. Conserv. Recycl.* **104**, 300-310 (2015).

31 Richa, K., Babbitt, C. W., Gaustad, G. & Wang, X. A future perspective on lithium-ion battery waste flows from electric vehicles. *Resour. Conserv. Recycl.* **83**, 63-76 (2014).

32 Gaines, L. & Nelson, P. Lithium-ion batteries: possible materials issues. in *13th international battery materials recycling seminar and exhibit, Broward County Convention Center, Fort Lauderdale, Florida* (2009).

33 Ziemann, S., Müller, D. B., Schebek, L. & Weil, M. Modeling the potential impact of lithium recycling from EV batteries on lithium demand: A dynamic MFA approach. *Resour. Conserv. Recycl.* **133**, 76-85 (2018).

34 Hao, H. et al. Impact of transport electrification on critical metal sustainability with a focus on the heavy-duty segment. *Nat. Commun.* **10**, 5398 (2019).

35 Deetman, S., Pauliuk, S., van Vuuren, D. P., van der Voet, E. & Tukker, A. Scenarios for Demand Growth of Metals in Electricity Generation Technologies, Cars, and Electronic Appliances. *Environ. Sci. Technol.* **52**, 4950-4959 (2018).

36 Weil, M., Ziemann, S. & Peters, J. in *Behaviour of Lithium-Ion Batteries in Electric Vehicles: Battery Health, Performance, Safety, and Cost* (eds. Pistoia, G. & Liaw, B.) 59-74 (Springer International Publishing, 2018).

37 Nordelöf, A., Messagie, M., Tillman, A.-M., Ljunggren Söderman, M. & Van Mierlo, J. Environmental impacts of hybrid, plug-in hybrid, and battery electric vehicles—what can we learn from life cycle assessment? *The International Journal of Life Cycle Assessment* **19**, 1866-1890 (2014).

38 Tagliaferri, C. et al. Life cycle assessment of future electric and hybrid vehicles: A cradle-to-grave systems engineering approach. *Chemical Engineering Research and Design* **112**, 298-309 (2016).

39 Hawkins, T. R., Singh, B., Majeau-Bettez, G. & Strømman, A. H. Comparative Environmental Life Cycle Assessment of Conventional and Electric Vehicles. *Journal of Industrial Ecology* **17**, 53-64 (2013).

40 Ellingsen, L. A.-W. et al. Life Cycle Assessment of a Lithium-Ion Battery Vehicle Pack. *Journal of Industrial Ecology* **18**, 113-124 (2014).

41 Hiremath, M., Derendorf, K. & Vogt, T. Comparative Life Cycle Assessment of Battery Storage

Systems for Stationary Applications. *Environmental Science & Technology* **49**, 4825-4833 (2015).

42 Zackrisson, M., Avellán, L. & Orlenius, J. Life cycle assessment of lithium-ion batteries for plug-in hybrid electric vehicles – Critical issues. *Journal of Cleaner Production* **18**, 1519-1529 (2010).

43 Ellingsen, L. A.-W., Hung, C. R. & Strømman, A. H. Identifying key assumptions and differences in life cycle assessment studies of lithium-ion traction batteries with focus on greenhouse gas emissions. *Transportation Research Part D: Transport and Environment* **55**, 82-90 (2017).

44 Peters, J. F., Baumann, M., Zimmermann, B., Braun, J. & Weil, M. The environmental impact of Li-Ion batteries and the role of key parameters – A review. *Renewable and Sustainable Energy Reviews* **67**, 491-506 (2017).

45 Peters, J. F. & Weil, M. Providing a common base for life cycle assessments of Li-Ion batteries. *Journal of Cleaner Production* **171**, 704-713 (2018).

46 Mohr, M., Peters, J. F., Baumann, M. & Weil, M. Toward a cell-chemistry specific life cycle assessment of lithium-ion battery recycling processes. *Journal of Industrial Ecology* **24**, 1310-1322 (2020).

47 Kelly, J. C., Dai, Q. & Wang, M. Globally regional life cycle analysis of automotive lithium-ion nickel manganese cobalt batteries. *Mitigation and Adaptation Strategies for Global Change* **25**, 371-396 (2020).

48 Spangenberger, J., Gaines, L. & Dai, Q. Recell; A Closed-Loop Battery Recycling Model. *ECS Meeting Abstracts* **MA2018-01**, 616-616 (2018).

49 Ciez, R. E. & Whitacre, J. F. Examining different recycling processes for lithium-ion batteries. *Nature Sustainability* **2**, 148-156 (2019).

50 Schulz-Mönninghoff, M., Bey, N., Nørregaard, P. U. & Niero, M. Integration of energy flow modelling in life cycle assessment of electric vehicle battery repurposing: Evaluation of multi-use cases and comparison of circular business models. *Resources, Conservation and Recycling* **174**, 105773 (2021).

51 Hawkins, T. R., Gausen, O. M. & Strømman, A. H. Environmental impacts of hybrid and electric vehicles—a review. *The International Journal of Life Cycle Assessment* **17**, 997-1014 (2012).

52 Knobloch, F. et al. Net emission reductions from electric cars and heat pumps in 59 world regions over time. *Nature Sustainability* **3**, 437-447 (2020).

53 Sovacool, B. K., Axsen, J. & Kempton, W. The Future Promise of Vehicle-to-Grid (V2G) Integration: A Sociotechnical Review and Research Agenda. *Annual Review of Environment and Resources* **42**, 377-406 (2017).

54 Sovacool, B. K., Noel, L., Axsen, J. & Kempton, W. The neglected social dimensions to a vehicle-to-grid (V2G) transition: a critical and systematic review. *Environmental Research Letters* **13**, 013001 (2018).

55 Ralon, P., Taylor, M., Ilas, A., Diaz-Bone, H. & Kairies, K. Electricity storage and renewables: Costs and markets to 2030. *International Renewable Energy Agency: Abu Dhabi, UAE* (2017).

56 *Global Renewables Outlook: Energy transformation 2050* (International Renewable Energy Agency, 2020). https://www.irena.org/publications/2020/Apr/Global-Renewables-Outlook-2020

57 *Global EV Outlook 2020* (IEA, 2020). https://www.iea.org/reports/global-ev-outlook-2020

58 *Second-life EV batteries: The newest value pool in energy storage* (McKinsey & Company, 2019). https://www.mckinsey.com/industries/automotive-and-assembly/our-insights/second-life-ev-batteries-the-newest-value-pool-in-energy-storage

59 Baghdadi, I., Briat, O., Delétage, J.-Y., Gyan, P. & Vinassa, J.-M. Lithium battery aging model based on Dakin's degradation approach. *Journal of Power Sources* **325**, 273-285 (2016).

60 Naumann, M., Spingler, F. B. & Jossen, A. Analysis and modeling of cycle aging of a commercial LiFePO4/graphite cell. *Journal of Power Sources* **451**, 227666 (2020).

61 Smith, K. et al. Life prediction model for grid-connected Li-ion battery energy storage system. in *2017 American Control Conference (ACC)* 4062-4068.

62 Deng, J., Bae, C., Denlinger, A. & Miller, T. Electric Vehicles Batteries: Requirements and Challenges. *Joule* **4**, 511-515 (2020).

63 *Global EV Outlook 2020: Entering the decade of electric drive?* (International Energy Agency, 2020). https://www.iea.org/reports/global-ev-outlook-2020

64 Ponrouch, A. & Rosa Palacín, M. Post-Li batteries: Promises and challenges. *Philos. Trans. R. Soc. A-Math. Phys. Eng. Sci.* **377** (2019).

65 Olivetti, E. A., Ceder, G., Gaustad, G. G. & Fu, X. Lithium-Ion Battery Supply Chain Considerations: Analysis of Potential Bottlenecks in Critical Metals. *Joule* **1**, 229-243 (2017).

66 Van den Brink, S., Kleijn, R., Sprecher, B. & Tukker, A. Identifying supply risks by mapping the cobalt supply chain. *Resour. Conserv. Recycl.* **156** (2020).

67 Banza Lubaba Nkulu, C. et al. Sustainability of artisanal mining of cobalt in DR Congo. *Nat. Sustain.* **1**, 495-504 (2018).

68 Thies, C., Kieckhäfer, K., Spengler, T. S. & Sodhi, M. S. Assessment of social sustainability hotspots in the supply chain of lithium-ion batteries. in *Procedia CIRP* 292-297.

69 Müller, D. B. Stock dynamics for forecasting material flows—Case study for housing in The

Netherlands. *Ecol. Econ.* **59**, 142-156 (2006).

70 *Modeling the Performance and Cost of Lithium-Ion Batteries for Electric-Drive Vehicles, Third Edition* (Argonne National Lab, 2019). https://www.osti.gov/servlets/purl/1503280

71 *Global EV Outlook 2019: Scaling-up the transition to electric mobility* (International Energy Agency, 2019). https://www.iea.org/reports/global-ev-outlook-2019

72 Sitty, G. & Taft, N. What Will the Global Light-Duty Vehicle Fleet Look like through 2050? (2016).

73 *World Energy Outlook 2020* (IEA, 2020). https://www.iea.org/reports/world-energy-outlook-2020

74 *Vehicle Size Classes Used in the Fuel Economy Guide* (EPA, 2019).

75 Severson, K. A. et al. Data-driven prediction of battery cycle life before capacity degradation. *Nature Energy* **4**, 383-391 (2019).

76 *Find Electric Vehicle Models* (US Department of Energy, 2019).

77 Ai, N., Zheng, J. & Chen, W.-Q. US end-of-life electric vehicle batteries: Dynamic inventory modeling and spatial analysis for regional solutions. *Resour. Conserv. Recycl.* **145**, 208-219 (2019).

78 Oguchi, M. & Fuse, M. Regional and longitudinal estimation of product lifespan distribution: a case study for automobiles and a simplified estimation method. *Environ. Sci. Technol.* **49**, 1738-1743 (2015).

79 Zhang, L., Yuan, Z. & Bi, J. Predicting future quantities of obsolete household appliances in Nanjing by a stock-based model. *Resour. Conserv. Recycl.* **55**, 1087-1094 (2011).

80 *Electrochemical energy storage technical team roadmap* (USDRIVE, 2017). https://www.energy.gov/sites/prod/files/2017/11/f39/EESTT%20roadmap%202017-10-16%20Final.pdf

81 *Inventing the sustainable batteries of the future* (BATTERY 2030+, 2020). https://battery2030.eu/digitalAssets/816/c_816048-l_1-k_roadmap-27-march.pdf

82 *Roadmap for an integrated cell and battery production in Germany* (The Federal Government's Joint Office for Electric Mobility, 2016). http://nationale-plattform-elektromobilitaet.de/fileadmin/user_upload/Redaktion/Publikationen/AG2_Roadmap_Zellfertigung_eng_bf.pdf

83 Chen, K., Zhao, F., Hao, H. & Liu, Z. Selection of lithium-ion battery technologies for electric vehicles under China's new energy vehicle credit regulation. *Energy Procedia* **158**, 3038-3044 (2019).

84 *NCM 811: The future of electric car batteries?* (INSIDEEVs, 2018).

85 *The Rechargeable Battery Market and Main Trends 2018-2030* (Avicenne Energy, 2019).

86 Faguy, P. The Low Co, Co-free Initiative for Next Generation Li-ion Cathode Materials. in *U.S. Department of Energy Vehicle Technologies Office 2019 Annual Merit Review* (2019).

87 *Tesla wins China approval to build Model 3 vehicles with LFP batteries: ministry - Reuters* (Reuters, 2020).

88 *LFP chemistry is emerging as the future of batteries* (Clean Future, 2020).

89 Cano, Z. P. et al. Batteries and fuel cells for emerging electric vehicle markets. *Nat. Energy* **3**, 279-289 (2018).

90 *It's safer with OXIS lithium sulfur rechargeable batteries* (OXIS Energy, 2016). http://oxisenergy.com/wp-content/uploads/2016/05/oxis-brochure.pdf

91 *Samsung's lithium-air battery could help double EV range* (World industrial reporter, 2017). https://worldindustrialreporter.com/samsungs-lithium-air-battery-could-help-double-ev-range/amp/?from=singlemessage&isappinstalled=0

92 *Comparison of plug-in hybrid electric vehicle battery life across geographies and drive-cycles* (National Renewable Energy Lab, 2012). https://www.nrel.gov/docs/fy12osti/53817.pdf

93 *Mineral Commodity Summaries 2020* (USGS, 2020). https://pubs.usgs.gov/periodicals/mcs2020/mcs2020.pdf

94 *EverBatt: A Closed-loop Battery Recycling Cost and Environmental Impacts Model* (Argonne National Lab, 2019). https://publications.anl.gov/anlpubs/2019/07/153050.pdf

95 Chen, M. et al. Recycling end-of-life electric vehicle lithium-ion batteries. *Joule* **3**, 2622-2646 (2019).

96 Reck, B. K. & Graedel, T. E. Challenges in metal recycling. *Science* **337**, 690-695 (2012).

97 Richa, K., Babbitt, C. W., Nenadic, N. G. & Gaustad, G. Environmental trade-offs across cascading lithium-ion battery life cycles. *Int. J. Life Cycle Assess.* **22**, 66-81 (2017).

98 *Identifying and Overcoming Critical Barriers to Widespread Second Use of PEV Batteries* (National Renewable Energy Lab, 2015). https://www.osti.gov/servlets/purl/1171780

99 Ahmadi, L., Young, S. B., Fowler, M., Fraser, R. A. & Achachlouei, M. A. A cascaded life cycle: reuse of electric vehicle lithium-ion battery packs in energy storage systems. *Int. J. Life Cycle Assess.* **22**, 111-124 (2017).

100 Kamath, D., Arsenault, R., Kim, H. C. & Anctil, A. Economic and Environmental Feasibility of Second-Life Lithium-Ion Batteries as Fast-Charging Energy Storage. *Environ. Sci. Technol.* **54**, 6878-6887 (2020).

101 Nitta, N., Wu, F., Lee, J. T. & Yushin, G. Li-ion battery materials: present and future. *Materials Today* **18**, 252-264 (2015).

102 Said, A. O., Lee, C. & Stoliarov, S. I. Experimental investigation of cascading failure in 18650 lithium ion cell arrays: Impact of cathode chemistry. *J. Power Sources* **446**, 227347 (2020).

103 Casals, L. C., García, B. A. & Canal, C. Second life batteries lifespan: Rest of useful life and environmental analysis. *J. Environ. Manag.* **232**, 354-363 (2019).

104 *Tesla is working on new ~110 kWh battery pack for more than 400 miles of range* (Electrek, 2020).

105 *SET-Plan ACTION n°7-Declaration of Intent "Become competitive in the global battery sector to drive e-mobility forward"* (European Commission, 2016).

106 *CATL batteries energise Powin's new 'long duration, long life' Li-Ion systems* (Energy Storage News, 2020).

107 Benveniste, G., Rallo, H., Casals, L. C., Merino, A. & Amante, B. Comparison of the state of Lithium-Sulphur and lithium-ion batteries applied to electromobility. *J. Environ. Manag.* **226**, 1-12 (2018).

108 *LEAF WARRANTY INFORMATION BOOKLET* (NISSAN, 2020). https://www.nissanusa.com/content/dam/Nissan/us/manuals-and-guides/leaf/2020/2020-nissan-leaf-warranty-booklet.pdf

109 Mayyas, A., Steward, D. & Mann, M. The case for recycling: Overview and challenges in the material supply chain for automotive li-ion batteries. *Sustain. Mater. Technol.* **19**, e00087 (2019).

110 Gaines, L. Lithium-ion battery recycling processes: Research towards a sustainable course. *Sustain. Mater. Technol.* **17**, e00068 (2018).

111 Richa, K., Babbitt, C. W., Nenadic, N. G. & Gaustad, G. Environmental trade-offs across cascading lithium-ion battery life cycles. *Int. J. Life Cycle Assess.* **22**, 66-81 (2015).

112 Lang, J. et al. High-purity electrolytic lithium obtained from low-purity sources using solid electrolyte. *Nat. Sustain.* **3**, 386-390 (2020).

113 *Study on Critical Raw Materials at EU Level* (Oakdene Hollins and Fraunhofer ISI, 2013). http://ec.europa.eu/DocsRoom/documents/5605/attachments/1/translations/en/renditions/native

114 Helbig, C., Bradshaw, A. M., Wietschel, L., Thorenz, A. & Tuma, A. Supply risks associated with lithium-ion battery materials. *J. Clean Prod.* **172**, 274-286 (2018).

115 Alves Dias, P., Blagoeva, D., Pavel, C. & Arvanitidis, N. Cobalt: demand-supply balances in the

transition to electric mobility. *European Commission, Joint Research Centre, EUR-Scientific and Technical Research Reports Publications Office of the European Union DOI* **10**, 97710 (2018).

116 Prior, T., Giurco, D., Mudd, G., Mason, L. & Behrisch, J. Resource depletion, peak minerals and the implications for sustainable resource management. *Glob. Environ. Change* **22**, 577-587 (2012).

117 Delogu, M., Zanchi, L., Dattilo, C. A. & Pierini, M. Innovative composites and hybrid materials for electric vehicles lightweight design in a sustainability perspective. *Mater. Today Commun.* **13**, 192-209 (2017).

118 Eberle, U. & Von Helmolt, R. Sustainable transportation based on electric vehicle concepts: a brief overview. *Energy Environ. Sci.* **3**, 689-699 (2010).

119 Saxena, S., Le Floch, C., MacDonald, J. & Moura, S. Quantifying EV battery end-of-life through analysis of travel needs with vehicle powertrain models. *Journal of Power Sources* **282**, 265-276 (2015).

120 Neubauer, J. & Wood, E. The impact of range anxiety and home, workplace, and public charging infrastructure on simulated battery electric vehicle lifetime utility. *J. Power Sources* **257**, 12-20 (2014).

121 Brown, S., Pyke, D. & Steenhof, P. Electric vehicles: The role and importance of standards in an emerging market. *Energy Policy* **38**, 3797-3806 (2010).

122 Prior, T., Wäger, P. A., Stamp, A., Widmer, R. & Giurco, D. Sustainable governance of scarce metals: The case of lithium. *Sci. Total Environ.* **461-462**, 785-791 (2013).

123 Zwolinski, P. & Tichkiewitch, S. An agile model for the eco-design of electric vehicle Li-ion batteries. *CIRP Annals* **68**, 161-164 (2019).

124 Meng, F., McNeice, J., Zadeh, S. S. & Ghahreman, A. Review of Lithium Production and Recovery from Minerals, Brines, and Lithium-Ion Batteries. *Miner. Process Extr. Metall. Rev.* (2019).

125 *Find Electric Vehicle Models* (US Department of Energy, 2019). https://www.energy.gov/eere/electricvehicles/find-electric-vehicle-models

126 *Electric Vehicle Outlook 2020* (Bloomberg NEF, 2020). https://bnef.turtl.co/story/evo-2020/?teaser=yes

127 *BP Energy Outlook 2019 edition* (BP, 2019). https://www.bp.com/content/dam/bp/business-sites/en/global/corporate/pdfs/energy-economics/energy-outlook/bp-energy-outlook-2019.pdf

128 *World Oil Outlook 2040* (OPEC, 2018). https://elperiodicodelaenergia.com/wp-content/uploads/2018/09/WOO_2018.pdf

129 *Charging upwards: BHP recharges its electric vehicle take-up forecasts* (BHP, 2019). https://www.smh.com.au/business/companies/bhp-recharges-its-electric-vehicle-take-up-forecasts-20190521-p51pix.html

130 *MOVIN'ON: TOTAL'S TAKE ON MOBILITY OF THE FUTURE* (TOTAL, 2018). https://www.total.com/en/news/movinon-totals-take-mobility-future?folder=9487

131 *Up to 50% of the global car fleet could be electric in 2050* (Enerdata, 2018). https://www.enerdata.net/publications/executive-briefing/half-car-fleet-electric-2050.html

132 *Global EV Outlook 2019* (IEA, 2019). https://www.iea.org/reports/global-ev-outlook-2019

133 Al-Alawi, B. M. & Bradley, T. H. Review of hybrid, plug-in hybrid, and electric vehicle market modeling studies. *Renew. Sust. Energ. Rev.* **21**, 190-203 (2013).

134 *Annual energy outlook 2020 with projections to 2050: light-duty vehicle sales by technology type* (U.S. Energy Information Administration, 2020). https://www.eia.gov/outlooks/aeo/data/browser/#/?id=48-AEO2020&sourcekey=0

135 Ko, M. et al. Scalable synthesis of silicon-nanolayer-embedded graphite for high-energy lithium-ion batteries. *Nat. Energy* **1**, 1-8 (2016).

136 *New lithium-air battery could drive huge performance gains* (ExtremeTech, 2015). https://www.extremetech.com/mobile/217191-new-lithium-air-battery-could-drive-huge-performance-gains?from=singlemessage&isappinstalled=0

137 Tsach, S., Tatievsky, A. & London, L. Future Commercial Aviation Trends. in *Israel Annual Conference on Aerospace Sciences* (2012).

138 *Why the future of batteries is lithium and why their impact will be bigger than you think* (Energy Post, 2017). https://energypost.eu/future-batteries-lithium-impact-will-bigger-think/?from=singlemessage&isappinstalled=0

139 Aurbach, D., McCloskey, B. D., Nazar, L. F. & Bruce, P. G. Advances in understanding mechanisms underpinning lithium–air batteries. *Nat. Energy* **1**, 1-11 (2016).

140 *Lithium-sulfur batteries: from materials understanding to device integration* (Yi Cui, 2017). https://www.energy.gov/sites/prod/files/2018/06/f52/bat361_cui_2018_o.pdf

141 Zhang, J.-G., Wang, D., Xu, W., Xiao, J. & Williford, R. E. Ambient operation of Li/Air batteries. *J. Power Sources* **195**, 4332-4337 (2010).

142 Park, J. O. et al. A 1000 Wh kg− 1 Li–Air battery: Cell design and performance. *J. Power Sources* **419**, 112-118 (2019).

143 Lee, H. C. et al. High-energy-density Li-O2 battery at cell scale with folded cell structure. *Joule* **3**, 542-556 (2019).

144 *Mineral Commodity Summaries 2020* (USGS, 2020). https://pubs.usgs.gov/periodicals/mcs2020/mcs2020.pdf

145 *What do we know about next-generation NMC 811 cathode?* (Research Interfaces, 2018). https://researchinterfaces.com/know-next-generation-nmc-811-cathode/

146 *Advanced battery materials for xEV and high-performance consumer products* (BASF, 2014).

147 Ryu, H.-H., Park, K.-J., Yoon, C. S. & Sun, Y.-K. Capacity Fading of Ni-Rich Li [Ni x Co y Mn1–x–y] O2 (0.6≤ x≤ 0.95) Cathodes for High-Energy-Density Lithium-Ion Batteries: Bulk or Surface Degradation? *Chem. Mater.* **30**, 1155-1163 (2018).

148 *Process development and manufacturing R&D at the national laboratories* (Argonne National Laboratory, 2016). https://www.energy.gov/sites/prod/files/2018/03/f49/FY2016_APR_Advanced_Batteries_R%26D_Part-3of5-opt.pdf

149 *Supplementary materials for cobalt in lithium-ion batteries* (Science, 2020).

150 Chae, S., Ko, M., Kim, K., Ahn, K. & Cho, J. Confronting issues of the practical implementation of Si anode in high-energy lithium-ion batteries. *Joule* **1**, 47-60 (2017).

151 Kumar, R. R. & Alok, K. Adoption of electric vehicle: A literature review and prospects for sustainability. *Journal of Cleaner Production* **253**, 119911 (2020).

152 Wells, P. & Nieuwenhuis, P. Transition failure: Understanding continuity in the automotive industry. *Technological Forecasting and Social Change* **79**, 1681-1692 (2012).

153 Baumstark, L. et al. REMIND2.1: transformation and innovation dynamics of the energy-economic system within climate and sustainability limits. *Geosci. Model Dev.* **14**, 6571-6603 (2021).

154 *PRospective EnvironMental Impact asSEment (premise): a streamlined approach to producing databases for prospective Life Cycle Assessment using Integrated Assessment Models* (2021). https://github.com/romainsacchi/premise

155 Chengjian, X. et al. Electric vehicle batteries alone could satisfy short-term grid storage demand by as early as 2030. *Submitted to Nature Communications* (2022).

156 Change, I. C. (Cambridge Univ. Press, 2013).

157 Steubing, B., de Koning, D., Haas, A. & Mutel, C. L. The Activity Browser — An open source LCA software building on top of the brightway framework. *Software Impacts* **3**, 100012 (2020).

158 Wernet, G. et al. The ecoinvent database version 3 (part I): overview and methodology. *The International Journal of Life Cycle Assessment* **21**, 1218-1230 (2016).

159 O'Neill, B. C. et al. A new scenario framework for climate change research: the concept of

shared socioeconomic pathways. *Climatic Change* **122**, 387-400 (2014).

160 Harpprecht, C., van Oers, L., Northey, S. A., Yang, Y. & Steubing, B. Environmental impacts of key metals' supply and low-carbon technologies are likely to decrease in the future. *Journal of Industrial Ecology* **25**, 1543-1559 (2021).

161 van der Meide, M., Harpprecht, C., Northey, S., Yang, Y. & Steubing, B. Effects of the energy transition on environmental impacts of cobalt supply: A prospective life cycle assessment study on future supply of cobalt. *Journal of Industrial Ecology* **n/a** (2022).

162 *GLOBAL ALUMINIUM CYCLE 2019* (International Aluminium Institute, 2019). https://alucycle.world-aluminium.org/public-access/

163 Ambrose, H. & Kendall, A. Understanding the future of lithium: Part 1, resource model. *Journal of Industrial Ecology* **24**, 80-89 (2020).

164 Ambrose, H. & Kendall, A. Understanding the future of lithium: Part 2, temporally and spatially resolved life-cycle assessment modeling. *Journal of Industrial Ecology* **24**, 90-100 (2020).

165 *Environmental impact assessment report in China* (Eiafans, 2022). http://www.eiafans.com/forum.php

166 Erakca, M. et al. Energy flow analysis of laboratory scale lithium-ion battery cell production. *iScience* **24**, 102437 (2021).

167 Bouter, A. & Guichet, X. The greenhouse gas emissions of automotive lithium-ion batteries: A statistical review of life cycle assessment studies. *Journal of Cleaner Production*, 130994 (2022).

168 Bieker, G. A global comparison of the life-cycle greenhouse gas emissions of combustion engine and electric passenger cars. *communications* **49**, 847129-847102 (2021).

169 Yang, X.-G., Liu, T. & Wang, C.-Y. Thermally modulated lithium iron phosphate batteries for mass-market electric vehicles. *Nature Energy* **6**, 176-185 (2021).

170 *Tesla Gigafactory* (Tesla, 2022). https://www.tesla.com/gigafactory

171 Kelly, J. C., Wang, M., Dai, Q. & Winjobi, O. Energy, greenhouse gas, and water life cycle analysis of lithium carbonate and lithium hydroxide monohydrate from brine and ore resources and their use in lithium ion battery cathodes and lithium ion batteries. *Resources, Conservation and Recycling* **174**, 105762 (2021).

172 Ratvik, A. P., Mollaabbasi, R. & Alamdari, H. Aluminium production process: from Hall–Héroult to modern smelters. *ChemTexts* **8**, 10 (2022).

173 Tilley, J. Automation, robotics, and the factory of the future. *McKinsey. https://www. mckinsey.*

*com/business-functions/operations/our-insights/automation-robotics-and-the-factory-of-the-future* (2017).

174 Manthiram, A., Yu, X. & Wang, S. Lithium battery chemistries enabled by solid-state electrolytes. *Nature Reviews Materials* **2**, 16103 (2017).

175 European, C. et al. *Determining the environmental impacts of conventional and alternatively fuelled vehicles through LCA : final report*. (Publications Office, 2020).

176 Albatayneh, A., Assaf, M. N., Alterman, D. & Jaradat, M. Comparison of the overall energy efficiency for internal combustion engine vehicles and electric vehicles. *Rigas Tehniskas Universitates Zinatniskie Raksti* **24**, 669-680 (2020).

177 Richardson, D. B. Electric vehicles and the electric grid: A review of modeling approaches, Impacts, and renewable energy integration. *Renewable and Sustainable Energy Reviews* **19**, 247-254 (2013).

178 Xu, C. et al. Future greenhouse gas emissions of automotive lithium-ion battery cell production. *submitted to Resources, Conservation & Recycling* (2022).

179 *Greenhouse Gas Emissions from a Typical Passenger Vehicle* (United States Environmental Protection Agency, 2022). https://www.epa.gov/greenvehicles/greenhouse-gas-emissions-typical-passenger-vehicle

180 Luderer, G. et al. Description of the REMIND model (Version 1.6). (2015).

181 *The road ahead for e-mobility* (McKinsey, 2020). https://www.mckinsey.com/~/media/mckinsey/industries/automotive%20and%20assembly/our%20insights/the%20road%20ahead%20for%20e%20mobility/the-road-ahead-for-e-mobility-vf.pdf

182 *THE GLOBAL BATTERY ARMS RACE: LITHIUM-ION BATTERY GIGAFACTORIES AND THEIR SUPPLY CHAIN* (The Oxford Institute for Energy Studies, 2021). https://www.oxfordenergy.org/wpcms/wp-content/uploads/2021/02/THE-GLOBAL-BATTERY-ARMS-RACE-LITHIUM-ION-BATTERY-GIGAFACTORIES-AND-THEIR-SUPPLY-CHAIN.pdf

183 *Lithium-ion battery supply chain technology development and investment opportunities* (Benchmark Mineral Intelligence, 2020). https://www.benchmarkminerals.com/wp-content/uploads/20200608-Vivas-Kumar-Carnegie-Mellon-Battery-Seminar-V1.pdf

184 Luksch, U., Steinbach, N. & Markosova, K. (2006).

185 Dunn, J. B., Gaines, L., Sullivan, J. & Wang, M. Q. Impact of recycling on cradle-to-gate energy consumption and greenhouse gas emissions of automotive lithium-ion batteries. *Environmental science & technology* **46**, 12704-12710 (2012).

186 Larouche, F. et al. Progress and Status of Hydrometallurgical and Direct Recycling of Li-Ion Batteries and Beyond. *Materials* **13** (2020).

187 Greenblatt, J. B. & Saxena, S. Autonomous taxis could greatly reduce greenhouse-gas emissions of US light-duty vehicles. *Nature Climate Change* **5**, 860-863 (2015).

188 Lund, P. D., Lindgren, J., Mikkola, J. & Salpakari, J. Review of energy system flexibility measures to enable high levels of variable renewable electricity. *Renewable and Sustainable Energy Reviews* **45**, 785-807 (2015).

189 Palensky, P. & Dietrich, D. Demand Side Management: Demand Response, Intelligent Energy Systems, and Smart Loads. *IEEE Transactions on Industrial Informatics* **7**, 381-388 (2011).

190 Brown, T., Schlachtberger, D., Kies, A., Schramm, S. & Greiner, M. Synergies of sector coupling and transmission reinforcement in a cost-optimised, highly renewable European energy system. *Energy* **160**, 720-739 (2018).

191 Naumann, M., Schimpe, M., Keil, P., Hesse, H. C. & Jossen, A. Analysis and modeling of calendar aging of a commercial LiFePO4/graphite cell. *Journal of Energy Storage* **17**, 153-169 (2018).

192 Guerra, O. J. Beyond short-duration energy storage. *Nature Energy* **6**, 460-461 (2021).

193 *Energy Storage Grand Challenge: Energy Storage Market Report* (U.S. Department of Energy, 2020). https://www.energy.gov/sites/prod/files/2020/12/f81/Energy%20Storage%20Market%20Report%202020_0.pdf

194 *Electric Insights Quarterly* (Drax, 2019). https://www.drax.com/wp-content/uploads/2019/12/191202_Drax_Q3_Report.pdf

195 *Global EV Data Explorer* (IEA, 2021). https://www.iea.org/articles/global-ev-data-explorer

196 *Electric vehicle capitals: Cities aim for all-electric mobility* (The International Council on Clean Transportation, 2020). https://theicct.org/publications/electric-vehicle-capitals-update-sept2020

197 *Electric Vehicle Industry in India: Why Foreign Investors Should Pay Attention* (India Briefing, 2021). https://www.india-briefing.com/news/electric-vehicle-industry-in-india-why-foreign-investors-should-pay-attention-21872.html/

198 *The Rechargeable Battery Market and Main Trends 2018-2030* (Avicenne Energy, 2019). https://www.bpifrance.fr/content/download/76854/831358/file/02%20-%20Presentation%20Avicenne%20-%20Christophe%20Pillot%20-%2028%20Mai%202019.pdf

199 *MPG and Cost Calculator and Tracker* (Spritmonitor, 2020). https://www.spritmonitor.de/en/

200 Plötz, P., Funke, S. A., Jochem, P. & Wietschel, M. CO2 Mitigation Potential of Plug-in Hybrid Electric Vehicles larger than expected. *Scientific Reports* **7**, 16493 (2017).

201 Hoekstra, A. The Underestimated Potential of Battery Electric Vehicles to Reduce Emissions. *Joule* **3**, 1412-1414 (2019).

202 Brooker, A. et al. (SAE International, 2015).

203 *Mitsubishi i-Miev charging cost and time calculator* (EVcompare.io, 2009). https://evcompare.io/cars/mitsubishi/mitsubishi_i-miev/charging/

204 *What does Elevated Self-discharge Do?* (Battery University, 2011). https://batteryuniversity.com/learn/article/elevating_self_discharge

205 *BatPaC: Battery Manufacturing Cost Estimation* (Argonne National Laboratory, 2021). https://www.anl.gov/partnerships/batpac-battery-manufacturing-cost-estimation

206 *Climate Data Online: Dataset Discovery* (National Oceanic and Atmospheric Administration, 2021). https://www.ncdc.noaa.gov/cdo-web/datasets

207 *CLIMATE DATA FOR CITIES WORLDWIDE* (CLIMATE-DATA.ORG, 2021). https://en.climate-data.org/

208 *Climates for travelers. Information on the climates in the world to plan a trip* (Climates to travel, 2021). https://www.climatestotravel.com/

209 *Climate Zone Finder* (Weather and Climate, 2021). https://tcktcktck.org/

210 Uddin, K., Dubarry, M. & Glick, M. B. The viability of vehicle-to-grid operations from a battery technology and policy perspective. *Energy Policy* **113**, 342-347 (2018).

211 Safari, M., Morcrette, M., Teyssot, A. & Delacourt, C. Multimodal Physics-Based Aging Model for Life Prediction of Li-Ion Batteries. *Journal of The Electrochemical Society* **156**, A145 (2009).

212 Zhang, Y. et al. Identifying degradation patterns of lithium ion batteries from impedance spectroscopy using machine learning. *Nat. Commun.* **11**, 1706 (2020).

213 Edge, J. S. et al. Lithium ion battery degradation: what you need to know. *Physical Chemistry Chemical Physics* **23**, 8200-8221 (2021).

214 Safari, M. & Delacourt, C. Modeling of a Commercial Graphite/LiFePO4 Cell. *Journal of The Electrochemical Society* **158**, A562 (2011).

215 Schimpe, M. et al. Comprehensive Modeling of Temperature-Dependent Degradation Mechanisms in Lithium Iron Phosphate Batteries. *Journal of The Electrochemical Society* **165**, A181-A193 (2018).

216 Peterson, S. B., Apt, J. & Whitacre, J. F. Lithium-ion battery cell degradation resulting from realistic vehicle and vehicle-to-grid utilization. *Journal of Power Sources* **195**, 2385-2392

(2010).

217 Martinez-Laserna, E. et al. Technical Viability of Battery Second Life: A Study From the Ageing Perspective. *IEEE Transactions on Industry Applications* **54**, 2703-2713 (2018).

218 Neubauer, J., Pesaran, A., Williams, B., Ferry, M. & Eyer, J. Techno-Economic Analysis of PEV Battery Second Use: Repurposed-Battery Selling Price and Commercial and Industrial End-User Value. (Sponsor Org.: USDOE Office of Energy Efficiency and Renewable Energy (EERE), Vehicle Technologies Office (EE-3V)).

219 Thompson, A. W. Economic implications of lithium ion battery degradation for Vehicle-to-Grid (V2X) services. *Journal of Power Sources* **396**, 691-709 (2018).

220 DeRousseau, M., Gully, B., Taylor, C., Apelian, D. & Wang, Y. Repurposing Used Electric Car Batteries: A Review of Options. *JOM* **69**, 1575-1582 (2017).

221 Reinhardt, R., Christodoulou, I., Gassó-Domingo, S. & Amante García, B. Towards sustainable business models for electric vehicle battery second use: A critical review. *Journal of Environmental Management* **245**, 432-446 (2019).

222 Casals, L. C., Amante García, B. & Canal, C. Second life batteries lifespan: Rest of useful life and environmental analysis. *Journal of Environmental Management* **232**, 354-363 (2019).

223 Podias, A. et al. Sustainability Assessment of Second Use Applications of Automotive Batteries: Ageing of Li-Ion Battery Cells in Automotive and Grid-Scale Applications. *World Electric Vehicle Journal* **9** (2018).

224 *The Present & Future Of Vehicle-To-Grid Technology* (CleanTechnica, 2020). https://cleantechnica.com/2020/09/05/the-present-future-of-vehicle-to-grid-technology/

225 Zonneveld, J. A. Increasing participation in V2G through contract elements: Examining the preferences of Dutch EV users regarding V2G contracts using a stated choice experiment.

226 Anwar, M. B. et al. Assessing the value of electric vehicle managed charging: a review of methodologies and results. *Energy & Environmental Science* (2022).

227 *A Vision for a Sustainable Battery Value Chain in 2030* (2019). https://www.globalbattery.org/media/publications/WEF_A_Vision_for_a_Sustainable_Battery_Value_Chain_in_2030_Report.pdf

228 Sapunkov, O., Pande, V., Khetan, A., Choomwattana, C. & Viswanathan, V. Quantifying the promise of 'beyond' Li–ion batteries. *Translational Materials Research* **2**, 045002 (2015).

229 Srdic, S. & Lukic, S. Toward Extreme Fast Charging: Challenges and Opportunities in Directly Connecting to Medium-Voltage Line. *IEEE Electrification Magazine* **7**, 22-31 (2019).

230 *What can 6,000 electric vehicles tell us about EV battery health?* (GEOTAB, 2020).

https://www.geotab.com/blog/ev-battery-health/

231 Park, Y.-U. et al. A New High-Energy Cathode for a Na-Ion Battery with Ultrahigh Stability. *Journal of the American Chemical Society* **135**, 13870-13878 (2013).

232 Alam, M. et al. Real-Time Smart Parking Systems Integration in Distributed ITS for Smart Cities. *Journal of Advanced Transportation* **2018**, 1485652 (2018).

233 Giordano, V. & Fulli, G. A business case for Smart Grid technologies: A systemic perspective. *Energy Policy* **40**, 252-259 (2012).

234 Zheng, Y. et al. Electric Vehicle Battery Charging/Swap Stations in Distribution Systems: Comparison Study and Optimal Planning. *IEEE Transactions on Power Systems* **29**, 221-229 (2014).

235 *Innovation in Batteries and Electricity Storage* (IEA, 2020). https://www.iea.org/reports/innovation-in-batteries-and-electricity-storage

236 *Global energy transformation: A roadmap to 2050 (2019 edition)* (IRENA, 2019). https://www.irena.org/publications/2019/Apr/Global-energy-transformation-A-roadmap-to-2050-2019Edition

237 *Electricity storage and renewables: Costs and markets to 2030* (IRENA, 2017). https://www.irena.org/publications/2017/oct/electricity-storage-and-renewables-costs-and-markets

238 *Energy Storage Investments Boom As Battery Costs Halve in the Next Decade* (BloombergNEF, 2019). https://about.bnef.com/blog/energy-storage-investments-boom-battery-costs-halve-next-decade/

239 *Global EV Outlook 2021* (IEA, 2021). https://www.iea.org/reports/global-ev-outlook-2021

240 Elwert, T., Hua, Q. S. & Schneider, K. Recycling of lithium iron phosphate batteries: future prospects and research needs. in *Materials Science Forum* 49-68(Trans Tech Publ).

241 Soundharrajan, V. et al. The advent of manganese-substituted sodium vanadium phosphate-based cathodes for sodium-ion batteries and their current progress: a focused review. *Journal of Materials Chemistry A* **10**, 1022-1046 (2022).

242 Zeng, X. et al. Commercialization of Lithium Battery Technologies for Electric Vehicles. *Advanced Energy Materials* **9**, 1900161 (2019).

243 Allwood, J. M., Ashby, M. F., Gutowski, T. G. & Worrell, E. Material efficiency: A white paper. *Resources, Conservation and Recycling* **55**, 362-381 (2011).

244 McManus, M. C. Environmental consequences of the use of batteries in low carbon systems: The impact of battery production. *Applied Energy* **93**, 288-295 (2012).

245 Child, M., Breyer, C., Bogdanov, D. & Fell, H.-J. The role of storage technologies for the transition to a 100% renewable energy system in Ukraine. *Energy Procedia* **135**, 410-423 (2017).

246 Lipu, M. S. H. et al. A review of state of health and remaining useful life estimation methods for lithium-ion battery in electric vehicles: Challenges and recommendations. *Journal of Cleaner Production* **205**, 115-133 (2018).

247 *Lithium Prices Surge on Increased Battery Demands* (Foley & Lardner LLP, 2022). https://www.foley.com/en/insights/publications/2022/04/lithium-prices-surge-on-increased-battery-demands

248 *Why lithium stocks are falling despite surging demand for EVs* (Money magazine, 2022). https://www.moneymag.com.au/why-lithium-stocks-are-falling-despite-surging-demand-for-evs

249 Eddy, J. et al. Metal mining constraints on the electric mobility horizon. (2018).

250 *The supply of critical raw materials endangered by Russia's war on Ukraine* (OECD, 2022). https://www.oecd.org/ukraine-hub/policy-responses/the-supply-of-critical-raw-materials-endangered-by-russia-s-war-on-ukraine-e01ac7be/

251 Sen, P. K. Metals and materials from deep sea nodules: an outlook for the future. *International Materials Reviews* **55**, 364-391 (2010).

252 *Billionaire group invests into mining project in Greenland for e-transportation* (POLAR JOURNAL, 2022). https://polarjournal.ch/en/2022/08/11/billionaire-group-invests-into-mining-project-in-greenland-for-e-transportation/

253 Curry, C. Lithium-ion battery costs and market. *Bloomberg New Energy Finance* **5**, 4-6 (2017).

## Summary

A rapid and large-scale shift from Internal Combustion Engine Vehicles (ICEVs) to Electric Vehicles (EVs) is one of the most effective pathways to meet climate mitigation goals for the transportation sector. Such a shift can reduce driving emissions of cars significantly, especially when combined with the supply of renewable electricity. At the same time, the use of batteries - dominated by lithium-ion batteries - will increase drastically. To maximize the greenhouse gas (GHG) mitigation potential of EVs, further efforts to lower the lithium-ion battery-related GHG emissions are essential. To guide such efforts, it is essential to have a quantitative understanding of both the sustainability challenges and opportunities that the large-scale use of EV batteries provides.

In this thesis, I built an integrated model that combines dynamic MFA (material flow analysis), prospective LCA (life cycle assessment), and battery technology modeling. We use the integrated model and scenario analysis in chapters 2 to 5 to answer the overall research question: What are the future environmental challenges and opportunities for automotive lithium-ion batteries from a life cycle perspective? By combining dynamic MFA and battery technology modeling, we estimate the global stocks and flows of battery materials until 2050 (Chapter 2). By combining prospective LCA and battery technology modeling, we assess life cycle GHG emissions of future battery production discerning different battery production regions, battery chemistries, and energy mix scenarios (Chapter 3). By combining dynamic MFA, prospective LCA, and battery technology modeling (*i.e.*, combining Chapter 2 and Chapter 3), we explore the total GHG emissions associated with global EV battery production and also discuss the effect of closed-loop material recycling (Chapter 4). Lastly, in addition to the above-mentioned battery environmental challenges, we evaluate the energy storage capacity potentially available from EV batteries by combining the dynamic MFA model and the battery technology modeling. We compare this storage potential to the demand for the grid storage capacity (Chapter 5). The model integration enables us to systematically investigate and analyze the sustainability challenges and opportunities of the large-scale deployments of EV batteries.

Chapter 2 assesses the future material demand for EV batteries, including critical materials (lithium, cobalt, and nickel) that are crucial to the global economy and

associated with environmental and social impacts. Our analysis in Chapter 2 is based on the detailed modeling of the future battery chemistry mix and the material compositions of each chemistry. For modeling battery material compositions, the parameter inputs include EV type (battery electric vehicle/plug-in hybrid electric vehicle), size (small/mid-size/large), and performance (EV range and fuel economy) as well as battery chemistry (positive and negative active material capacity of 8 chemistries) and performance (*e.g.*, specific energy). Results show the dynamic development of battery stock, the demand for 8 battery materials, and the number of end-of-life batteries. We find a strong demand growth for battery materials (a factor of ~20 from 2020 to 2050). The modeling results for three battery chemistry scenarios assert that the material demand strongly depends on the battery chemistry. The demand for nickel and cobalt is lower when deploying more lithium iron phosphate batteries and lithium-sulfur/lithium-air solid-state batteries instead of lithium nickel cobalt aluminum/ lithium nickel cobalt manganese batteries. This, in turn, reflects the importance of modeling future battery chemistry mixes and the material compositions of each chemistry.

Chapter 3 quantifies the GHG emissions of future battery production using a prospective LCA model that simulates the life cycle inventories (LCIs) of future battery production. The data source for the foreground LCIs is based on the EverBatt model (Argonne's closed-loop battery life-cycle model), China battery industry reports (environmental assessment reports for battery production), and others (such as literatures); the background LCIs are based on the integration of ecoinvent 3.6 (world's most consistent and transparent life cycle inventory database), future energy mix scenarios with an ambitious and moderate GHG emission reduction policy based on the REMIND (Regional Model of Investment and Development) Integrated Assessment model, and future technology changes for the supply of key battery metals. The analysis is performed for different combinations of battery production regions, battery chemistry, and energy mix. The results show that the future life cycle GHG emissions of battery production relies heavily on the future energy mix. The scenario that includes a low-carbon energy transition, which aims well below 2 degrees Celsius for global warming, can result in an 50%-75% reduction in the life cycle GHG emissions of EV batteries.

Chapter 4 shows the total GHG emission of global EV battery production. This chapter

is based on the dynamic MFA model from Chapter 2, but develops three more specific future battery demand scenarios (low/medium/high) considering EV fleet size and battery capacity per vehicle. Taking into account the life cycle GHG emissions of battery production including differences therein between battery production regions (China/EU/US), Chapter 4 presents the magnitude and range of total GHG emissions related to global EV battery production. The decreasing life cycle GHG emissions of battery production result in a relative decoupling between total GHG emissions of battery production and global battery demand. Despite this relative decoupling, results show that there is no absolute decoupling due to the strong demand increase overall until 2050. Reduction of the production emission requires an even faster penetration of renewable energy production, using battery chemistries (such as lithium iron phosphate batteries) that emit less GHG during production, etc.

Finally, Chapter 5 presents an opportunity of EV battery use: the co-benefit of providing grid storage. This is important, since in future a significant part of electricity production will come from intermittent sources such as wind and solar power. Chapter 5 uses the results of Chapter 2 on future battery stocks and outflows, which are differentiated by battery capacity and chemistry. Further, based on a detailed dataset on the daily driving distance of various EV types/sizes/models, Chapter 5 models the EV driving behavior and battery use states. The battery use states (driving/charging) over time, combined with the battery chemistry and information on ambient temperature, are used to estimate battery degradation over time (*i.e.*, the dynamic battery capacity under various conditions). Results present the total gird storage capacity from EV batteries until 2050, including both vehicle-to-grid and second-use, under assumed market participation rates of vehicle-to-grid and second-use. By comparing this total grid storage capacity with demand scenarios for storage capacity, we find that EV batteries alone could satisfy short-term grid storage demand by as early as 2030.

Combining the results of Chapters 2-5, increasing battery demand and battery production driven by EV fleet penetration will continue to pose challenges to raw materials supply and GHG mitigation in the context of achieving climate goals. Large-scale production of EV batteries would weaken the driving emission reduction benefits resulting from EVs. The results point out the important factors (*e.g.*, battery chemistry, production region, and low-carbon energy transition) and their effects on the

magnitude of the challenges. This has fundamental implications for the guidance with respect to relieving these challenges and even turning challenges into opportunities for achieving environmentally sustainable batteries.

A lower emission and even net-zero battery industry can be achieved by the adoption of new battery production processes using low-carbon electricity, in addition to other potential low-carbon energy sources. Reducing life cycle emissions from battery production should require further coordinated actions throughout battery value chains to promote all mitigation options. This includes reducing battery demand (such as stimulating the use of small EVs that can be driven with low-capacity batteries); improved and innovative battery technologies that enhance battery lifetimes, and are less dependent on materials that are critical or require high levels of energy to be produced; increasing material and energy efficiency during battery production; implementing circular economy principles (such as close-loop recycling).

# Samenvatting

Een snelle en grootschalige overstap van voertuigen met een verbrandingsmotor (ICEV's) naar elektrische voertuigen (EV's) is een van de efficiënste manieren om de klimaatdoelen voor de transportsector te halen. Deze omschakeling kan de uitstoot van auto's aanzienlijk verminderen, vooral in combinatie met de levering van hernieuwbare elektriciteit. Tegelijkertijd zal het gebruik van batterijen - met name lithium-ionbatterijen - drastisch toenemen. Om de klimaatimpact van EV's te minimaliseren, is het essentieel om de uitstoot van broeikasgassen (BKG's) van de productie van lithium-ionbatterijen te verlagen. Om dergelijke inspanningen in goede banen te leiden, is het essentieel om een kwantitatief inzicht te hebben in zowel de duurzaamheidsuitdagingen als de kansen die het grootschalige gebruik van EV batterijen biedt.

Deze dissertatie beschrijft een geïntegreerd model dat dynamische MFA (Material Flow Analysis of materiaalstroomanalyse), ex-ante of toekomstgerichte LCA (levenscyclusanalyse) en modellering van batterijtechnologie combineert. We gebruiken het geïntegreerde model en een scenario-analyse in de hoofdstukken 2 tot 5 om de hoofdonderzoeksvraag te beantwoorden: Wat zijn de toekomstige milieu-uitdagingen en kansen voor lithium-ion batterijen voor EV's vanuit een levenscyclus perspectief? Met de combinatie van dynamische MFA en het batterijtechnologiemodel schatten we de wereldwijde voorraden en stromen van batterijmaterialen tot 2050 (hoofdstuk 2). Door ex-ante LCA en het batterijtechnologiemodel te combineren, beoordelen we de toekomstige broeikasgasemissies van de batterijproductie gedurende de levenscyclus, waarbij wij verschillende productieregio's, batterijtypen en energiescenario's onderscheiden (hoofdstuk 3). Door alle drie de modellen (d.w.z. door hoofdstuk 2 en hoofdstuk 3) te combineren, onderzoeken we de totale broeikasgasemissies die gepaard gaan met de wereldwijde productie van EV-batterijen en bespreken we ook het effect van recycling van materialen in gesloten kringlopen (hoofdstuk 4). Naast de bovengenoemde milieu-uitdagingen voor batterijen evalueren we tenslotte de potentiële opslagcapaciteit van EV-batterijen om de stabiliteit van een door wind- en zonne-energie gevoed elektriciteitsnet te vergroten, door het dynamische MFA-model en het batterijtechnologiemodel te combineren. We vergelijken dit opslagpotentieel met de behoefte aan opslagcapaciteit voor elekticiteit

(Hoofdstuk 5). De modelintegratie stelt ons in staat om de batterijtechnologie systematisch te onderzoeken en te analyseren met betrekking tot de duurzaamheid van de grootschalige inzet van EV batterijen.

Hoofdstuk 2 onderzoekt de toekomstige vraag naar materialen voor EV-batterijen, inclusief kritieke materialen (lithium, kobalt en nikkel) die cruciaal zijn voor de wereldeconomie en wier productie gepaard gaat met ecologische en sociale problemen. Onze analyse in hoofdstuk 2 is gebaseerd op een gedetailleerde modellering van de toekomstige mix van batterijtypen en de materiaalsamenstellingen van elke type. Het model van de samenstelling van batterijmaterialen heeft als invoerparameters het EV-type (Batterij Electrische Voertuigen/Plug-in Hybride Electrische Voertuigen), de grootte (klein/middengroot/groot), en de prestaties (rijbereik en brandstofrendement) alsook de batterijchemie (8 combinaties van verschillende anode- en kathodematerialen) en de prestaties (zoals opslagcapaciteit). De resultaten tonen de ontwikkeling van de batterijvoorraad, de vraag naar 8 batterijtypes, en het aantal afgedankte batterijen. Wij constateren een sterke groei van de vraag naar batterijmaterialen (een factor ~20 van 2020 tot 2050). De modelresultaten voor drie specifieke batterijchemiescenario's bevestigen dat de vraag naar materialen sterk afhangt van de batterijsamenstelling. De vraag naar nikkel en kobalt is lager wanneer meer LFP- en Li-S/Li-Air-batterijen worden gebruikt in plaats van NCA/NCM-batterijen. Hieruit blijkt hoe belangrijk het is om modellen te maken van de toekomstige samenstellingen van batterijen en batterijmaterialen.

In hoofdstuk 3 worden de toekomstige broeikasgasemissies van batterijproductie gekwantificeerd met behulp van een ex-ante LCA-model dat de Levenscyclusinformatie (LCI) van de toekomstige batterijproductie simuleert. De gegevensbronnen voor de LCI's van de batterijproductie zelf (de zogenaamde voorgronddata) zijn onder anderen het EverBatt-model en een rapport van de Chinese batterijindustrie. De LCI's van toeleverende productieprocessen (de zogenaamde achtergronddata) zijn gebaseerd op de integratie van de LCI database ecoinvent 3.6, toekomstige energiemixscenario's met een ambitieus en gematigd BKG-emissiereductiebeleid op basis van het Remind Integrated Assessment Model, en toekomstige technologische veranderingen voor het produceren van de belangrijkste metalen gebruikt in batterijen. De analyse wordt uitgevoerd voor verschillende combinaties van batterijproductieregio's, batterijsamenstellingen en energiemixen. Uit

de resultaten blijkt dat de toekomstige broeikasgasemissies van de batterijproductie sterk afhangen van de toekomstige energiemix. Het scenario met een energietransitie die gericht is op minder dan 2 graden Celsius opwarming kan resulteren in een vermindering van de broeikasgasemissies van de productie van EV-batterijen met 50%-75%.

Hoofdstuk 4 toont de totale broeikasgasemissies van de wereldwijde productie van EV-batterijen. Dit hoofdstuk is gebaseerd op het dynamische MFA-model van hoofdstuk 2, maar ontwikkelt drie specifiekere scenario's voor de toekomstige vraag naar batterijen (laag/gemiddeld/hoog) rekening houdend met de omvang van het EV-wagenpark en de batterijcapaciteit per voertuig. Rekening houdend met de broeikasgasemissies van batterijproductie, met inbegrip van de verschillen tussen de batterijproductieregio's (China/EU/VS), wordt in hoofdstuk 4 de omvang en de bandbreedte van de totale broeikasgasemissies met betrekking tot de wereldwijde productie van EV-batterijen gepresenteerd. De afnemende broeikasgasemissie van batterijproductie resulteert in een relatieve ontkoppeling tussen de totale broeikasgasemissies en de wereldwijde vraag naar batterijen. Ondanks deze relatieve ontkoppeling blijkt uit de resultaten dat er geen absolute ontkoppeling is als gevolg van de sterke toename van de totale vraag tot 2050. Een vermindering van de productie-emissies vereist een nog snellere overstap naar hernieuwbare energie, het gebruik van batterijtypes die minder energie vergen tijdens de productie (zoals LFP), enz.

Tot slot wordt in hoofdstuk 5 een mogelijkheid gepresenteerd voor het gebruik van EV-batterijen: de mogelijkheid om elektriciteit van het net te bufferen. Dit is van belang omdat in de toekomst naar verwachting een aanzienlijk deel van de elektriciteitsproductie uit niet continue bronnen zoals wind en zon zal komen. Hoofdstuk 5 maakt gebruik van de resultaten van hoofdstuk 2 over toekomstige instroom, uitstroom en totale voorraad van batterijen in de economie, die worden gedifferentieerd naar batterijcapaciteit en -chemie. Verder, gebaseerd op een gedetailleerde dataset over de dagelijkse rijafstand van verschillende EV-modellen, worden in hoofdstuk 5 het rijgedrag en gebruik van batterijen van EV's in de tijd gemodelleerd. De gebruiksstatus van de batterij (rijden/laden) in de tijd, gecombineerd met de batterijchemie en informatie over de omgevingstemperatuur, wordt gebruikt om de degradatie van de batterij in de tijd te schatten (d.w.z. de

dynamische batterijcapaciteit onder verschillende omstandigheden). De resultaten tonen de totale netopslagcapaciteit van EV-batterijen tot 2050, met inbegrip van zowel voertuig-naar-net als tweedehands gebruik, onder veronderstelde marktdeelname van beide toepassingen. Door deze totale netopslagcapaciteit te vergelijken met scenario's voor de vraag naar opslagcapaciteit, komen we tot de bevinding dat EV-batterijen al in 2030 in de volledige vraag naar korte-termijnopslag kunnen voorzien.

Uit de combinatie van de resultaten uit hoofdstukken 2-5 blijkt het volgende. De stijgende vraag naar en productie van batterijen als gevolg van de elektrificatie van het wagenpark resulteert in aanzienlijke materiaalbehoeften en BKG emissies. Grootschalige productie van batterijen kan dus de netto vermindering beperken van BKG uitstoot door gebruik van elektrische voertuigen. Dit proefschrift geeft echter ook inzicht in de belangrijkste factoren die BKG emissies van de productie van batterijen kan verminderen (zoals batterijtype, de productieregio, en de snelheid van de energietransitie). Deze inzichten zijn cruciaal om voornoemde uitdagingen te lijf te gaan of zelfs om te zetten in kansen.

Een batterijproductie met een BKG emissie die laag of zelfs nihil is kan productie te richten op batterijtypes die weinig energie vergen in de productie en waarbij gebruik wordt gemaakt van emissiearme elektriciteit, naast andere potentiële duurzame energiebronnen. Verder moet in de hele waardeketen van batterijen gezocht worden naar reductie-opties om alle kansen te benutten. Dit omvat het verminderen van de vraag naar batterijen (zoals het stimuleren van het gebruik van kleine EV's die kunnen worden aangedreven met batterijen met een kleinere capaciteit); verbeterde en innovatieve batterijtechnologieën die de levensduur van batterijen verlengen en minder afhankelijk zijn van materialen die kritisch zijn of veel energie vergen om te worden geproduceerd; het verhogen van de materiaal- en energie-efficiëntie tijdens de batterijproductie; en het toepassen van de beginselen van de kringloopeconomie (zoals hoogwaardige recycling).

## Acknowledgements

This thesis is about challenges and opportunities related to the use of lithium-ion batteries. Similarly, I met challenges and opportunities during my PhD journey. I cannot describe the whole story of this PhD journey in this short acknowledgment. But in short, the journey was like a long-distance roller coaster ride where I entered a world of unfamiliar surroundings, exciting collaborations with top-ranking institutes, how to publish high-quality papers, *etc.*

Here I would like to thank my supervisor, Professor Arnold Tukker, for his support in my PhD trajectory. I am very impressed by his very good organizational skills and cutting-edge research perspectives. Thanks to his help, I managed to finalize Chapters 3 and 4 of this thesis and the overall thesis in time. Also, I would like to thank my two co-supervisors, Dr. Bernhard Steubing and Dr. Mingming Hu. They always gave very detailed comments and encouraged me to do impactful and meaningful research. I would like to express a special appreciation for Bernhard's contribution to Chapter 2. Thanks to the collaboration Bernhard set up with the US Argonne National Laboratory we managed to write this paper, called "Future material demand for automotive lithium-based batteries" which by now has received 62k access and 159 citations since its publication in Dec 2020. It would have been impossible to achieve this without the help of Bernhard, Mingming, and Arnold, and the contributions of Dr. Qiang Dai and Dr. Linda Gaines from US Argonne National Laboratory. With regard to Chapter 3, I would like to thank Carina Harpprecht for her help on developing future metal supply scenarios and Marc van der Meide for his help in using the activity browser software to implement life cycle assessment. With regard to Chapter 5, I would like to thank Dr. Paul Gasper and Dr. Kandler Smith from the US National Renewable Energy Laboratory, for their excellent support on battery degradation modeling. In addition, I would like to thank Dr. Paul Behrens for his ideas about the structure and editorial help in Chapter 5. I would also thank Sander van Nielen for his help in editing the Dutch Summary of this thesis.

I would also like to thank the colleagues at the Institute of Environmental Sciences (CML) at Leiden University for the meetings, workshops, speeches, conversations, and other activities that we had. Such an environment enriched me with knowledge in different research fields in the area of environmental sciences, and at the same time

helped me to have a good work-life balance. Special thanks to my Chinese colleagues for their help in my life at Leiden University. I would like to thank Dr. Jeroen Guinee and Dr. Bernhard Steubing for their class on life cycle assessment, as well as Dr. Mingming Hu for her class on Industry ecology tools. Special thanks to Dr. Gjalt Huppes and Professor Haixiang Lin for the interesting exchanges on a wide range of subjects, as well as to Dr. Rene Kleijn for the organization of Circular Industry Talks. Especially, I would like to appreciate the China Scholarship for the financial support, as well as the secretaries and management team of the CML for their kind help.

Last but not least, I would like to express appreciation to my family members for their kind support and attention. Special thanks to Professor Zhiming Zhao from the University of Amsterdam for his help in every aspect of my PhD journey in the Netherlands, as well as my parents for their encouragement to be an excellent researcher.

## Curriculum Vitae

Chengjian Xu was born on the 22th of April 1993 in Yancheng, China. After completing his study at the second high school in Jianhu county in 2011, he joined the Jiangsu University of Technology for a Bachelor program with a major in science and technology for circular resource use. From 2011 to 2015, he studied a wide range of courses in Mathematics, Physics, and Chemistry, with a focus on environmental engineering. Between 2015 and 2018, he did a MSc. in environmental engineering at Tongji University, Shanghai. There, he studied waste management and recycling of Waste Electrical and Electronic Equipment. He finished a Master's thesis on the application of ultrasound technology to recover valuable materials from mobile phone batteries. He was part of a team that won the 1st Prize in the 3rd University Challenge China during IEexpo 2017 in Shanghai/China, awarded by Tongji University and the German Water, wastewater, and waste disposal association.

After finalizing his Master's degree in 2018, the Chinese Scholarship Council (CSC) awarded him a grant to do his PhD at the Institute of Environmental Sciences (CML), Leiden University. Between September 2018 and September 2022, he analysed the environmental challenges and opportunities of Electric Vehicle Batteries from a life cycle perspective. In this work, he applied dynamic material flow analysis, prospective life cycle assessment, and battery technology modeling to investigate the future battery material demand and environmental impacts of battery production. In 2021, he won the Stans Award for the best PhD paper from 2020 at CML, Leiden University, for his paper in Nature Communications Materials "Future material demand for automotive lithium-based batteries". From September 2022, he has been hired on a short-term contract by the United Nations Institute for Training and Research in Bonn, to contribute to the Future of Raw Materials (FUTURAM) Horizon Europe project.

## List of peer-reviewed publications:

1. Xu, C., Dai, Q., Gaines, L., Hu, M., Tukker, A. & Steubing, B. Future material demand for automotive lithium-based batteries. *Communications materials* **1**, 1-10 (2020).
2. Xu, C., Behrens, P., Gasper, P., Smith, K., Hu, M., Tukker, A. & Steubing, B. Electric vehicle batteries alone could satisfy short-term grid storage demand by as early as 2030. (under revision in Nature Communications)
3. Xu, C., Steubing, B., Hu, M., Harpprecht, C., van der Meide, M. & Tukker, A. Future greenhouse gas emissions of automotive lithium-ion battery cell production. *Resources, Conservation & Recycling* **187**, 106606 (2022).
4. Xu, C., Steubing, B., Hu, M. & Tukker, A. Future greenhouse gas emissions of global automotive lithium-ion battery cells and recycling potential till 2050. (Submitted to Renewable and Sustainable Energy Reviews)
5. Xu, C., Dai, Q., Gaines, L., Hu, M., Tukker, A. & Steubing, B. (2020). Reply to: Concerns about global phosphorus demand for lithium-iron-phosphate batteries in the light electric vehicle sector. *Communications materials* **3**, 15 (2022).

## Additional publications:

6. Xu, C., Zhang, W., He, W., Li, G. & Huang, J. The situation of waste mobile phone management in developed countries and development status in China. *Waste management* **58**, 341-347 (2016).
7. Xu, C., Zhang, W., He, W., Li, G., Huang, J., & Zhu, H. Generation and management of waste electric vehicle batteries in China. *Environmental Science and Pollution Research* **24**, 20825-20830 (2017).
8. Zhang, W., Xu, C., He, W., Li, G. & Huang, J. A review on management of spent lithium ion batteries and strategy for resource recycling of all components from them. *Waste Management & Research* **36**, 99-112 (2018).
9. Zhang, W., Liu, Z., Xu, C., He, W., Li, G., Huang, J., & Zhu, H. Preparing graphene oxide–copper composite material from spent lithium ion batteries and catalytic performance analysis. *Research on Chemical Intermediates* **44**, 5075-5089 (2018).